ORNL 919, Series A
PROGRESS REPORT
REACTORS

AIRCRAFT NUCLEAR PROPULSION PROJECT

QUARTERLY PROGRESS REPORT
FOR PERIOD ENDING DECEMBER 10, 1950

OAK RIDGE NATIONAL LABORATORY
OPERATED BY
CARBIDE AND CARBON CHEMICALS DIVISION
UNION CARBIDE AND CARBON CORPORATION
UCC
POST OFFICE BOX P
OAK RIDGE, TENNESSEE

SECRET

[redacted]

ORNL 919

This document consists of 290 pages.
Copy 10 of 192. Series A

Contract No. W-7405, eng 26

AIRCRAFT NUCLEAR PROPULSION PROJECT

QUARTERLY PROGRESS REPORT

for Period Ending December 10, 1950

R. C. Briant
Director, ANP Division

Edited by:

C. B. Ellis and W. B. Cottrell

DATE ISSUED FEB 26 1951

OAK RIDGE NATIONAL LABORATORY
operated by
CARBIDE AND CARBON CHEMICALS DIVISION
Union Carbide and Carbon Corporation
Post Office Box P
Oak Ridge, Tennessee

INTERNAL DISTRIBUTION

1. G. T. Felbeck (C&CCD)
2-3. Chemistry Library
4. Physics Library
5. Biology Library
6. Health Physics Library
7. Metallurgy Library
8-9. Training School Library
10-13. Central Files
14. C. E. Center
15. C. E. Larson
16. W. B. Humes (K-25)
17. W. D. Lavers (Y-12)
18. A. M. Weinberg
19. J. A. Swartout
20. E. D. Shipley
21. E. J. Murphy
22. F. C. VonderLage
23. R. C. Briant
24. C. B. Ellis
25. E. H. Taylor
26. A. H. Snell
27. A. Hollaender
28. F. L. Steahly
29. K. Z. Morgan
30. D. W. Cardwell
31. M. T. Kelley
32. W. H. Pennington
33. C. E. Winters
34. J. A. Lane
35. M. M. Mann
36. G. E. Boyd
37. R. W. Stoughton
38. F. R. Bruce
39. H. W. Savage
40. W. K. Eister
41. A. S. Householder
42. C. B. Graham
43. R. N. Lyon
44. R. E. Engberg
45. W. R. Gall
46. R. M. Jones
47. E. C. Miller
48. D. S. Billington
49. E. P. Blizard
50. W. K. Ergen
51. C. E. Clifford
52. M. L. Nelson
53. G. H. Clewett
54. C. P. Keim
55. O. Sisman
56. A. D. Callihan
57. R. S. Livingston
58. W. D. Manly
59. J. L. Meem
60. C. D. Susano
61. W. B. Cottrell
62. A. S. Kitzes
63-72. ANP Library
73-78. Central Files (O.P.)

EXTERNAL DISTRIBUTION

79-83. Air Force Engineering Office, Oak Ridge
84-95. Argonne National Laboratory
96-103. Atomic Energy Commission, Washington
104. Atomic Energy Commission, Wilmington
105. Battelle Memorial Institute
106-109. Brookhaven National Laboratory
110. Bureau of Aeronautics
111. Bureau of Ships
112-117. Carbide and Carbon Chemicals Division (Y-12)
118. Chicago Patent Group
119. Chief of Naval Research
120-123. Du Pont Company
124-127. General Electric Company, Richland
128. Hanford Operations Office
129-132. Idaho Operations Office
133. Iowa State College
134-137. Knolls Atomic Power Laboratory
138-140. Los Alamos
141. Massachusetts Institute of Technology (Kaufmann)
142-143. National Advisory Committee for Aeronautics, Cleveland
144. National Advisory Committee for Aeronautics, Washington
145-163. NEPA Project
164. New Operations Office
165-166. New York Operations Office
167-169. North American Aviation, Inc.
170. Office of Naval Research
171. Patent Branch, Washington
172-186. Technical Information Service, Oak Ridge
187-188. University of California Radiation Laboratory
189-192. Westinghouse Electric Corporation

S[redacted]

TABLE OF CONTENTS

[redacted]

SE[redacted]

TABLE OF CONTENTS (Cont'd)

[redacted]

[redacted]

TABLE OF CONTENTS (Cont'd)

[redacted]

TABLE OF CONTENTS (Cont'd)

[redacted]

TABLE OF CONTENTS (Cont'd)

[redacted]

LIST OF FIGURES

[redacted]

SUMMARY

The Aircraft Nuclear Propulsion Project at the Oak Ridge National Laboratory has expanded considerably during the past quarter. There are now 236 technical people engaged in all phases of the research work. Thirteen divisions of the Laboratory are represented on this Project.

Design of the Aircraft Reactor Experiment (ARE) is continuing, with particular emphasis on shielding, control, and fuel material. The NEPA Division, Fairchild Engine and Aircraft Corporation, has loaned 14 men to assist in the design and construction of the ARE.

Three major facilities have been completed: the Shielding Reactor, the ANP Critical Facility, and the 86-in. cyclotron, which will be used part-time for radiation damage studies. Also, work has begun on increasing the power level of the MTR mock-up so that it may serve as a Low Intensity Training Reactor (LITR) and may also be used part-time for radiation damage studies.

ANP SHIELDING BOARD

One of the major activities of the members of the ANP Project at the Laboratory this quarter was the work on the joint ORNL-NEPA Shielding Board. During the summer the ANP Technical Advisory Board was able to carry shielding analysis only through the stage of the idealized shield which contains no ducts, pumps, heat exchangers, structural elements, or other mechanical arrangements. The ANP Shielding Board was assembled and asked to carry the work through the next stage and to estimate minimum weights for fully engineered shields containing all the necessary mechanical features. The work of this Board culminated in the publication of a summary report of 215 pages, ANP-53, on Oct. 16, 1950. The following quotation from this report lists its conclusions on shield weights:

> "Weights quoted in this section include all shields, structure within shields, reactor, reflector, ducts, pumps, and heat exchangers.
>
> 1. The weight of a divided shield for the assumed standard conditions (3.0-ft-diameter right circular cylindrical reactor core, 200,000 kw output, sodium in both primary and secondary coolant circuits, and 1 r/hr at the crew compartment) was estimated to be 98,000 lb.

[redacted]

2. The weight of one possible unit shield was found to be over 200,000 lb for the same conditions as above, but with the additional ground tolerance requirement that the radiation at the surface of the shield not exceed 0.8 r in the first 8 hr after shutdown. This latter requirement nearly doubled the weight of the shield because of the necessity of keeping the sodium in the secondary circuit from becoming radioactive.

3. Substantial savings in shield weight can be effected both by rounding the corners of the square cylindrical core and by reducing the core diameter. Further savings can be effected through the use of coolants less inclined to become radioactive with such an inconvenient half-life as that of sodium (14.8 hr). Estimated weights for two representative cases are as follows:

   a. A 30-in.-diameter reactor core with ellipsoidal ends and Li^7 and Li as coolants gave a unit shield weight of 116,000 lb. For the same conditions but a 36-in.-diameter core the shield weight was found to be 122,000 lb.

   b. A 30-in.-diameter reactor core with rounded ends and lead or bismuth as the primary coolant gave a unit shield weight of 105,000 lb.

4. The weight of a unit shield for a circulating-fuel reactor not having a large amount of sodium in the primary circuit would probably not be much greater than that for the Li^7-Li case cited above unless — as seems likely — the heat exchanger volume must be increased because of a lower heat transfer coefficient for the fused salt carrying the fuel. If sodium hydroxide were used in the primary circuit, a shield weight increase of the order of 25,000 lb would be required to satisfy the ground tolerance condition. In any case, sodium could not be used in the secondary circuit with any circulating-fuel reactor because of activation from delayed neutrons in the intermediate exchanger.

5. If the ground tolerance for the Na-Na cooled reactor is relaxed to 1 r/hr at the shield surface 15 min after shutdown, the unit shield weight for a 30-in.-diameter core with ellipsoidal ends is estimated to be 148,000 lb.

6. A divided shield near to the lower limit in weight has been designed using somewhat relaxed design specifications. For a 2.5-ft-square cylindrical reactor, 65 ft separation, 150 mw power, 3 to 4 man crew compartment, Li^7-Li system, the total weight was 66,450 lb."

For shields which are similar to ideal shields the principal sources of uncertainty in these quoted weights are in the accuracy of each of the following: (1) the Lid Tank detector calibration (since the Lid Tank measurements form the basis for the computed weights), (2) the effective cross section for boron, (3) the capture gamma-ray intensity from structural metals, and (4) the effective oxygen scattering cross section. For shields with large deviations from the ideal shape, such as a unit shield for a Na-Na system, geometrical factors become the largest source of uncertainty. Shielding Reactor measurements are required to remove this uncertainty. For systems using sodium as a secondary coolant, the effective activation cross section of sodium is another major uncertainty. All these points of uncertainty will be attacked experimentally in the near future. It is to be noted that all the above calculations are based on Lid Tank measurements with lead and borated water. There is some theoretical evidence that no other materials will be found to give weights which are significantly smaller. Other materials, however, will soon be checked by Lid Tank measurements.

ANP CONTROL BOARD

A parallel effort to the ANP Shielding Board was the work on the joint ORNL-NEPA Control Board.[1] This group studied the control properties of the solid-fuel aircraft reactor design developed by Oak Ridge National Laboratory which has been described in previous reports.[2] The Control Board found that although this solid-fuel reactor would have a negative short-time coefficient of reactivity owing to temperature changes of the fuel elements alone, it would have a positive temperature coefficient of reactivity over time intervals of 10 sec or longer owing to temperature changes in the moderator. The Control Board also believed that this reactor would require 10 or more absorber control rods. The mechanical actuation system and the heat-removal system would be somewhat complex. Subsequent reactivity calculations, as described in the Reactor Physics section of this report, have shown that the positive temperature coefficient difficulties can be greatly diminished by a decrease in the fraction of moderator in the core so as to raise the mean energy for fission. However, it is clear that the control of a solid-fuel high-temperature reactor will not be simple.

(1) *Interim Report of the ANP Control Board,* NEPA-ORNL, ANP-54, (Nov. 1, 1950).

(2) *Aircraft Nuclear Propulsion Project Quarterly Progress Report for Period Ending August 31, 1950,* ORNL-858 (Dec. 4, 1950); *Preliminary Feasibility Report for the Aircraft Reactor Experiment,* Oak Ridge National Laboratory, Y-12 Site, Y-F5-15, (July 4, 1950).

ARE DESIGN

Largely as a result of the above findings of the ANP Control Board, a decision was made to suspend work temporarily on the solid-fuel ARE design, while attempting to develop a suitable liquid-fuel arrangement. It is to be expected that a "stationary" liquid-fuel system can be designed which will be almost self-regulating, and which will require only one or two control rods. The self-regulating feature will arise from the strong negative temperature coefficient of reactivity since increases in reactor temperature will expand the fuel-bearing liquid and force some of the uranium outside the active core, thus leading to a compensating decrease in power. The most promising fuel mixture to date is a solution of UF_4 in NaF, with possible admixtures of other fluorides to lower the melting point to a convenient range. Design is now underway on such a liquid-fuel aircraft reactor and ARE prototype and, as described in this report, research is also in progress on the properties of other possible fuel liquids.

STUDIES ON ALTERNATIVE LINES

In addition to design and research toward a "stationary" liquid-fuel liquid-metal-cooled aircraft reactor and ARE, a certain amount of work is being continued by the Laboratory on various alternative lines which show promise for future aircraft reactors. These studies are described in Part II of this report. They include:

1. Calculations on vapor-cycle systems by North American Aviation, Inc., together with research on the corrosive effects of Na vapor.
2. A complete design study including reactor, engine, and aircraft analysis for a nuclear XB-52 plane powered by a circulating-fuel reactor based on a suspension of uranium-bearing particles in NaOH, carried out by the H. K. Ferguson Company.
3. A detailed analysis of the supercritical water-cooled reactor by Nuclear Development Associates, Inc.
4. Research on the most economical method of separating the isotope Li^7 in quantity for possible use as a high-performance coolant.
5. Studies on the Supersonic Tug-Tow system.

SUMMARY OF RESEARCH RESULTS

From the body of research now underway on all the problems mentioned above, some of the other tangible results obtained during the last quarter are listed below:

Physics

1. The Reactor Physics Group has performed extensive computations of criticality and thermal xenon coefficients in bare reactors, and similar calculations for reflected reactors are in progress. Graphs of the spectra of several solid-fuel reactors are included. The determination of the kinetic response of some liquid-fuel stationary-moderator reactor designs has been begun.

2. For the Na—BeO—stainless steel reactors studied, having moderator volume fractions lying in the range 40 to 70%, the following points are clear:

   a. The temperature coefficient of reactivity with solid fuel decreases rapidly as the mean energy of fission of the reactor is increased by cutting out moderator. With a moderator volume fraction less than about 60%, the temperature coefficient of the solid-fuel reactor becomes negative.

   b. The reactivity effect due to thermal expansion of the moderator amounts to 1 to 3% in k in going from 183 to 1286°F.

   c. The reactivity effect due to maximum transient xenon decreases from 11% for the near thermal reactor to less than the equilibrium xenon when the mean energy of fission is raised to 100 ev.

   d. For a core containing 52% moderator, using a 6.5-in. reflector which was made of 75% BeO, the reflector savings came out about equal to the reflector thickness.

3. A preliminary analysis of the fuel kinetics of the $NaF\text{-}UF_4$ reactor shows the existence of oscillation in the reactor power following a change in reactivity, which arises from the coupling between fuel displacement and neutron flux. However, this oscillation damps out in a few seconds, and in any event the preliminary result was obtained without taking account of delayed neutrons. In a more exact calculation which is to follow, any power oscillations are expected to be negligible.

4. A resonance at approximately 49 ev was found from the preliminary neutron cross-section measurements on molybdenum at Columbia.

5. Nuclear Development Associates, Inc. have computed, as a function of temperature, both the xenon cross section averaged over a Maxwellian distribution and the temperature derivative of this quantity.

6. Preliminary studies show that it should be possible to prepare a 1000-curie source of Xe^{135} if a measurement of the intermediate xenon cross section proves advisable. The most efficient source for preparing such a quantity of Xe^{135} would probably be the Homogeneous Reactor Experiment.

Shielding

7. Since the close of the ANP Shielding Board, a new divided shield for a Na-Na reactor with 30-in. rounded-end core has been computed to weigh 127,000 lb if the ground radiation condition is made to be 1 r/hr at a point 50 ft from the reactor with the latter operating at one-tenth power. Thus, for a moderate increase in weight over the purely air-safe divided shields of the Shielding Board, one might gain the ability to inspect the aircraft engines, operating one at a time, without special ground shielding.

8. A Lid Tank test of a shield proposed by the ANP Technical Advisory Board has been completed. The design consisted simply of 55 cm of iron next to the core, followed by 35 cm of borated water. The results show this arrangement to be impractical, since intermediate-energy neutrons penetrate the iron to such an extent that their capture gammas cannot be suppressed in the water.

9. Preliminary results are listed on Lid Tank measurements of neutron and gamma attenuation in slabs of solid B_4C followed by borated water. First analysis of the data indicates a relaxation length of 6.2 cm for B_4C of theoretical density, 2.5 g/cc. However, more precise determinations are in progress.

10. A sulfur threshold detector has been put into use in the Lid Tank for measurement of fast-neutron intensity. The effective threshold of this instrument is about 3 Mev.

11. Analysis of recently published Pb-H_2O and Fe-H_2O measurements in the Lid Tank indicates effective neutron absorption cross sections for these experiments of 3.4 barns for Pb and 2.0 barns for Fe.

Heat Transfer

12. Theoretical analyses of heat transfer have been completed on three situations which approximate the entrance conditions involved in current ARE core designs. Heat transfer within a wide range of duct shapes has been analyzed.

13. Equipment has been designed for the measurement of thermal conductivity, specific heat, and other high-temperature properties of various liquid metals and molten salts. The specific heat of lithium between 550 and 900°C has been measured as 1.0 ± 10%.

14. Both a type 316 and type 347 stainless steel convection harp containing liquid sodium have now been operated almost 800 hr at 1500°F without failure.

Metallurgy

15. Static corrosion measurements have been made on numerous materials in Pb at 1800°F. Tungsten and Armco iron showed no evidence of any attack; Cb, Mo, Ta, Ni, Be, Zr, and several stainless steels are attacked in varying degrees; 18-8 molybdenum type alloy shows encouraging preliminary results.

16. The attack on stainless steels by Li at 1800°F is found to be largely intergranular in nature with a considerable amount of decarburization and phase transformation in some cases.

17. Substances so far found to have good resistance to Na at 1800°F include types 316 and 347 stainless steel and Ni. Fair resistance under these conditions is shown by Co, Mo, Ta, Alloy N-155, Inconel, and Inconel X.

18. Molten U-Al alloy has been suggested as a possible liquid fuel. Materials to contain this liquid at 1800°F have not yet been found. Ti, Fe, Zr, Co, and Mo are severely attacked.

19. Preliminary tests at 2000°F for 100 hr on the compatibility of materials suggested for fuel elements show moderate reactions occurring between type 316 stainless steel and both UO_2 and Mo.

20. Between type 316 stainless steel and Be, in the above circumstances, there was a strong reaction. With BeO and 316 stainless steel no reaction was observed.

Radiation Damage

21. Radiation damage experiments on various metals exposed to a neutron flux of 1.2×10^{12} at 500°F and 1000 psi pressure for as much as four months have shown no significant changes in shape, electrical resistivity, permeability, or hardness of the metals.

22. A creep test is now underway on type 316 stainless steel in the Oak Ridge reactor at 1050°F under a stress of 4000 psi. Preliminary results show at least a transient increase in creep rate under these conditions, although possible spurious effects caused by gamma and neutron heating of the specimen have not yet been excluded.

Liquid Fuels

23. Attempts have been made to find a liquid fuel consisting of a uranium compound dissolved or suspended in NaOH. All uranium materials tested to date have been found to react rapidly with NaOH to form a finely divided compound which is probably sodium uranate. The possibility of developing stable suspensions in this system is being studied.

24. The equilibrium diagram of the molten salt system $LiF-UF_4$ has been established, and study of such systems as $NaF-KF-UF_4$ is underway.

25. Preliminary corrosion studies of numerous metals in $NaF-UF_4$ at 1300°F for 160 hr show hastelloy C, Inconel, and Mo to be the least attacked.

Alternative Systems

26. Neither the helium turbojet system nor the two mercury vapor compressor-jet systems so far studied by North American Aviation, Inc. looks desirable for use in nuclear aircraft. However, the sodium vapor compressor-jet system still shows great promise if high reactor temperatures can be attained.

27. Corrosion tests of samples in sodium vapor at 1650°F for 20 hr show no attack on type 316 stainless steel or on AWG graphite. These experiments will be carried to higher temperatures.

28. Nuclear Development Associates, Inc. has pointed out that estimates contained in the Lexington report indicate the possibility of a reactor shield for the tug-tow system weighing no more than about 15,000 lb. Such a weight, if substantiated, would permit the use of extremely small, easily built aircraft.

29. With the 48-compartment electroexchanger for separating Li isotopes, samples of 94.5% Li^7 have been obtained. A separation factor of approximately 1.05 per stage is found. Large-scale production appears to be feasible if this material turns out to be really needed. The principal economic factors which are still under study are the large power costs and the very large quantities of mercury which would be required with the present arrangement.

Part I

RESEARCH CONTRIBUTING TO THE ARE

1. DESIGN OF THE AIRCRAFT REACTOR EXPERIMENT

1. DESIGN OF THE AIRCRAFT REACTOR EXPERIMENT

R. C. Briant R. W. Schroeder
A. P. Fraas J. H. Wyld
ANP Division

The reactor designs now being studied for possible use in the Aircraft Reactor Experiment all involve some arrangement of a quiescent liquid fuel and the use of liquid sodium as both the primary and secondary coolant. Five such core designs are presented. The coolant circuit specifications which have been adopted are discussed.

Core Design. Several core designs utilizing a quiescent liquid fuel are being considered for possible use in the Aircraft Reactor Experiment. The liquid which is believed most likely to serve for this purpose is a solution of UF_4 in NaF, with the probable addition of one or more other fluorides to reduce the melting point of the solution. The simplest method of containing the liquid fuel appears to be in tubes. The fuel-container wall thickness should be kept down to the order of 0.010 in. so as to minimize the uranium inventory necessary to overcome neutron absorption in the container metal. The combined effects of changes in thermal gradients and pressure gradients under transient conditions would probably be serious for any container shape other than a round tube.

A number of different types of construction have been proposed. The five designs shown in Figs. 1.1 to 1.8 are representative of the more promising of these proposals. The major features of these may be sketched as follows:

1. Helical coil arrangement, Figs. 1.1 and 1.2. This design contains fuel inside tubing which is wound in helical form between cylindrical shells of moderator. The arrangement permits the use of long fuel containers, thereby minimizing the number of welds required.

2. Hairpin ("U") tube fuel-element design, Figs. 1.3 and 1.4. This configuration features about 12,000 closely spaced U-tube fuel elements, with inlet and outlet headers both located at the top of the reactor for convenience of access and to simplify thermal expansion problems. Any desired degree of compartmentalization may be achieved by dividing the headers.

3. Parallel-tube fuel-element design, Fig. 1.5. This arrangement is essentially the same as the U-tube type except that the tubes

are interconnected by headers at both top and bottom to facilitate filling and draining.

4. Annular fuel-tube arrangement, Fig. 1.6. This design consists of moderator cylinders surrounded successively by coolant annuli, fuel annuli, and coolant annuli. Approximately three hundred such concentric elements are housed in a moderator matrix.

5. Individual fuel-pin arrangement, Figs. 1.7 and 1.8. In this case the fuel is contained in individual noninterconnected tubes with void volumes provided for fuel expansion and fission product gas accumulation. The design has the disadvantage that the fuel could not be drained from the core and replaced by means of a purely liquid-flow operation.

The first three of these are similar in that they all involve about 30,000 ft of 0.100-in.-O.D., 0.080-in.-I.D. tubing. The fourth type, having the fuel in the annulus between concentric tubes, requires less total footage of tubing but presents a more complex set of fabrication problems.

In comparing these various designs, the fuel element itself is, of course, the item requiring the most study. The nature of the heat transfer through the liquid fuel to the tube wall presents a major question. As many pieces of data as possible have been assembled on the physical properties of substances which might be involved in this problem, and these are shown in Tables 1.1 and 1.2 and Fig. 1.9. When necessary, thermal conductivities have been calculated by Bridgmann's formula for nonmetallic liquids [*Proc. Natl. Acad. Sci.*, **9**, 341 (1923)]; specific heats have been calculated by Kopp's rule [Lange, N. A., *Handbook of Chemistry*, 7th ed, Handbook Publishers, Sandusky, Ohio (1949)].

The temperature drop in the liquid-fuel tube from the center to the wall is very high if computed on the basis that thermal conduction is the sole heat transfer mechanism. However, the effects of thermal convection and of any change in the properties of the liquid due to radiation would be expected to reduce this temperature differential. In any case, the coolant tubes will have to be rather small to minimize trouble from this source.

It is expected that the core diameter will fall between 30 and 36 in. and the volume percentage of moderator between 50 and 60%. The core shape will be a right circular cylinder with the corners rounded off to give ellipsoidal ends.

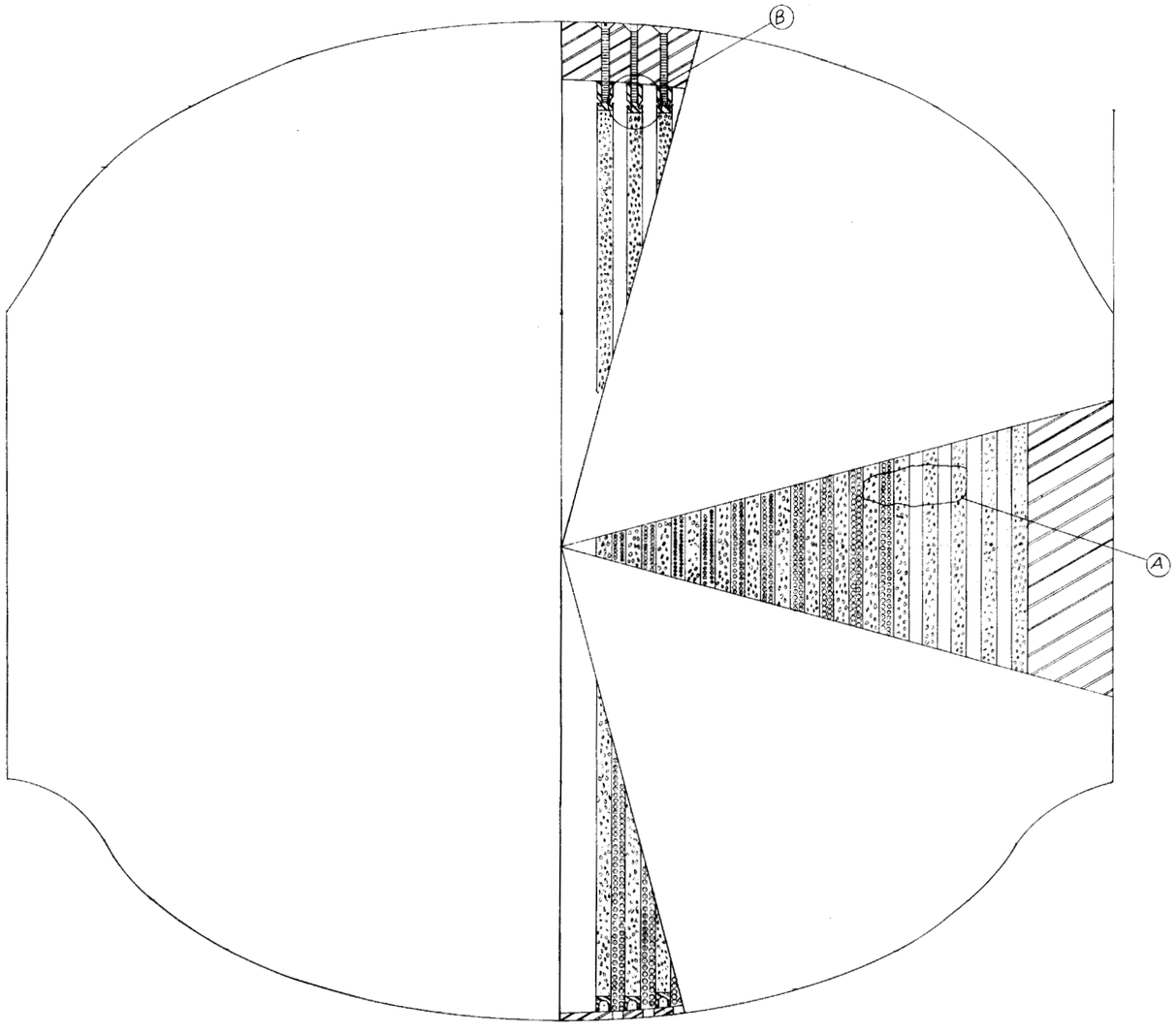

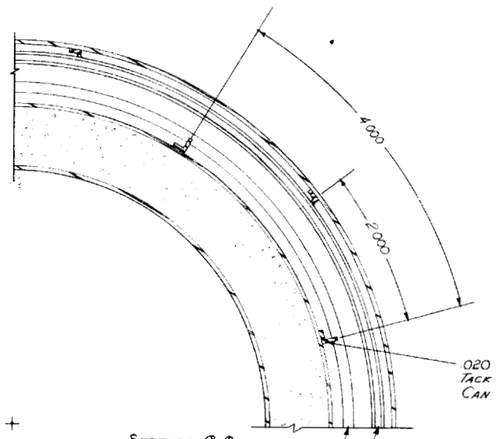

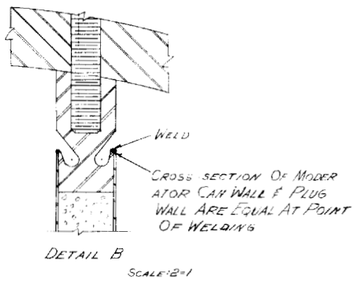

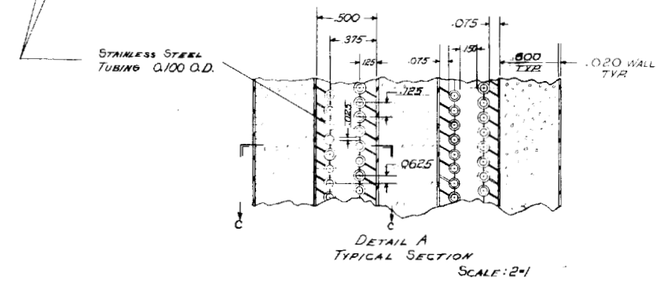

DRAWING NO. Y-F7-31 [redacted]

FIGURE 1.1 HELICAL COIL ARRANGEMENT (Reactor Core)

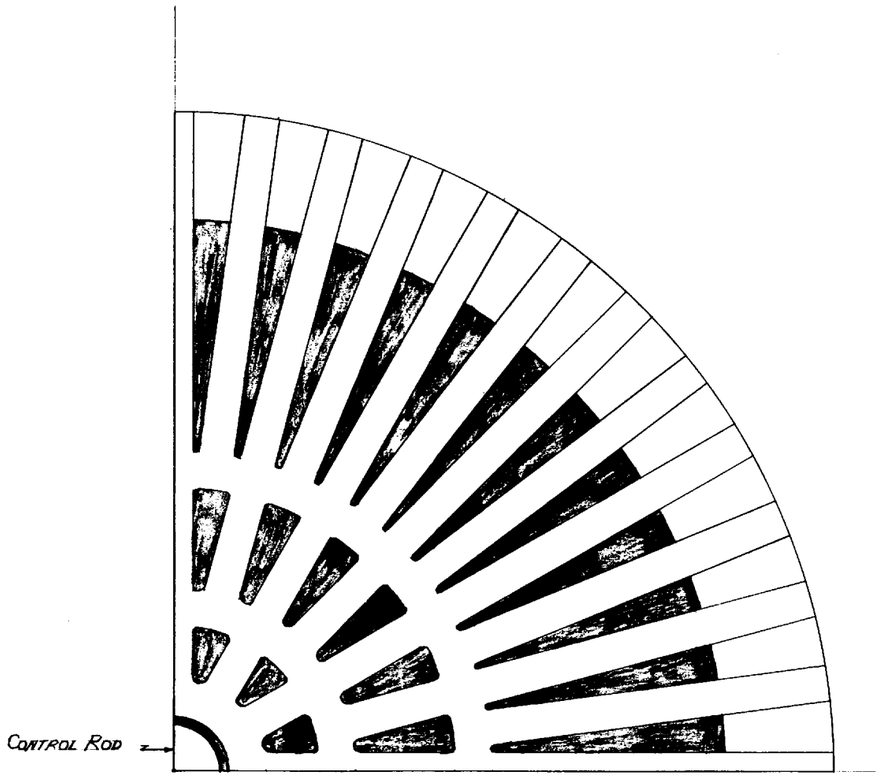

SECTION A-A

PLAN VIEW OF RIB TYPE DOME

NA FLOW PASSES IN RED

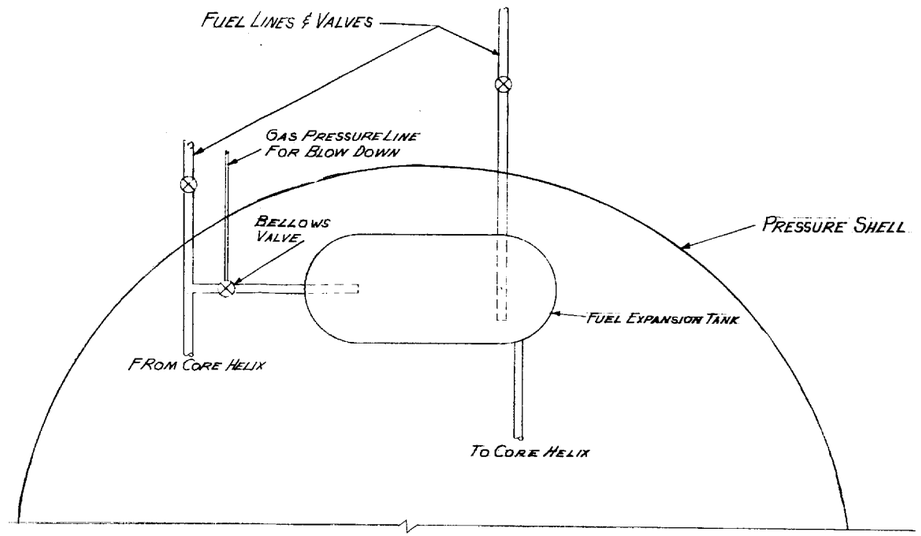

TYPICAL FUEL FLOW DIAGRAM

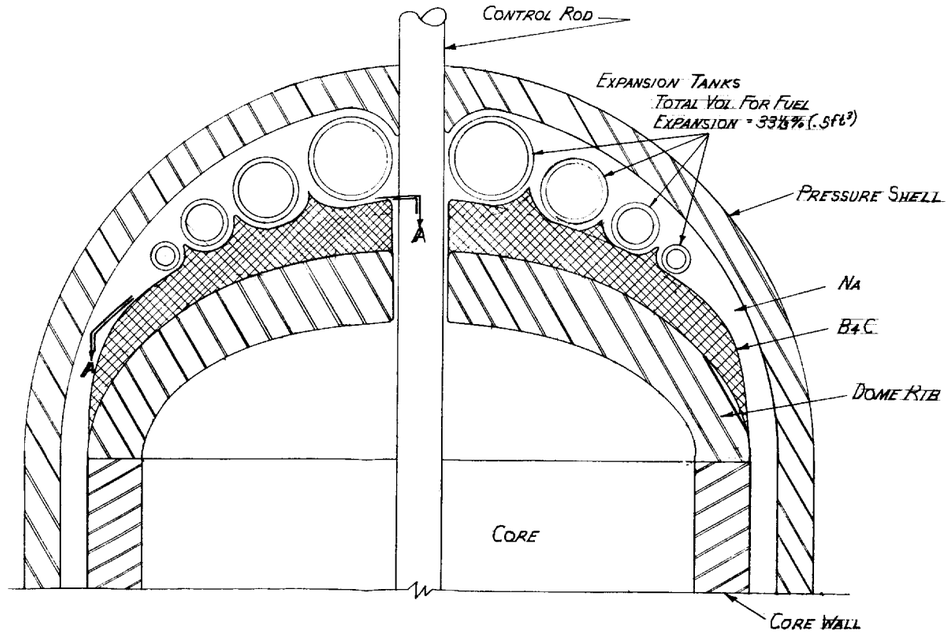

DRAWING NO. Y-F7-32

FIGURE 1.2 HELICAL COIL ARRANGEMENT (Dome & Fuel Tanks)

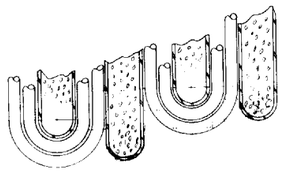

DETAIL B
TYPICAL SECTION

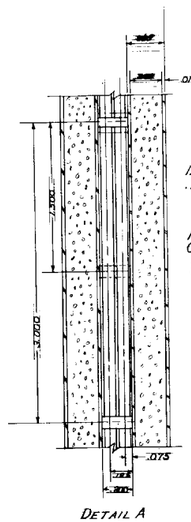

INCONEL 'X' TUBING
.125 O.D. · 0.95 I.D.

INCONEL 'X' MODERATOR
CAN WALL .010 THICK
THIN SODIUM FILM BETWEEN
CAN WALL & MODERATOR BLOCKS

DETAIL A
TYPICAL SECTION
SCALE 2=1

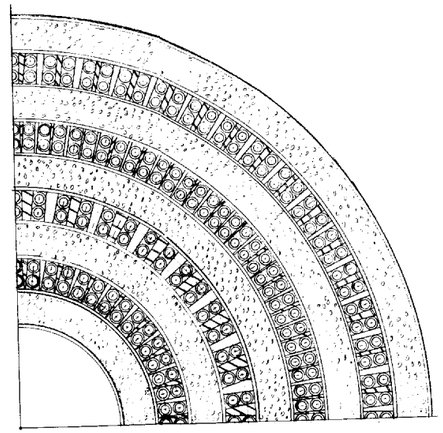

SECTION C-C

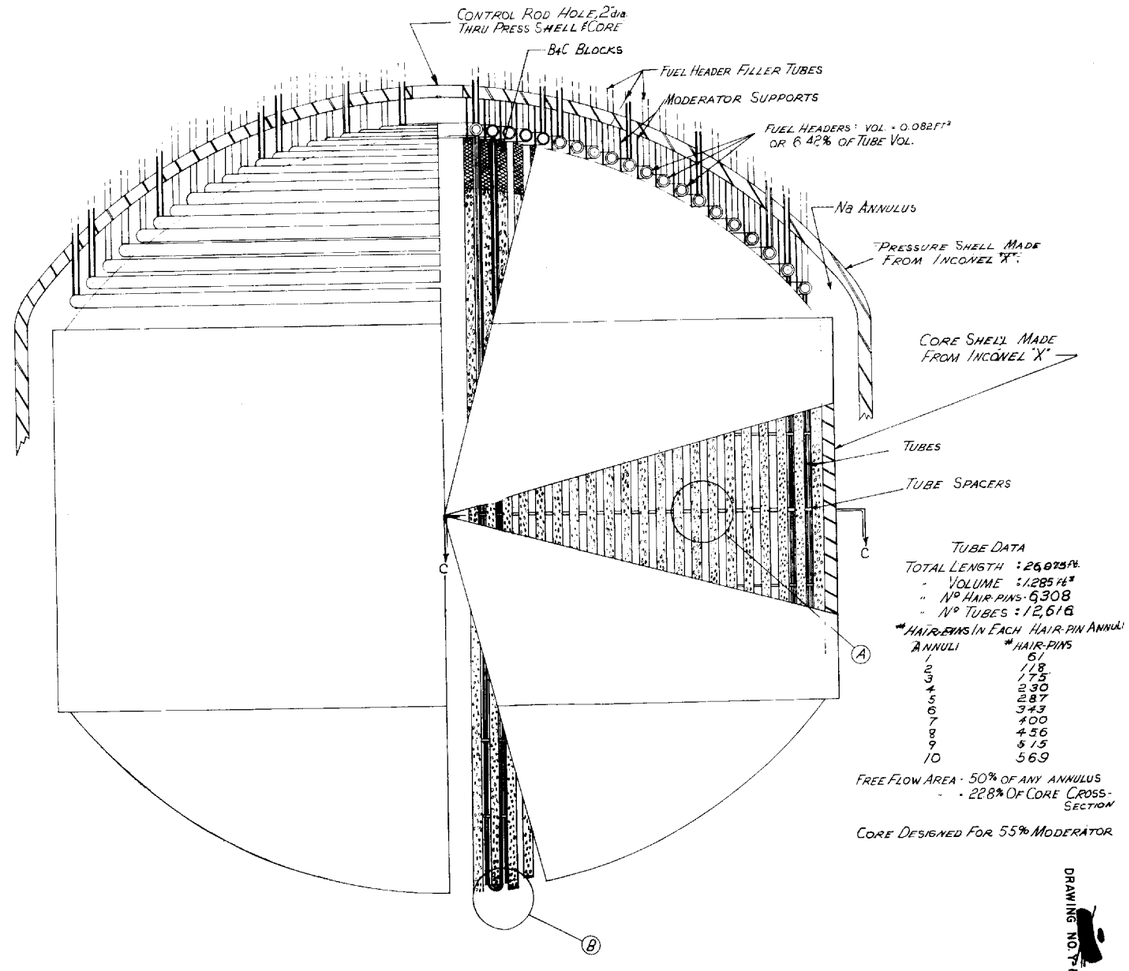

TUBE DATA
TOTAL LENGTH : 26.075 Ft.
" VOLUME : 1.285 Ft³
" Nº HAIR-PINS : 6308
" Nº TUBES : 12,616

HAIR-PINS IN EACH HAIR-PIN ANNULI

ANNULI	# HAIR-PINS
1	61
2	118
3	175
4	230
5	287
6	343
7	400
8	456
9	515
10	569

FREE FLOW AREA · 50% OF ANY ANNULUS
" · 228% OF CORE CROSS-SECTION

CORE DESIGNED FOR 55% MODERATOR

DRAWING NO. PF7-35

FIGURE 1.3 HAIR-PIN ("U") TUBE FUEL ELEMENT DESIGN (Reactor Core)

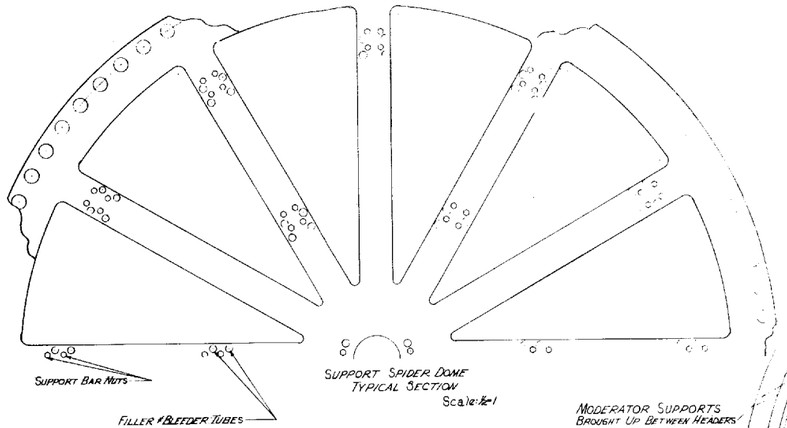

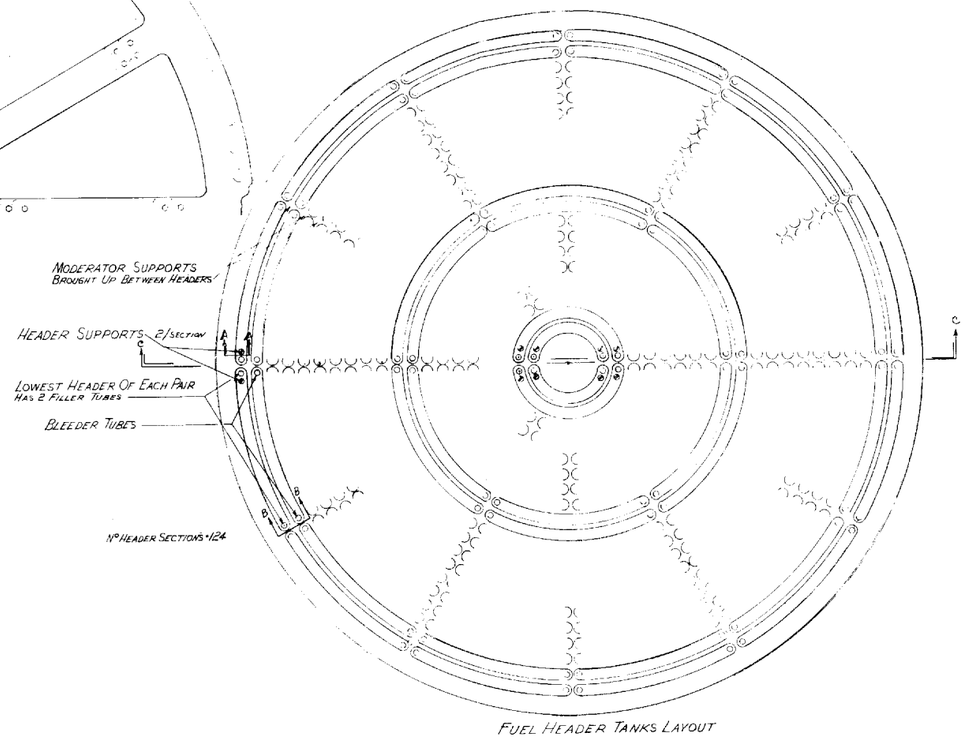

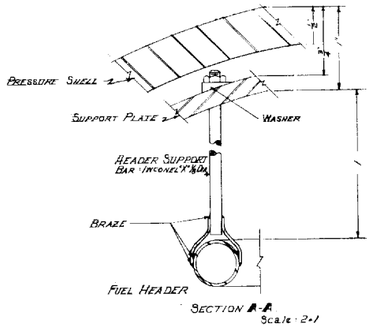

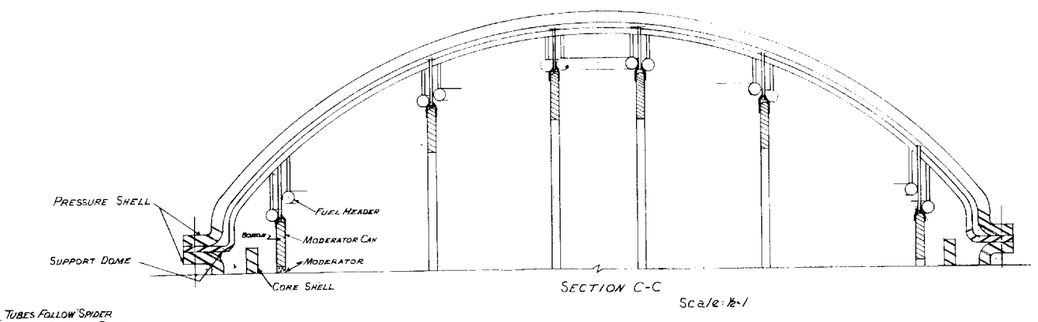

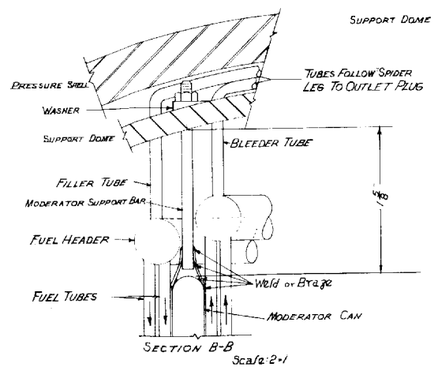

DRAWING NO. Y-F7-38

FIGURE 1.4 HAIR PIN (U) TUBE FUEL ELEMENT DESIGN (Support Details)

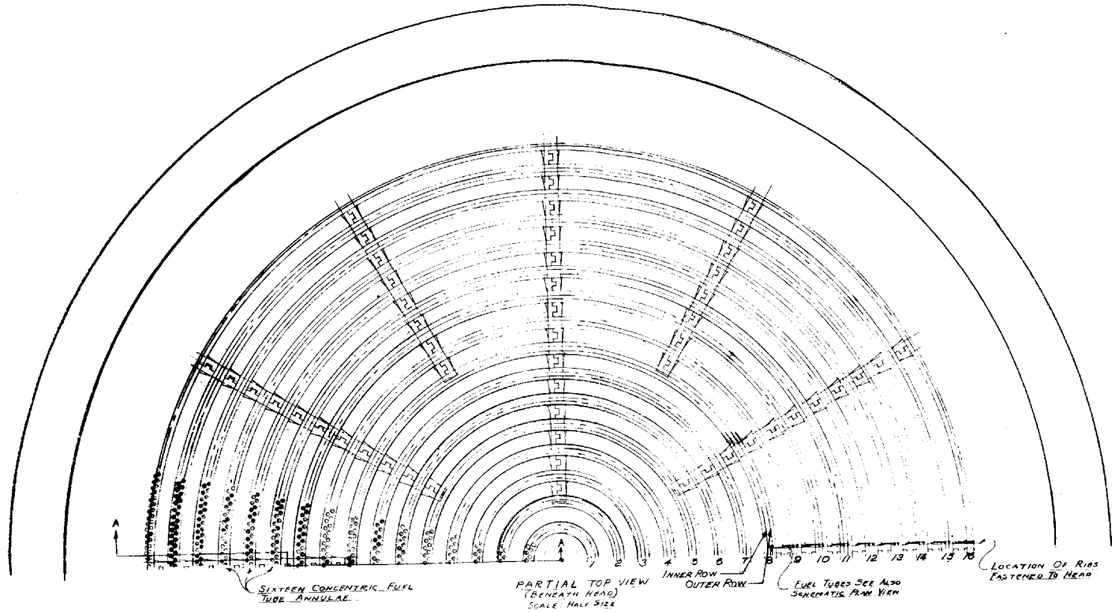

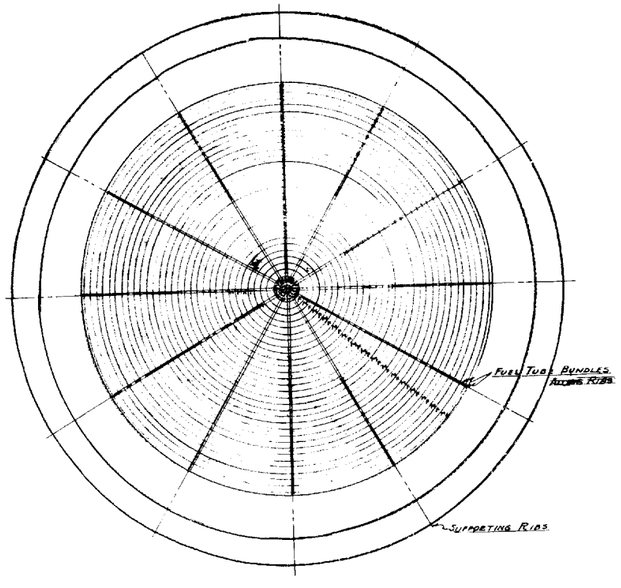

Schematic Plan View
Scale: Quarter Size

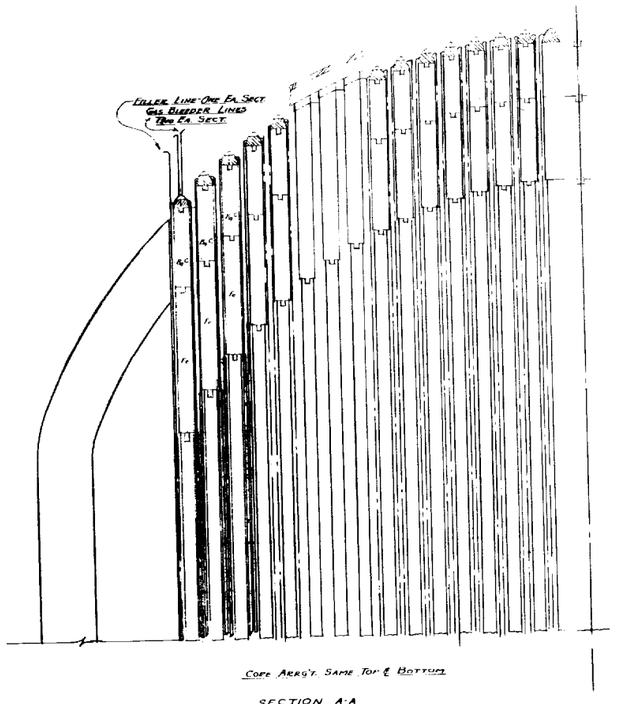

Section Alizing Table				
Row		Row		Sections
1	Inner			1
1	Outer	2	Inner	2
2	"	3	"	3
3	"	4	"	3
4	"	5	"	3
5	"	6	"	6
6	"	7	"	6
7	"	8	"	6
8	"	9	"	12
9	"	10	"	12
10	"	11	"	12
11	"	12	"	12
12	"	13	"	12
13	"	14	"	12
14	"	15	"	12
15	"	16	"	12

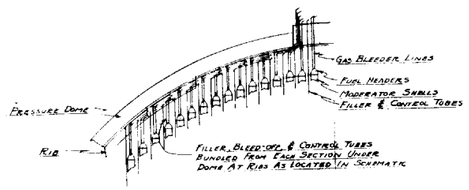

Partial Tube Schematic
Scale Quarter Size

FIGURE 1.5 PARALLEL TUBE FUEL ELEMENT DESIGN (General Arrangement)

DRAWING NO. Y-F7-33

[redacted]

DRAWING NO. YF7-28

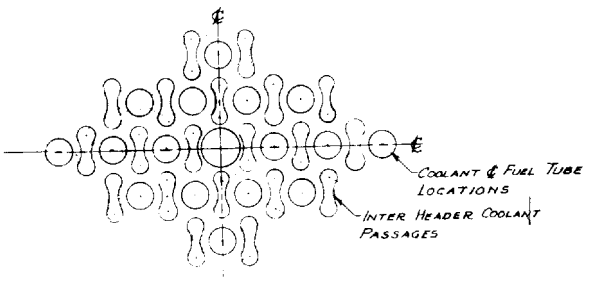

PORTION OF TOP
SHOWING ROD CONFIGURATION

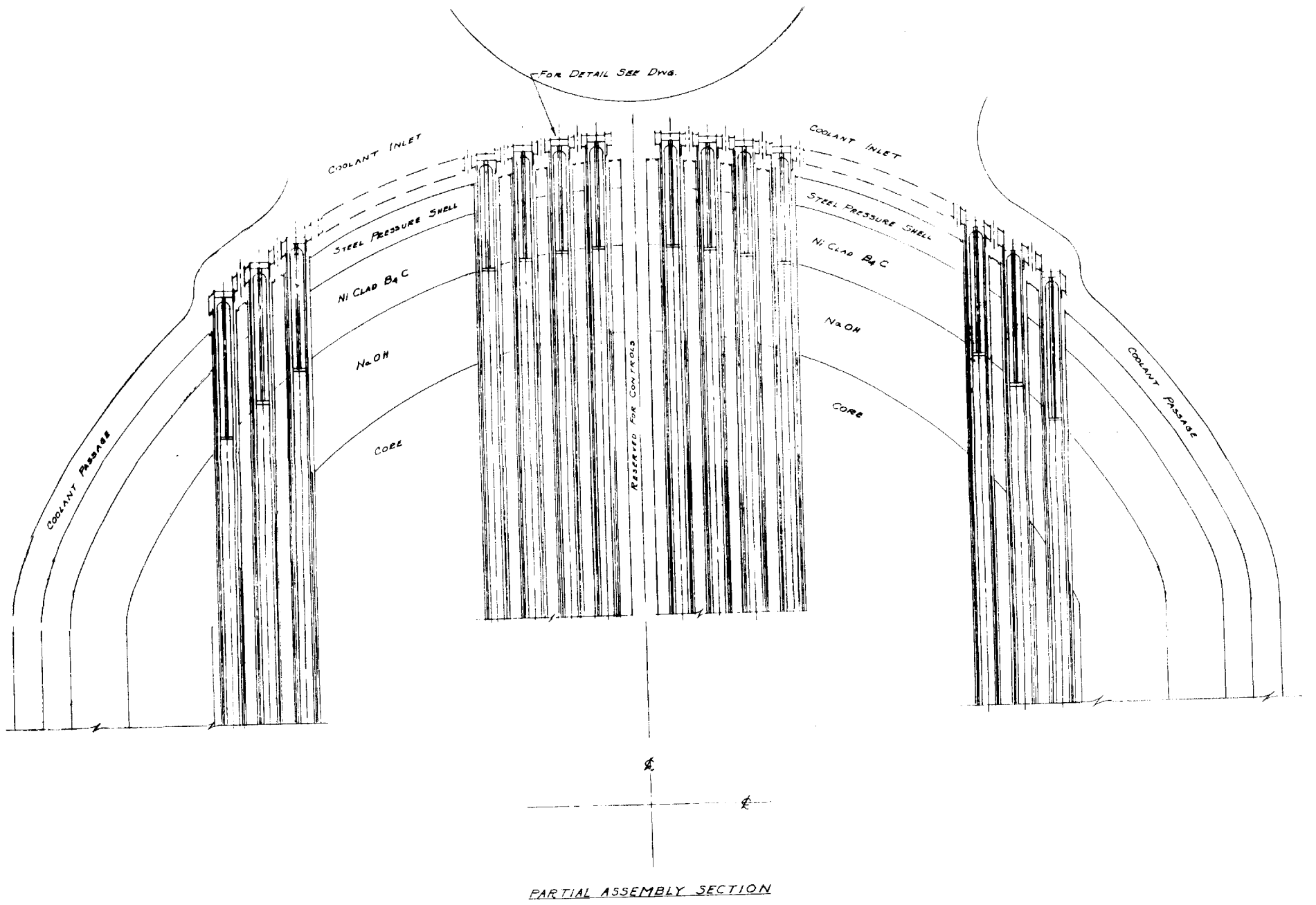

PARTIAL ASSEMBLY SECTION

FIGURE 1.6 ANNULAR FUEL TUBE ARRANGEMENT (General Assembly)

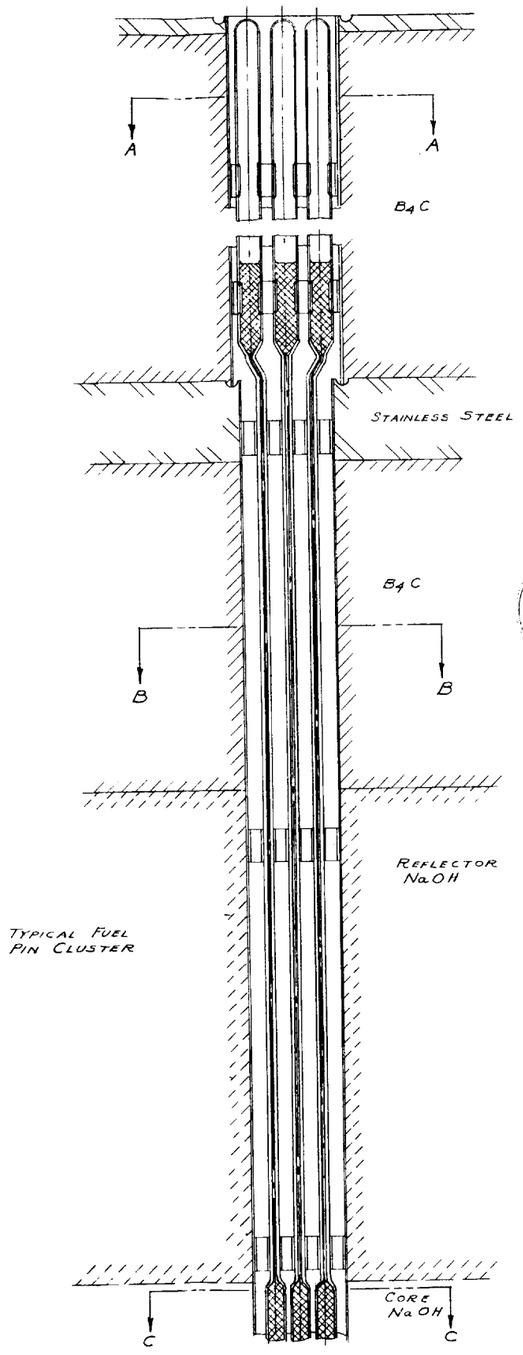

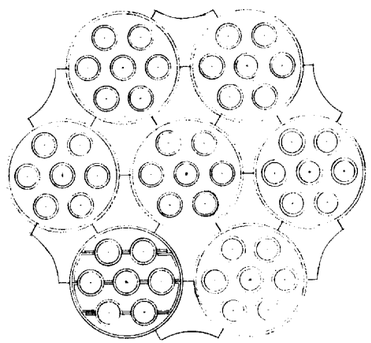

SECTION A-A

SECTION B-B

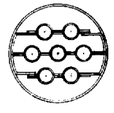

SECTION C-C

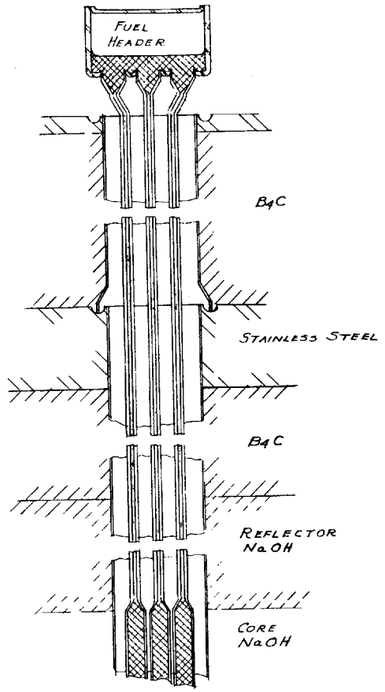

TYPICAL FUEL PIN
CLUSTER
(AT FUEL HEADER)

FIGURE 1.7 FUEL PIN ARRANGEMENT
(Typical Pin Assembly)

DRAWING NO. Y-F7-30

DRAWING NO. YF7-29

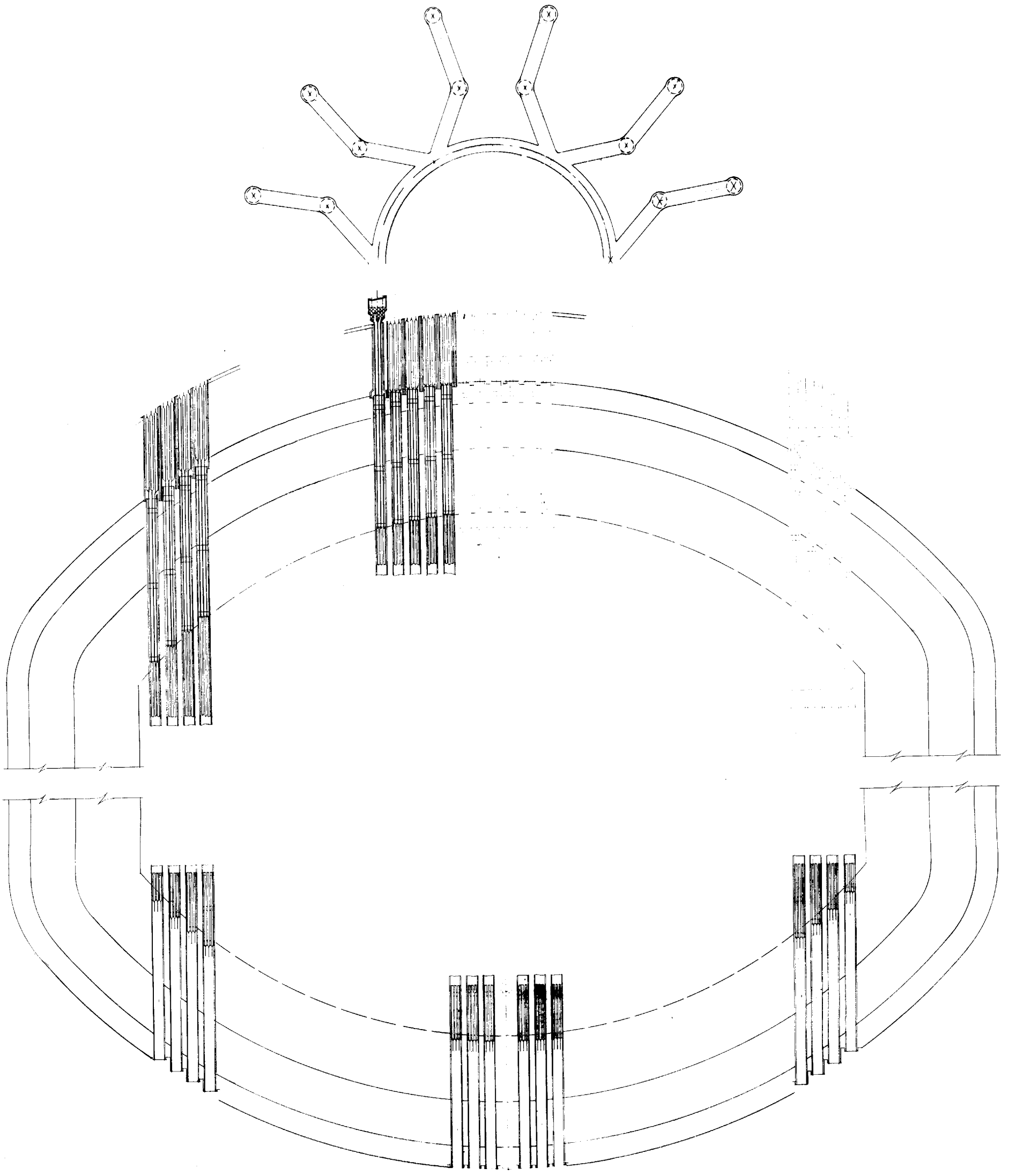

FIGURE 1.8 INDIVIDUAL FUEL PIN ARRANGEMENT (General Assembly)

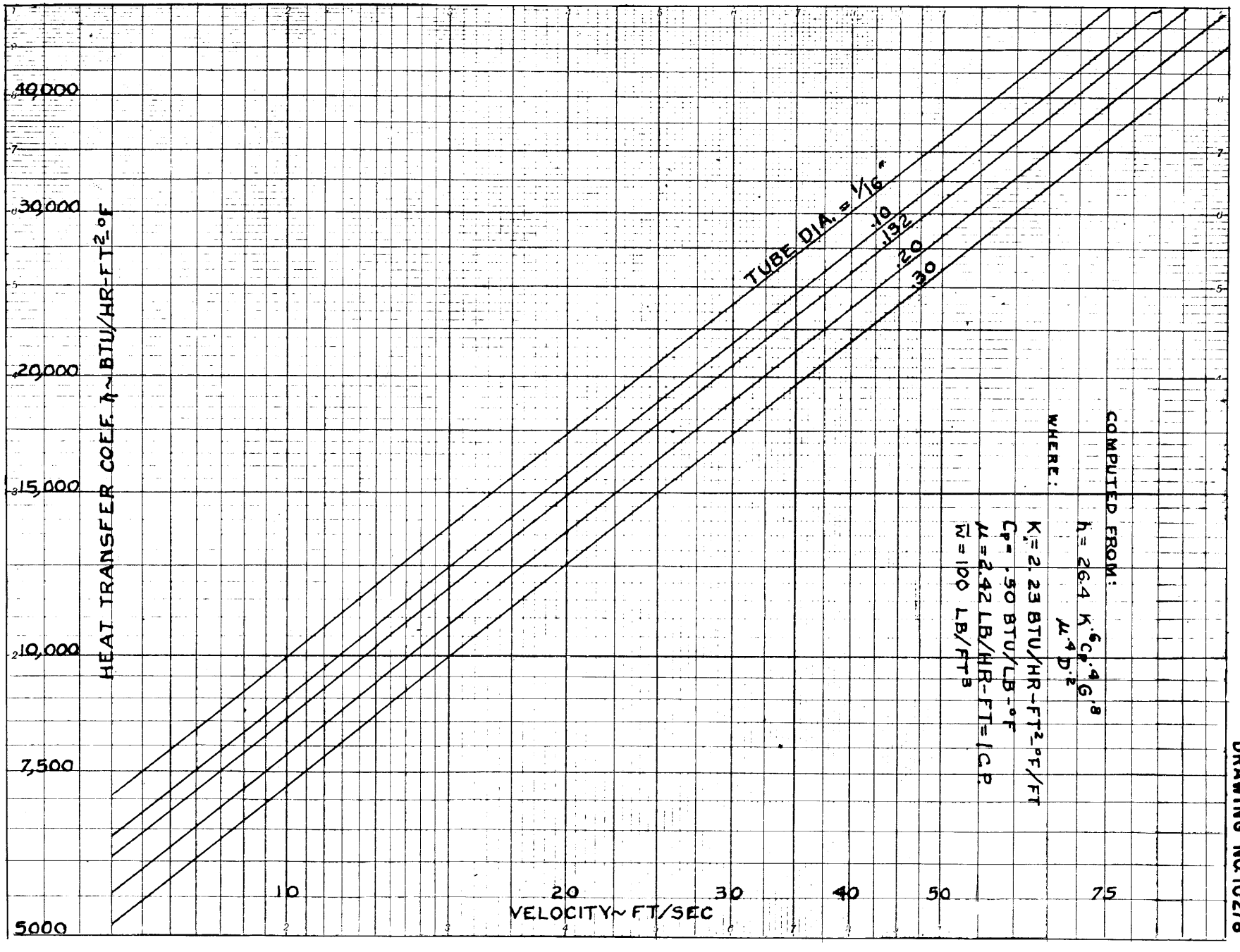

FIGURE 1.9 HEAT TRANSFER COEFFICIENT FOR NaOH AT 1350°

UNCLASSIFIED
DRAWING NO. 10278

TABLE 1.2

Physical Data of Fluorides in the Fused State

FORMULA	M.P. (°C)	B.P. (°C)	SPECIFIC GRAVITY	SPECIFIC HEAT* (Btu/lb °F)	VISCOSITY (centipoises)	THERMAL CONDUCTIVITY (Btu/hr ft °F)
LiF	870[1]	1676[1]	1.798 - 0.000437 (t - 850) at t°C[2] 1.789 at 868.5°C[3] 1.753 at 944°C[3] 1.713 at 1029°C[3] 1.672 at 1117°C[3] 1.629 at 1208°C[3] 1.599 at 1270°C[3]	0.578		~1.5 (calculated)[5]
NaF	980 - 997[1]	1700[1]	1.942 - 0.000564 (t - 1000) at t°C[2] 1.936 at 1010°C[3] 1.887 at 1097°C[3] 1.859 at 1147°C[3] 1.810 at 1234°C[3] 1.766 at 1313°C[3] 1.714 at 1405°C[3] 1.662 at 1497°C[3] 1.634 at 1546°C[3]	0.357	~1 (estimated from NaBr and NaCl)	~1 (estimated from LiF and KF)
KF	880[1]	1500[1]	1.878 - 0.000669 (t - 900) at t°C[2]	0.258		~0.7 (calculated)[5]
BeF	800[1]	Subl.[4]	1.986 for the solid**	0.319		
RbF	760[1]	1410[1]	2.873 - 0.000967 (t - 825) at t°C[2]	0.144		
CsF	684[1]	1250[1]	3.611 - 0.001234 (t - 700) at t°C[2]	0.099		
AlF_3	1040[1]	(1,4)	3.07[1] for the solid**	0.197		
CaF_2	1360[1]	(1,4)	3.18[1] for the solid**	0.281		~1 (calculated)[5]
MgF_2	1396[1]	2239[1]	2.9 to 3.2[1] for the solid**	0.353		
BaF_2	1280[1]	2137[1]	4.83[1] for the solid**	0.125		
$AlF_3 \cdot 3NaF$				0.352		

* Specific heat calculated by Kopp's rule for liquids.

** For LiF, NaF, and KF, $(C_p$ liq$)/(C_p$ solid$) \sim 0.6$ to 0.75; for CsF, $(C_p$ liq$)/(C_p$ solid$) \sim 1$(?).

(1) *Handbook of Chemistry and Physics*, Ed. C. D. Hodgman, 31st ed., Chemical Rubber Publishing Co., Cleveland, Ohio, 1949.

(2) Jäger, F. M., *Z. anorg. Chem.*, 101, 1 (1917). (3) International Critical Tables, McGraw-Hill, New York, 1929.

(4) Lange, N. A., *Handbook of Chemistry*, 7th ed., Handbook Publishers, Sandusky, Ohio, 1949.

(5) Manson, S. V., Theoretical Equations for Estimating Thermal Conductivity of Liquids, ORNL, Y-12 Site, Y-F8-6 (Nov. 13, 1950).

TABLE 1.1

Physical Data for Hydroxides In the Fused State

FORMULA	M.P. (°C)	B.P. (°C)	SPECIFIC GRAVITY	SPECIFIC HEAT (Btu/lb °F)	VISCOSITY (centipoises)(3)						THERMAL CONDUCTIVITY (Btu/hr ft °F)
					350°C	400°C	450°C	500°C	550°C	600°C	
NaOH	318.4(4)	1390(4)	2.11 - 0.00063t for t between 340 and 440°C(1) 1.746 $[1 - 2.74 \times 10^{-4}(t - 400)]$(2a) 1.786 at 320°C(2a) 1.771 at 350°C(2a) 1.746 at 400°C(2a) 1.722 at 450°C(2a) 1.90 at 320°C(2b) 1.89 at 340°C(2b) 1.88 at 360°C(2b) 1.87 at 380°C(2b) 1.86 at 400°C(2b) 1.85 at 420°C(2b) 1.84 at 440°C(2b) 110 lb/ft^3 at m.p.(6)	0.50(6) 0.47 by Kopp's rule for liquids(5)	4.0	2.8	2.2	1.8	1.5		2.23(7) 1(6)
KOH	360.4 ± 0.7(4) 380(5)	1320-1324(4) 1320(5)	2.25 - 0.001t for t from 380 to 440°C(1) 1.717 $[1 - 2.56 \times 10^{-4}(t - 400)]$(2c) 1.717 at 400°C(2c) 1.695 at 450°C(2c) 1.673 at 500°C(2c) 1.651 at 550°C(2c) 1.629 at 600°C(2c)	0.34 by Kopp's rule for liquids(5)		2.3	1.7	1.3	1.0	0.8	If the compressibility of KOH were about 1.5 times that of NaOH, the thermal conductivity of KOH would be about 0.65. (thermal conductivity of NaOH; see Bridgmann's equation and items b and d of Y-F8-6)

(1) International Critical Tables, McGraw-Hill, New York, 1929.

(2) Landolt-Börnstein Tables, J. Springer, Berlin:
- (a) Eq. II, Part I, Table 81K, p. 223.
- (b) Eq. I, Table 81F, p. 177.
- (c) Eq. II, Part I, Table 81F, p. 219.

(3) Arndt and Ploetz, *Z. phys. Chem.* 121, 439 (1926)

(4) *Handbook of Chemistry and Physics*, Ed. C. D. Hodgman, 31st ed., Chemical Rubber Publishing Co., Cleveland, Ohio, 1949.

(5) Lange, N. A., *Handbook of Chemistry*, 7th ed., Handbook Publishers, Sandusky, Ohio, 1949.

(6) NEPA Report IC-50-4-20 (April, 1950).

(7) Battelle Memorial Institute, telephone conversation.

If the various problems associated with reactors of this type can be solved satisfactorily, designs 1, 2, 3, and 4 would afford great flexibility in loading and unloading the fuel. The entire core could be fabricated and assembled within the shield and the liquid metal coolant put in the system and the various pumps brought up to operating levels and temperatures before the reactor contains any fuel. The fuel could then be added slowly and might have its concentration varied over a fairly wide range. The initial start-up problems thus seem much less difficult than with solid-fuel reactors.

By compartmentalization and the use of various concentrations of uranium in the fuel solution, a considerable variation of fuel distribution across the reactor core could be obtained, if desired for adjustment of the flux pattern. Another potential advantage of the liquid fuel for an aircraft reactor is that most of the radioactivity could be drained from the system at one step, thus greatly simplifying the ground handling problems if a divided shield is used.

Coolant Circuit Design. It is expected, as indicated in previous reports, that sodium will be both the primary and the secondary coolant for the ARE. Coolant circuit design work currently is in progress with particular emphasis on the components which affect the design of the building. Fundamental coolant circuit specifications which have been adopted at the present time are:

1. The fluid circuit will simulate the airplane system as far as practicable within the shield if a unit shield is adopted. The secondary circuit outside the shield is to be designed primarily for safety and convenience. Flow rates are to be as required to remove power at the rate developed by the ARE.

2. Final heat rejection is to be by transfer from the secondary circuit to air.

3. Multiple primary coolant pumps will be used.

4. Multiple intermediate heat exchangers will be used.

5. The ARE is expected to contain two completely independent secondary systems with separate pipes, pumps, radiators, radiator blowers, and accessories.

6. Two independent power sources of auxiliary power will serve the secondary loops and will transmit power to the primary pumps so as to maintain circulation in the event of failure of one power source.

In addition to the above features, which are similar to those expected in the final aircraft system, several special items are planned for the ARE for protection of personnel and reactor under experimental conditions. These include the following:

7. Dump systems for control of liquid-metal fires will be provided.

8. A pressure shell will be constructed about the reactor-shield assembly, to contain materials that might escape from the shield in the event of an accident.

9. The pump room will be isolated and shielded to protect personnel from radioactive gases in the event of partial failure.

Building Design for the ARE. The Test Facility building design now proposed consists of a steel, concrete, and masonry fire-resistant structure 80 ft wide by 90 ft long. The building is expected to contain a crane bay approximately 42 ft high, so that large pieces of the reactor or of the shield may be lifted out of the assembly. A basement level is expected to house the liquid-metal pumps and the disassembly and decontamination rooms.

2. REACTOR PHYSICS

N. M. Smith, Jr., Chairman
ANP Physics Group, Physics Division

2. REACTOR PHYSICS

N. M. Smith, Jr., Chairman

ANP Physics Group, Physics Division

A. INTRODUCTION

The principal efforts of the ANP Reactor Physics Group during the last quarter have been directed toward two general types of calculations: computations of criticality and thermal xenon coefficients in both bare and reflected reactors, and calculations on the kinetic response of some liquid-fuel stationary-moderator reactor designs.

The criticality calculations summarized in the following sections are applicable in principle to both solid- and liquid-fuel reactors of the types discussed for the ARE. This arises from the fact that both types of ARE designs use approximately the same volume percent of the same moderator, BeO, and use the same coolant, Na. The difference between the criticality calculations for the oxygen in the UO_2 of the solid-fuel designs and the fluorine in the $NaF\text{-}UF_4$ of the liquid-fuel designs is likely to lie within the uncertainty limits of the present results.

These calculations deal with homogeneous reactors, both bare and reflected. The principal effect which must be added to the picture in order to apply the answers in detail to designs of the ARE type is the one brought about by the heterogeneous nature of the core, i.e., the effect of self-shielding caused by lumping. Thus the present calculation of the critical mass of uranium may be in error from 50 to 100%. The effects of perturbations, however, are obtained more accurately. The application of methods of calculating "effective homogeneous" cross sections to replace the atomic cross sections now used should reduce the pre-experimental errors of critical mass to around 30%. Experience with calculating results of critical assemblies should ultimately permit making calculations on a new reactor within 10 to 15%. In spite of these uncertainties, the present refinement of the calculation is valuable in guiding design in a semiquantitative sense and for gaining an understanding of the overall field of intermediate reactors through exploratory calculations.

It is to be noted that the "bare reactor" calculations described in Section B really represent the first approximation to an actual reflected ARE reactor, since the effect of a reflector was simulated by modification of the core diameter to allow for estimated reflector savings. The so-called "reflected reactor" calculations (Section C) represent a second, and more difficult, approximation in which the core-plus-reflector combination is treated explicitly as a two-region problem.

In addition to the calculations of critical masses and associated core fluxes, neutron lifetimes, and control rod effects, particular attention has been paid to that contribution to the temperature coefficient of reactivity which arises from the shift of the thermal base across the xenon absorption curve. This parameter is vitally important for reactor control. For those ARE designs which involve a large volume percentage of moderator, the positive xenon coefficient is so large that it yields a net positive temperature coefficient for the reactor as a whole. This coefficient is, however, associated with the temperature of the moderator. It is quite clear that the design to be used for the aircraft reactor must be arranged to have either a total temperature coefficient of reactivity which is negative, or else a thermal response time of the moderator which is so long that slow-acting servo controls are adequate and safe.

As described previously in this report, the liquid-fuel designs for the ARE offer the attractive possibility of gaining a rapidly acting negative temperature coefficient of reactivity through expansion of the fuel to points outside the active core. This allows control by means of a relatively sluggish temperature-sensing device in place of a neutron-flux-sensing receptor. However, the problem of the kinetics of a "stationary" liquid-fuel reactor is intricate. It requires study not only of the nuclear response of the system to a change in reactivity, but also an investigation of the time-temperature-density transients of the liquid fuel, the coolant, and the moderator. Studies of maximum stresses in the fuel tubes, etc., under emergency conditions are also required. This large body of analyses is now being undertaken. Some initial perturbation-theory results are presented in Section D on the flux behavior and the kinetics of the liquid fuel for the simplified case where delayed neutrons are neglected. These perturbation theory calculations apply to infinitesimal effects and serve to determine designs having stable kinetics. Numerical integration of more exact equations are required for analysis of the stresses resulting from large perturbations.

In Section E some of the background problems are listed which contribute to the broader calculations. They include studies on the Doppler effect, on adjoint functions, and on cylindrical multigroup age equations. Further work is in progress, as mentioned in Section F, in preparation for interpreting the results from forthcoming ANP critical experiments.

B. BARE-REACTOR CRITICALITY CALCULATIONS[1]

Four solid-fuel reactors having the same heat-transfer area but covering a range of mean neutron energy from epithermal to epiresonance were considered. The shift of spectrum was made by changing the moderator volume. Thus analysis has been directed toward:

1. The establishment of a rough lower limit to the median energy for fission of a BeO reactor such that xenon poisoning does not create a control problem.
2. The calculation of pile parameters such as critical mass, neutron life, core flux, and control effectiveness.

At the high operating temperature of the aircraft reactor the kT energy associated with the peak of the thermal neutron distribution is above the energy of the peak of the xenon cross section (if the Breit-Wigner fit is assumed). Thus the xenon creates a positive component of the overall temperature coefficient ($\Delta k/kT$). If the overall coefficient is positive an unstable condition results which could present a very difficult control problem. However, if the moderator temperature increases slowly as the reactor power is increased, the velocities of the thermal neutrons will then change slowly and the resultant slow change in reactivity could probably be handled. This temperature behavior of the moderator is being studied. The secondary aims of the calculations were to obtain rough estimates of critical mass, potential reactivity changes that must be offset by shim control rods, mean neutron lifetimes, mean xenon lifetime for absorption, total core flux, and the effectiveness of B_4C as a control rod material.

The calculations were made by reducing reflected reactors to equivalent bare reactors and using bare reactor computational methods. In computing the temperature coefficients several effects, such as the Doppler effect, effects of heterogeneity, and effect of the spatial variation of temperature, were neglected. Work is in progress to set up a method of accounting for these omissions.

(1) Except for minor editorial changes, this section is the same as the following report: Webster, J. W. (NEPA), and Macauley, B. T. (USAF), *Results of Some Bare Calculations of Critical Mass and Reactivity Effects*, Oak Ridge National Laboratory, Y-12 Site, Y-F10-22 (Dec. 1, 1950).

Theory and Assumptions. The four reactors considered constitute a family, each with about the same heat transfer area. In each case the fuel was UO_2 of density 10.9 g/cc, the moderator was BeO of density 2.8 g/cc, the coolant was sodium of density 0.75 g/cc, the structural material was type 347 stainless steel of density 7.67 g/cc, and the control material when present was B_4C of density 2.5 g/cc. These densities are quoted for the operating temperature of the aircraft reactor. The dimensions and compositions were as follows:

REACTOR NO.	DIAMETER OF EQUIVALENT SPHERICAL CORE (ft)	VOLUME FRACTION		
		BeO	STAINLESS STEEL	Na
1	2.604	0.4700	0.08723	0.3986
2	2.690	0.5200	0.07900	0.3610
3	2.790	0.5700	0.07077	0.32341
4	3.000	0.7005	0.05020	0.2227

The core in each case was arbitrarily taken to have a reflector equivalent to 10 cm of additional core mixture. For a good reflecting material the consequent savings from the reflector should be about equal to the reflector thickness. (This assumption is verified in the first IBM calculation of a reactor reflected with BeO, as discussed in Section C.) The extrapolation distance was assumed to be 2 cm for all energy groups.

The reactor core at its operating temperature is taken to have a uniform temperature of 1286°F. The cold reactor temperature was assumed to be 183°F, which is approximately the melting point of the coolant. The power was 200 megawatts. The detailed data used in the xenon calculations are given elsewhere.[2]

The solution of the pile equations as used in these calculations is also given elsewhere.[3] However, the relation

(2) Webster, J. W. (NEPA), *Xe Effect in an Epi-thermal Reactor*, Oak Ridge National Laboratory, Y-12 Site, Y-F10-17 (Oct. 10, 1950).

(3) Nielsen, M. J. (USAF), *Bare Pile Adjoint Solution*, pp. 4-6, Oak Ridge National Laboratory, Y-12 Site, Y-F10.18 (Oct. 27, 1950).

$$n\nu(u) = \frac{q(u)}{\zeta\sigma_T}$$

was substituted for

$$n\nu(u) = \frac{q(u)}{\zeta\sigma_s}$$

where absorption was large.

The method of handling the xenon effect is described in an earlier report.[4] Figure 2.1, taken from this report, illustrates the origin of the positive temperature coefficient of reactivity contributed by xenon. The operating temperature and the shape of the xenon resonance are such that the effective absorption of xenon decreases with an increase in the temperature of the thermal base.

Results and Conclusions. The following results and conclusions are discussed in terms of the median energy for fission (MEF) of the reactors. Table 2.1 relates the MEF to the size and composition of the reactor. It is to be remembered that these calculations were made for solid-fuel reactors and therefore do not include thermal coefficient effects arising from fuel expansion, as in the $NaF-UF_4$ designs.

1. With maximum transient xenon present, the temperature coefficient (neglecting any contribution by the Doppler effect) decreases rather rapidly with increasing MEF of the reactor and becomes negative at a MEF of approximately 3 ev. *It therefore appears from these rough calculations that, even with short time lags in moderator temperature rise, the solid-fuel reactor could be designed to have acceptable control characteristics.* This controllable reactor would have a core diameter equal to or less than approximately 2.9 ft, with 10 cm reflector savings and a moderator percentage less than approximately 60%.
2. The number of moles of B_4C necessary to provide shim control remains roughly constant as the MEF of a reactor increases; therefore the necessary number of control rods for an intermediate reactor should be no more than for a thermal reactor.

(4) Webster, *op. cit.*

DRAWING NO. 10217

The xenon and cadmium cross-sections, compared with the thermal flux distribution for kT = .0836 ev. (i.e., 1283°F). The shape of the xenon is asymmetrical, hence the flux corresponding high-energy tail of the Maxwellian is in a region of lower poisoning. A shift to a higher temperature results in a decrease in the overall poisoning, giving a positive component to the temperature coefficient of reactivity.

The cadmium cross-section is shown for comparison. The suggestion that cadmium be used to mask out the xenon has not been here investigated.

FIGURE 2.1 Xe + Cd CROSS-SECTIONS + THERMAL FLUX DIST.

TABLE 2.1

Miscellaneous Reactivity Results for Reactors of Various Core Sizes and 10 cm Reflector Savings

CORE DIAMETER (ft)	VOLUME FRACTION			CRITICAL MASS (lb)	MEDIAN ENERGY FOR FISSION (ev)	TOTAL FLUX AT 200 Mw [neutrons/(cm^2)(sec)]	NEUTRON LIFETIME (sec)	AVERAGE LIFETIME OF Xe FOR ABSORPTION (hr)	$\delta k/k$ FOR COMPLETE REMOVAL OF COOLANT	B_4C TO PROVIDE SHIM CONTROL (moles)
	Be	SS 347	Na							
2.604	0.4700	0.08723	0.3986	~125	321	6.5×10^{15}	3.4×10^{-6}	300	-0.076	~9
2.69	0.5200	0.07900	0.3610	~100	114	6.0×10^{15}	6.2×10^{-6}	40		~6
2.79	0.5700	0.07077	0.3234	~75	27	6.0×10^{15}	1.5×10^{-5}	5		~5
3.00	0.7005	0.0502	0.2227	~55	0.4	3.1×10^{15}	3.0×10^{-5}	1	-0.002	~7

3. The change in reactivity due to the rise of thermal base in the clean reactor from cold to operating temperature is small (<1%) for those reactors having MEF greater than ~0.4 ev.

4. The change in reactivity caused by equilibrium xenon decreases only slightly as the MEF increases up to approximately 20 ev, at which point it falls off rapidly. (This behavior arises, of course, because the equilibrium xenon concentration increases as the burn-out decreases in the less thermal reactors, and the decrease in effectiveness of the xenon tends to be offset by this increase in quantity. Ultimately, however, as the reactor spectrum becomes faster the xenon concentration approaches a maximum value determined from the equation

Rate of natural decay = rate of formation

The decrease in xenon effectiveness is no longer offset by increase in quantity and the reactivity effect drops off rapidly.)

5. The reactivity effect due to thermal expansion rises approximately linearly with log MEF and ranges from about 1 to 3% in k for the reactors studied here. [In the more thermal reactors considered, the moderator atoms are at a high concentration and the core size is large. Consequently, the neutron leakage is small. Upon expansion, with the resultant change in distance between scattering nuclei, the chance that a neutron will escape from the reactor remains small since the neutron still sees, on the average, many nuclei in its path. The reactivity change is consequently small. (In the limiting case of infinite size a uniform change in density obviously causes no change in reactivity.) For the smaller reactor with less moderator, it follows by reverse argument that the reactivity effect due to expansion is larger.]

6. The reactivity effect due to *maximum transient xenon* is very large (~11%) for the near thermal reactor considered and drops approximately linearly with log MEF, until it becomes no greater than that due to equilibrium xenon at MEF = 100 ev. The concentration of the xenon at its maximum transient value is essentially independent of the reactor spectrum. It is determined primarily from the concentration of the iodine at shutdown, and the equilibrium iodine concentration is a function only of reactor power density. Since the power density is large for these reactors, the effect on k of the after-shutdown xenon is large for the near thermal cases. As the mean neutron energy gets above the xenon resonance, the effect drops off. Apparently, when the reactor MEF is about 100 ev, the equilibrium xenon concentration is determined primarily by xenon decay, and there is no appreciable rise in concentration after shutdown.

7. The temperature coefficient due to thermal base plus expansion is roughly constant with change of MEF ($\sim 2.5 \times 10^{-5}$ units).

8. In the range of reactors studied, the temperature coefficient due to equilibrium xenon + expansion + thermal base change was calculated to be always negative.

9. The effect of the sodium coolant in these reactors as opposed to void is to decrease the uranium requirement.

10. Other pertinent results are shown in Table 2.1 and Figs. 2.2 through 2.14, which are self-explanatory.

C. REFLECTED REACTOR CRITICALITY CALCULATIONS

D. K. Holmes and O. A. Schulze

The large amount of time required to make hand calculations for a reflected reactor made desirable the setting up of a machine method of calculations. Accordingly, the G.E. multigroup method was adopted with modifications and set up on IBM machines by the uranium Control Department (F. C. Uffelman) at Y-12. The corresponding step has already been taken by the IBM division at G.E., and they are now able to make calculations for two complete 13-group reflected reactors per day, which is contrasted with 10 computer-days needed for the same calculation by hand.

In conversation and correspondence with the theoretical section of the Physics Division of KAPL at Schenectady the essentials of the KAPL technique for adapting the method for IBM calculation were obtained.[5] However, a slight variation of their present procedure has actually been used here, although the variation is in reality equivalent to a method, called "scheme *b*," which has been discussed in a KAPL report.[6] Whereas KAPL obtains the relation between the average flux over a lethargy group and the values of the flux at the group limits by an iterative, self-consistency method, the present method assumes that the flux is linear over a group. Thus, the present method avoids a certain amount of calculation time which would be devoted to repeating groups. It has been decided that the calculation time on the IBM would

(5) Letter from Hurwitz and Ehrlich to N. M. Smith, Aug. 14, 1950.

(6) Tonks, L., *Analyses of Errors in Method for Computing Critical Masses of Intermediate Piles Which Arise from a Spatially Discontinuous Source Distribution and Other Factors*, GE-LT-2 (1947).

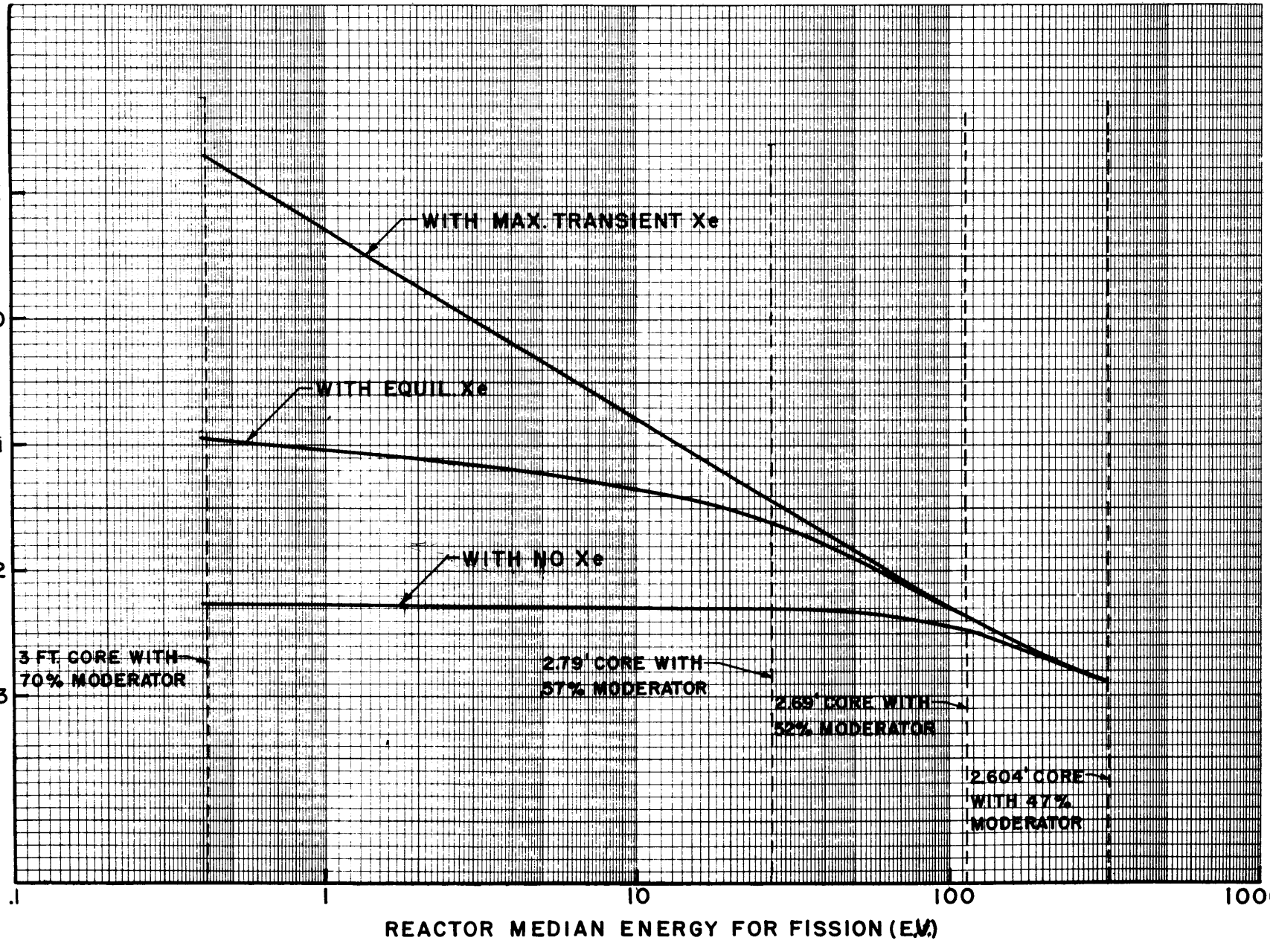

FIGURE 2.2 TEMP. COEFF. $\left(\frac{\Delta k}{k}/^{\circ}F\right)$ AT MEAN CORE TEMPERATURE = 1286°F

DRAWING NO. 10218

DRAWING NO. 10219

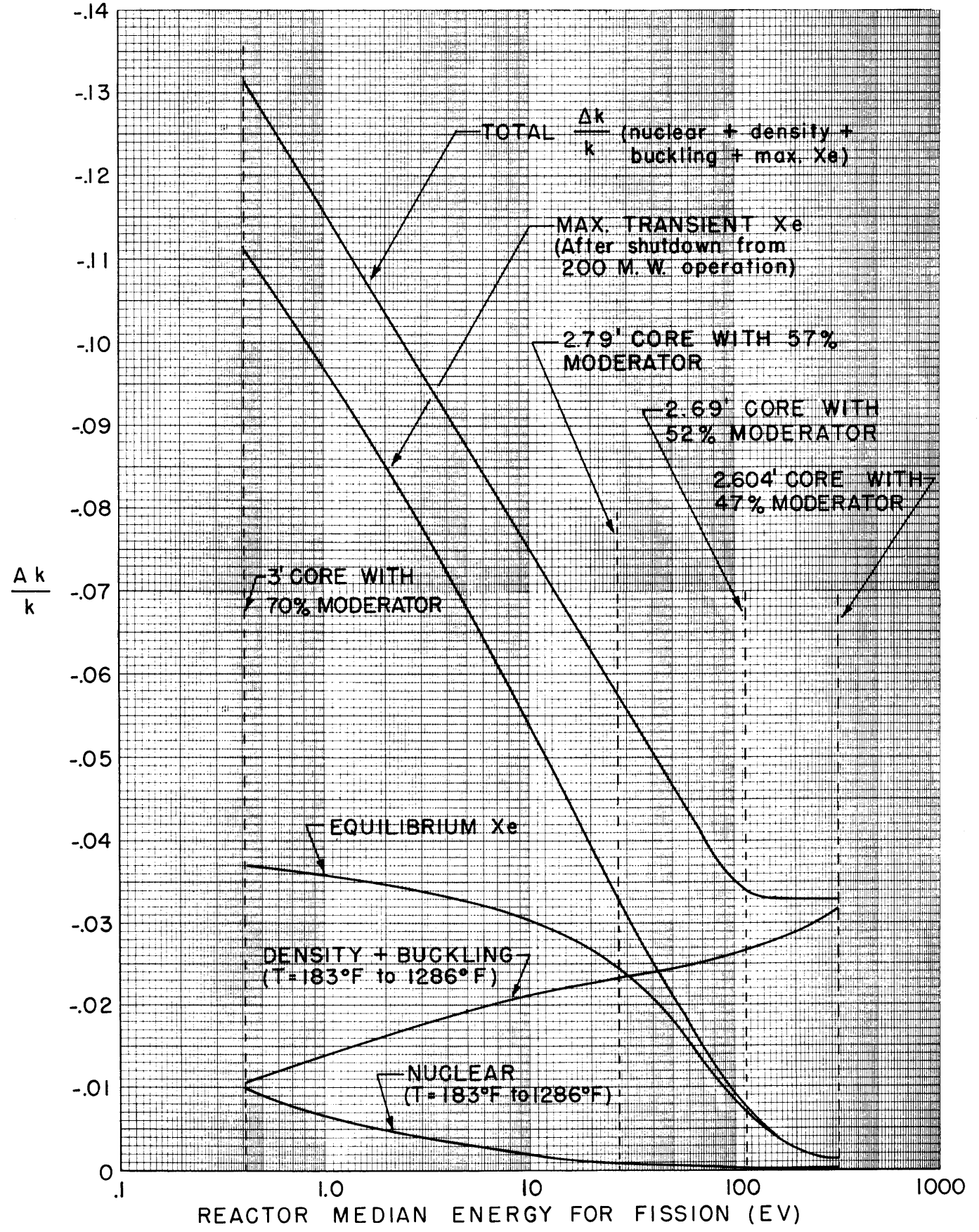

FIGURE 2.3 REACTIVITY EFFECTS AS A FUNCTION OF REACTOR SPECTRUM

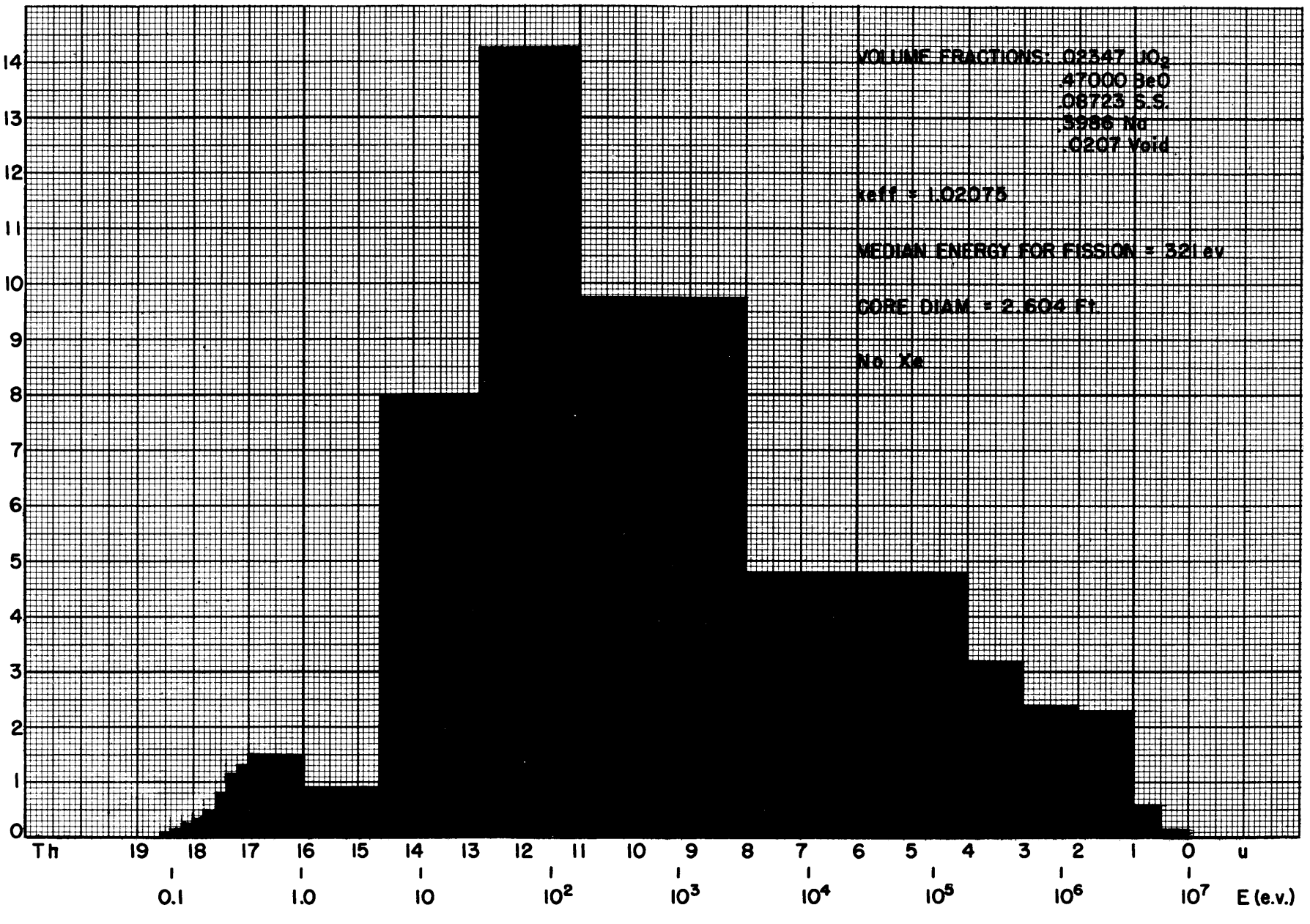

DRAWING NO. 10220

FIGURE 2.4 PRODUCTION SPECTRUM

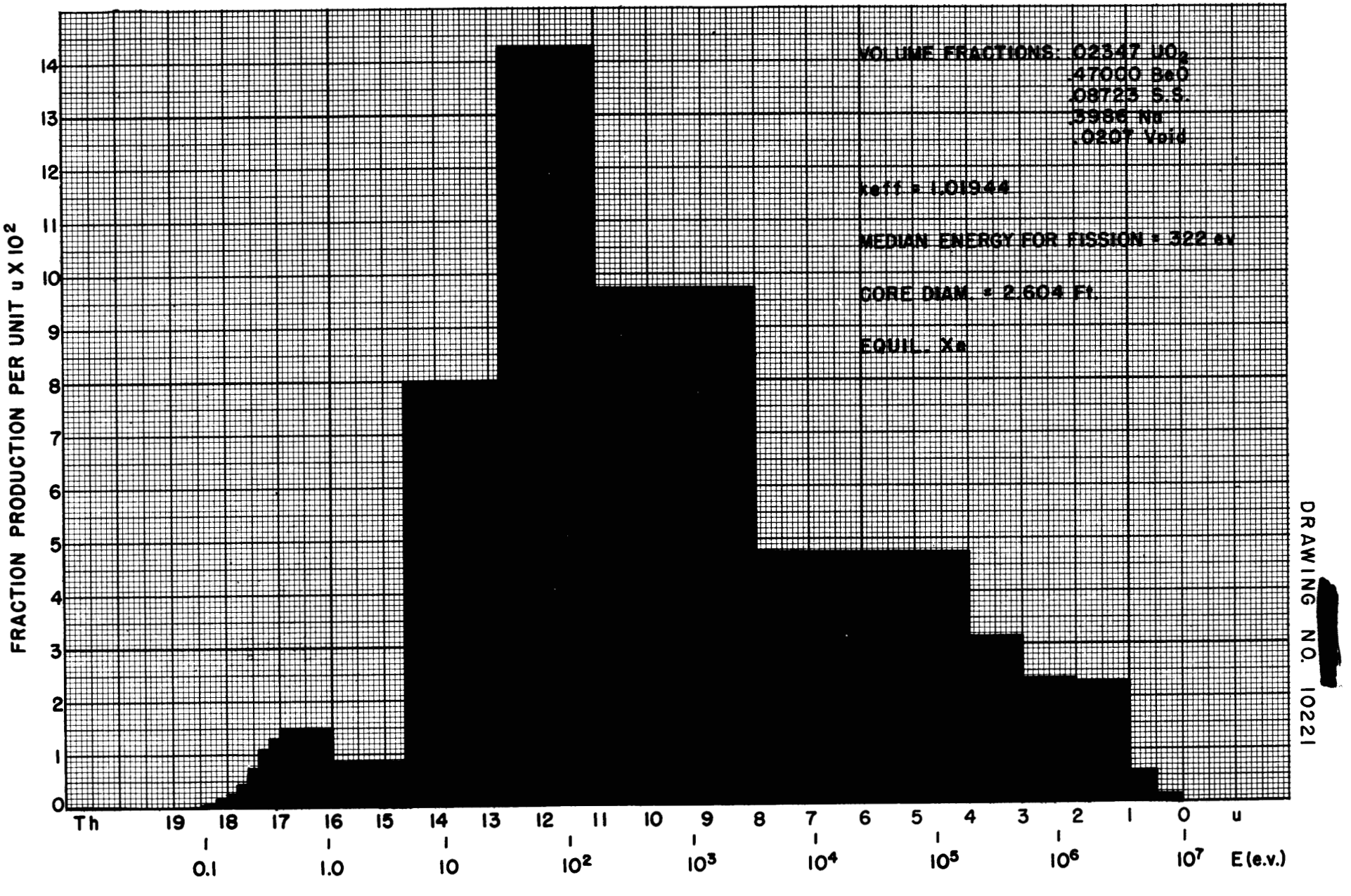

FIGURE 2.5 PRODUCTION SPECTRUM

DRAWING NO. [redacted] 10221

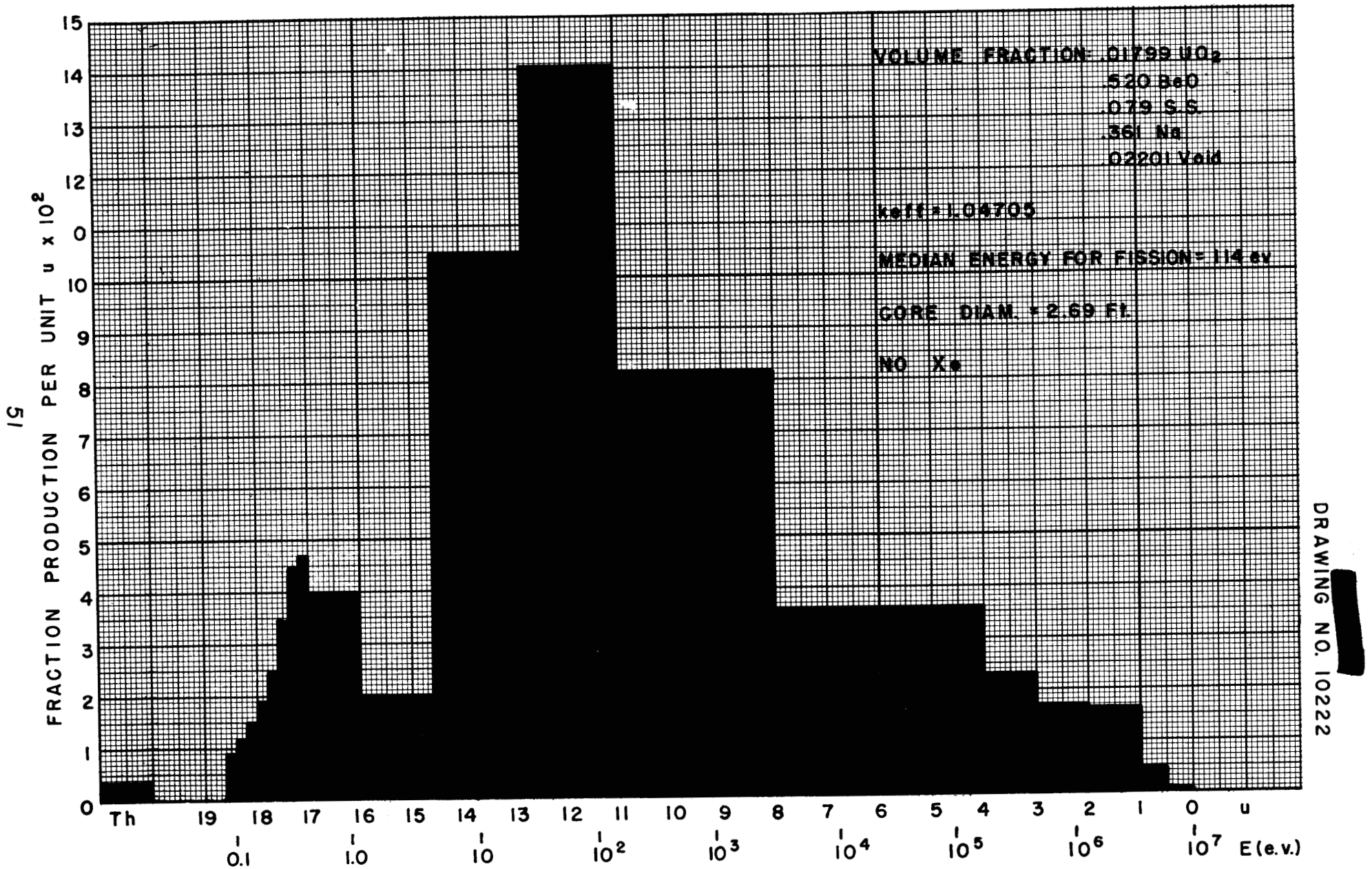

FIGURE 2.6 PRODUCTION SPECTRUM

DRAWING NO. 10222

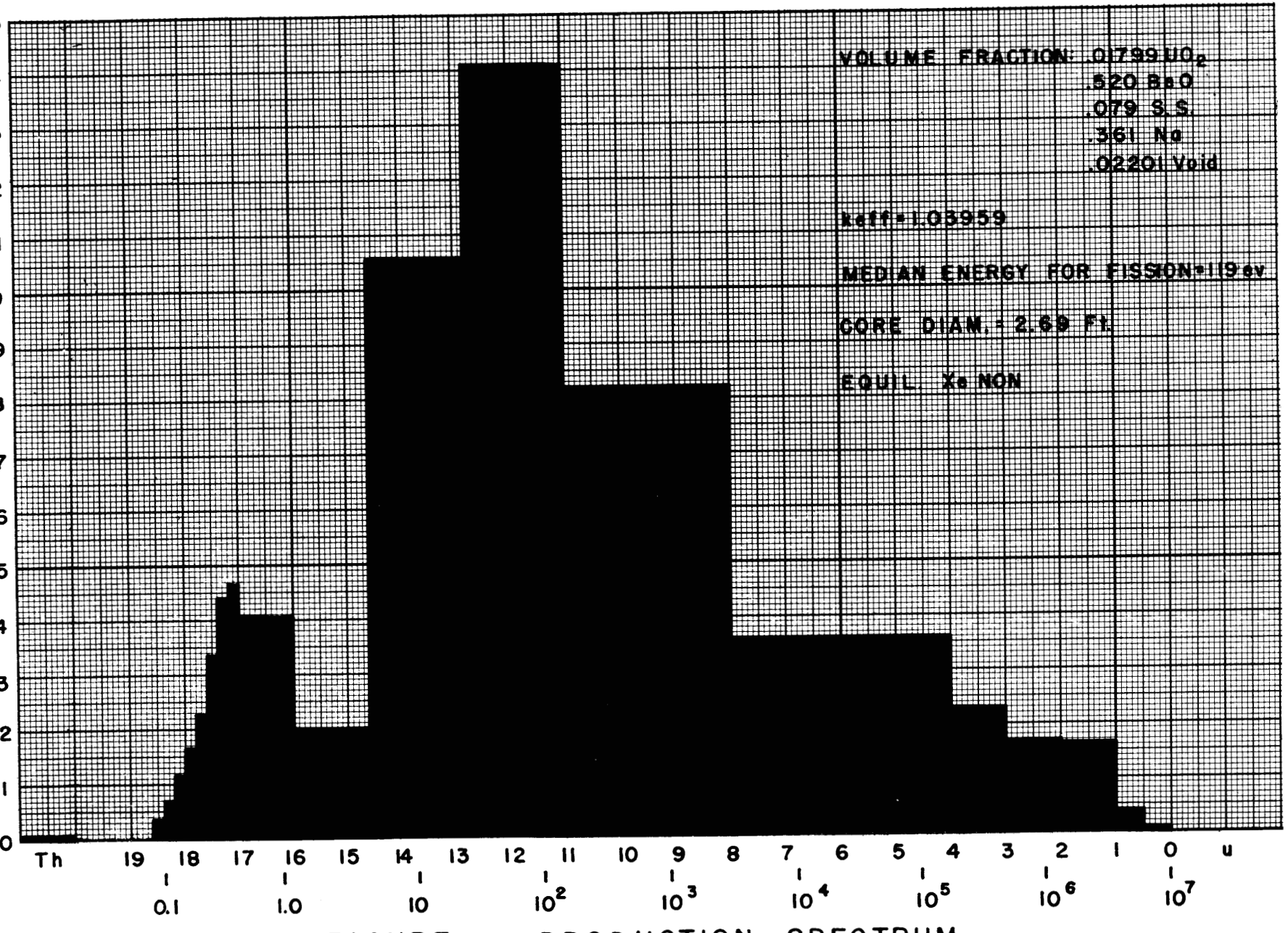

FIGURE 2.7 PRODUCTION SPECTRUM

DRAWING NO. 10223

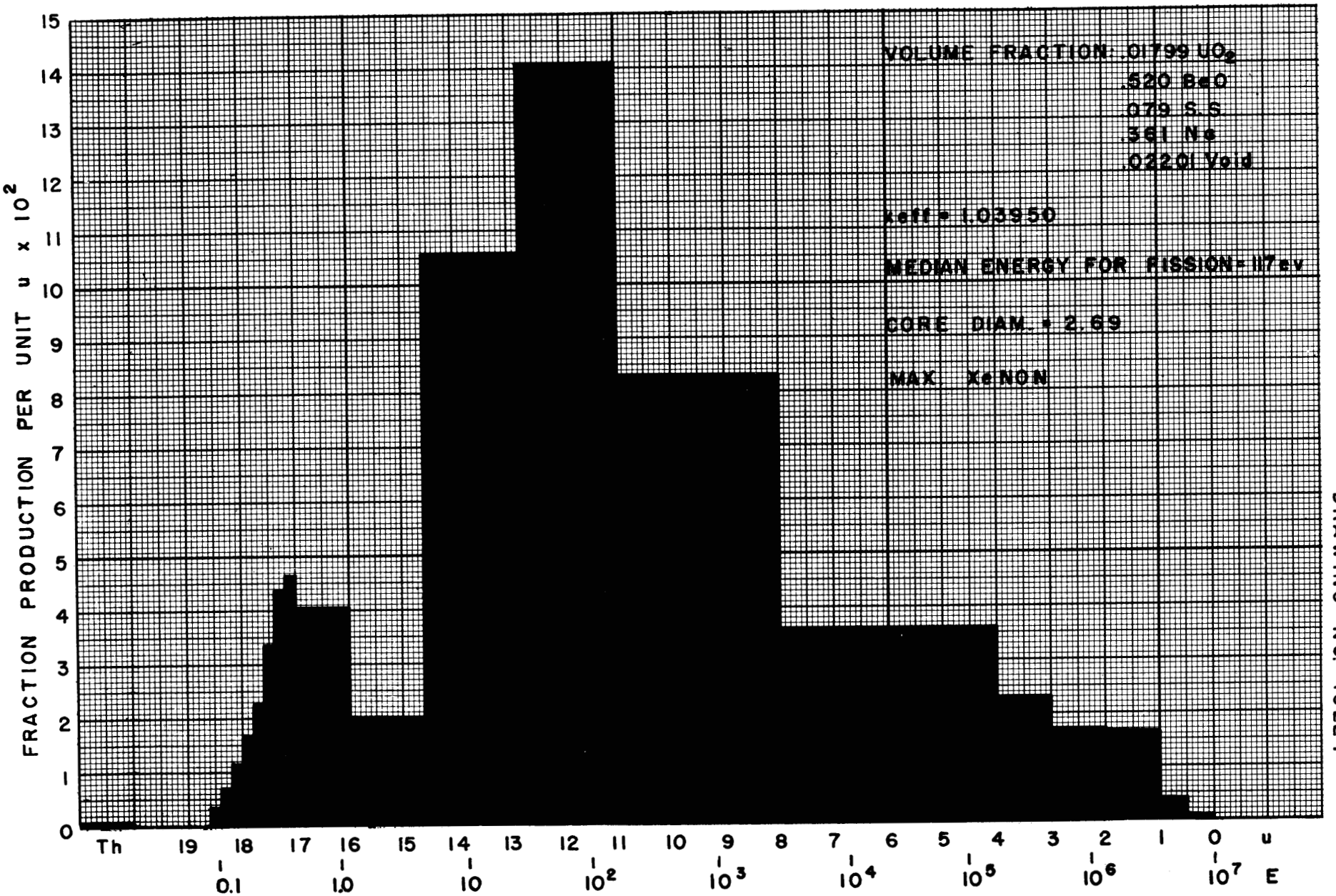

FIGURE 2.8 PRDUCTION SPECTRUM

DRAWING NO. 10224

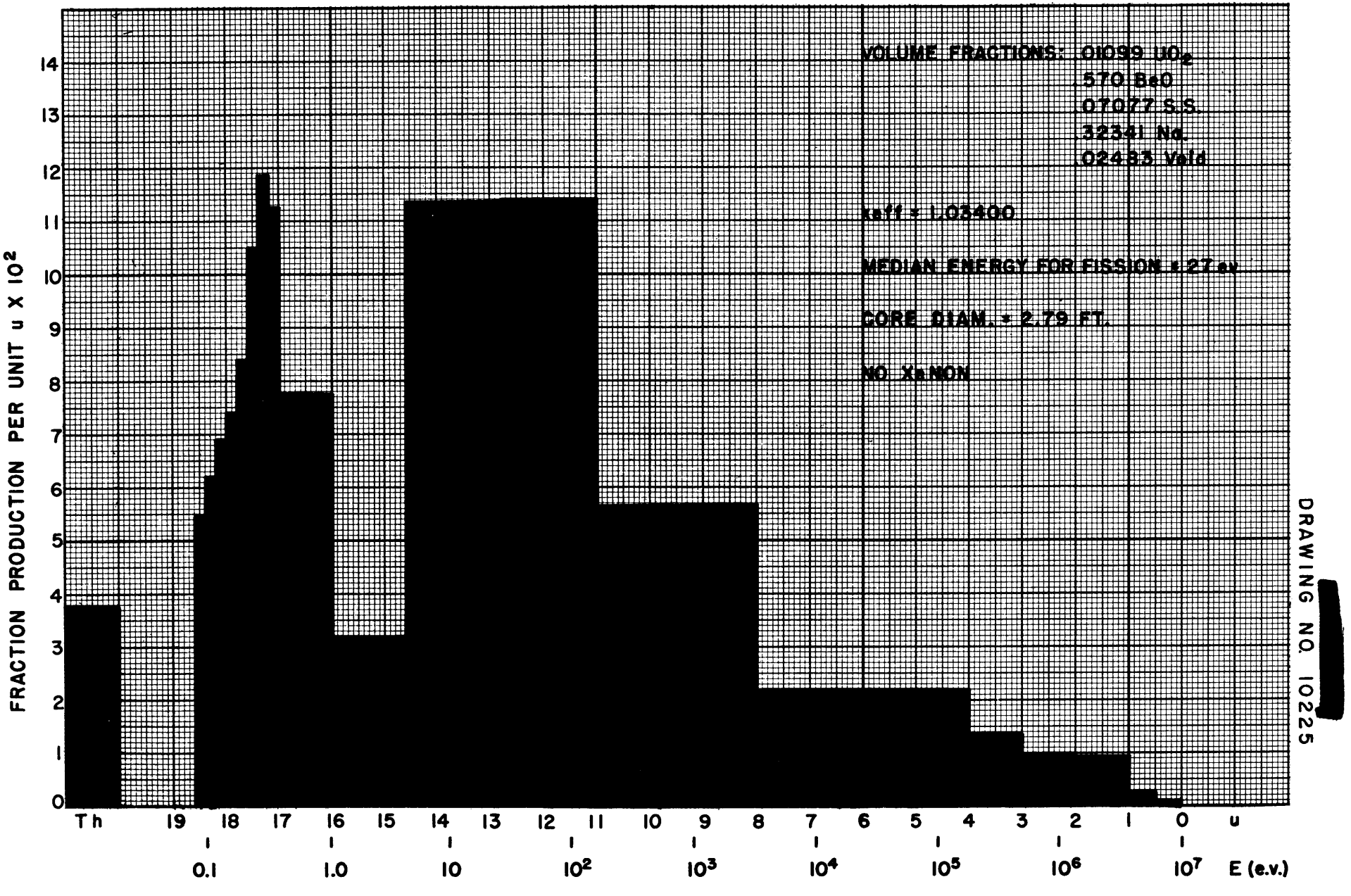

FIGURE 2.9 PRODUCTION SPECTRUM

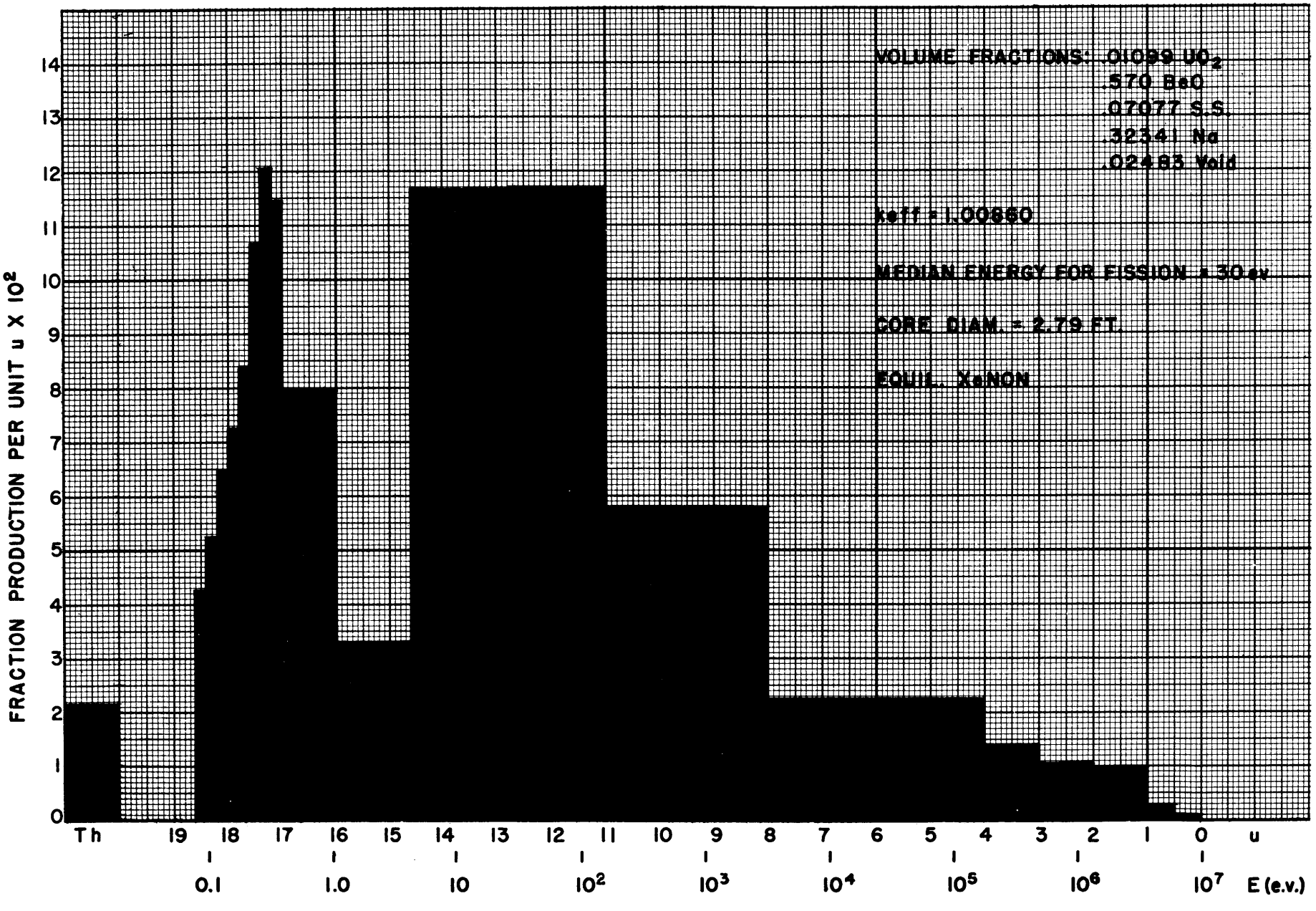

FIGURE 2.10 PRODUCTION SPECTRUM

DRAWING NO. 10226

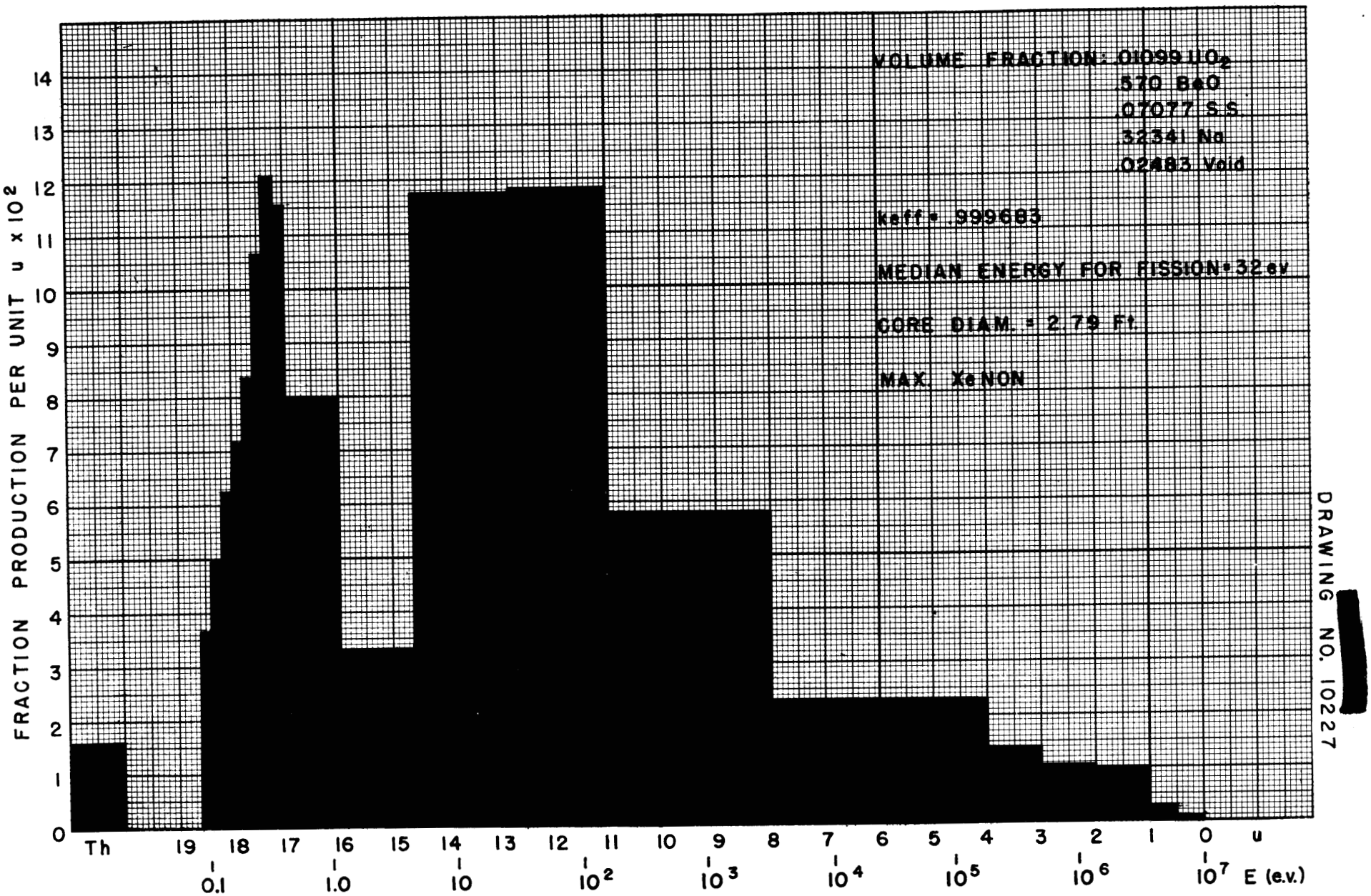

FIGURE 2.11 PRODUCTION SPECTRUM

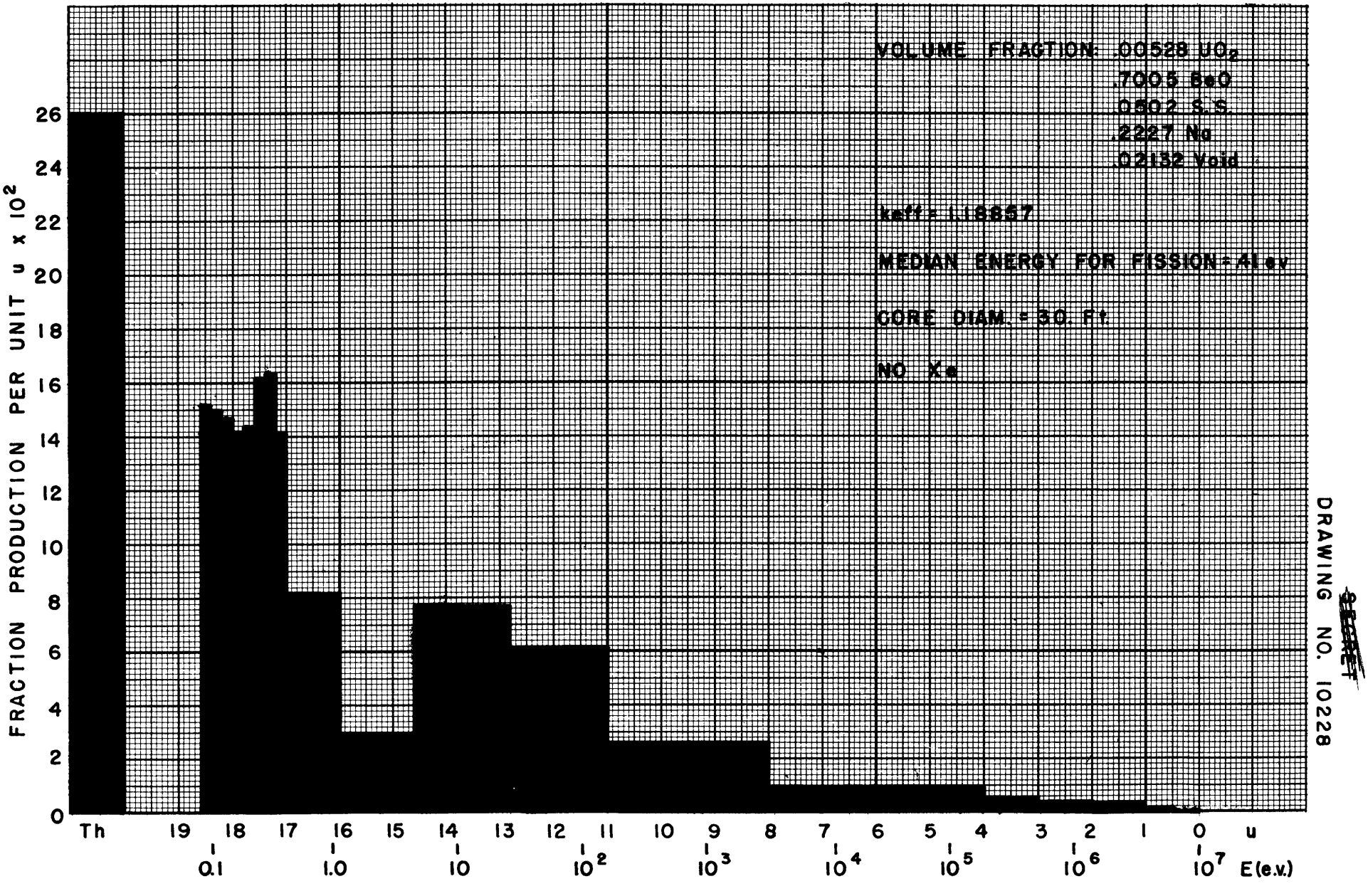

FIGURE 2.12 PRODUCTION SPECTRUM

DRAWING NO. 10228

SECRET

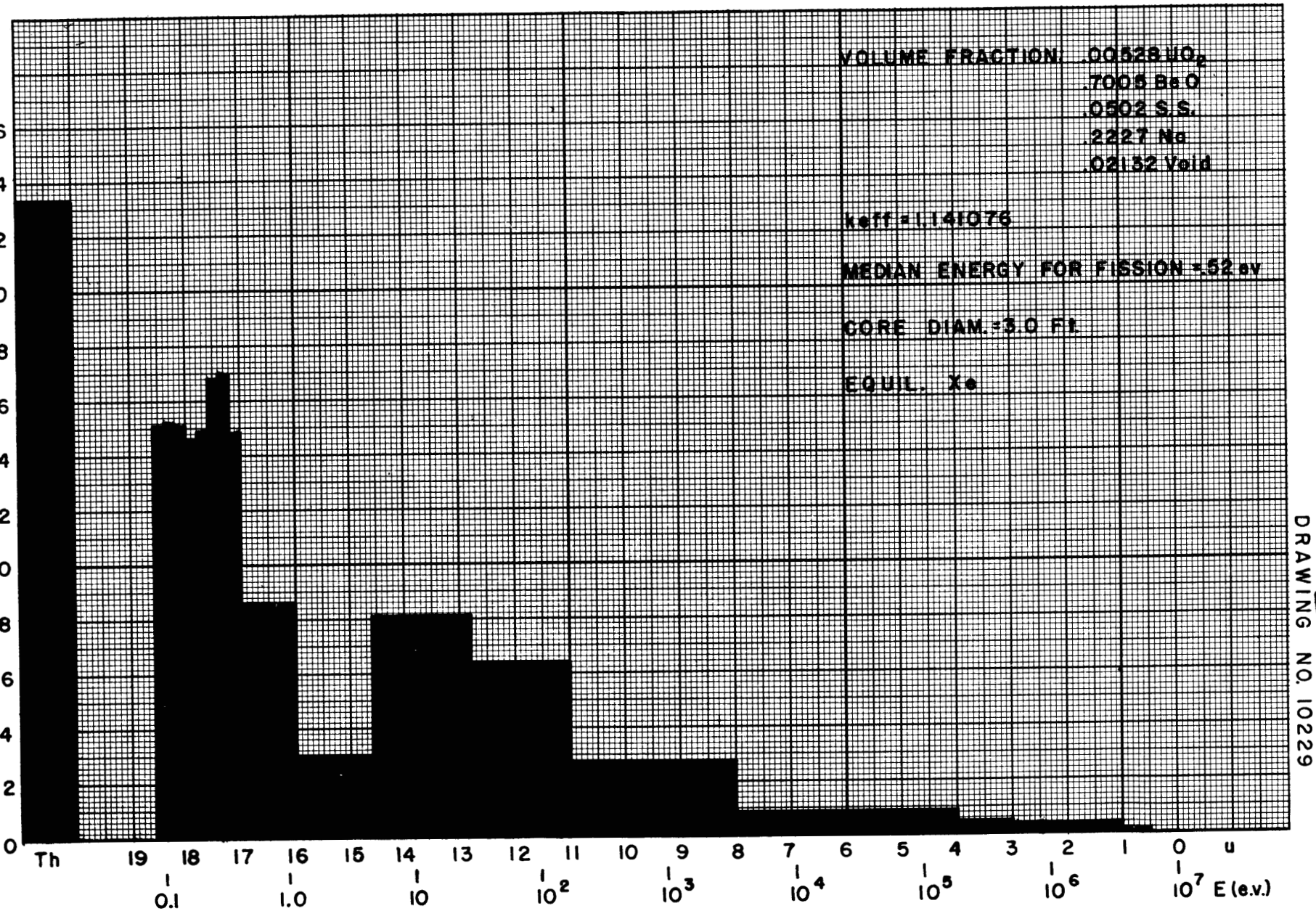

FIGURE 2.13 PRODUCTION SPECTRUM

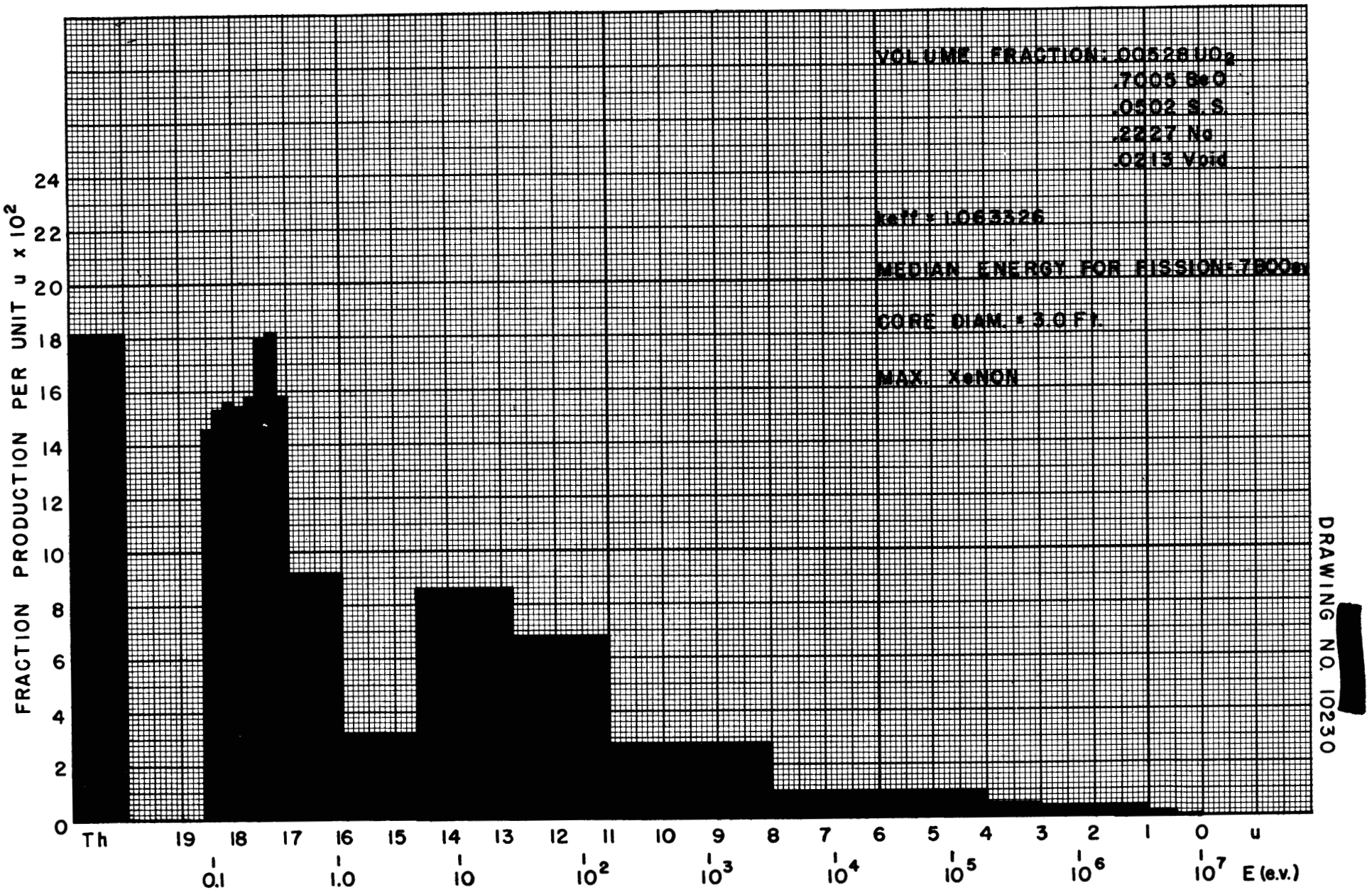

FIGURE 2.14 PRODUCTION SPECTRUM

not increase linearly with the number of groups, and that, to increase the validity of the general method, it would be acceptable to use 32 groups over the energy range.

Table 2.2 presents the results of a comparison of the two methods for the first six groups of a 13-group reflected reactor. The physical quantities tabulated are the total leakage of neutrons in a group (E), the total number of neutrons slowing down from a group (D), and the total number of neutrons absorbed in a group (A), all normalized to one neutron produced throughout the reactor. A more complete discussion of the linear approximation has been made.[7] A report on the detailed procedure which has now been adopted for multigroup calculations on spherical reflected reactors has been issued.[8]

The complete reactor calculation involves computations to obtain each of the following:

1. Average macroscopic cross sections for the core and reflector from basic cross-section data.
2. Various constants for each group from the average cross sections.
3. Auxiliary functions needed for fitting the boundary conditions in each group.
4. Fluxes and slowing-down densities over the reactor for each group.
5. Net neutron leakage, absorption, and total fissions in each group.
6. Power distribution and the k_{eff} for the reactor.

The setup of all these steps on the IBM machines has been very laborious, requiring, for example, the wiring of 16 electronic control panels and seven supplementary boards. However, the preparation period is now essentially completed so that spherical reactors of the UO_2—BeO—Na—stainless steel type may be calculated on a production basis. In addition, partial preparation has been made for the following calculations:

1. Adjoint functions for reflected reactors.
2. Reactors of the UF_4-BeF_2-NaF liquid-fuel types.
3. Multiregion spherical reactors.

(7) Holmes, D. K., *Results of a Test of the Linear Approximation Multigroup Calculations*, Oak Ridge National Laboratory, Y-12 Site, Y-F10-20 (Nov. 6, 1950).

(8) Holmes, D. K., and Schulze, O. A., *IBM Multigroup Numerical Procedures*, Oak Ridge National Laboratory, Y-12 Site, Y-F10-21 (Nov. 28, 1950).

TABLE 2.2

SUMMARY OF TEST OF LINEAR METHOD

GROUP NO.	CORE		REFLECTOR	
	G.E. METHOD	LINEAR METHOD	G.E. METHOD	LINEAR METHOD
I	E_1 0.00484387	0.00484380	E' 0.00293864	0.0029387
	D_1 0.0180802	0.0180804	D' 0.00190526	0.0019051
	A_1 0.0000768409	0.00007675	A' 3.81052×10^{-8}	2.858×10^{-8}
II	E 0.0161205	0.0164871	E' 0.00778762	0.00797926
	D 0.103625	0.103246	D' 0.0102378	0.0104133
	A 0.000335745	0.000345174	A' 1.02378×10^{-7}	1.23184×10^{-7}
III	E 0.0924723	0.0926290	E' 0.0535788	0.0533433
	D 0.453414	0.452860	D' 0.0491315	0.0496958
	A 0.00275676	0.00275551	A' 9.82630×10^{-7}	9.01638×10^{-7}
IV	E 0.0483388	0.0480298	E' 0.0237181	0.0243173
	D 0.702250	0.701981	D' 0.0737526	0.0734080
	A 0.00283709	0.00284091	A' 7.37526×10^{-7}	1.23104×10^{-6}
V	E 0.0452667	0.0453560	E' 0.0285398	0.0277470
	D 0.783166	0.782790	D' 0.0904788	0.0910144
	A 0.00382968	0.00382328	A' 9.04788×10^{-7}	8.22112×10^{-7}
VI	E 0.121533	0.122265	E' 0.126826	0.121989
	D 0.636685	0.635922	D' 0.0851816	0.0912816
	A 0.0249708	0.0246217	A' 5.11090×10^{-6}	5.46888×10^{-6}

Spherical Reflected Reactor. The first spherical reflected reactor computed by the IBM group had the following basic properties:

1. Core composition: 1.96% UO_2, 52.0% BeO, 7.9% stainless steel, 36.1% Na.
2. Core diameter: 2.68 ft.
3. Reflector composition: 75% BeO, 20% Na, 5% stainless steel.
4. Reflector thickness: 6.5 in.

The results of the calculation, including the neutron fluxes in the various groups, the power distribution, the fissions per unit lethargy interval, and the neutron leakage as a function of lethargy, are presented graphically. The k_{eff} at the operating temperature is 1.043, while the temperature coefficient, computed on the change of thermal base alone, is $+4.6 \times 10^{-6}$ per degree Fahrenheit.

The flux distribution in each group, all plotted with the same vertical scale, is shown in Fig. 2.15. Table 2.3 gives the energy limits of the various groups. The flux is large in groups 1 through 9, into which are thrown the fission neutrons. It is interesting to note the build-up in the lower groups of the flux in the reflector.

This build-up explains the up-turn of the power distribution curve (Fig. 2.16) near the reflector; in the lower energy groups the net neutron current at the core-reflector interface is from the reflector into the core. The neutrons having nearly thermal energies cause fissioning before they have penetrated far into the core. Figure 2.16 also compares the power distribution of the reflected reactor with that of the equivalent bare reactor, normalized to the same number of fissions in the core volume. The reflector effectively flattens the power distribution, thus increasing the importance of the outer regions. (It must be remembered in examining Fig. 2.16 that we are treating a spherical reactor, so that the regions at greater radii are more important than the curve would indicate.)

That the peak in power distribution near the reflector is actually due to near-thermal fissions is shown by the number of fissions per unit lethargy. This is shown (Fig. 2.17) for three regions of the reactor. The outstanding feature of these curves is the peak, near thermal, for the region near the reflector. This result also indicates that the xenon effect, which from the

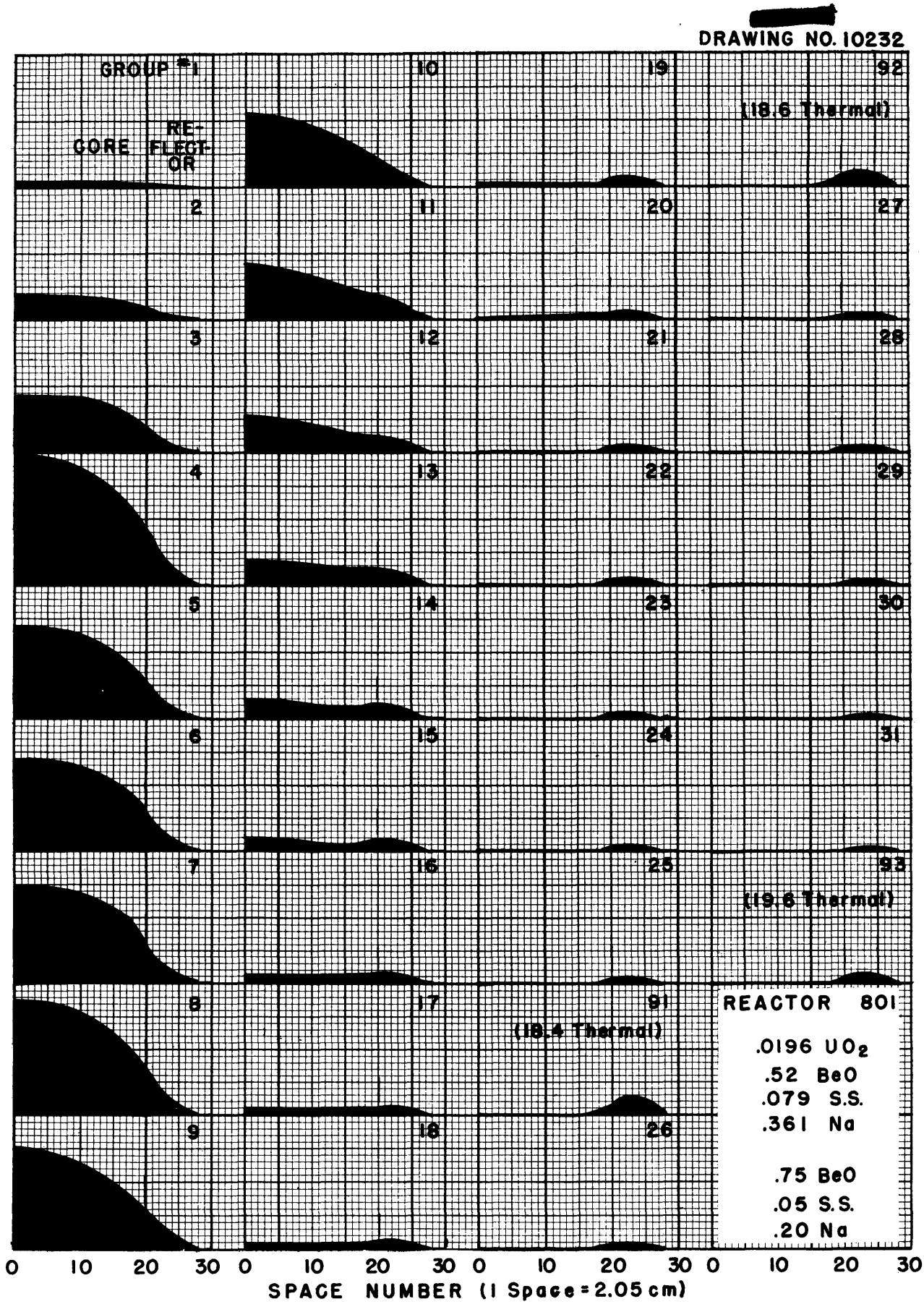

FIGURE 2.15 FLUX DISTRIBUTION

TABLE 2.3

Energy and Lethargy Intervals Used in IBM Multigroup Calculations

GROUP NO.	LETHARGY INTERVALS*	ENERGY INTERVALS (ev)
1	0.0 - 0.5	10^7 - 6.07×10^6
2	0.5 - 1.0	6.07×10^6 - 3.68×10^6
3	1.0 - 1.5	3.68×10^6 - 2.23×10^6
4	1.5 - 2.0	2.23×10^6 - 1.35×10^6
5	2.0 - 2.5	1.35×10^6 - 0.82×10^6
6	2.5 - 3.0	0.82×10^6 - 0.498×10^6
7	3.0 - 3.5	0.498×10^6 - 0.302×10^6
8	3.5 - 4.0	0.302×10^6 - 0.183×10^6
9	4.0 - 7.0	0.183×10^6 - 9120
10	7.0 - 10.0	9120 - 450
11	10.0 - 11.4	450 - 105
12	11.4 - 12.6	105 - 33
13	12.6 - 13.4	33 - 15
14	13.4 - 13.8	15 - 10
15	13.8 - 14.6	10 - 4.5
16	14.6 - 15.8	4.5 - 1.36
17	15.8 - 16.2	1.36 - 0.91
18	16.2 - 16.6	0.91 - 0.61
19	16.6 - 17.0	0.61 - 0.41
20	17.0 - 17.4	0.41 - 0.275
21	17.4 - 17.6	0.275 - 0.225
22	17.6 - 17.8	0.225 - 0.185
23	17.8 - 18.0	0.185 - 0.150
24	18.0 - 18.2	0.150 - 0.126
25	18.2 - 18.4	0.126 - 0.101
26	18.4 - 18.6	0.101 - 0.085
27	18.6 - 18.8	0.085 - 0.068
28	18.8 - 19.0	0.068 - 0.055
29	19.0 - 19.2	0.055 - 0.045
30	19.2 - 19.4	0.045 - 0.038
31	19.4 - 19.6	0.038 - 0.0305

* Lethargy, u, is defined by $u = \ln 10^7/E$, where E = energy in electron volts.

[redacted] DRAWING NO. 10233

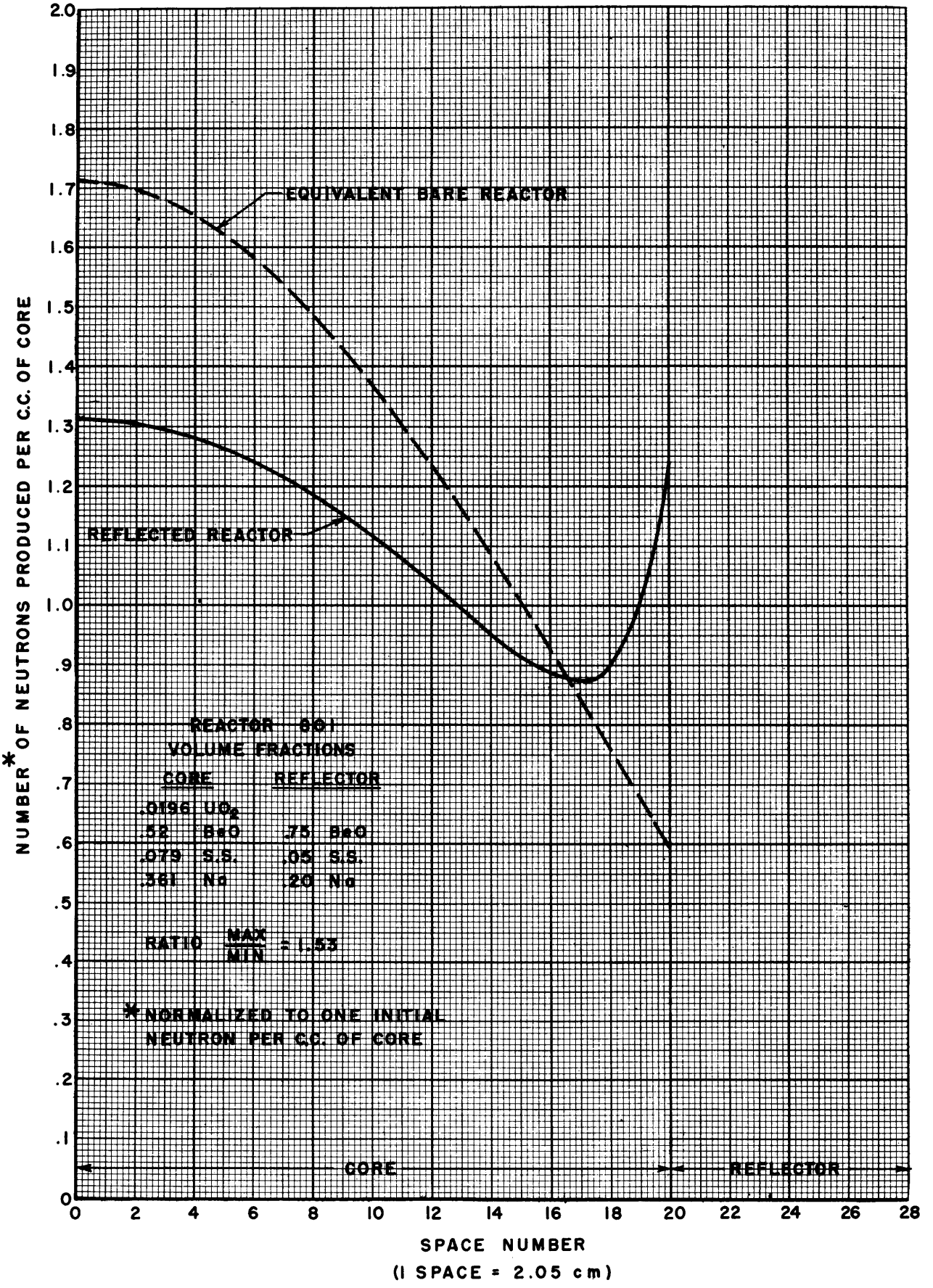

FIGURE 2.16 POWER PRODUCTION

~~SECRET~~

DRAWING NO. 10234

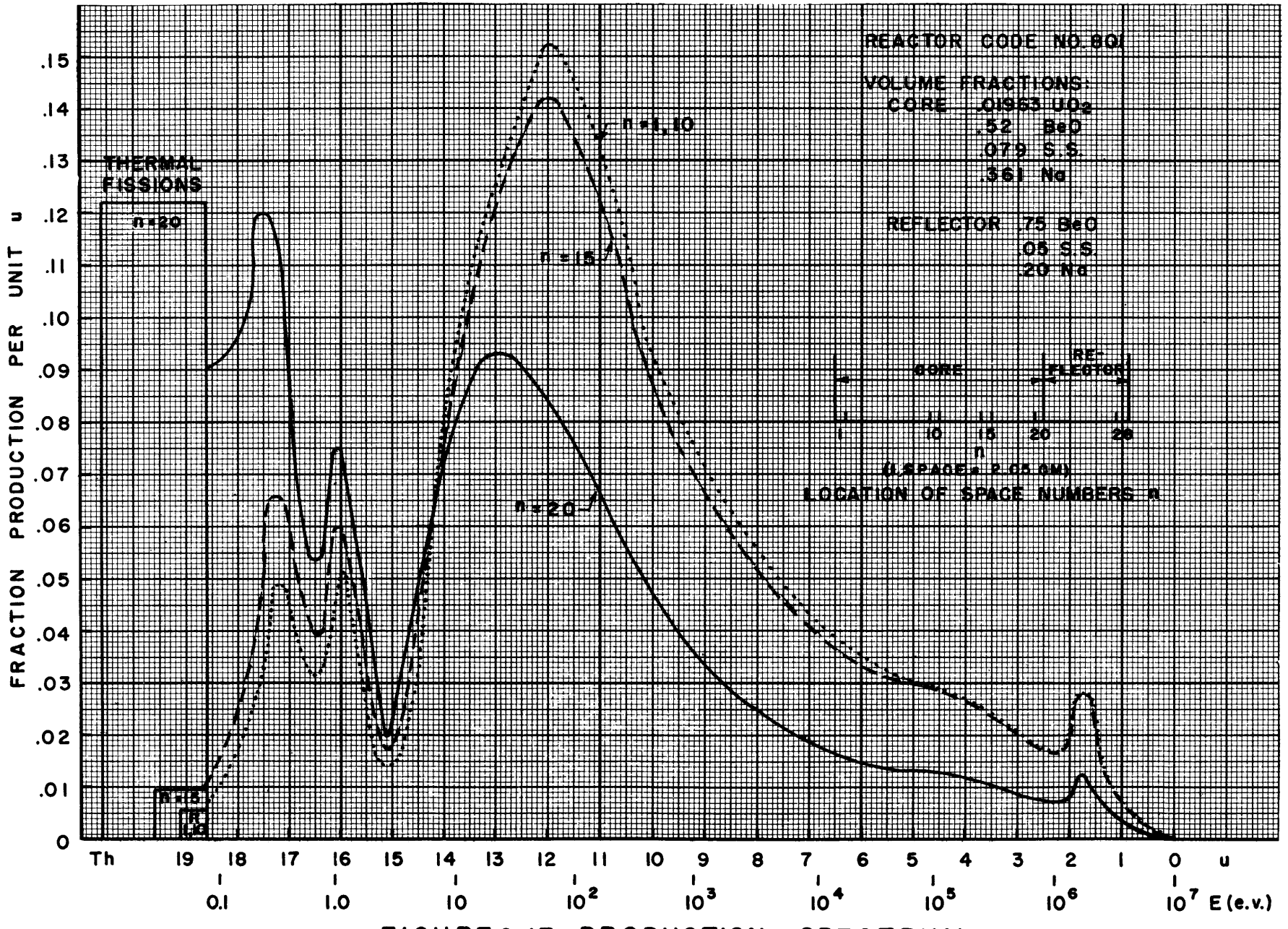

FIGURE 2.17 PRODUCTION SPECTRUM

total production spectrum (Fig. 2.18) would be large for the reflected reactor, will actually be most important out near the reflector. Thus the total xenon effect will be greater in the reflected reactor than in the bare (because of the larger number of thermal fissions), but this is mitigated by the fact that in the reflected reactor the xenon is produced out near the reflector, where neutron absorptions are less important to the overall reactivity.

The interesting feature of the curve (Fig. 2.19) of the fraction of the neutrons which escape from the reactor in each group is the very high leakage in group 4. This is a real effect resulting from a dip in the BeO scattering cross section in that energy range.

Reflector Saving Computations. In order to check the reflector saving which has been assumed in the calculation of equivalent bare reactors, three bare reactors having the same composition as the core of the reflected reactor were computed with the following results:

(1) 2.68 ft plus 10 cm shell for reflector savings plus 2 cm shell for extrapolation distance $k_{eff} = 0.943$.

(2) 2.68 ft plus 12 cm shell for reflector savings plus 2 cm shell for extrapolation distance, $k_{eff} = 0.982$.

(3) 2.68 ft plus 15 cm shell for reflector savings plus 2 cm shell for extrapolation distance $k_{eff} = 1.035$. Evidently the reflector savings for this reactor is about 15 cm, nearly equal to the reflector thickness.

The second reactor computed by the IBM group is the same as the first except for the total amount of uranium, which is 100 lb as compared to 120 lb for the first reactor (corresponding to the 1.96% UO_2 listed on p. 62). The k_{eff} for the second reactor is 1.0065; the two values allow the following preliminary estimate of the relationship between the k_{eff} and the mass of uranium:

$$\frac{\delta k_{eff}}{k_{eff}} = 0.18 \frac{\delta M_v}{M_v}$$

Future Program. The immediate program for the IBM group is the investigation of UO_2—BeO—Na—stainless steel reactors, with the following goals:

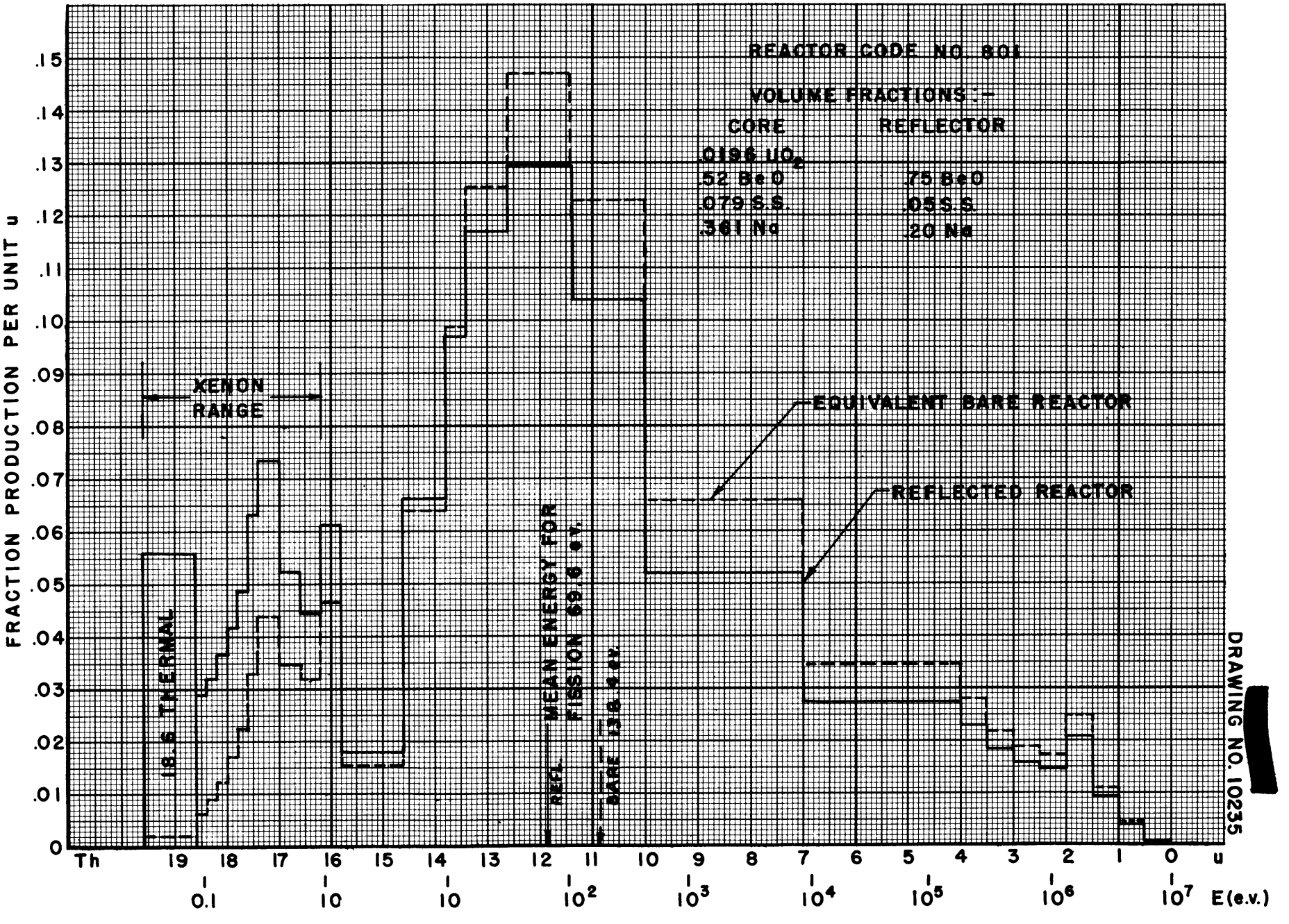

FIGURE 2.18 PRODUCTION SPECTRUM

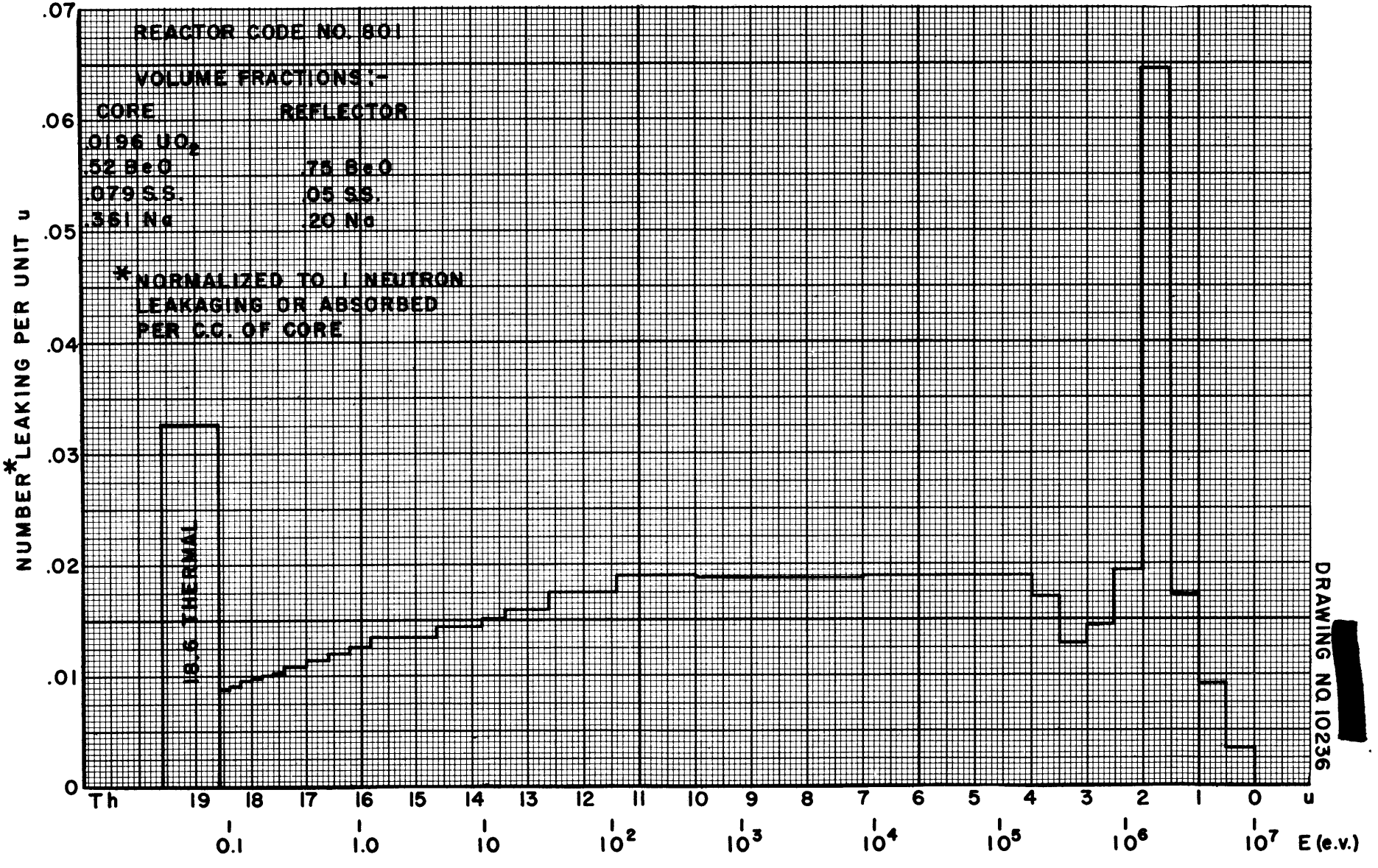

FIGURE 2.19 LEAKAGE SPECTRUM

1. Establish the optimum reflector thickness.

2. Obtain the relationship between the change in uranium mass and the change in k_{eff}

3. Establish the optimum core size and moderator percentage for meeting the requirements that the solid-fuel reactor be

   a. Large enough to allow sufficient heat extraction,

   b. Small enough to keep the shield weights within required limits, and

   c. Fast enough that the xenon parts of the temperature coefficients are tolerable, and that the reactor has optimum median energy of fission-production spectrum from control requirements.

4. Estimate the xenon effect on k_{eff} and temperature coefficient of reactivity.

5. Perform calculations which will permit an estimate of the errors involved in the approximations of the multigroup method.

D. KINETICS OF LIQUID-FUEL REACTORS

Perturbation Calculations[9] (N. M. Smith, Jr.). Perturbation calculations of the kinetic response of a liquid-fuel reactor have been initiated. Such calculations are useful in searching for instabilities, for surveying a broad field for desirable characteristics, and for general self-education into reactor kinetics. Space does not permit the detailed description of the calculations, but these may be obtained from the reference. Furthermore, the physical data on heat transfer, expansion coefficients, and heat capacity of the $NaF-BeF_2-UF_4$ systems are not available at the time of the preparation of this report. Hence the results described must be considered largely as illustrative.

The standard method of calculation was followed as used by Nordheim in his first calculations of xenon effects. The present reactor is complicated by having reactivity coefficients associated with the temperature and density of the moderator, the density of the liquid fuel, and, in the high-spectrum reactors, a coefficient associated with the density of the coolant. The

(9) This describes the beginning of a series of exploratory perturbation calculations to be made on reactor kinetics. The parts will be published separately, with very limited distribution as the calculations proceed and later collected together in one publication with more extensive distribution. The work described here will be included in Y-F10-30 (ANP memorandum at Oak Ridge National Laboratory, Y-12 Site), *Perturbation Equations for the Kinetic Response of a Liquid-fuel Reactor*, by N. M. Smith, Jr., T. Rubin, M. J. Nielsen, and R. R. Coveyou. Copies of any ANP Physics Group report may be obtained by an authorized person by request from the ANP Library.

thermal relaxation time of the liquid fuel and containing tube is small, with estimates varying, from one design to another, from 0.3 to 0.09 sec; that of the moderator is larger, with estimates from 5 sec to many tens of seconds. The situation is further complicated by the possibility of neutron flux thermal elastic oscillations of the tube and liquid fuel systems in a single tube, and, since the tubes may be connected by a header at top and bottom, of space-modal neutron flux elastic oscillations. Still further complications arise from the movement of fuel and fission poisons from regions of one importance to another.

Obviously, no attempt is made to consider all these effects simultaneously at first, but, through a series of increasingly realistic approximations, they are added one by one. The reference report contains equations for reactor impedance, including contributions of delayed neutrons, fuel response, moderator response, xenon poisoning, and temperature coefficient and provides for reactor admittance calculations for control rod and for coolant temperature perturbations.

The chief interest is in the characteristics of a three-medium system, with coefficients of reactivity associated with the temperatures of the moderator and of fuel only. The following constants were calculated, estimated, or assumed for the 70 lb uranium—70% BeO 3-ft bare reactor:

	FUEL	MODERATOR
Thermal relaxation time (sec)	0.25	5.0
Total heat capacity (cal/°C)	2.5×10^4	2.4×10^5
Temperature rise rate in absence of coolant (°C/sec)	1800	12
Reactivity coefficient (per °C)	-3.3×10^{-5}	-3.6×10^{-5}
Cooling capacity (cal/°C/sec)	3.1×10^5	
Integrated flux (neutrons/cm^2/sec)	3.1×10^{15}	
Neutron lifetime (sec)	2.5×10^{-5}	

For these constants the temperature increase over the operating temperature of the liquid fuel following a step change in reactivity of 10^{-3} and in the absence of delayed neutrons and xenon effects is shown to be, in degrees centigrade,

$$\theta_1'(t) = 16.22 + 13.87e^{-0.3597t} - 30.10e^{-0.4422t} \cos(48.54t + 0.002255)$$

This expression is plotted in Fig. 2.20.

The accompanying integrated excess flux is shown to be given by

$$\phi' = 2.70 \times 10^{13} + 2.02 \times 10^{13}e^{-0.3597t} + 2.59 \times 10^{15}e^{-0.4422t} \sin(48.54t - 0.01818)$$

and is plotted in Fig. 2.21.

Both θ_1' and ϕ' are inversely proportional to the neutron lifetime. It is therefore advantageous to have as long a lifetime as possible. The lifetime in a reflected reactor, particularly in a moderating reflector, will be considerably increased over the corresponding value in the "equivalent" bare reactor (i.e., a bare reactor of the same composition as the core of the reflected reactor but increased in size until its reactivity is that of the reflected reactor). The lifetime also is greater in the reactors of lower median fissioning energy. As the reactor is made more nearly thermal, however, the xenon fission poison introduces a positive temperature coefficient of reactivity associated with the moderator.

This positive coefficient is tolerable or not, depending on the thermal relaxation time of the moderator (i.e., the average time required to each equilibrium after a thermal transient). If this time is short compared to the response time of the liquid-fuel-level—temperature-sensing control system, then a positive coefficient of reactivity associated with the moderator is not allowable. However, if this relaxation time is long, a temperature-sensing servo-control system will have adequate time to act. Such a reactor would not be self-regulating in the broad sense but only within a time defined by the moderator thermal relaxation time. Indeed, it is true that there is no meaning to a "completely self-regulating reactor." The so-called "self-regulating features" designed in systems are merely characteristics which allow the requirements of the external servo-control systems to be relaxed to such an extent that control is simple and safe.

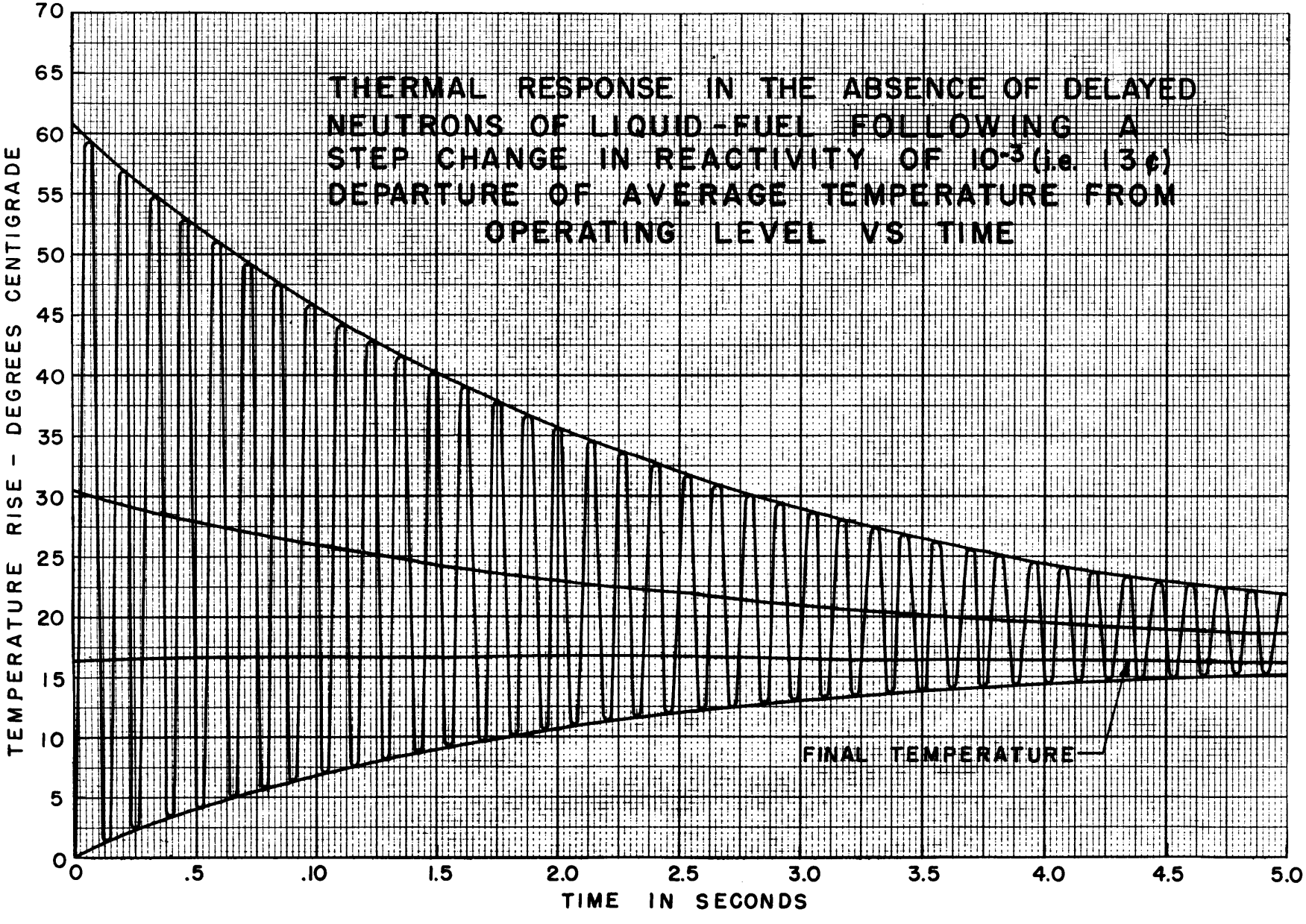

FIGURE 2.20

DRAWING NO. 10237

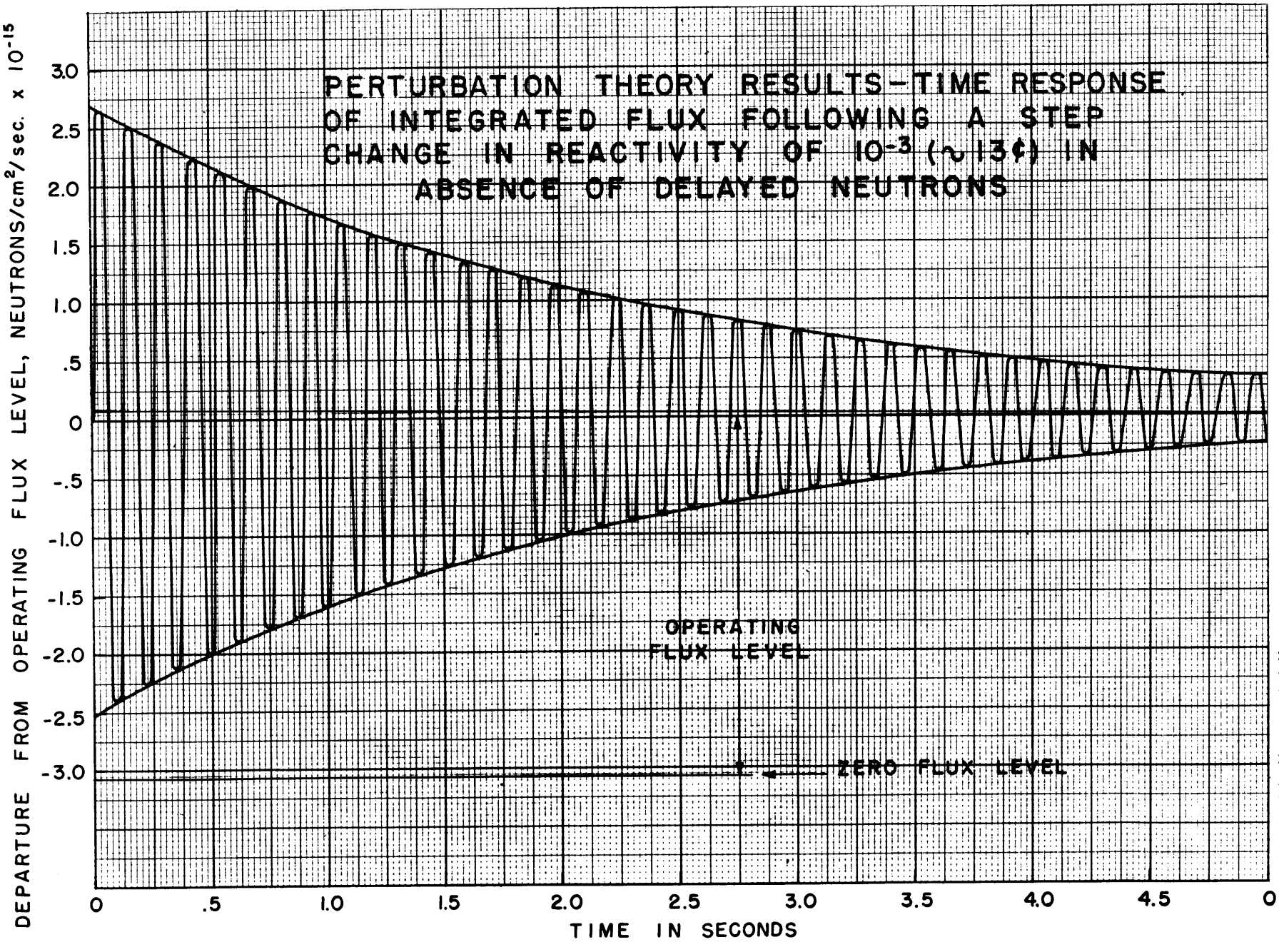
PERTURBATION THEORY RESULTS-TIME RESPONSE OF INTEGRATED FLUX FOLLOWING A STEP CHANGE IN REACTIVITY OF 10^{-3} (~13¢) IN ABSENCE OF DELAYED NEUTRONS
DEPARTURE FROM OPERATING FLUX LEVEL, NEUTRONS/cm²/sec. x 10^{-15}
3.0
2.5
2.0
1.5
1.0
.5
0
-.5
-1.0
-1.5
-2.0
-2.5
-3.0
OPERATING FLUX LEVEL
ZERO FLUX LEVEL
0
.5
1.0
1.5
2.0
2.5
3.0
3.5
4.0
4.5
0
TIME IN SECONDS
DRAWING NO. 10238

FIGURE 2.21

It is not yet clear what combination of fissioning spectrum, neutron lifetime, xenon effect, etc., will yield an optimum system for control. The discovery of these specifications is the objective of the present course of calculations. It is apparent, however, that the optimum exists and may well be in the direction of the epithermal reactor. Other considerations, such as shield size and weight, may, of course, affect these specifications. The possibility of compensation of a positive xenon coefficient by means of an external mechanical-thermal system exists.

The perturbation calculations are being extended to include:

1. An average group of delayed neutrons.
2. Xenon poisoning.
3. Response to ramp changes of control rod or of entrance coolant.
4. Coolant loop and ramp changes of power demand.
5. Mechanical-elastic response of the liquid-fuel system.

The exact integration of the equations of motion for large perturbations is the subject of a separate investigation.

Thermal Relaxation Time for Fuel Rods (T. Rubin, NEPA). An important quantity in determining the kinetic response of a reactor is the time it takes for a fuel rod to reach temperature equilibrium after having been subjected to a change in flux. This quantity is determined by considering the following heat conduction problem:

A cylinder has finite radius and an initial temperature $v = 0$; heat is produced for time $t > 0$ at the constant rate A_0 per unit volume per unit time; the surface of the cylinder is kept at constant temperature $t = 0$. The solution given[10] is

$$\frac{v}{A_0} = \frac{a^2 - r^2}{4K} - \frac{2}{aK} \sum_{n=1}^{\infty} e^{-k\alpha_n^2 t} \frac{J_0(r\alpha_n)}{\alpha_n^3 J(a\alpha_n)} \qquad (1)$$

(10) Carslaw, H. S., and Jaeger, J. C., *Conduction of Heat in Solids*, p. 277, Oxford, Toronto, 1947.

where v = temperature of cylinder at radius r and time t

K = thermal conductivity

a = radius of cylinder

k = diffusivity of material; $k = K/\rho c$, where ρ = density and c = specific heat

α_n = roots of the equation $J_0(a\alpha_n) = 0$

The temperature of a cylindrical fuel rod, when subjected to a step increase in power, due to an increase in flux, and whose walls are kept at constant temperature by coolant flow, would respond in the manner given by Eq. (1). Note that changing the boundary condition to $v(t = 0) = a > 0$ and $v(r = a) = b > 0$, where a and b are constants, introduces only slight modifications into the given solution of the problem.

Included in this report are plots, Fig. 2.22, of v/A_0 for a given r as a function of time for a fuel rod whose radius is 0.13 cm and which consists of a mixture of UO_2 and BeO. Also included is a plot, Fig. 2.23, of v/A_0 as a function of time, where

$$\frac{v}{A_0} = \frac{2}{A^2} \int_0^a \frac{v}{A_0} r \, dr$$

The time constant for the fuel rod is computed from the following equation:

$$\lambda_0 = \frac{\int_0^\infty [\bar{v}(\infty) - \bar{v}(t)] t \, dt}{\int [\bar{v}(\infty) - \bar{v}(t)] \, dt}$$

The time constant was found to be 0.09 sec. Note that λ_0 does not depend on the magnitude of A_0.

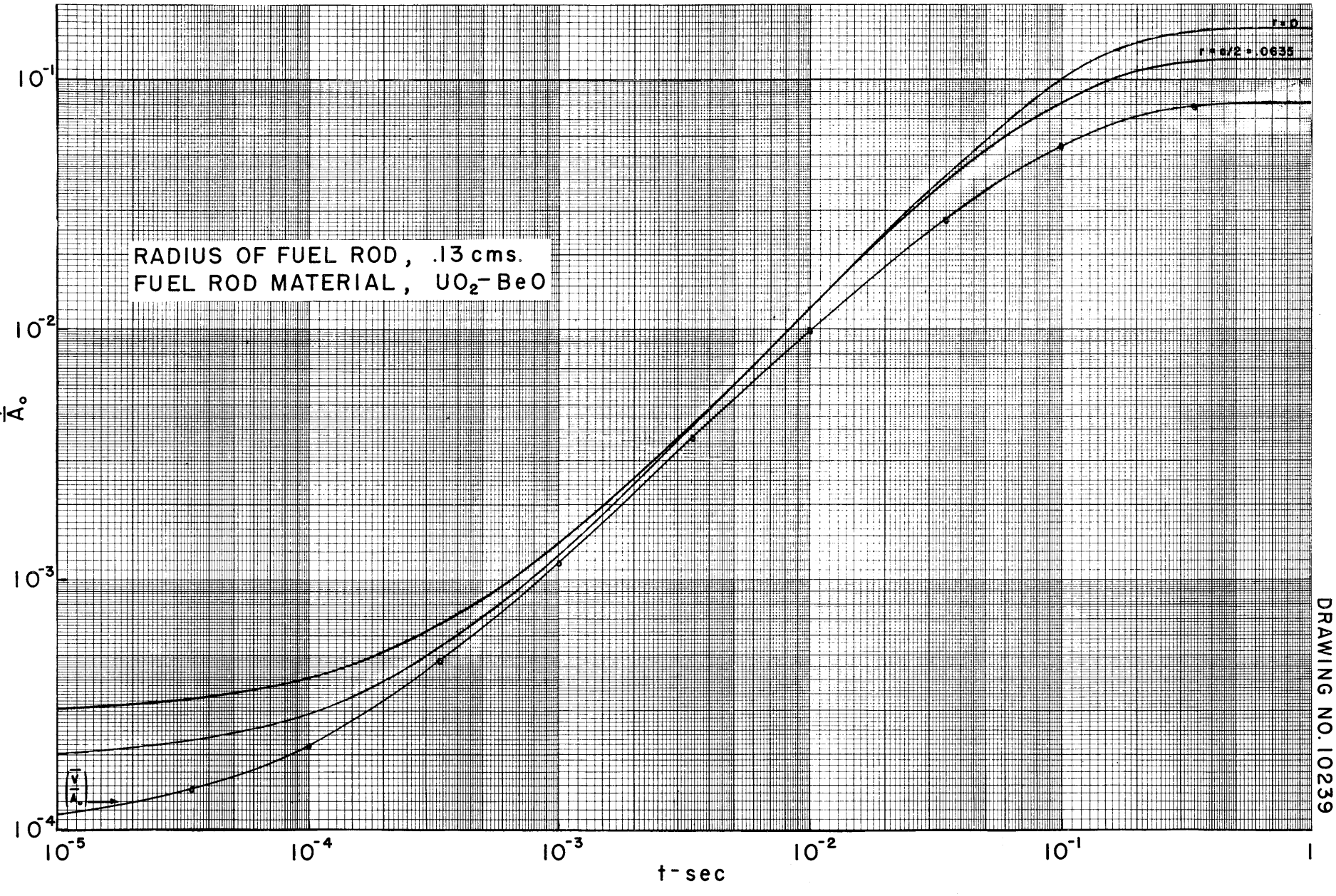

77

DRAWING NO. 10239 [redacted]

FIG. 2.22 $\left(\frac{\overline{V}}{A_o}\right)$ AND $\frac{V}{A_o}$ VS. TIME IN FUEL ROD

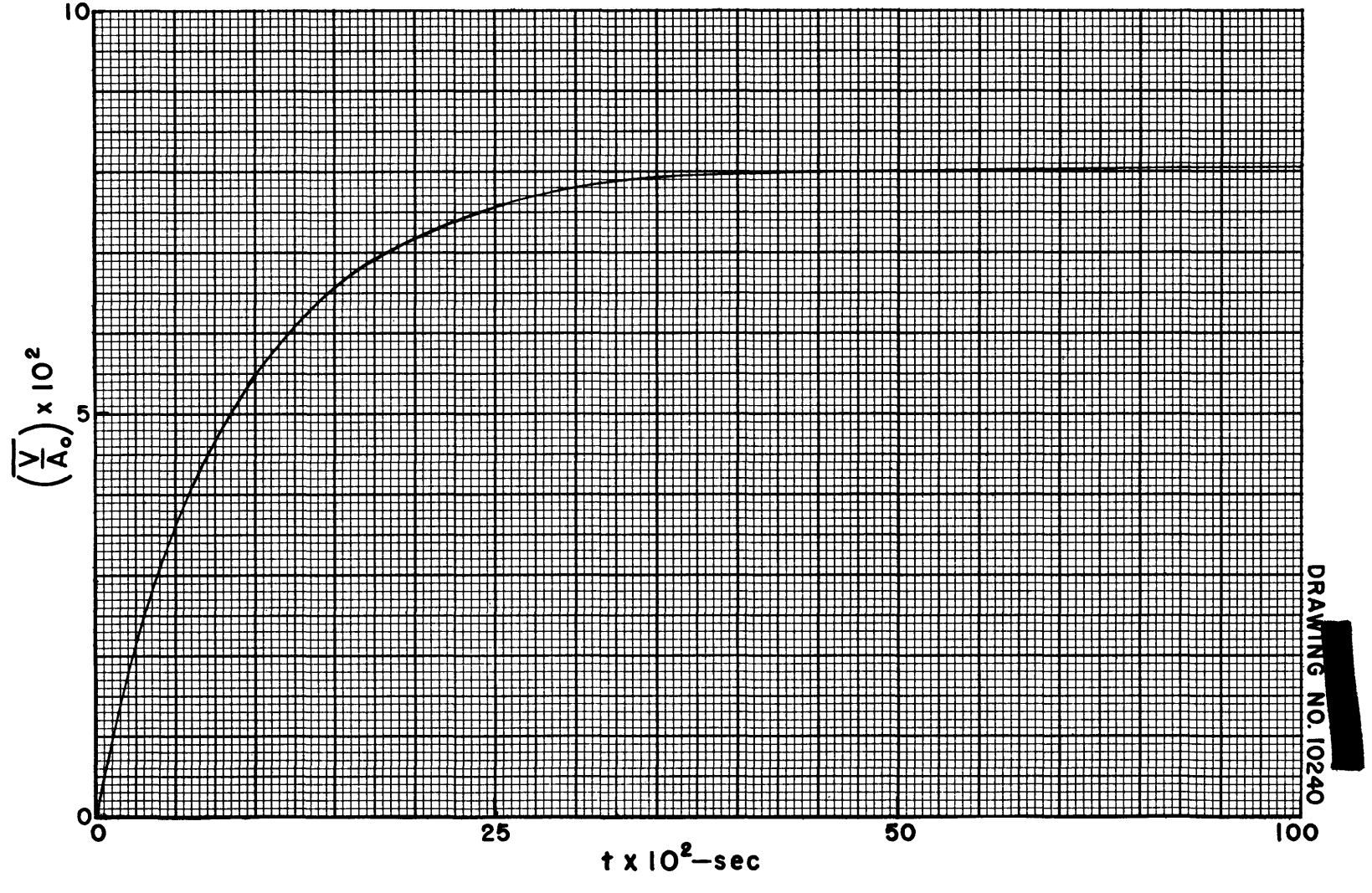

FIGURE 2.23 AVERAGE TEMPERATURE IN FUEL ROD VS. TIME

In an attempt to determine the time of response of the moderator to a sudden power increase, the following analogous heat conduction problem has been solved:

Two concentric cylinders of radius a and b ($b > a$), respectively, are initially at temperature $v = 0$. A sudden uniform and steady source of A_0 units of heat per cubic centimeter per second is initiated at time $t = 0$ in the interior cylinder. The following boundary conditions are imposed on the solution:

(1) At $r = a$, $\quad v_1 = v_2$ and $K_1 \, dv_1/dr = K_2 \, dv_2/dr$

(2) At $r = b$, $\quad dv_2/dr = 0$

The symbols have previously been defined. It is necessary only to note that subscript 1 refers to fuel and subscript 2 to moderator.

Note that boundary condition (1) means that, in this approximation, the fuel rod is assumed to be in direct contact with the moderator and that contact resistance is neglected. Therefore the resultant calculated time constant is expected to be shorter than the actual case, in which there is coolant flowing between moderator and fuel rod.

The fuel rod—moderator system considered in the problem was a typical "cell" of the reactor. Boundary condition (2) is a statement that the solution in this cell repeats itself in the other units.

The solution obtained is

$$\frac{v_2}{A_0} = \frac{K_1 k_2 a^2 t}{K_1 k_2 a^2 + K_2 k_1 (b^2 - a^2)}$$

$$+ 2k_1 k_2^{1/2} \sum_{n=0}^{\infty} \left\{ \frac{1 - e^{-a_n^2 t}}{a_n} J_1(\epsilon a_n) \left[J_1(\eta a_n) \, Y_0\left(\frac{a_n}{k_2^{1/2}} r\right) - Y_1(\eta a_n) \, J_0\left(\frac{a_n}{k_2^{1/2}} r\right) \right] \right\}$$

where the a_n's are the roots of the following equation:

$$K_1 k_2^{1/2} J_1(\mu u)\{J_1(\eta a)\, Y_0(\epsilon u) - J_0(\epsilon u)\, Y_1(\eta u)\}$$

$$+ K_2 k_1^{1/2} - J_0(\mu u)\{J_1(\epsilon u)\, Y_1(\eta u) - Y_1(\epsilon u)\, J_1(\eta u)\} = 0$$

and where

$$\epsilon = \frac{a}{k_2^{1/2}} \qquad \eta = \frac{b}{k_2^{1/2}} \qquad \mu = \frac{a}{k_1^{1/2}}$$

Numerical work will soon be in progress to determine the quantities that were obtained for the fuel rod.

E. BACKGROUND PROBLEMS

Effect on Cross Sections of Atomic Motion* (R. R. Coveyou, Mathematics Panel). In this and succeeding studies methods will be set down for taking into account the effect on various diffusion phenomena of the finite velocity of the atoms of the medium in which neutrons are diffusing. This first study will concern itself with the effect of this motion on values of nuclear cross sections.

Consider a neutron of speed s in collision with an atom of speed t, selected out of a distribution isotropic in direction. Then the relative speed of neutron and atom is given by

$$r^2 = s^2 + 2\lambda s t + t^2$$

* To appear later as part of another report.

where r is the relative speed and λ is the cosine of the angle between the velocities. Denoting by $P(X)$ the probability of the event described by X, we have

$$\begin{aligned} P(r \leqslant x) &= P(r^2 \leqslant x^2) \\ &= P(s^2 + 2\lambda s t + t^2 \leqslant x^2) \\ &= P\left[\lambda \leqslant \frac{x^2 - s^2 - t^2}{2st}\right] \end{aligned}$$

By the hypothesis of isotropy, λ is uniformly distributed on $(-1, 1)$. Hence,

$$P_t(r \leqslant x) = \frac{1}{2}\left[1 + \frac{x^2 - s^2 - t^2}{2st}\right], \qquad s - t \leqslant x \leqslant |s + t| \tag{3}$$

or

$$P_t(x \leqslant r \leqslant x + dx) = \frac{x\,dx}{2st}, \qquad |s - t| \leqslant x \leqslant |s + t| \tag{4}$$

Now suppose the distribution of atomic speeds is Maxwellian, i.e.,

$$P(Z \leqslant t \leqslant Z + dZ) = \frac{4\beta^3}{\sqrt{\pi}} Z^2 e^{-\beta^2 Z^2}\, dZ \tag{5}$$

where $\beta^2 = M/2kT$, M is the atomic mass, k is Boltzmann's constant, and T is the absolute temperature.

Then the distribution of relative speeds "seen" by a neutron of speed S is in this case given by

$$P(x \leqslant r \leqslant x + dx) = \int \frac{x\ dx}{2st} \frac{r\beta^3}{\sqrt{\pi}} t^2 e^{-\beta^2 t^2}\ dt \qquad (6a)$$

where the integration is with respect to t and the limits are given by $|s - t| \leqslant x \leqslant |s + t|$. But this is the condition that x, s, and t form a triangle, hence is symmetric and can be written $|s - x| \leqslant t \leqslant |s + x|$. Thus,

$$P(x \leqslant r \leqslant x + dx) = \frac{\beta x\ dx}{\sqrt{\pi}\ s} \int_{|x-s|}^{|x+s|} (2\beta^2 t\ dt) e^{-\beta^2 t^2}$$

$$= \frac{\beta x\ dx}{\sqrt{\pi}\ s} \left[e^{-\beta^2 (x-s)^2} - e^{-\beta^2 (x+s)^2} \right] \qquad (6b)$$

Suppose now that the cross section for a given process is $\sigma(s)$, as a function of relative speed. Let $\sigma^*(s)$ be the effective cross section for this process as a function of neutron speed. Then,

$$\sigma^*(s) = (\beta/\sqrt{\pi}\ s) \int_0^\infty x\ \sigma(x) \left[e^{-\beta^2 (x-s)^2} - e^{-\beta^2 (x+s)^2} \right] dx \qquad (7)$$

If

$$\sigma(s) = \frac{\sigma_0 s_0}{s} \quad (1/v \text{ absorption})$$

then

$$\sigma^*(s) = \frac{\sigma_0 s_0}{s} \left[\frac{2}{\sqrt{\pi}} \int_0^{\beta s} e^{-u^2} \, du \right]$$

$$= \frac{\sigma_0 s_0}{s} \text{ erf } (\beta s)$$

Since erf $(Z) \longrightarrow 1$ as $s \longrightarrow \infty$, this states that the cross section at high neutron volocities is unaffected, as would be expected. If

$$\sigma(s) = \sigma_0 \delta(s - s_0) \quad \{\text{sharp resonance}\}$$

then

$$\sigma^*(s) = \frac{\beta \sigma_0 s_0}{\sqrt{\pi}} \left[\frac{e^{-\beta^2 (s-s_0)^2} - e^{-\beta^2 (s+s_0)^2}}{s} \right]$$

The effective cross-section curves have been calculated for the case of a material of atomic weight 135 and a sharp resonance at 0.0863 ev, at temperatures 300, 1000, and 1500°C (see Fig. 2.24). We note that the maximum of the effective curve always lies below the resonance energy, though the displacement is negligible in the cases considered.

For other cross-section curves $\sigma^*(s)$ can be computed by numerical integration. Existing measurements of cross sections made at room temperature, such as the xenon absorption resonance, can be taken and Eq. (7) can be written as a matrix. Inversion of the matrix by machine computational methods will,

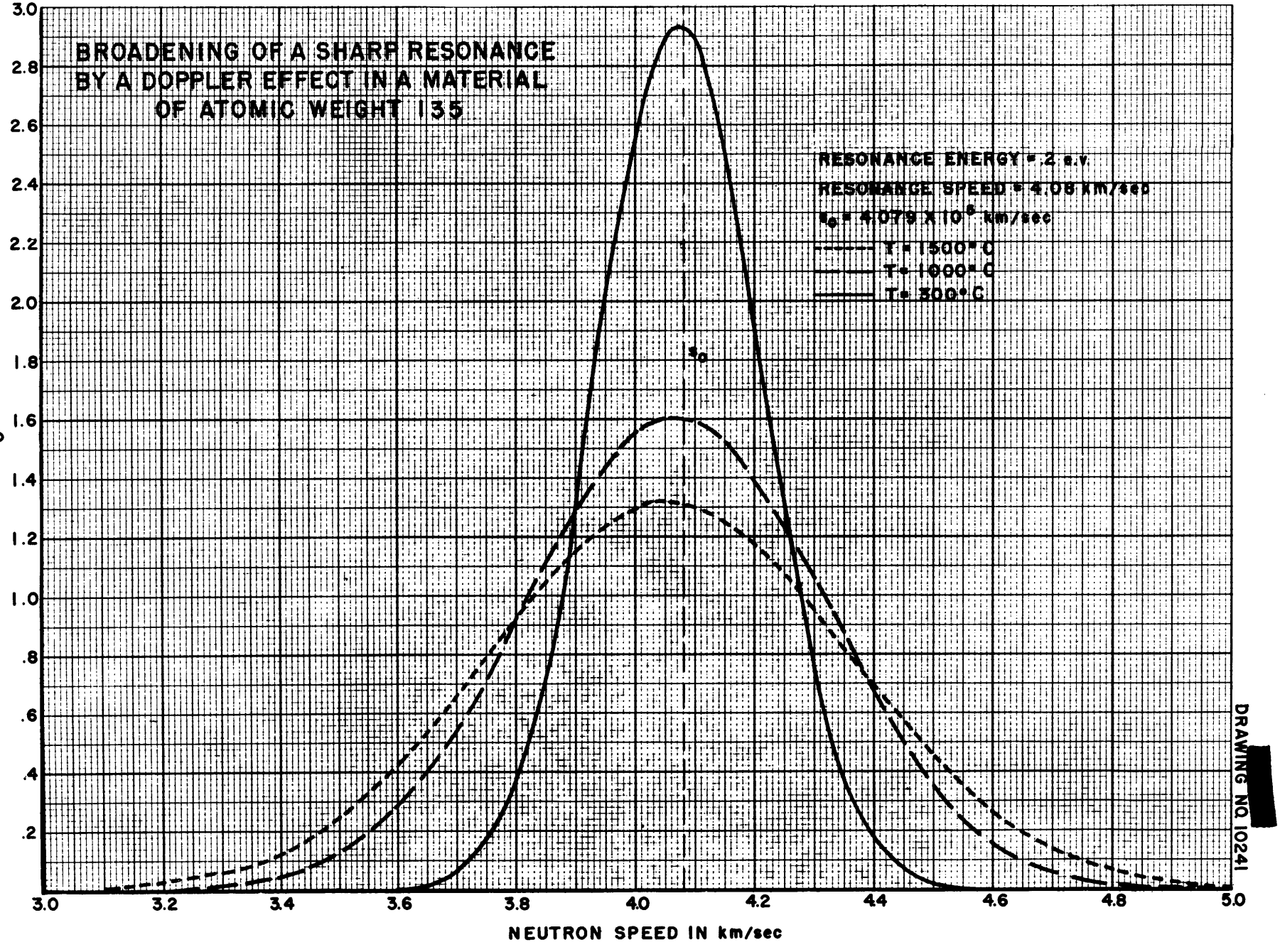

FIGURE 2.24

DRAWING NO. 10241

in principle, give the true cross section. The xenon resonance, for instance, may be somewhat narrower than that given in the published curves. A narrower xenon resonance would produce a larger positive temperature coefficient of reactivity.

Adjoint Fluxes and perturbation Theory (M. J. Nielsen, USAF). For each of the family of bare reactors discussed above, the differential equation adjoint to the assumed reactor equation was solved numerically. In solving the adjoint equation, the probability that the ultimate fate of a neutron in the reactor is to cause a fission is computed as a function of energy. This permits the assignment to various neutron groups of an "importance to the reactor" parameter. In addition, using first-order perturbation theory, the change in reactivity resulting from small changes in the pile parameters such as size and fuel content can be computed. (Since most perturbation calculations for the bare reactor involve approximately the same labor as an additional reactor calculation, this use of the adjoint function has so far been very limited.) The adjoint solution also yields a numerical check on the determination of k_{eff}. Calculations of the reactors in the preceding section were checked in this manner.

The lifetimes given above were computed in the standard manner as perturbation calculations by assuming that for $k_{eff} = 1 + \Delta k$, the neutron density as a function of time is given by

$$n(t) = n(0)e^{(\Delta k/l)t}$$

where l is the lifetime. Then

$$\frac{\partial n(t)}{\partial t} = \frac{\Delta k}{l} n(t) = \frac{1}{v}\frac{\Delta k}{l}\phi$$

where $\phi = nv$, the neutron flux. The quantity $\frac{1}{v}\frac{\Delta k}{l}$ is then regarded as a perturbation on the absorption cross section of the pile and the corresponding reactivity change is computed, giving

$$\Delta k = (\text{constant}) \frac{\Delta k}{l}$$

The constant is in the form of a definite integral which can be evaluated numerically, giving the lifetime directly.

As part of a computational handbook the derivation of the bare-pile adjoint equation and equations for all types of perturbations as integral equations and as difference equations are assembled in report Y-F10-18.[11] Other references are given.[12-14] A compilation of methods planned for multiregion piles is in preparation. The slowing-down density, the importance function, and the statistical weight for the 2.79-ft reactor are shown in Fig. 2.25 as a function of energy. The slowing-down density is the number of neutrons per unit of lethargy slowing down in unit time. The importance function is the net increase in neutron inventory resulting from the introduction of one neutron. The curve labeled "statistical weight" is the product of the other two curves. The ordinate scale is for the importance function.

Cylindrical Multigroup Calculations (M. C. Edlund and T. Rubin). The multigroup age equations have been transformed into difference equations in cylindrical geometry.[15] Hand calculations are now in progress to check the method prior to setting up the problem for the IBM. A satisfactory approximation to the correct boundary conditions for this geometry has not yet been found.

F. CALCULATIONS FOR THE CRITICAL EXPERIMENT

It is planned that the ANP Physics Group will devote considerable time in the future to calculations pertaining to experiments with the critical assemblies. The principal activity will be devoted to interpretation of results from the critical experiments, guiding the experiments so that the results will be useful and interpretable, and using the experiments to check present calculational techniques. Some effort has already been made toward selecting the first few experiments to be of sufficiently simple geometry that a reliable comparison can be made using the IBM calculation.

(11) Nielsen, M. J., *Bare Pile Adjoint Solution,* Oak Ridge National Laboratory, Y-12 Site, Y-F10-18 (Oct. 27, 1950).

(12) Goertzel, G., "Variational Derivation of Adjoint Function and Perturbation Equation," Appendix, p. 13, in *Numerical Integration of Criticality Equations and Use of Perturbation Theory for Bare Intermediate Reactors,* by A. R. Gruber, Oak Ridge National Laboratory, Y-12 Site, TAB-96 (Aug. 15, 1950).

(13) Nordheim, L. W., and Soodak, H., *Application of the Rayleigh-Schroedinger Perturbation Method to the Theory of Piles,* Chicago CP-1638 (June 15, 1944).

(14) Wigner, E. P., *Effect of Small Perturbations on Pile Period,* Chicago CP-G-3048 (June 13, 1945).

(15) Edlund, M. C., *Numerical Integration of the Multigroup Reactor Equations in Cylindrical Geometry,* Oak Ridge National Laboratory, Y-12 Site, Y-F5-22 (Sept. 27, 1950).

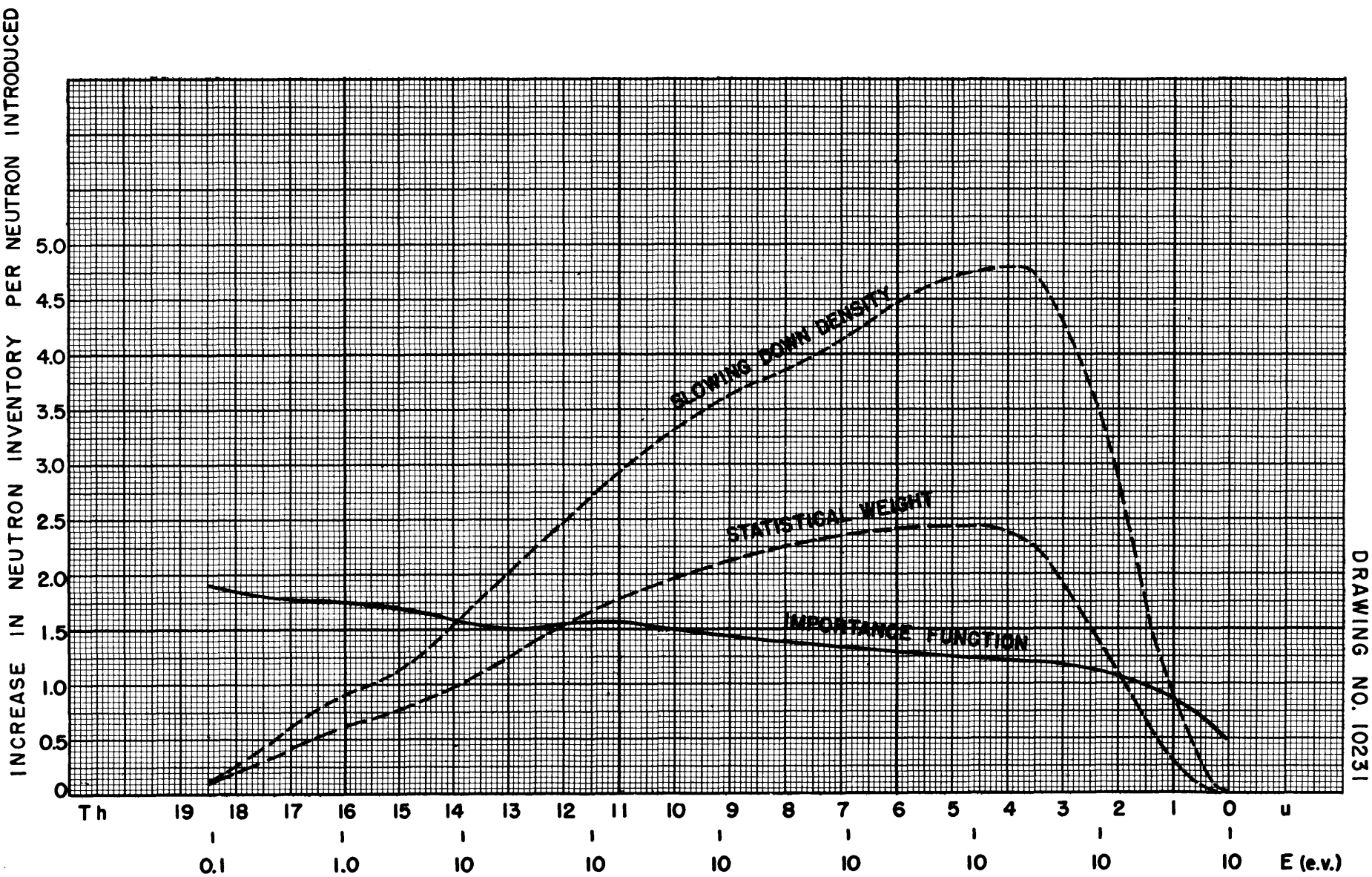

FIGURE 2.25 IMPORTANCE FUNCTION - 2.79 FT. REACTOR

3. CRITICAL EXPERIMENTS

3. CRITICAL EXPERIMENTS

A. D. Callihan, Physics Division, and J. F. Coneybear, NEPA

Preparations for joint ORNL-NEPA critical experiments have continued. The installation of equipment in the laboratory is almost complete, the major exceptions being the control and safety rods and the personnel shield. An allotment of uranium has been received and is in the process of fabrication. Some graphite has been received, and the beryllium is being machined. At the time of this writing it was expected that materials and equipment would be ready for the initial experiments about Jan. 1, 1951.

Conferences between ORNL and NEPA personnel have resulted in slight modifications in the initial program described in NEPA-1522. Owing to changes in the ARE design and a desire by the theoretical groups to check the accuracy of calculations, it is likely that the first assembly will be a simple lattice rather than one patterned after a particular ARE reactor. The initial experiments will be done with the moderator and reflector of graphite or beryllium, depending upon the materials on hand at the time the uranium is delivered. The median energy for fissions in the ARE design now considered is between 1 and 100 ev, probably closer to the former. This change has necessitated consideration of Xe^{135} danger-coefficient measurements.

The assembly tables which carry the reactor halves have been installed and are being tested. The aluminum honeycomb structure has been assembled on the tables and fixed into position in an iron framework. The mechanism for inserting a neutron source has been operated. Part of the support for a personnel shield for use during assembly operations has been placed. The control and safety rods have been built, but have not been installed in the assembly because of a delay in obtaining the supporting structure.

The actuating circuits for the table drive and for the control and safety rods have been assembled. Eight radiation-level-measuring circuits, used for safety and for operation, have also been installed. This equipment is being tested.

An allotment of 75 kg of enriched uranium has been made and is now being fabricated into fuel disks 0.01 in. thick. Beryllium is being cast and finish-machined by the Brush Beryllium Corporation. The delivery schedule calls for

500 lb to be shipped during December, 1950, and the total of approximately 2 tons to be delivered by March 1, 1951. The normal density of AGOT graphite (~1.6 g/cm^3) is being machined by the Y-12 Shop, and partial delivery has been made. Analysis of this graphite indicates acceptable purity.

Samples of the special high-density graphite (~2.0 g/cm^3) have been received but difficulties with the dies have delayed delivery. Analysis after fabrication of test samples indicates acceptable purity.

Since sodium is being considered as the coolant for the ARE it is necessary to investigate its effect in the critical experiments. It may be built into these experiments as NaF or as Na metal. Satisfactory samples of NaF, formed by either hot or warm pressing, have been received from two vendors. One vendor is considering canning sodium in type 304 stainless steel, 0.008 in. thick, and it is believed that the cans may be filled to at least 95% of their volumes.

Stainless steel, type 310, for the heavy-metal reflector studies, is now being fabricated in the Y-12 Shop, and spectrographic analyses have been made of the steel.

Conferences with the NEPA Materials Section concerning danger-coefficient samples have continued. It appears now that samples will be available by the time they are needed.

4. NUCLEAR MEASUREMENTS

4. NUCLEAR MEASUREMENTS

The cross-section curve of molybdenum, being determined at Columbia University, indicates a resonance at 49 ev. Consideration is being given to the measurement of the xenon cross section at intermediate energies, and consequently the practicality of the preparation of large xenon sources has been investigated. The chopper time-of-flight velocity selector for operation in this intermediate energy range is still under construction. The 5-Mev Van de Graaff accelerator may be in operation in three or four months.

MECHANICAL VELOCITY SELECTOR

G. Pawlicki and E. C. Smith, Physics Division

The chopper time-of-flight velocity selector for operation in the neutron energy region up to several thousand electron volts is still in the process of design and construction. Design of the rotor is complete, and construction has started in the shops. Construction of the rather elaborate electronic equipment is proceeding satisfactorily in the Instrument Shop. The BF_3-filled ionization chamber to be used for counting the transmitted neutrons is under preliminary test.

MOLYBDENUM CROSS-SECTION MEASUREMENTS

Columbia University*

The cross section of molybdenum is being measured at Columbia University by Prof. W. W. Havens. This measurement is of great interest to reactor engineers since molybdenum has not only exceptional high-temperature strength but also a relatively high resistance to liquid-metal corrosion. The nuclear requirement for aircraft reactors, however, is that the nucleus should have a reasonably low intermediate absorption cross section. A preliminary total cross-section curve, Fig. 4.1, of molybdenum indicates a resonance at 49 ev, with a height of a few barns. Higher resolution work is in progress, and more data are expected shortly.

* Work performed under contract with the AEC New York Operations Office.

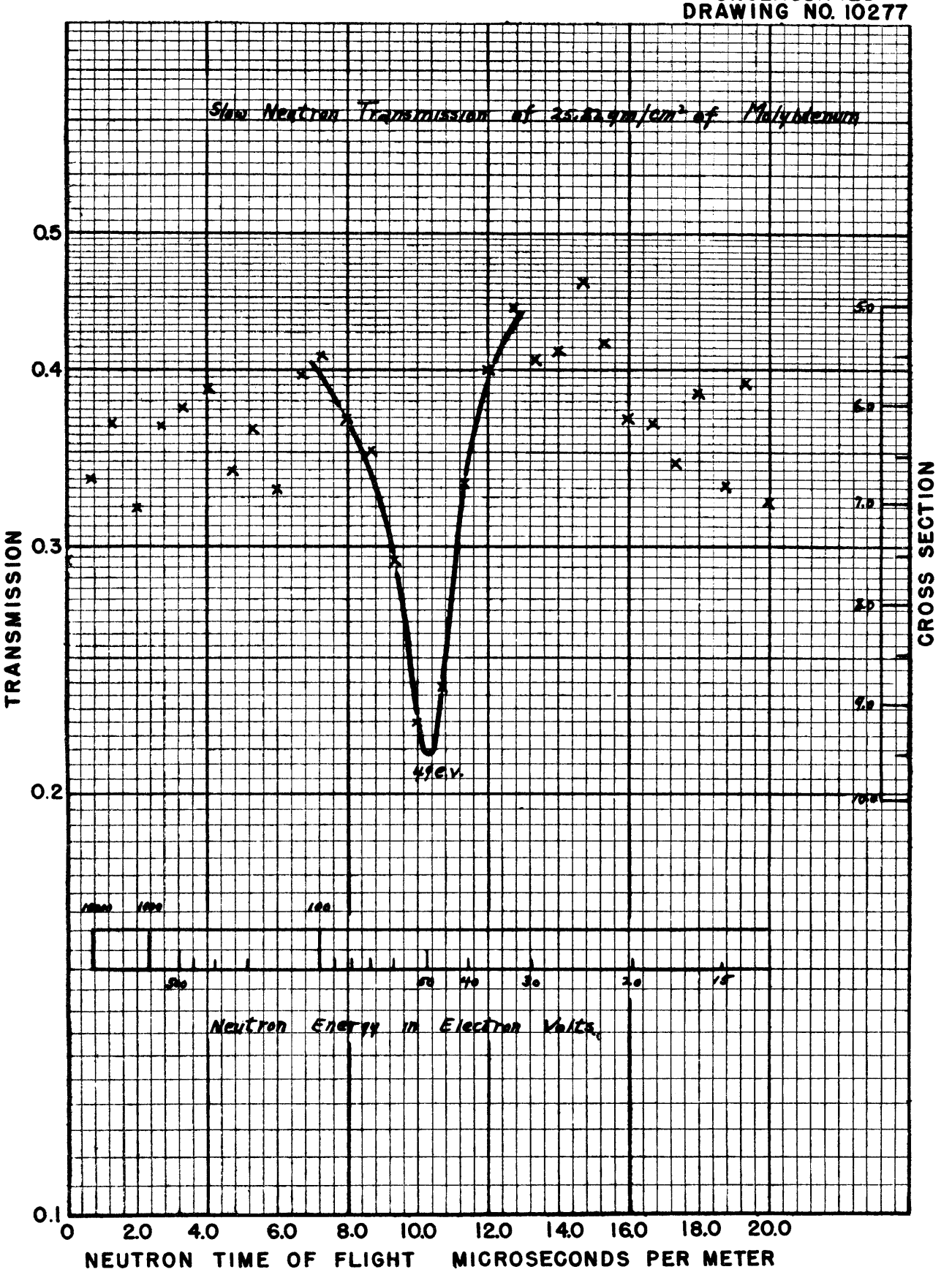

FIG. 4.1 PRELIMINARY TOTAL CROSS-SECTION CURVE OF MOLYBDENUM
(Measured at Columbia University by Professor W.W. Havens)

INTERMEDIATE XENON CROSS-SECTION MEASUREMENTS

During the past quarter some study has been given to the desirability and practicality of measuring the xenon cross section at somewhat higher energies than those reached in the previous ORNL work. Some rough calculations indicate that a danger-coefficient measurement might be possible if 1000 curies of xenon were available.[1] A study was therefore made by the Chemistry Division on the feasibility of preparing a xenon source of this magnitude. As described in the following section, it appears that such an operation would be possible, although it would require work on a rather large scale. However, some theoretical reasons have been advanced[2] for believing that the contribution of possible higher resonances to the resonance integral of xenon will turn out to be negligible in the region of interest for the ARE, compared to the tail of the known xenon absorption band. The matter is, therefore, being considered further before embarking upon such a large experimental program as would be required for complete exploration of this spectrum.

Practicality of Preparing Large Xenon Sources.[3] A xenon source of sufficiently high level may probably be realized from each of the following three reactors:

1. Low Intensity Training Reactor (LITR)
2. Hot Pilot Plant
3. Homogeneous Reactor Experiment (HRE)

The parameters pertinent to the production of xenon are summarized in Table 4.1 for each of these reactors.

Of the three methods for the production of xenon, the minimum yield, in curies, from the Hot Pilot Plant would be lower than desired, whereas that from the LITR should be adequate, and the yield from the HRE should be more than ample. In regard to availability, the production—essentially the collection—of xenon could probably be arranged to fit in with the current program of the Hot Pilot Plant. Neither the LITR nor HRE is now in operation,

(1) Weinberg, A. M., *Resonance Absorption by Xe*, CF 50-8-116 (Aug. 29, 1950).

(2) Arfken, G. B., Jr., and Welton, T. A., *Estimates of Effects of Higher Levels on the Resonance Integrals of* Xe^{135}, CF 50-12-25 (Dec. 6, 1950).

(3) From a letter of Dec. 15, 1950, from G. W. Parker to C. B. Ellis *re* high-level sources of 9.2-hr xenon, CF 50-12-45.

TABLE 4.1

High-level Sources of 9.2-hr Xenon

REACTOR	ESTIMATED POWER (kw)	PORTION AVAILABLE	HALFLIVES TO PROCESS	AMOUNT AT SATURATION (curies)	MAXIMUM YIELD (curies)
Hot Pilot Plant (Clinton Pile)	0.2/slug	100 slugs	2*	1000	200
Low intensity Training Reactor	300	1 of 18 elements	0.5**	1000	750
Homogeneous Reactor Experiment	1000	All	1***	40,000	20,000

* Type of process for Hot Pilot Plant slugs: (1) dissolution in HNO_3; (2) bulk gas fractionation

** Type of process for LITR element: (1) melting of unit in vacuum; (2) minor gas fractionation

*** Type of process for HRE off-gas: (1) collection of 24-hr gas sample; (2) minor gas fractionation

although preparations for placing the LITR in operation are proceeding rapidly. The HRE is expected to operate at low level in mid-1951, and full-level operation may possibly be reached by the end of 1951.

(1) *Low Intensity Training Reactor.* While the operation of the Low Intensity Training Reactor (LITR) has not yet been definitely settled with the Safeguards Committee, preparations for placing the reactor in operation are proceeding rapidly. A shield estimated to weigh at least 8 tons is necessary to safely handle a green fuel assembly of the size and activity required to produce the xenon. Since such a shield would be generally useful for other purposes, it has already been designed and is expected to be built soon.

It is anticipated that the element would be removed from the reactor after a short cooling period and transported quickly to the laboratory working area, where the xenon could be collected and purified by a relatively small charcoal bed and fractionating column. With a flux of 5×10^{12} neutrons per second the time after shutdown for maximum xenon growth has been calculated[4] as 4.2 hr, which is adequate for the required operations.

The amount of xenon available would be about 1 kilocurie at 300 kw at whatever flux at which the LITR may be operated. The processing time after the 4 hr growth period could be short, and the yield might therefore be as high as 80 to 90%.

(2) *Hot Pilot Plant.* The equipment (scrubbers, condenser, etc). now being installed in the Hot Pilot Plant for the absorption of the 10-year krypton of mass 85 from the off-gas stream of the dissolver operation will also concentrate xenon, although the latter is cooled to a stable gas in the process. The Pilot Plant may be mentioned as a possible source of 9.2-hr xenon if and when the problem of handling large quantities of oxides of nitrogen and foreign gases can be overcome. Conceivably, a fair portion of a 100-slug charge could be dissolved in 4 to 6 hr, and if the time for fractionation were not excessive, yields of 200 or more curies might be expected.

(3) *Homogeneous Reactor.* The most attractive prospect for future large-scale xenon work is the Homogeneous Reactor Experiment (HRE), from which a continuous flow of hydrogen, oxygen, and water vapor will sweep out kilocurie quantities of xenon and krypton. The off-gas treatment system now proposed includes a large charcoal bed, through which 40,000 curies of xenon will eventually be discharged after around 100 days of holdup for decay. In order to obtain similar quantities of xenon in a portable container, it would be necessary only to pass the off gas through a shielded charcoal cold trap and collect samples of the mixed gases which could then be purified. The equilibrium xenon activity of 40,000 curies will give off heat at the rate of 500 watts, thereby introducing an extra requirement for handling.

(4) Lane, J. A., *Xenon Poisoning at Varying Power Levels*, CF-49-12-83 (Dec. 14, 1949).

THE 5-MEV VAN DE GRAAFF ACCELERATOR

W. M. Good, Physics Division, and Conway Snyder, NEPA

A 5-Mev Van de Graaff accelerator, constructed by the High Voltage Engineering Corporation of Cambridge, Mass., has been purchased by NEPA. The final design has been approved, and delivery is expected in the immediate future. Upon receipt the accelerator will be erected in the Y-12 area. It is expected that a period of three months will be required to place it in operation, following which research will begin on shielding, radiation damage, and other problems in nuclear research pertinent to the nuclear propulsion of aircraft.

5. SHIELDING RESEARCH

5. SHIELDING RESEARCH

E. P. Blizard, Physics Division

During the past quarter the Shielding Groups at ORNL and NEPA collaborated in an effort to apply the available information to the actual design of several realistic aircraft shields. There resulted a number of configurations which were light enough to be highly interesting and sufficiently well founded in experiment to lend considerable confidence as to their adequacy. Iron and water shields were investigated in the Lid Tank, but to a limited extent only, since the shield weights appear to be excessive for these materials. The shielding properties of B_4C are currently being measured, and several interesting effects have been discovered with this material. Measurements using the liquid-metal duct are being made, but as yet no conclusions can be reached regarding its effectiveness in the shield. Completion of the new Bulk Shielding Facility has been delayed by the building contractor. The first test, probably of an ideal unit shield, will commence sometime in March. Some previous Lid Tank experiments on lead, iron, and water have now been analyzed according to simple theory. A more general approach to shield optimizing is being explored, with the hope of carrying out this procedure theoretically as well as experimentally.

THE ANP SHIELDING BOARD*

This Board, a joint effort of NEPA and ORNL, was convened from September 5 to October 16, primarily to demonstrate the best possible weight estimates of pertinent, fully engineered shields for the subsonic aircraft. In addition, any conclusions which could be inferred from the work were to be reported, especially if doing so would aid in allocation of effort for the ANP.

The first designs were based on standard specifications which were given to the Board at its inception for a Na - Na fixed-fuel cycle: 3 ft diameter, 3-ft-long cylindrical reactor, 200 megawatts power, 50 ft reactor-crew separations, 1 r/hr flight tolerance. The tolerance for ground servicing was left to the discretion of the Board, and after discussions with engineers

* ORNL membership included E. P. Blizard, Chairman, C. E. Clifford, A. P. Fraas, K. E. Keyes, R. W. Schroeder, T. A. Welton, and J. H. Wyld.

0.1 r/hr was adopted. Since the unit shields for this set of specifications appeared to weigh over 200,000 lb, competitive designs were investigated. It was then demonstrated in some detail that for a 30-in.-diameter nearly spherical core with lead or bismuth as the primary coolant, other conditions remaining the same, the weight of reactor, shield, structure within shield, reflectors, ducts, pump, and heat exchangers was approximately 105,000 lb. Other designs, with somewhat greater weights and lithium as the coolant, were also completed. In view of the fact that neither lead nor lithium could surely be used as a coolant because of their corrosive properties, the Na-Na cycle was re-examined for a smaller core more nearly spherical in size. Furthermore, the ground tolerance was relaxed to 1 r/hr at the shield surface 15 min after shutdown. For this configuration the weight was estimated to be 148,000 lb.

The divided shield for the Na-Na cycle was, on the other hand, not excessive in weight, being estimated to be 98,000 lb for the standard conditions given above. In view of this fact, it appeared interesting to investigate what might be a lower limit for shield weight; consequently a divided shield for a 2.5-ft-square cylindrical reactor, 65 ft separation, 3 to 4 man crew compartment, Li^7-Li system was designed. The total weight was 66,450 lb.

General conclusions of the Shielding Board were that a serious weight penalty must be paid for using the Na-Na system in the unit shield. The same conclusion applies for a unit shield circulating-fuel system using NaOH as the fuel vehicle and Na as the secondary coolant. On the other hand, a divided shield for either of these systems will probably be below 100,000 lb in weight. In comparing unit and divided shields it was pointed out that the divided shield weighs at least 30,000 lb less than the unit shield in most cases of significance. Furthermore, the frontal area of a divided shield will always be appreciably less than that of a unit shield. The obvious disadvantage of the divided shield, the extreme radiation intensity near the reactor during and after operation, appears not to be prohibitive since the outer section of the reactor shield consists of a rather thick layer of gasoline which can be replaced while on the ground by a much denser material, for example, steel shot in oil. It is also pointed out that both unit- and divided-shield aircraft will require facilities for handling very radioactive components during reactor replacement, and, if long flights and low burn-up become necessary, this will be a frequent operation. The complete findings of the Board are reported in ANP-53.

DIVIDED SHIELDS FOR MORE CONSERVATIVE GROUND SPECIFICATIONS[1]

T. R. Mitchell*

It appeared desirable to initiate an investigation of shields which would satisfy ground tolerance specifications intermediate to those of ground-safe unit shields and the air-safe divided shields described in the Shielding Board Report.[2] Such shields would necessarily be of the divided type but would retain some heavy gamma-ray shielding material completely around the reactor. The tolerance conditions chosen for this study were as follows:

(*a*) 1 r/hr outside the crew compartment at 50 ft from the reactor center, with reactor operating at one-tenth power (20,000 kw).

(*b*) ¼ r/hr in the crew compartment with reactor operating at full power (200,000 kw); rear of crew compartment to be located 50 ft from center of reactor.

These specifications are not so stringent as those for the ground-safe unit shields defined in ANP-53, which require that the radiation intensity at 50 ft be no more than 1 r/hr when operating at full power. They are considerably more conservative, however, than the specifications for the air-safe divided shields of ANP-53, which limited only the radiation level inside the crew compartment while the radiation intensity outside the compartment was allowed to be extremely high. The radiation specifications being considered here would allow maintenance personnel to remain at the engines for a short time without auxiliary shielding with the engines running, one at a time, at about half power.

Shield Specifications. The weights and sizes of the divided shields investigated in this study are given in Table 5.1 along with similar data for unit shields around the same reactors. Of the weights listed for the divided shields, 22,000 lb is attributed to the crew shield.

* On loan from NEPA to the ANP Division for assistance in designing the ARE.

(1) Except for minor editorial changes, this section is the same as the following report: Mitchell, T. R., *Divided Shields for More Conservative Ground Specifications*, Oak Ridge National Laboratory, Y-12 Site, Y-F15-4 (Nov. 20, 1950).

(2) *Report of the ANP Shielding Board*, ~~NEPA-ORNL~~, ANP-53 (Oct. 16, 1950).

TABLE 5.1

Weights and Sizes of Shields

SHIELD	Na-Na COOLED REACTOR WITH ELLIPSOIDAL ENDS; 30-IN.-DIAMETER CORE		Na-Na COOLED REACTOR WITH ELLIPSOIDAL ENDS; 36-in.-DIAMETER CORE		Li^7-Li COOLED REACTOR WITH ELLIPSOIDAL ENDS; 36-in.-DIAMETER CORE	
	SHIELD WEIGHT (lb)	SHIELD DIAMETER (in.)	SHIELD WEIGHT (lb)	SHIELD DIAMETER (in.)	SHIELD WEIGHT (lb)	SHIELD DIAMETER (in.)
Divided Shield	127,000	130	136,000	132	111,800	132
Ground-safe unit shield,[3] 1 r/hr at 50 ft	148,000	145	160,000	147	122,000	147
Ground-safe unit shield,[3] ¼ r/hr at 50 ft	179,000	155	199,000	157	148,000	157

The radiation intensity at the surface of the 1 r/hr unit shields, 15 min after reactor shutdown, is approximately 1 r/hr.[3] This will be greater by more than a factor of 10 at the surface of the reactor portions of these divided shields.

Performance of Divided Shields. To satisfy the first of the two radiation tolerance conditions stated above, it is necessary simply to remove a one-tenth attenuation thickness of neutron and gamma-ray shielding materials from the outer layers of the existing ground-safe shield designs (ANP-53) which were designed to give 1 r/hr at 50 ft when operating at full power (200,000 kw). The second condition is then met by designing a crew shield for a factor-of-10 total attenuation of neutrons plus gamma rays. Thus, while the weights given here for the shielding around the reactor were obtained by perturbation of previously reported shield weights, the crew shield weight was computed independently.

(3) ANP-53, *op. cit.*, p. 53

Specifically, an equivalent of 7.7 in. of water and 1.71 in. of lead were removed from the outer portions of the ground-safe shields (1 r/hr at 50 ft at 200,000 kw) for the following three reactors:

1. Na-Na cooled reactor having a 30-in.-diameter core with ellipsoidal ends.[4]
2. Na-Na cooled reactor having a 36-in.-diameter core with ellipsoidal ends (design similar to 1).
3. Li^7-Li cooled reactor having a 36-in.-diameter core with ellipsoidal ends.[5]

Assuming that the neutron shielding outside the last lead layer consists of gasoline contained in plastic, this removes 43,000, 45,600, and 32,000 lb, respectively, from the unit shields (1 r/hr at 50 ft) for the reactors listed above. Using the weights which have been previously[6] computed for these unit shields, the shielding around the reactor for the three divided shields being considered will weigh 105,000, 114,400, and 89,800 lb, respectively.

Decreasing the thickness of the reactor shielding materials as described in the preceding paragraph increases the neutron and gamma-ray leakage from the reactor shield by a factor of 10, but allows the relative leakage of gamma rays and neutrons to remain the same, i.e., 75% gamma rays and 25% neutrons in terms of radiation dosage per unit time. The crew shield, however, is designed so that the allowable ¼ r/hr received by a crew member will be caused 50% by neutrons and 50% by gamma rays. Therefore the crew shield must attenuate the gamma rays by a factor of 60 and the neutrons by a factor of 20 in order to give the required total attenuation factor of 40. The required thicknesses of shielding materials around the crew compartment (sides, rear, front) were calculated using the same methods developed by W. B. Thomson and H. E. Stern in computing the crew shields for the air-safe shields described in ANP-53. In this case, of the neutrons which penetrate into the crew compartment, 60% were allowed to come through the sides, 10% through the rear face, and 30% through the front of the compartment. These percentages were chosen rather arbitrarily, but even an optimum choice of these parameters

(4) ANP-53, *op. cit.*, Fig. 5.
(5) ANP-53, *op. cit.*, Fig. 4.
(6) ANP-53, *op. cit.*, p. 53.

would not greatly lower the crew shield weight. The calculations indicated that 5, 15.2, and 1.7 in. of plastic were required at the sides, rear, and front of the crew compartment, respectively. The plastic was assumed to be polyethylene, $(CH_2)_n$, having a density of 0.93 g/cc. All the gamma rays entering the crew compartment were assumed to penetrate through the rear face, because the plastic at the sides and at the front was more than enough to stop all but a negligible portion of the scattered gamma radiation. Therefore lead is used only at the rear of the crew compartment, where a 2.3-in. thickness is required in addition to the 15.2 in. of plastic which also affords some gamma shielding.

The crew compartment of this study was that used[7] for the divided shield for the Na-Na cooled reactor. Based upon this configuration and the thicknesses of shielding materials indicated above, the weight of the crew shield was calculated to be 22,000 lb, i.e.,

Plastic	13,100 lb
Lead	8,200
Aluminum Structure (Estimated)	700
Total	22,000 lb

Thus the total divided shield weights for the three cases being considered are 127,000, 136,000, and 111,800 lb, respectively.

If polyethylene, $(CH_2)_n$, is used in the outer portion of the reactor shield instead of gasoline, the shield weights tabulated on p. 102 of this report will remain very nearly the same. The resultant shields, however, would be about 8 in. smaller in diameter. This would require, roughly, an additional 30,000 lb of the plastic per shield, at a cost of approximately $3.50 per pound.

LID TANK

C. E. Clifford E. P. Blizard
J. D. Flynn T. V. Blosser
Physics Division
L. H. Ballweg, USAF

A shield design consisting of iron next to the core, followed by well-borated water, was tested in the Lid Tank. Such a design, proposed by the

(7) ANP-53, *op. cit.*, p. 68.

TAB,[8] was attractive because of its simplicity and low weight, although there was a recognized question regarding its effectiveness upon intermediate-energy neutrons. These latest Lid Tank measurements have shown that the intermediate-energy neutrons can penetrate the iron to such an extent that suppression of their capture gammas is virtually impossible. In another experiment the attenuation of neutrons and gammas in solid B_4C and water was measured.

Iron and Borated Water. The Technical Advisory Board included in its report a shield design which was very attractive from the standpoint of simplicity and ease of construction, which exhibited the smallest overall diameter of any recent design, and which appeared to be in contention on a weight basis as well. Therefore it was decided that this shield should be mocked-up and tested (Expt. 10)[9] during the waiting period between promise and delivery of the B_4C slabs.

The TAB shield design consists simply of 55 cm of Fe next to the core followed by 35 cm of well-borated H_2O.[10] The Shielding Group at ORNL was strongly of the opinion that the design violated the principle that gamma-attenuating material could not be lumped next to the core because of the great importance of secondary gammas produced at the outside edge of this material from neutron capture or inelastic scattering. The TAB thesis was that

1. The iron would attenuate fast neutrons adequately to eliminate the latter, and on this there was agreement.

2. Sufficient boron could be located outside the iron to suppress the captures, and on this there was not agreement.

It should be pointed out that on item 1 the TAB was able to make a calculation which proved to be reasonably close to the experiment, but on item 2 the information required for a detailed calculation included capture cross sections in the intermediate-energy range which were completely unavailable, as well as some estimate of neutron-energy spectra which would likewise have been very difficult to obtain.

(8) *Report of the Technical Advisory Board to the Technical Committee of the Aircraft Nuclear Propulsion Program*, ANP-53 (Aug. 4, 1950).

(9) Blizard, E. P., and Clifford, C. F., *Measurements of an Iron and Borated Water Shield in the Lid Tank*, CF-50-12-47 (Dec. 14, 1950).

(10) ANP-53, *op. cit.*, p. 29.

Accordingly a shield mock-up was measured in which the first section consisted nearly entirely of iron; a second, transition, region was made up of varying thicknesses of B_4C; and the third region was the usual borated water. The iron samples used in the experiment were in the form of rectangular plates 7/8 in. thick by 56½ in. high by 66½ in. wide, the total number available for the experiment being 24. These plates were placed in the tank adjacent to the source, four at a time. When they were placed in the Lid Tank it was found that since the plates were not perfectly flat there remained, on the average, a 1/8-in. water gap between plates. Thermal-neutron measurements, gamma measurements, and fast-neutron dosimeter measurements were taken in the water behind the iron.

A layer of B_4C 1/8 in. thick, in the form of plastic 50% B_4C by volume, was fastened to the rear face of the last plate in each configuration to reduce capture gamma production in the iron at this most sensitive position. After the addition of 24 iron slabs the gamma level was still very high; therefore a layer of B_4C (density 1.8 g/cc) in the form of 1-in. slabs was added up to a thickness of 5 in.

Since the 1-in. B_4C slabs were not watertight it was necessary to place them in a 15-in. by 6-ft by 5-ft dry tank with 1/8-in. steel walls. In order to avoid the introduction of a large void, the dry tank was so placed that it also contained the outer slabs of Fe. At this point it became clear that the gamma level could not be reduced sufficiently by a reasonable further addition of B_4C, and the design was considered inadequate.

Since the walls of the dry tank are bowed by the water pressure, it was difficult to determine the exact amount of water displaced. For this reason two measurements were carried out (Table 5.2 last column, Table 5.3 first column) with and without water in the dry tank. The effect of the addition of B_4C slabs is best inferred by comparison with the "no-water" condition.

Figure 5.1 and Table 5.2 give the gamma attenuation data for the foregoing experiments, and include as well a comparison of gammas in pure and borated water. Figure 5.2 and Table 5.3 show more truly the effect of the B_4C slabs.

Figure 5.3 and Tables 5.4 and 5.5 show the attenuation of neutrons in H_2O behind the various thicknesses of Fe, demonstrating the well-known superiority of Fe over H_2O which accounted for the thinness of the TAB shield design.

Figure 5.4 and Table 5.6 show neutron attenuation behind Fe and B_4C, and from this figure the effect of the latter on the emergent neutrons is evident.

The reason that the Fe cannot be lumped next to the core now becomes evident. Examination of Figs. 5.3 and 5.4 shows that the neutrons emerging must be predominantly of energy in the neighborhood of 1 Mev since the neutron attenuation next to the Fe is very great, by both H_2O and B_4C. This is not unexpected since Fe possesses a "window" in this neighborhood just below the inelastic scattering region and above that of great absorption. Hence these intermediate-energy neutrons were penetrating the iron in such large numbers that the suppression of their capture gammas is essentially impossible.

To prove that the gammas observed at the outer side of the shield mock-up were produced as supposed, the experiment was extended by remeasuring the gammas as slab after slab of Fe was removed (and, of course, replaced by borated water) from the source side of the innermost (Fe) region. Since H_2O does not possess this low-energy window, it would be expected that the removal of the iron would result initially in a reduction of gamma intensity at the outer side of the shield. Such was observed to be the case throughout the removal of eight slabs, as is shown in Fig. 5.5 and Table 5.7. A schematic drawing of the slab arrangement is shown in Fig. 5.6.

The investigation of the Fe-H_2O system was extended by a measurement of neutrons and gammas behind a region of 50% Fe by volume, and then by a measurement of the relative effectiveness of the iron as compared to water at various positions within the mixed region. This latter amounts merely to a determination of the l described in the last quarterly report[11] as the important parameter for shield optimization. The results are shown in Figs. 5.7 and 5.8, which correspond to Tables 5.8 and 5.9, respectively. A schematic drawing of the slab arrangement is shown in Fig. 5.9. Dosimeter measurements of the Fe-B_4C system are shown in Fig. 5.10 and Table 5.10. Since some difficulties were encountered in the electronic circuits during these measurements, they are probably not accurate to better than ±30%.

(11) *Aircraft Nuclear Propulsion Project Quarterly Progress Report for Period Ending August 31, 1950*, ORNL-858, p. 17 (Dec. 4, 1950).

[redacted]
DWG. 9978

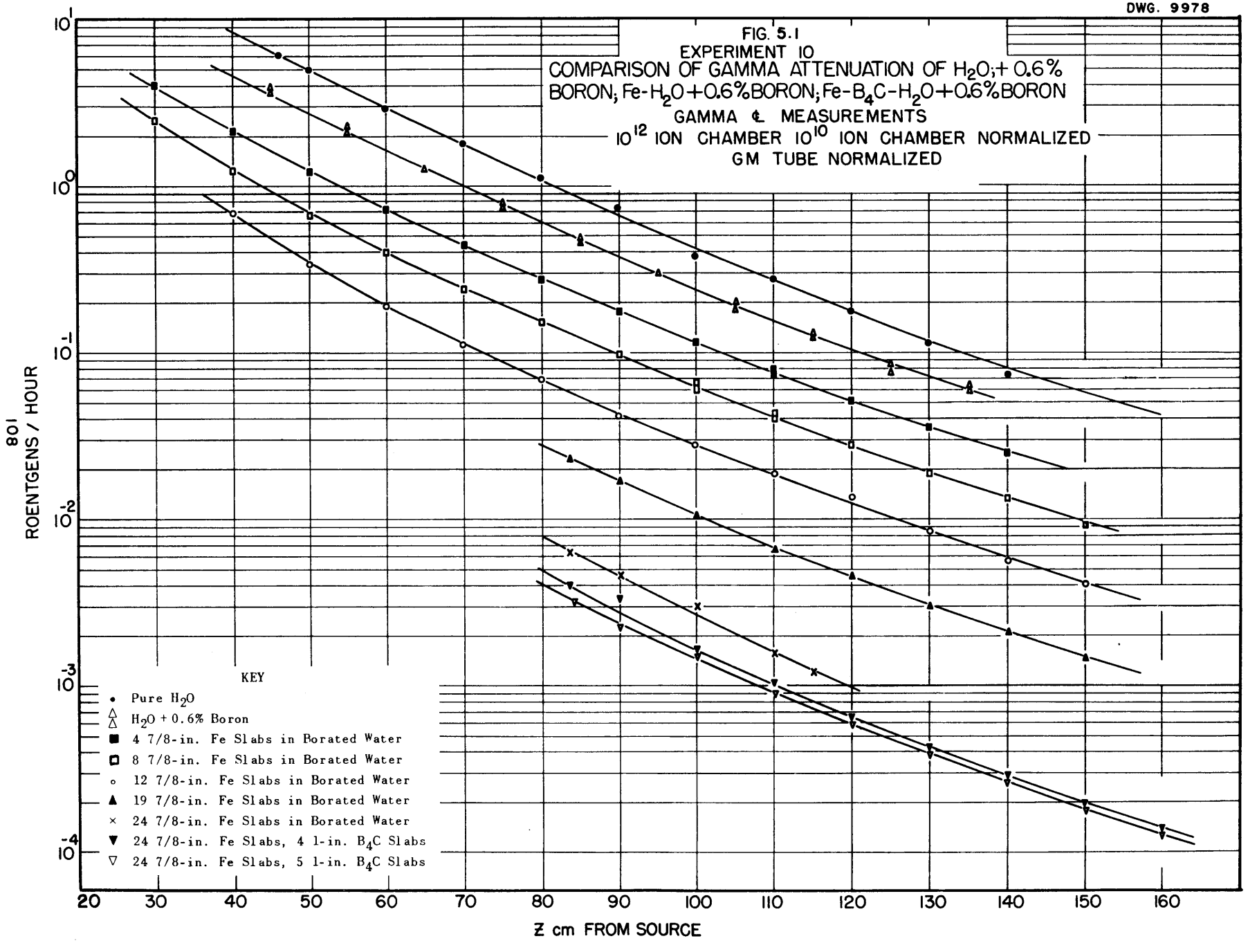

TABLE 5.2

Comparison of Gamma Attenuation by H_2O; H_2O + 0.6% B; Fe-H_2O + 0.6% B; Fe-B_4C-H_2O + 0.6% B

(10^{12} and 10^{10} Ion Chambers Normalized, GM Tube Normalized)

DISTANCE FROM SOURCE (cm)	(roentgens/hour)									
	NO SLABS		4 Fe SLABS*		8 Fe SLABS*		12 Fe SLABS*		19 Fe SLABS*	24 Fe SLABS, WATER IN "DRY" TANK
	10^{10} I.C.	10^{10} I.C.	10^{10} I.C.	10^{10} I.C.	10^{10} I.C.	10^{12} I.C.	10^{10} I.C.	10^{12} I.C.	10^{12} I.C.	10^{12} I.C.
30			3.99	3.98	2.48					
40			2.10	2.14	1.21		0.686			
45	3.81	3.95								
46										
50			1.22	1.20	0.671		0.335			
55	2.19	2.29								
60			0.721	0.703	0.397		0.191			
65	1.27	1.26								
70			0.447	0.431	0.241		0.111			
75	0.765	0.782								
80			0.273	0.273	0.151		0.070			
83.5									0.0227	0.00637
85	0.474	0.485								
90			0.174	0.175	0.097		0.041	0.0434	0.0170	0.00466
95	0.299	0.305								
100			0.117	0.113	0.064	0.0608		0.0278	0.0103	0.00302
105	0.181	0.205								
110			0.0713	0.0771	0.0413	0.0407		0.0186	0.00655	0.00159
115	0.123	0.126								0.00120
120			0.051	0.0516	0.0276	0.0275		0.0133	0.00445	
125	0.076	0.087								
130			0.0359	0.0355		0.0187		0.00852	0.00295	
135	0.063	0.058								
140			0.0249	0.0245		0.0133		0.00575	0.00206	
150						0.00917		0.00394	0.00142	
160										

* 7/8 in. thick.

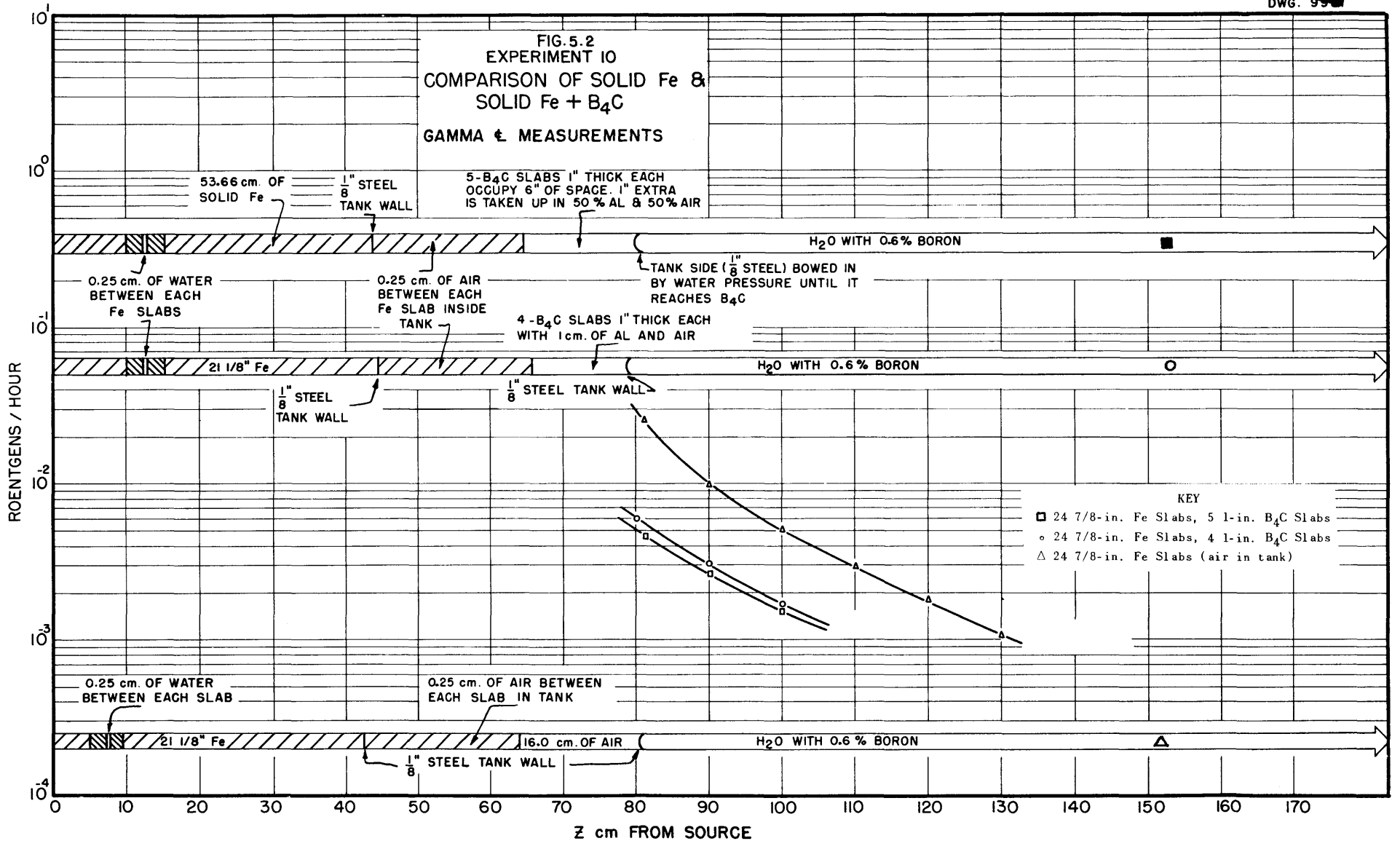
DWG. 99
FIG. 5.2
EXPERIMENT 10
COMPARISON OF SOLID Fe & SOLID Fe + B_4C
GAMMA & MEASUREMENTS
53.66 cm. OF SOLID Fe
1/8" STEEL TANK WALL
5-B_4C SLABS 1" THICK EACH OCCUPY 6" OF SPACE. 1" EXTRA IS TAKEN UP IN 50% AL & 50% AIR
H_2O WITH 0.6% BORON
0.25 cm. OF WATER BETWEEN EACH Fe SLABS
0.25 cm. OF AIR BETWEEN EACH Fe SLAB INSIDE TANK
TANK SIDE (1/8" STEEL) BOWED IN BY WATER PRESSURE UNTIL IT REACHES B_4C
4-B_4C SLABS 1" THICK EACH WITH 1 cm. OF AL AND AIR
21 1/8" Fe
H_2O WITH 0.6% BORON
1/8" STEEL TANK WALL
1/8" STEEL TANK WALL
KEY
□ 24 7/8-in. Fe Slabs, 5 1-in. B_4C Slabs
○ 24 7/8-in. Fe Slabs, 4 1-in. B_4C Slabs
△ 24 7/8-in. Fe Slabs (air in tank)
0.25 cm. OF WATER BETWEEN EACH SLAB
0.25 cm. OF AIR BETWEEN EACH SLAB IN TANK
21 1/8" Fe
16.0 cm. OF AIR
H_2O WITH 0.6% BORON
1/8" STEEL TANK WALL
ROENTGENS / HOUR
10^{1}
10^{0}
10^{-1}
10^{-2}
10^{-3}
10^{-4}
0 10 20 30 40 50 60 70 80 90 100 110 120 130 140 150 160 170
Z cm FROM SOURCE

011

TABLE 5.3

Effect on Gamma Intensity of B_4C Added Outside Fe Region

(10^{12} Ion Chamber)

DISTANCE FROM SOURCE (cm)	(roentgens/hour)		
	24 Fe SLABS,* NO WATER IN "DRY" TANK	24 Fe SLABS,* 4 B_4C SLABS**	24 Fe SLABS,* 5 B_4C SLABS**
80		0.0058	
81	0.0257		
81.2			0.00452
90	0.00995	0.00302	0.00260
100	0.00516	0.00170	0.00154
105		0.1329	
110	0.00293		
120	0.00180		
130	0.00107		

* 7/8 in. thick.

** 1 in. thick.

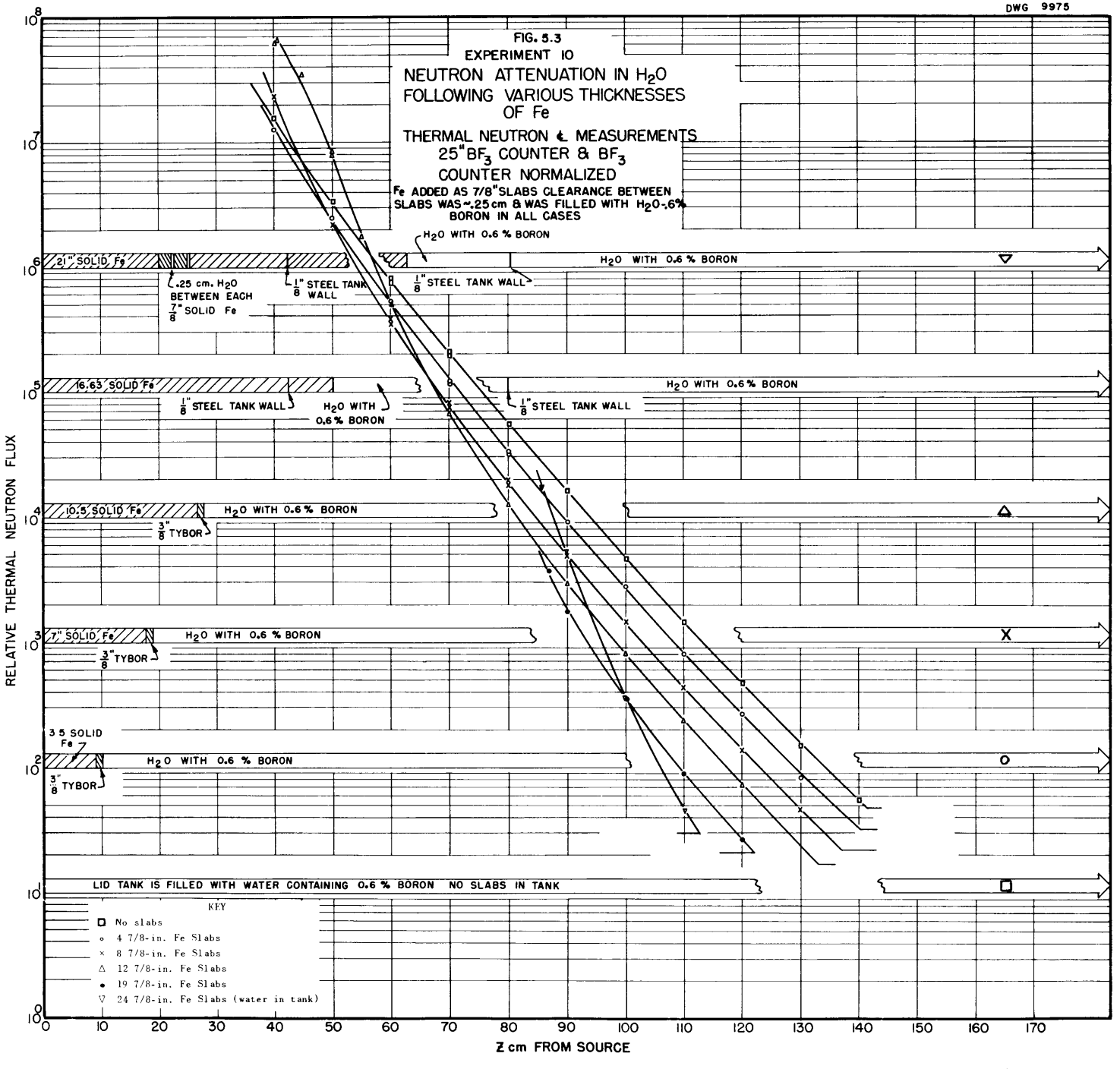
FIG. 5.3
EXPERIMENT 10
NEUTRON ATTENUATION IN H_2O FOLLOWING VARIOUS THICKNESSES OF Fe
THERMAL NEUTRON MEASUREMENTS
25" BF_3 COUNTER & BF_3 COUNTER NORMALIZED
Fe ADDED AS 7/8" SLABS CLEARANCE BETWEEN SLABS WAS ~.25 cm & WAS FILLED WITH H_2O-.6% BORON IN ALL CASES
H_2O WITH 0.6 % BORON
2" SOLID Fe
.25 cm. H_2O BETWEEN EACH 7/8" SOLID Fe
1/8" STEEL TANK WALL
16.63 SOLID Fe
10.5 SOLID Fe
3/8" TYBOR
7" SOLID Fe
3.5 SOLID Fe
LID TANK IS FILLED WITH WATER CONTAINING 0.6 % BORON NO SLABS IN TANK
KEY
No slabs
4 7/8-in. Fe Slabs
8 7/8-in. Fe Slabs
12 7/8-in. Fe Slabs
19 7/8-in. Fe Slabs
24 7/8-in. Fe Slabs (water in tank)
RELATIVE THERMAL NEUTRON FLUX
Z cm FROM SOURCE

TABLE 5.4

Neutron Attenuation by Solid Fe-H_2O + 0.6% B

[8-in. BF_3 Counter Normalized to 25-in. BF_3 Counter (i.e., × 35.7)]

DISTANCE FROM SOURCE (cm)	(counts/minute)				
	NO SLABS	4 Fe SLABS*	8 Fe SLABS*	12 Fe SLABS*	
				RUN 1	RUN 2
40	15,200,000	12,900,000	23,000,000	62,900,000	
40.6					65,600,000
45					34,900,000
50	3,380,000	2,450,000	2,221,000	7,990,000	8,340,000
55					1,785,000
60	803,000	515,000	356,000	494,000	
70	205,000	123,000	73,100	67,700	
80	55,500	31,700	17,974	8,380	
90	10,900			2,920	

* 7/8 in. thick.

TABLE 5.5

Neutron Attenuation by Solid Fe-H_2O + 0.6% B

(25-in. BF_3 Counter)

DISTANCE FROM SOURCE (cm)	(counts/minute)					
	NO SLABS	4 Fe SLABS*	8 Fe SLABS*	12 Fe SLABS*	19 Fe SLABS*	24 Fe SLABS,* WATER IN "DRY" TANK
60	740,247	482,082	373,855	489,661		
70	199,753	119,707	80,119	65,766		
80	54,668	32,274	19,104	12,745		
82.1					3,685	
85.9						17,439
90	16,038	9,032	4,991	2,970	1,754	5,176
100	4,692	2,731	1,486	814	346	349
110	1,455	791	430	234	89	45
120	469	264	138	71	26	
130	148	81	46			
140	54					

* 7/8 in. thick.

FIG. 5.4
EXPERIMENT 10

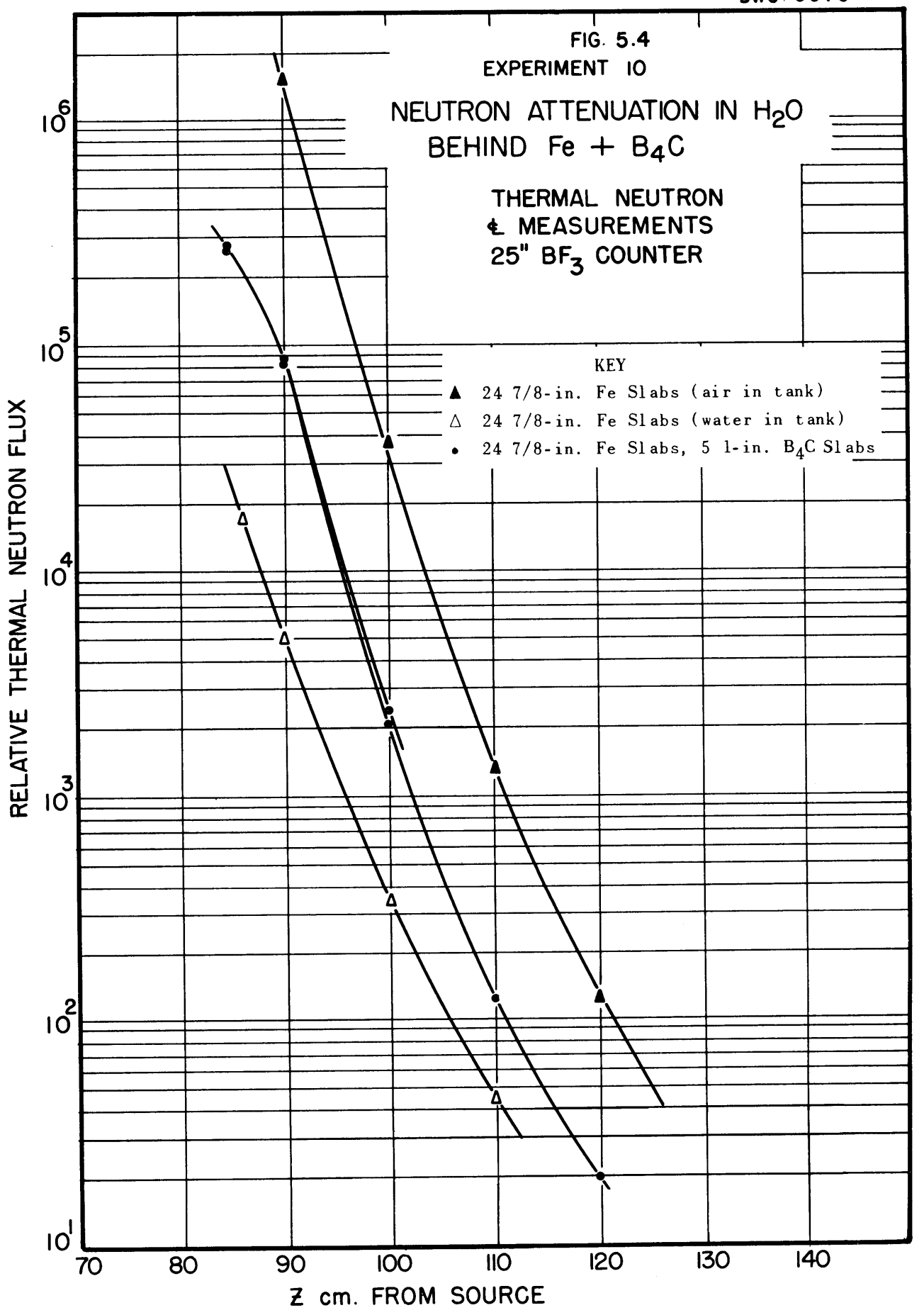

TABLE 5.6

Neutron Attenuation of B_4C Behind Fe

(25-in. BF_3 Counter)

DISTANCE FROM SOURCE (cm)	(counts/minute)			
	24 Fe SLABS*		24 Fe SLABS,* 5 B_4C SLABS**	
	WATER IN "DRY" TANK	NO WATER IN "DRY" TANK	RUN 1	RUN 2
84.7			267,022	
84.8				269,051
85.9	17,439			
90	5,176	1,507,812	87,448	84,191
100	349.3	37,140	2,351	2,062
110	45.1	1,326		122.8
120		125.14		19.9

* 7/8 in. thick.

** 1 in. thick.

DWG. 9982

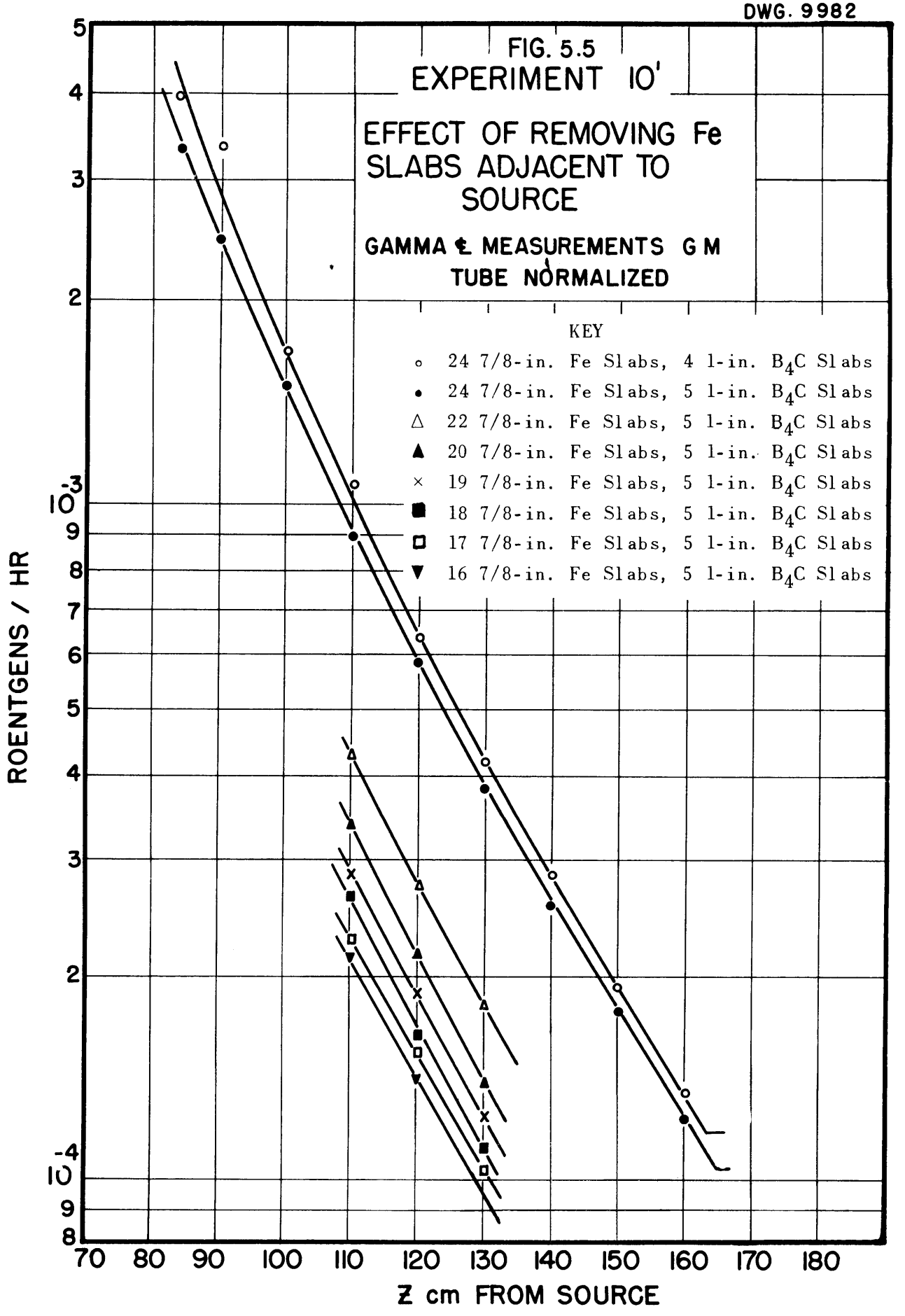
FIG. 5.5
EXPERIMENT 10'
EFFECT OF REMOVING Fe SLABS ADJACENT TO SOURCE
GAMMA & MEASUREMENTS G M TUBE NORMALIZED
KEY
24 7/8-in. Fe Slabs, 4 1-in. B4C Slabs
24 7/8-in. Fe Slabs, 5 1-in. B4C Slabs
22 7/8-in. Fe Slabs, 5 1-in. B4C Slabs
20 7/8-in. Fe Slabs, 5 1-in. B4C Slabs
19 7/8-in. Fe Slabs, 5 1-in. B4C Slabs
18 7/8-in. Fe Slabs, 5 1-in. B4C Slabs
17 7/8-in. Fe Slabs, 5 1-in. B4C Slabs
16 7/8-in. Fe Slabs, 5 1-in. B4C Slabs
ROENTGENS / HR
10^-3
10^-4
5
4
3
2
9
8
7
6
70 80 90 100 110 120 130 140 150 160 170 180
Z cm FROM SOURCE

TABLE 5.7

Effect of Removing Fe Slabs Adjacent to Source on Gamma Attenuation

(GM Tube Normalized)

DISTANCE FROM SOURCE (cm)	(roentgen/hour)							
	16 Fe SLABS,* 5 B_4C SLABS**	17 Fe SLABS,* 5 B_4C SLABS**	18 Fe SLABS,* 5 B_4C SLABS**	19 Fe SLABS,* 5 B_4C SLABS**	20 Fe SLABS,* 5 B_4C SLABS**	22 Fe SLABS,* 5 B_4C SLABS**	24 Fe SLABS,* 4 B_4C SLABS**	24 Fe SLABS,* 5 B_4C SLABS**
83.4							0.00397	
84								0.00332
90							0.00335	0.00246
100							0.00168	0.00150
110	0.00215	0.000227	0.000263	0.000285	0.000338	0.000422	0.00107	0.000894
120	0.000140	0.000154	0.000162	0.000187	0.000216	0.000271	0.000634	0.000585
130	0.000102	0.000102	0.000110	0.000122	0.000138	0.000180	0.000419	0.000382
140							0.000283	0.000256
150							0.000193	0.000177
160							0.000133	0.000122

* 7/8 in. thick.

** 1 in. thick.

FIG. 5.6

DWG. 9983

EXPERIMENT 10'

SCHEMATIC DRAWING OF LID TANK
WITH 24 IRON AND 5 B_4C SLABS

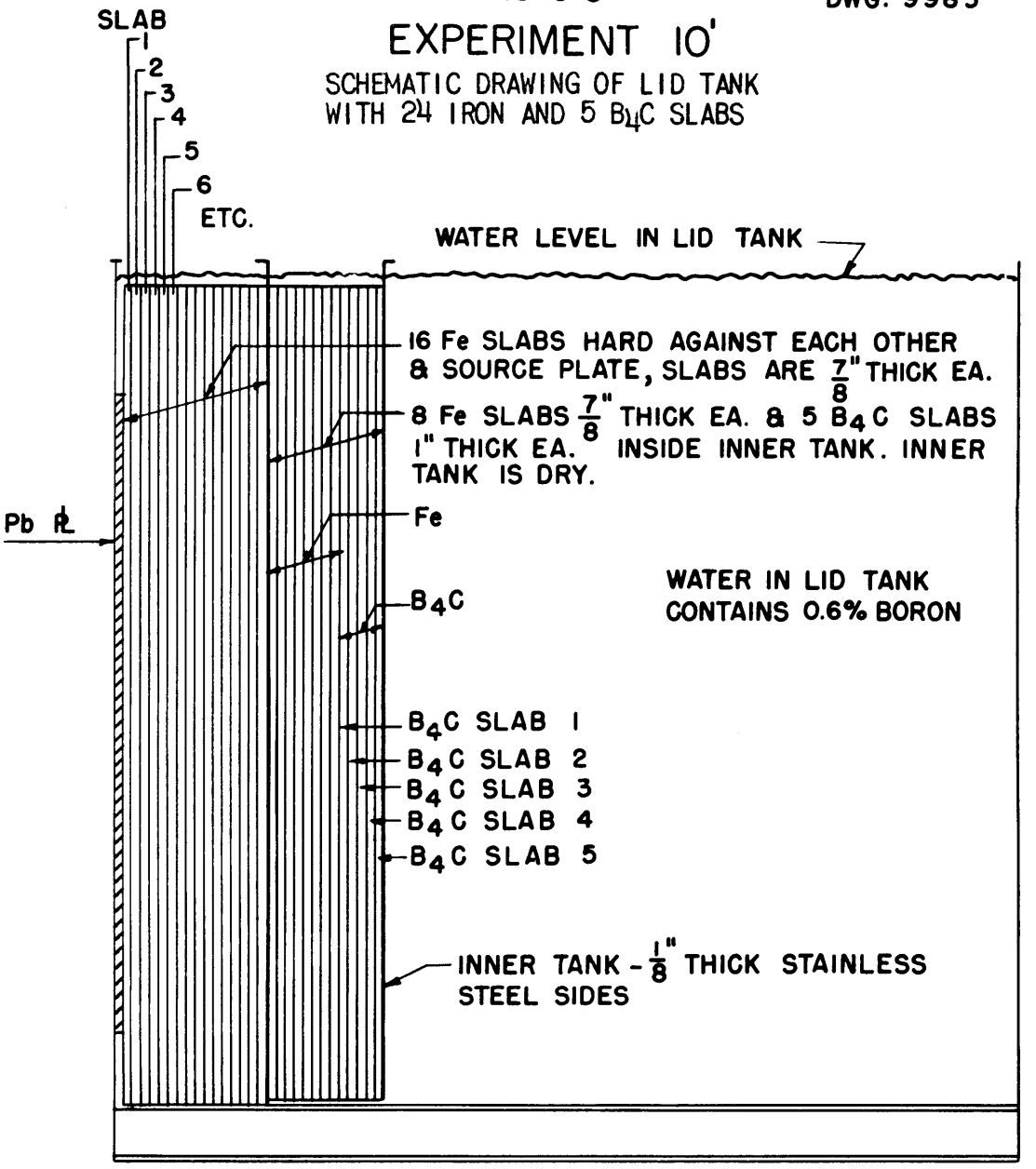

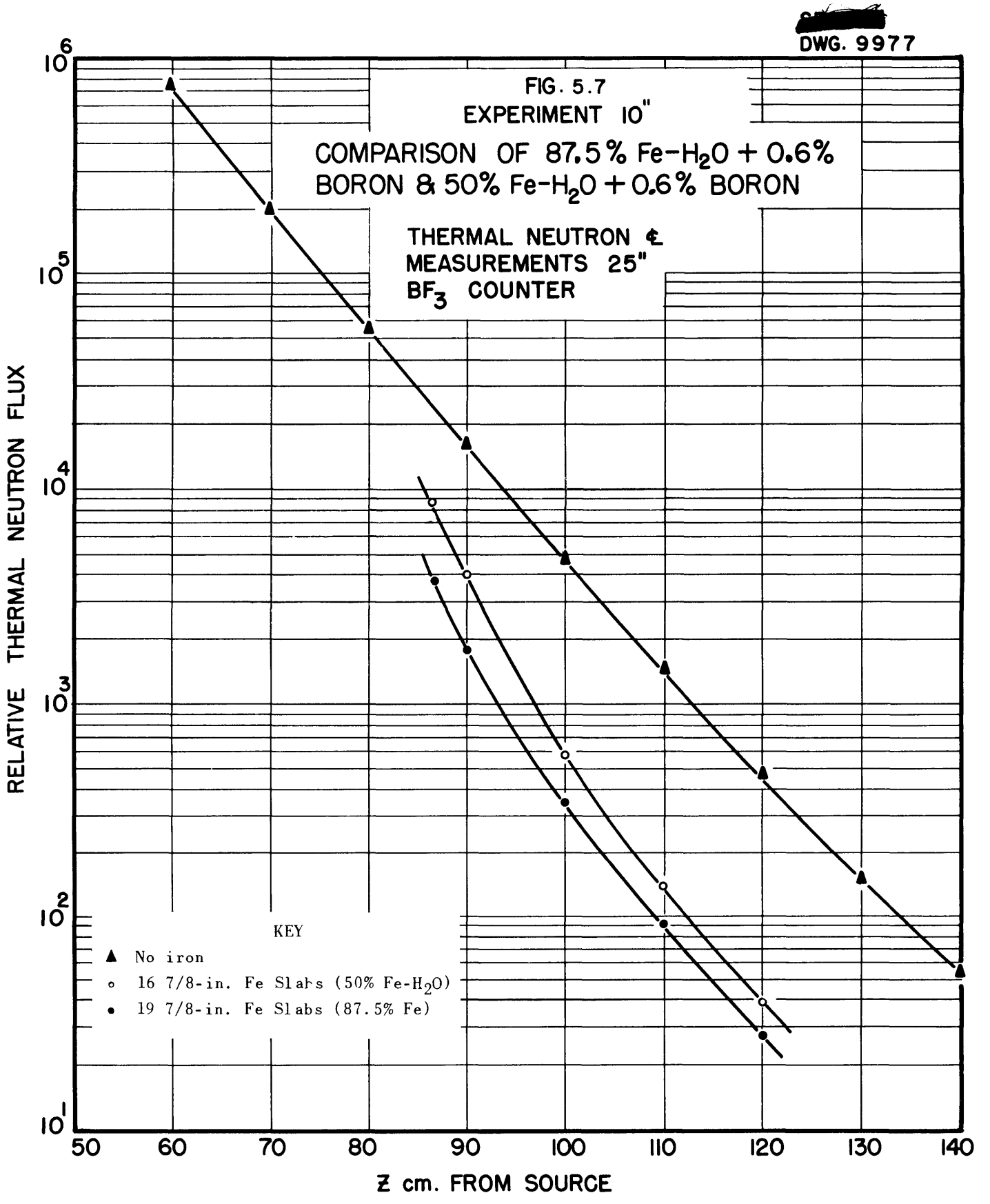
DWG. 9977
FIG. 5.7
EXPERIMENT 10"
COMPARISON OF 87.5% Fe-H_2O + 0.6% BORON & 50% Fe-H_2O + 0.6% BORON
THERMAL NEUTRON ℄ MEASUREMENTS 25"
BF_3 COUNTER
RELATIVE THERMAL NEUTRON FLUX
10^6
10^5
10^4
10^3
10^2
10^1
KEY
▲ No iron
o 16 7/8-in. Fe Slabs (50% Fe-H_2O)
• 19 7/8-in. Fe Slabs (87.5% Fe)
50 60 70 80 90 100 110 120 130 140
Z cm. FROM SOURCE

TABLE 5.8

Comparison of Neutron Attenuation by 87.5% Fe-H_2O + 0.6%B vs. 50% Fe-H_2O + 0.6% B

(25-in. BF_3 Counter)

DISTANCE FROM SOURCE (cm)	(counts/minute)		
	NO SLABS, 100% H_2O	19 Fe SLABS,* 87.5% Fe-H_2O	16 Fe SLABS,* 50% Fe-H_2O
60	740,247		
70	199,753		
80	54,668		
82.1		3685	
86.4			8541
90	16,038	1754	3904
100	4,692	346.2	572
110	1,455	88.8	137
120	469	26.43	38
130	148		
140	54		

* 7/8 in. thick.

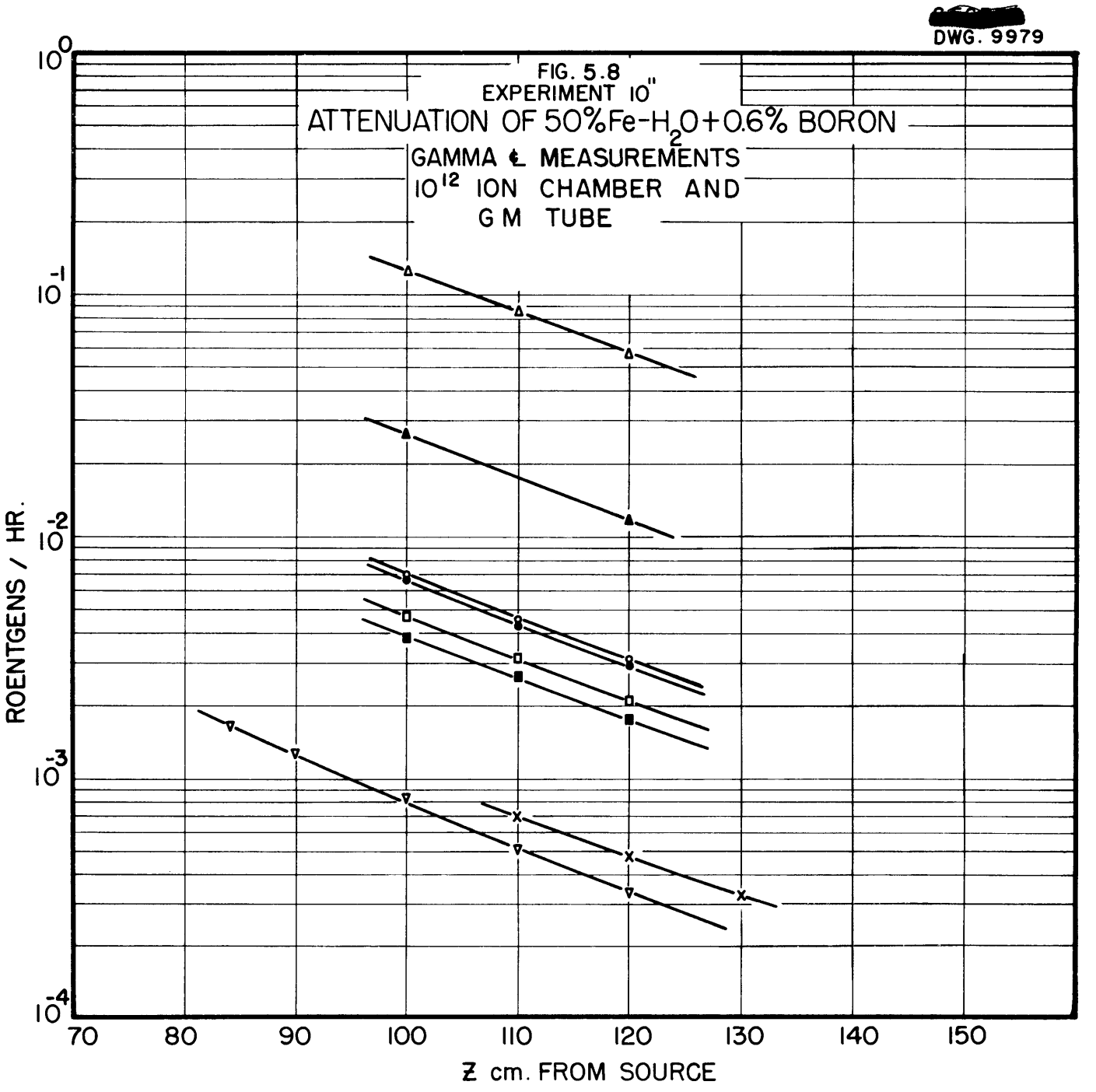

KEY

- △ 4 7/8-in. Fe Slabs (50% Fe-H_2O)
- ▲ 8 7/8-in. Fe Slabs (50% Fe-H_2O)
- × 16 7/8-in. Fe Slabs (Water in Tank)
- ▽ 16 7/8-in. Fe Slabs (50% Fe-H_2O)
- ○ Slab No. 12 Out
- ● Slab No. 7 Out
- □ All Slabs In
- ■ Slab No. 1 Out

} 12 7/8-in. Fe Slabs (50% Fe-H_2O)

TABLE 5.9

Gamma Attenuation of 50% Fe-H_2O + 0.6% B

(10^{12} and 10^{10} Ion Chambers Normalized, GM Tube Normalized; 50% Fe-H_2O)

DISTANCE FROM SOURCE (cm)	(roentgens/hour)						
			12 Fe SLABS*				
	4 Fe SLABS*	8 Fe SLABS*	SLAB 12 OUT	SLAB 7 OUT	ALL SLABS IN	SLAB 1 OUT	16 Fe SLABS*
84							0.00166
90							0.00128
100	0.124	0.0267	0.00698	0.00660	0.00464	0.00385	0.00084
110	0.0849	0.0140	0.00459	0.00429	0.00314	0.00266	0.00051
120	0.0570	0.0120	0.00308	0.00291	0.00208	0.00179	0.00038

* 7/8 in. thick.

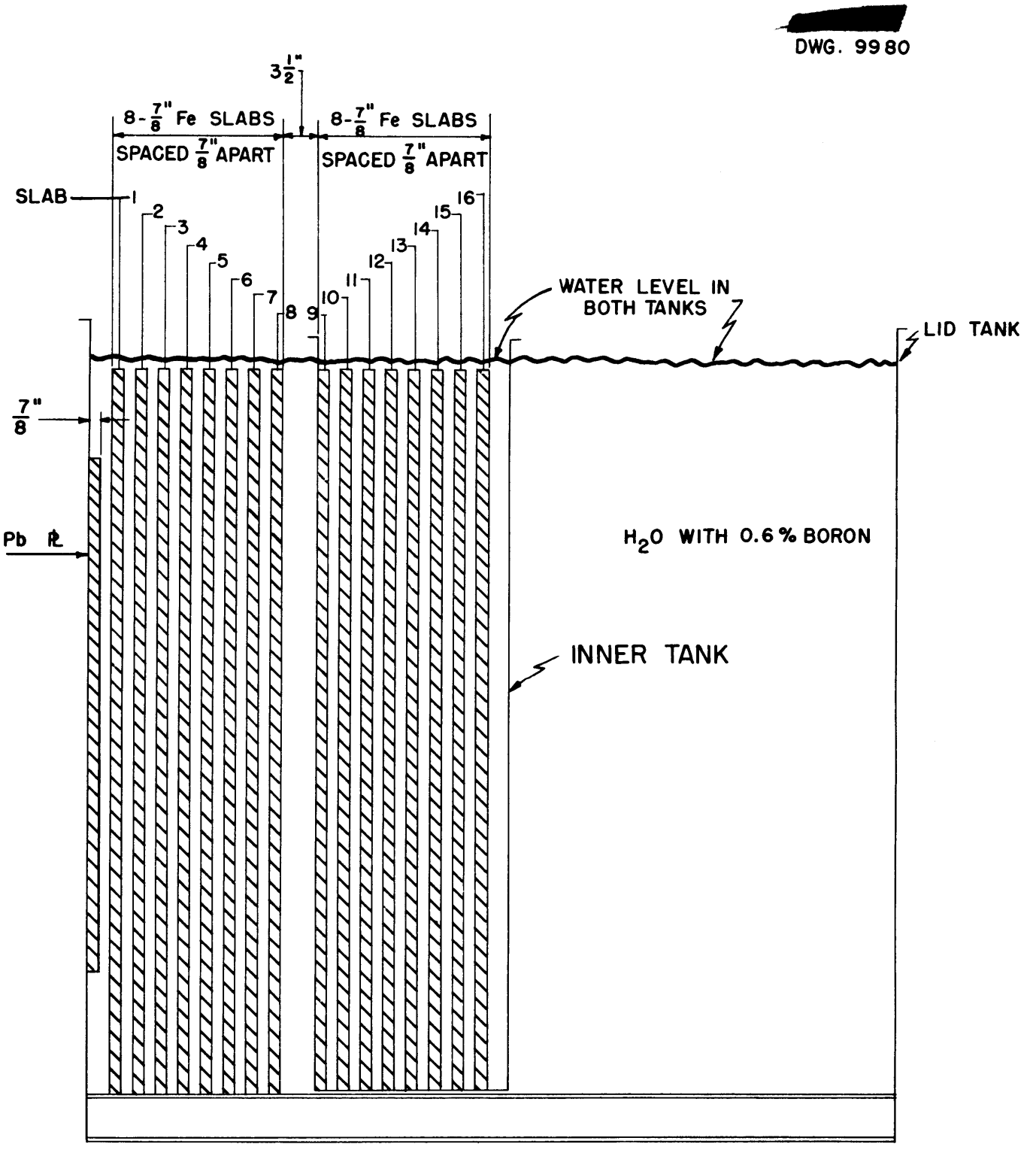

LID TANK (NOT TO SCALE)

FIG. 5.9

EXPERIMENT 10"

SCHEMATIC DRAWING OF LID TANK
WITH 16 7/8-IN. IRON SLABS (50% Fe-H_2O)

DWG. 9984

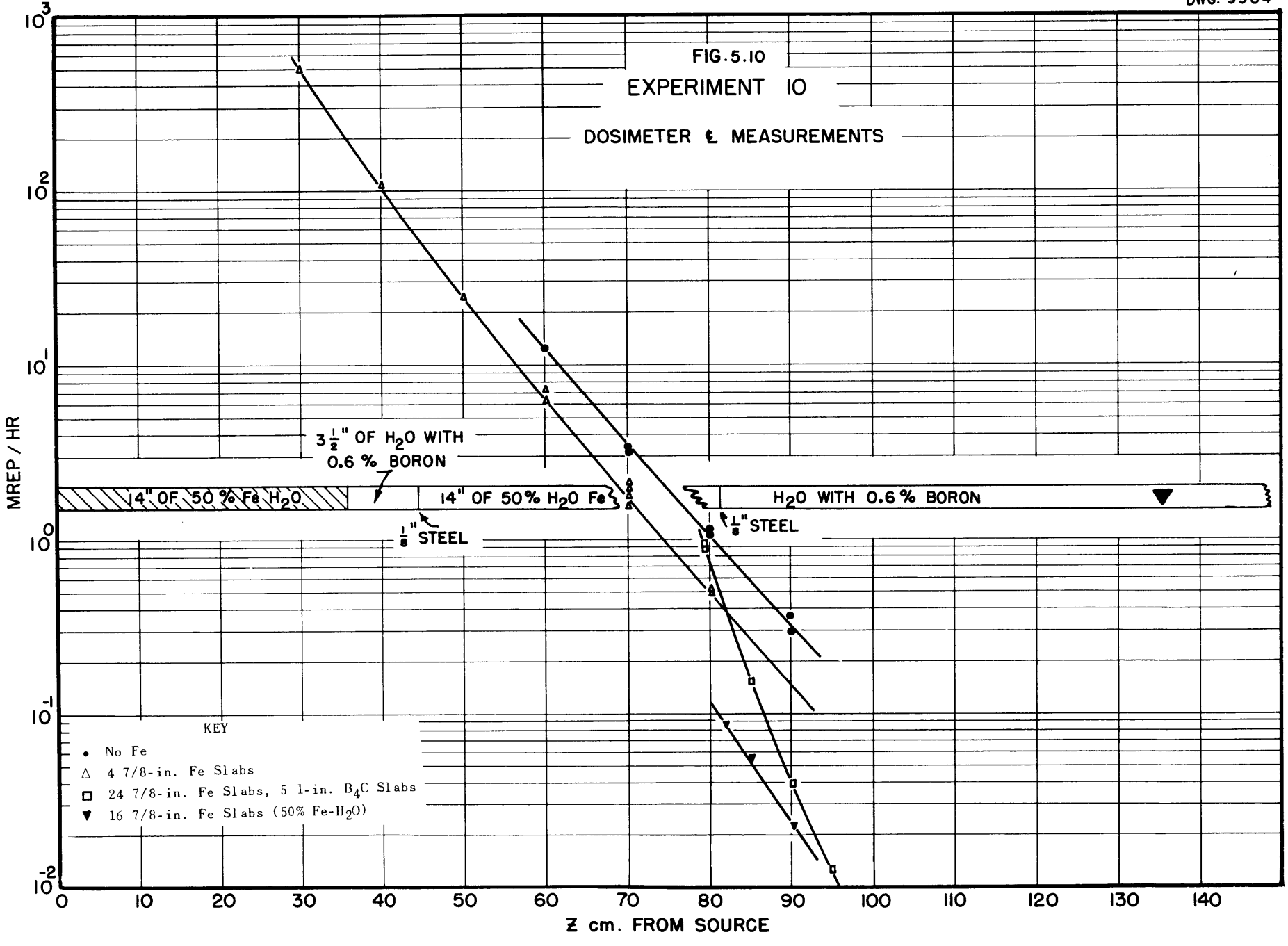
FIG. 5.10
EXPERIMENT 10
DOSIMETER & MEASUREMENTS
MREP / HR
Z cm. FROM SOURCE
10^3
10^2
10^1
10^0
10^{-1}
10^{-2}
0
10
20
30
40
50
60
70
80
90
100
110
120
130
140
$3\frac{1}{2}$" OF H_2O WITH 0.6 % BORON
14" OF 50 % Fe H_2O
14" OF 50% H_2O Fe
$\frac{1}{8}$" STEEL
H_2O WITH 0.6 % BORON
$\frac{1}{8}$" STEEL
KEY
• No Fe
△ 4 7/8-in. Fe Slabs
□ 24 7/8-in. Fe Slabs, 5 1-in. B_4C Slabs
▼ 16 7/8-in. Fe Slabs (50% Fe-H_2O)

TABLE 5.10

Dosimeter Centerline Measurements

DISTANCE FROM SOURCE (cm)	(millirep/hour)							
	NO SLABS		4 Fe SLABS*		24 Fe SLABS,* 5 B_4C SLABS**		50% Fe-H_2O, 16 Fe SLABS*	
	RUN 1	RUN 2	RUN 1	RUN 2	RUN 1	RUN 2	RUN 1	RUN 2
30			494	496				
40			107.3	109.1				
50			24.2	25.3				
60	12.13		6.67	6.38				
70	3.05	3.35	1.81	1.87				
79.2					0.878	0.8096		
80	1.12	1.06	0.498	0.593				
81.5							0.0620	
81.9								0.0845
85					0.148		0.0554	
90	0.29	0.36			0.0389		0.0222	
95						0.0126		

* 7/8 in. thick.

** 1 in. thick.

Boron Carbide and Water. Attenuation of neutrons and gammas in solid B_4C followed by H_2O containing 0.5% boron by weight is currently being measured in the Lid Tank (Expt. 11).[11a] Quantities of particular interest are the variation of the biological dose with the thickness of B_4C at the outer side of the B_4C-H_2O shield, and the activation to be expected in a coolant (particularly sodium) located at various depths of B_4C.

The B_4C samples are in the form of one 20-in.-thick block, 5 by 4 ft, supplied by KAPL, and seventeen 1-in. slabs, 5 by 4 ft, supplied by NEPA. The 20-in. block contains B_4C of density 1.95 g/cc plus 0.135 g/cc of occluded H_2O. The NEPA slabs have an average density of B_4C of 1.8 g/cc and are less than 0.5% water by weight.

The amount of B_4C in each test is given in Tables 5.11 and 5.12. The following quantities, which were measured in the borated water behind various thicknesses of B_4C, are shown in the corresponding tables and figures:

QUANTITY MEASURED	DETECTOR	FIGURE NO.	TABLE NO.
Comparison of fast-neutron dosimeter and thermal-neutron counter measurements for borated water	25-in. BF_3 proportional counter vs. proton recoil dosimeter	5.11	5.13
Fast-neutron dosimeter centerline measurements	Proton recoil dosimeter	5.12	5.14
Thermal-neutron centerline measurements	25-in. BF_3 proportional counter	5.13	5.15
Gamma dose centerline measurements	10^{10} and 10^{12} ion chamber	5.14	5.16
Neutron absorption by boron within solid B_4C	25-in. BF_3 proportional counter within B_4C jacket	5.15	5.17

Since the 1-in. slabs were not watertight they were placed in a 15-in. by 6-ft by 5-ft dry tank with 1/8-in. steel walls. The remaining space in the dry tank was occupied by an aluminum tank full of water. The amount of Fe, Al, and occluded water in each configuration measured is given in Table 5.11. Some water always unavoidably remained between the source and the samples and also between the dry tank and the 20-in. block, since none of the surfaces are perfectly flat. The amount of this water is indicated in Tables 5.11 and 5.12.

(11a) Blizard, E. P., and Clifford, C. E., *Measurements of an Iron and Borated Water Shield in the Lid Tank, Experiment 11*, CF-50-12-48 (Dec. 15, 1950).

The experiment (Table 5.17) reversing the position of the boron slabs was carried out to determine the effect of the relative position of occluded water in the 20-in. block. It will be noted that lower neutron intensities at the shield exterior (about 140 cm) are obtained with the wet boron preceding the dry. This is tentatively explained qualitatively as being due to the relative effectiveness of scattering and absorption in a shield. The difference between wet and dry boron is that the former has a larger fraction of effective absorber, since hydrogen degrades neutrons so greatly in elastic collisions. The effect of reversing the position of the boron slabs can then be thought of as being due to an interchange of scatterer and absorber between two regions of the shield, one next to the source and the other intermediate between source and outer side of the shield. A scatterer is important in a shield only if it is introduced where neutrons are already collimated, so that deflection seriously affects the probability of its escape. Thus the dry boron, which, comparatively speaking, is a scatterer, is less effective in the relatively isotropic flux next to the source.

The measurements with the 25-in. BF_3 counter enclosed in a jacket of B_4C were taken to determine the activation of a $1/v$ absorber in neutrons of the spectrum existing behind a solid B_4C shield. Measurements in the water following the B_4C will also be taken since these attenuation data give a rough indication of the spectrum.

TABLE 5.11

Description of Materials in B_4C-H_2O Experiment

EXPERIMENT	THICKNESS OF B_4C AT DENSITY 2.5 (cm)	THICKNESS OF H_2O OCCLUDED IN B_4C OR BETWEEN SLABS (cm)	THICKNESS OF Fe (cm)	THICKNESS OF Al (cm)
20-in. B_4C block	39.62	7.7	1.27	
20-in. B_4C block followed by 4 1-in. slabs	47.03	8.7*	1.91	1.58**
20-in. B_4C block followed by 10 1-in. slabs	57.86	8.7*	1.91	3.46***
20-in. B_4C block followed by 12 1-in. slabs	61.65	8.7*	1.91	3.78****

* About 1 cm of H_2O between 20-in. block and tank of 1-in. slabs.

** 4 slabs + 1 aluminum tank containing 0.315 cm of aluminum.

*** 10 slabs and 1 aluminum tank containing 0.315 cm of aluminum.

**** 12 slabs but no tank.

TABLE 5.12

Description of NEPA 1-in. B_4C Slabs

POSITION	SLAB IDENTIFICATION NO.	WEIGHT OF B_4C (lb)	DENSITY OF B_4C (g/cc)	THICKNESS OF B_4C OF DENSITY 2.5 (cm)
1	17	191	1.84	1.87
2	19	190	1.83	1.86
3	16	191	1.84	1.87
4	15	185	1.78	1.81
5	4	177	1.70	1.73
11*	13	197	1.89	1.92
6	20	200	1.92	1.95
7	10	189	1.82	1.85
12*	1	193	1.86	1.87
8	6	172	1.65	1.68
9	9	176	1.69	1.72
10	18	194	1.87	1.90

* Positions 11 and 12 between slabs as shown

Position 1 is adjacent to the source

Aluminum face plates are 0.062 in. thick; 2 per slab = 0.315 cm/slab

Volume of B_4C slabs = 5 x 4 x 1/12 = 20/12 = 1.67 cu ft

Description of 20-in. B_4C block:

Density of dry B_4C, 1.95 g/cc

Thickness, 20-in. B_4C + two ¼-in. Fe face plates

Occluded H_2O = 6.48% of B_4C + H_2O by weight

g/cm^2 of B_4C = 20 x 2.54 x 1.95 = 99.06

g/cm^2 of occluded H_2O = 99.06 x 0.648/0.9352 = 6.90 g/cm^2

H_2O between block and source, 0.8 cm

Total H_2O = 6.9 + 0.8 = 7.7 g/cm^2

Equivalent centimeters of B_4C at density 2.50 = 99.06/2.50 = 39.62

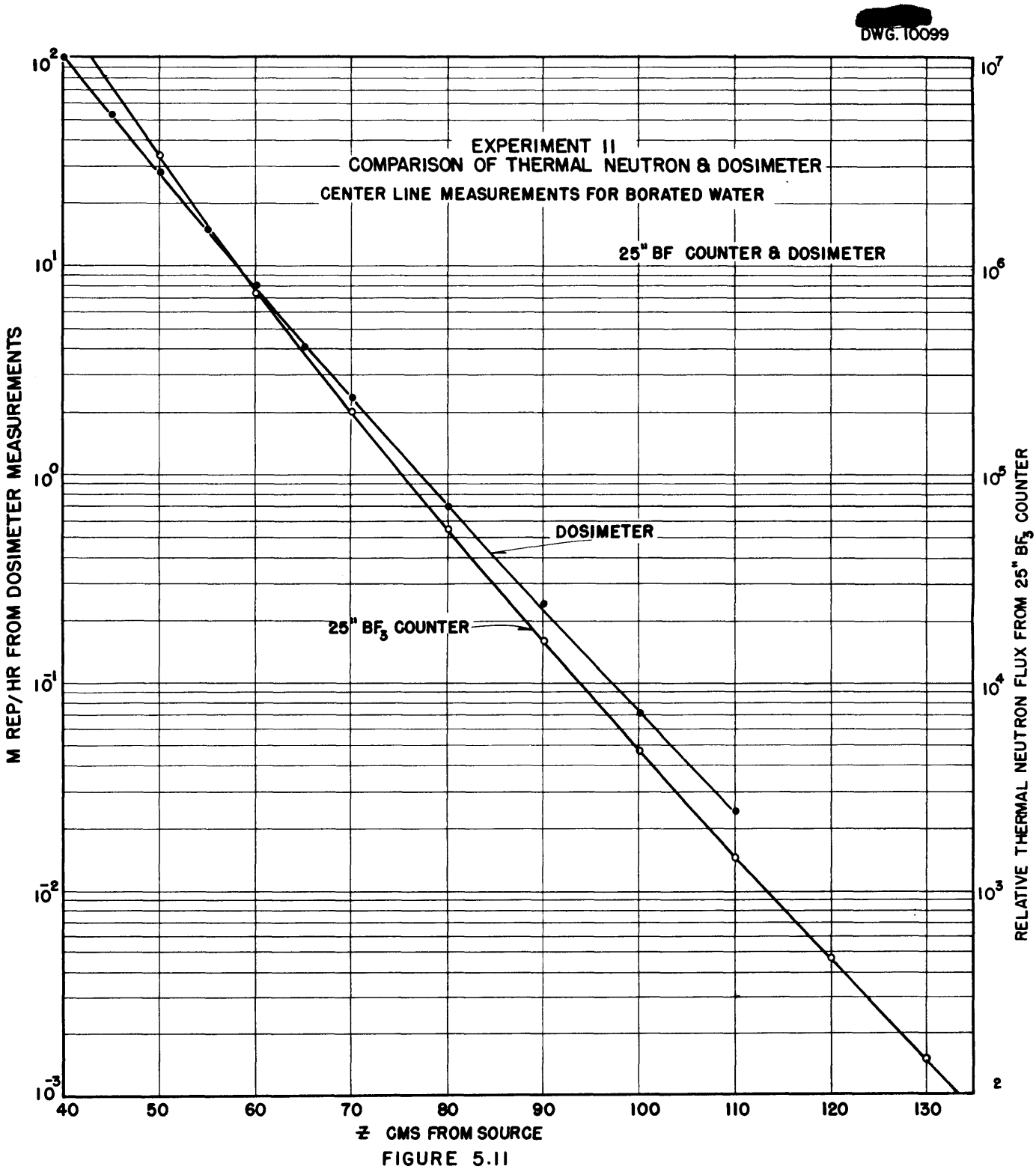
DWG. 10099
EXPERIMENT II
COMPARISON OF THERMAL NEUTRON & DOSIMETER
CENTER LINE MEASUREMENTS FOR BORATED WATER
25" BF COUNTER & DOSIMETER
DOSIMETER
25" BF3 COUNTER
M REP/HR FROM DOSIMETER MEASUREMENTS
RELATIVE THERMAL NEUTRON FLUX FROM 25" BF3 COUNTER
Z CMS FROM SOURCE
10^2
10^1
10^0
10^-1
10^-2
10^-3
10^7
10^6
10^5
10^4
10^3
2
40
50
60
70
80
90
100
110
120
130

FIGURE 5.11

TABLE 5.13

Comparison of Fast-neutron Dosimeter and Thermal-neutron Counter Measurements for Borated H_2O, No Slabs

DISTANCE FROM SOURCE (cm)	FAST-NEUTRON DOSIMETER, H_2O + 0.5% B (millirep/hour)		THERMAL-NEUTRON COUNTER, H_2O + 0.6% B (counts/minute)	
	RUN 1	RUN 2	8-in. BF_3 COUNTER NORMALIZED TO 25 in.	25-in. BF_3 COUNTER
40	107	91.5	15,230,000	
45	54.9	51.6		
50	28.61	27.3	3,380,000	
55	15.1	14.7		
60	8.1	7.88	803,000	740,000
65	4.10	4.25		
70	2.35	2.26	205,000	200,000
80	0.70	0.67	55,500	54,700
90	0.25	0.22	10,900	16,000
100		0.071		4,700
110		0.0241		1,460
120				469
130				148
140				54

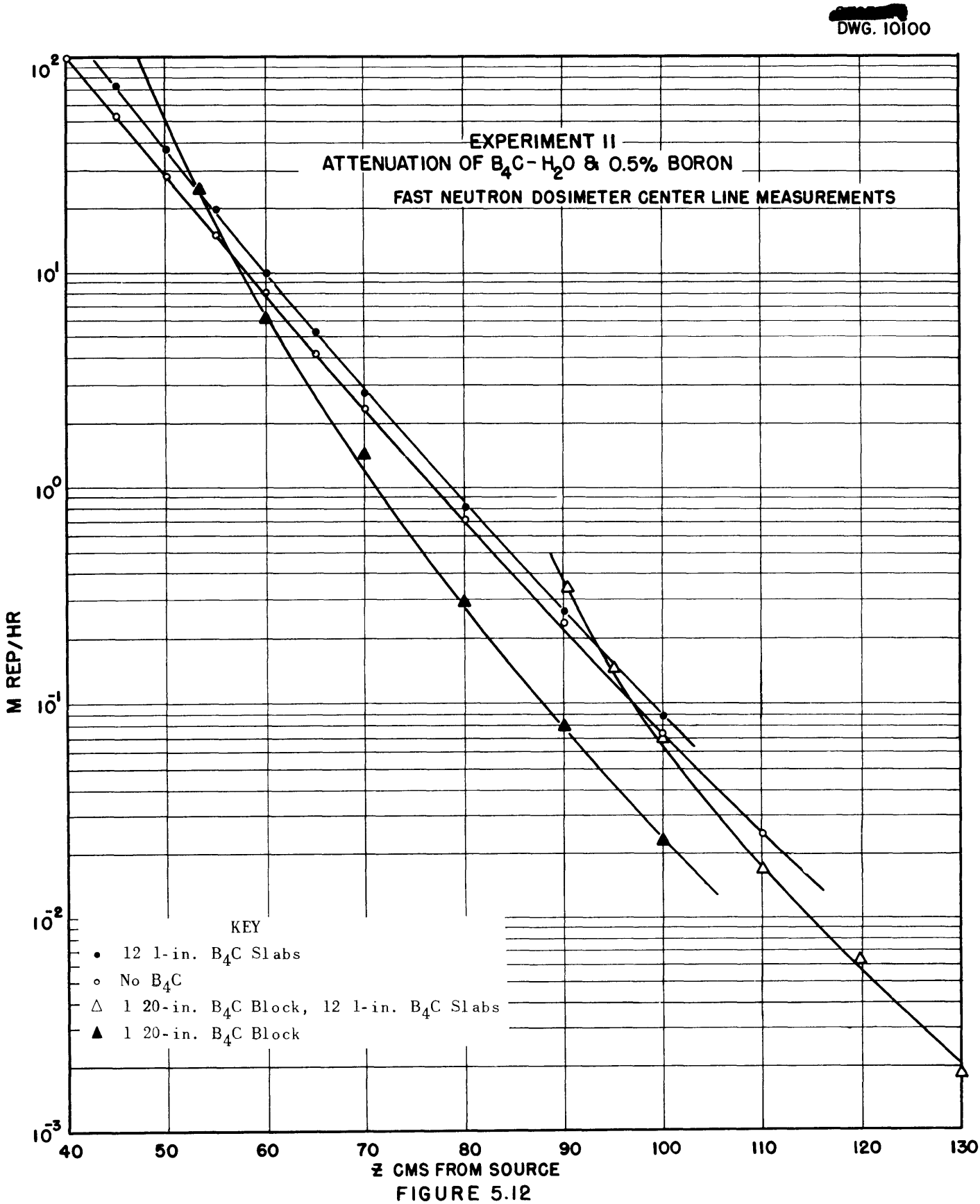
DWG. 10100
EXPERIMENT II
ATTENUATION OF B_4C-H_2O & 0.5% BORON
FAST NEUTRON DOSIMETER CENTER LINE MEASUREMENTS
M REP/HR
10^2
10^1
10^0
10^{-1}
10^{-2}
10^{-3}
KEY
• 12 1-in. B_4C Slabs
○ No B_4C
△ 1 20-in. B_4C Block, 12 1-in. B_4C Slabs
▲ 1 20-in. B_4C Block
40
50
60
70
80
90
100
110
120
130
Z CMS FROM SOURCE

FIGURE 5.12

TABLE 5.14

Neutron Attenuation of B_4C-H_2O + 0.5% B

(Fast-neutron Dosimeter Centerline Measurements)

DISTANCE FROM SOURCE (cm)	(millirep/hour)				
	2 1-in. B_4C SLABS	1 20-in. B_4C SLAB			1 20-in. B_4C SLAB, 12 1-in. B_4C SLABS
		RUN 1	RUN 2	RUN 3	
40.5	128.3				
45	72.1				
50	36.9				
53.5		30.2	18.9		
55	19.6				
60	9.90	5.81	6.47	6.29	
65	5.23				
70	2.78	1.43	1.49	1.31	
80	0.814		0.262	0.326	
90	0.265			0.078	
90.5					0.340
95					0.145
100	0.087			0.023	0.069
110					0.0154
115					0.0063
120					0.00183*

* Poor statistics.

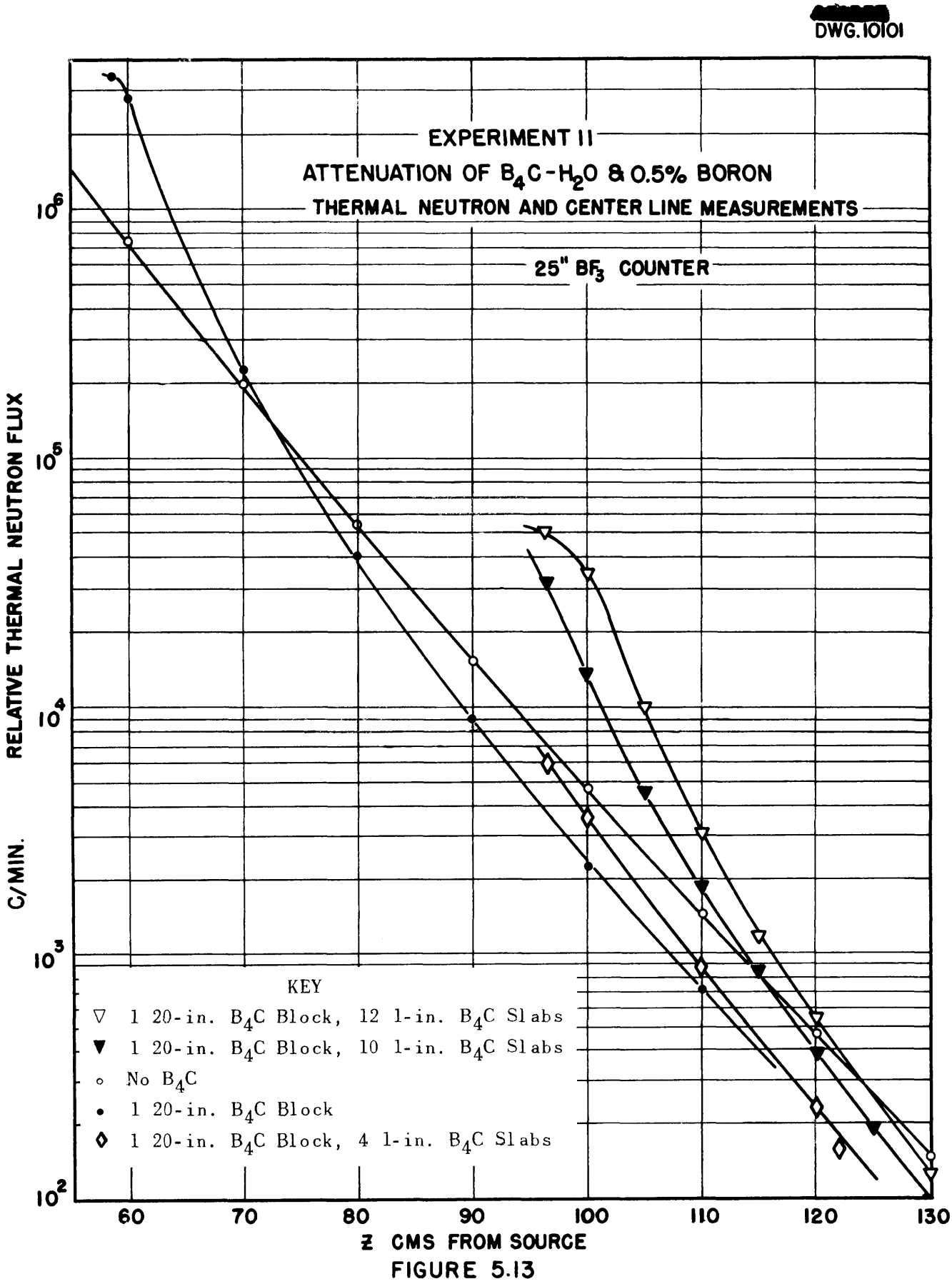
DWG. 10101
EXPERIMENT 11
ATTENUATION OF B_4C-H_2O & 0.5% BORON
THERMAL NEUTRON AND CENTER LINE MEASUREMENTS
25" BF_3 COUNTER
RELATIVE THERMAL NEUTRON FLUX
C/MIN.
10^6
10^5
10^4
10^3
10^2
60
70
80
90
100
110
120
130
Z CMS FROM SOURCE
KEY
▽ 1 20-in. B_4C Block, 12 1-in. B_4C Slabs
▼ 1 20-in. B_4C Block, 10 1-in. B_4C Slabs
○ No B_4C
● 1 20-in. B_4C Block
◇ 1 20-in. B_4C Block, 4 1-in. B_4C Slabs

FIGURE 5.13

TABLE 5.15

Thermal-neutron Attenuation by B_4C and H_2O + 0.5% B

(25-in. BF_3 Counter in H_2O Behind Solid B_4C)

DISTANCE FROM SOURCE (cm)	(counts/minute)						
	EXPT. 10 NO SLABS* (borated water)	EXPT. 11 NO SLABS* (borated water)	1 20-in. B_4C SLAB				
			RUN 1		RUN 2		RUN 3
58.7			1,339,000**		1,270,000**		1,261,000**
60			1,280,000**		1,252,000**		1,181,000**
70	199,753	199,357	224,000		233,000		213,000
80	54,668	53,640	40,600		42,000		38,400
90	16,038	15,178	9,030		9,400		8,975
100	4,692		2,070		2,400		2,250
110	1,455		705		672		612
120	469				182		
130	148						
140	54						
	1 20-in. B_4C SLAB, 4 1-in. B_4C SLABS		1 20-in. B_4C SLAB, 10 1-in. B_4C SLABS		1 20-in. B_4C SLAB, 12 1-in. B_4C SLABS		12 1-in. B_4C SLABS, 1 20-in. B_4C SLAB
	RUN 1	RUN 2	RUN 1	RUN 2	BARE	Cd-COVERED	BARE
96.4			31,400	31,700	49,800	5,350	
96.7	5,990	5,840					
97.4							19,535
100	3,615	3,630	13,700	13,700	35,000	3,107	17,431
105				4,560	9,970	810	
110	882	867	1,860	1,870	3,100	268	2,922
115				827	1,180		
120	230	232	392	394	541		663
125				194			
130	67.6	68		99.8	126		175
135				54.9			
140	19.7		28	30	32.7		48

* 0.6% boron was used in this experiment.

** Not reliable owing to counting loss at high counting rate.

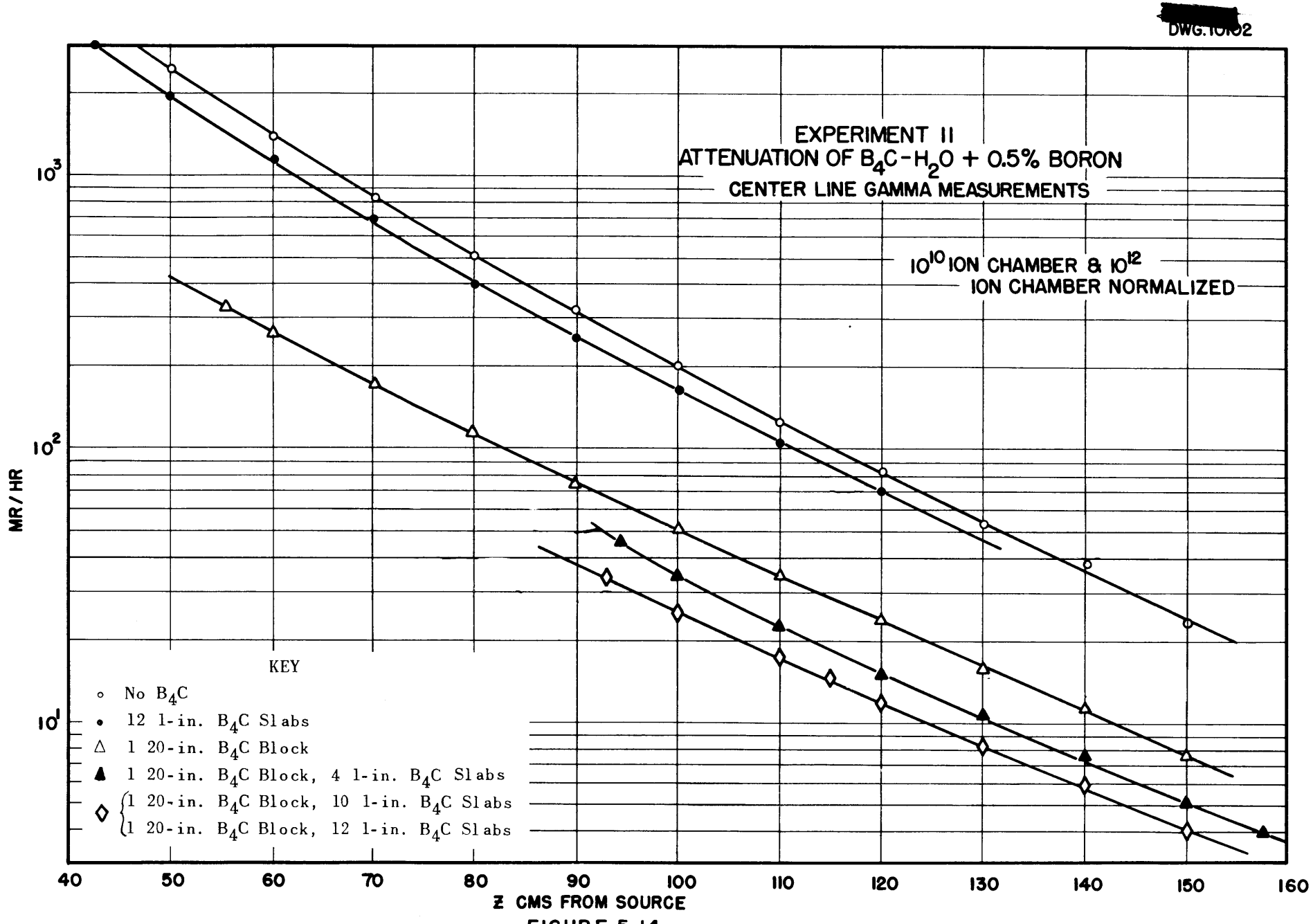
DWG. 10102
EXPERIMENT 11
ATTENUATION OF B_4C-H_2O + 0.5% BORON
CENTER LINE GAMMA MEASUREMENTS
10^{10} ION CHAMBER & 10^{12} ION CHAMBER NORMALIZED
MR/HR
10^3
10^2
10^1
KEY
○ No B_4C
• 12 1-in. B_4C Slabs
△ 1 20-in. B_4C Block
▲ 1 20-in. B_4C Block, 4 1-in. B_4C Slabs
◇ 1 20-in. B_4C Block, 10 1-in. B_4C Slabs
◇ 1 20-in. B_4C Block, 12 1-in. B_4C Slabs
40 50 60 70 80 90 100 110 120 130 140 150 160
Z CMS FROM SOURCE

FIGURE 5.14

TABLE 5.16

Gamma Attenuation by B_4C and H_2O + 0.5% B

(10^{10} and 10^{12} Ion Chambers Normalized)

DISTANCE FROM SOURCE (cm)	(milliroentgens/hour) NO SLABS	2 1-in. B_4C SLABS	1 20-in. B_4C SLAB	1 20-in. B_4C SLAB, 4 1-in. B_4C SLABS	1 20-in. B_4C SLAB, 10 1-in. B_4C SLABS	1 20-in. B_4C SLAB, 12 1-in. B_4C SLABS
42.5		2993				
50	2440	1941				
55.3			330			
60	1380	1152	262			
70	825	690	176			
80	506	400	119			
90	321	255	74.8			
92.8						31.4
93					33.8	
94.4				46.1		
100	200	163	51.3	34.1	25.1	26.0
110	124	105	34.2	22.5	17.1	17.9
115					14.6	
120	83	70	23.4	15.0	11.9	11.9
130	53		15.9	10.5	8.4	8.4
140	38		11.2	7.6	5.9	6.0
150	23		7.8	5.0	4.0	3.8
157.7				3.9		

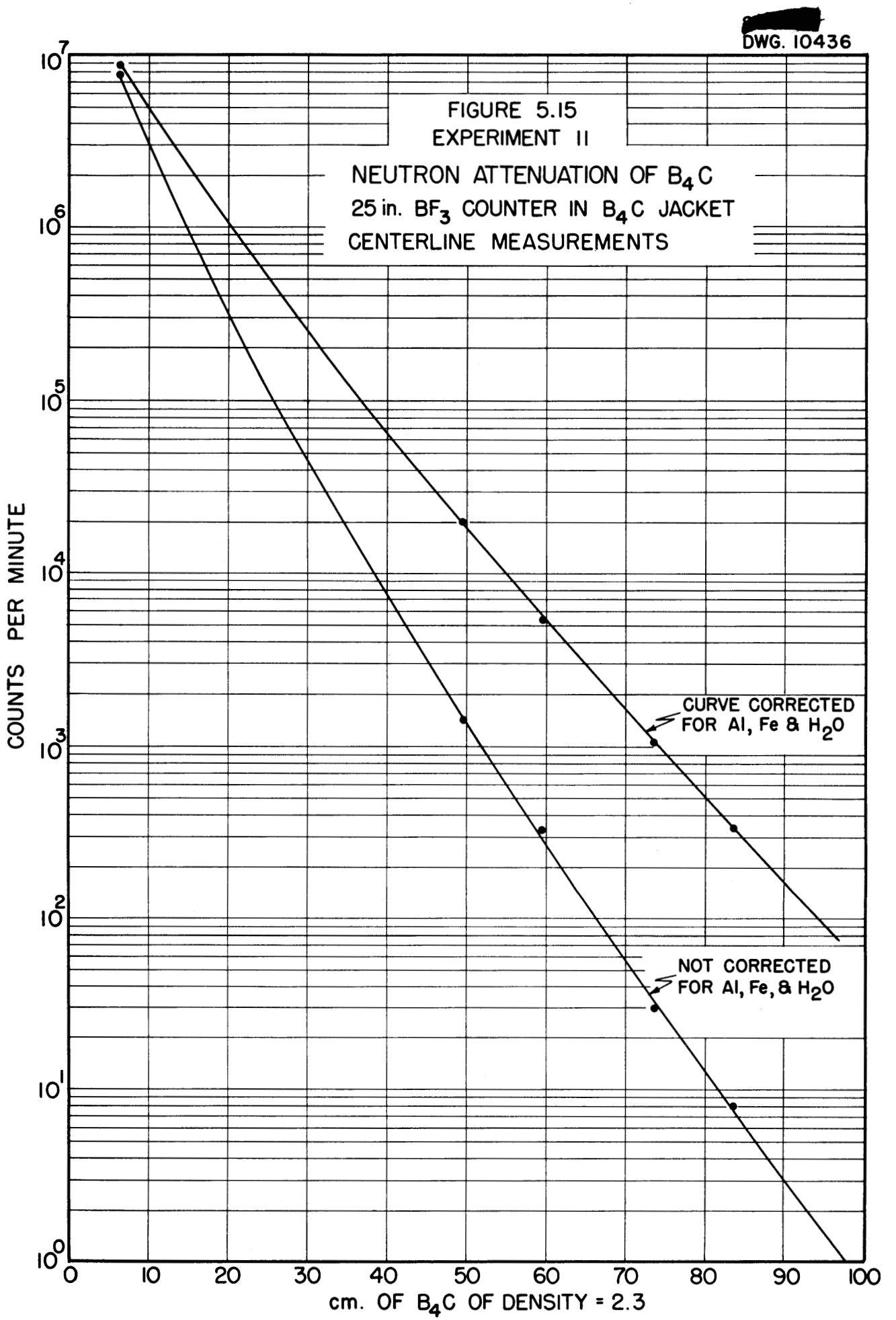
DWG. 10436
FIGURE 5.15
EXPERIMENT II
NEUTRON ATTENUATION OF B_4C
25 in. BF_3 COUNTER IN B_4C JACKET
CENTERLINE MEASUREMENTS
CURVE CORRECTED FOR Al, Fe & H_2O
NOT CORRECTED FOR Al, Fe, & H_2O
COUNTS PER MINUTE
10^7
10^6
10^5
10^4
10^3
10^2
10^1
10^0
0
10
20
30
40
50
60
70
80
90
100
cm. OF B_4C OF DENSITY = 2.3

TABLE 5.17

Measurements of B_4C Attenuation

(25-in. BF_3 Counter in B_4C Jacket Behind Solid B_4C Slabs)

EXPERIMENT	THICKNESS OF B_4C OF DENSITY 2.3* (cm)	THICKNESS OF Al** (cm)	THICKNESS OF Fe** (cm)	THICKNESS OF H_2O** (cm)	COUNTS/MIN WITH 25-IN. BF_3 COUNTER
3 in. B_4C in jacket	6.30	1.27	0	0.5	7,673,680
1 20-in. B_4C slab	43.1		1.27	7.7	
1 20-in. B_4C slab 3 in. B_4C in jacket	49.4	1.27	1.46	10.4	1,400.8
1 20-in. B_4C slab 5 1-in. B_4C slabs 3 in. B_4C in jacket	59.43	2.85	1.46	10.4	323.4
1 20-in. B_4C slab 12 1-in. B_4C slabs 3 in. B_4C in jacket	73.47	5.05	2.095	12.9	29.53
1 20-in. B_4C slab 17 1-in. B_4C slabs 3 in. B_4C in jacket	83.50	6.625	2.095	12.9	7.96

* Includes B_4C in jacket between source and counter.

** If these materials are treated as impurities, corrections should be made using the following relaxation lengths: Al, 12 cm; Fe, 12 cm; H_2O, 4.3 cm.

Description of B_4C counter jacket:

Outside dimensions of B_4C, 40 in. high by 16 in. wide by 6-1/8 in., rectangular
Inside dimensions of B_4C,, 25 in. high by 12 in. wide by 3-1/8 in., rectangular
B_4C thickness between detector and source, 3 in.
¼-in. aluminum can over B_4C exterior, 1/8-in. aluminum can inside B_4C
Density of B_4C, 1.90 g/cc
Water content, 1.4% by weight

Measurements of Fast Neutrons in the Lid Tank Using a Sulfur Threshold Detector (H. E. Hungerford, Physics Division). During the past quarter Lid Tank Measurements of fast neutrons using a sulfur threshold detector were completed. The reaction used was the $S^{32}(n,p)P^{32}$ reaction. Samples of ammonium sulfate powder were exposed to fast-neutron flux in the Lid Tank in appropriate containers. After exposure the radioactive phosphorus was separated from the inert material by precipitation as ammonium phosphomolybdate. Details of the separation and preliminary results have already been reported in the preceding quarterly report.[12]

The purpose of these measurements has been twofold: (1) to test the feasibility of using such a detector for measuring fast-neutron attenuation, and (2) to obtain independent measurements of the fast neutrons along the centerline of the Lid Tank.

Up until the time of the present measurements workers had not had much success in the use of sulfur detectors.[13] In the present experiments a technique was developed and refined until a fair amount of reproducibility was possible. Losses during chemical separation were cut down to less than 2%, and the counters were standardized using P^{32} from the Isotopes Division, which guaranteed that the activity specification was within 3%. This calibration gives flux values about 15% lower than values of the phosphorus standardization previously reported.

It should be pointed out that although the actual reaction threshold is about 1 Mev, the effective threshold is nearly 3 Mev, so that, for all practical purposes, the values reported here and previously give the flux for neutrons of energies of 3 Mev and greater. In Table 5.18 and Fig. 5.18 (p.147) are presented the most reliable points obtained. Measurements were taken in the 33% Pb—borated water shield mock-up. Their accuracy is within 25% for points far from the source, and within 10% for those near the source.

(12) ORNL-858, *op. cit.*, p. 35.

(13) See Taschek, R. F., *Radioactive Threshold Detectors for Neutrons*, MDDC-360 (Sept. 17, 1946); Bopp, C. D., and Sisman, O., *The Neutron Flux Spectrum and Fast and Epithermal Flux in Hole 19 of the ORNL Reactor*, ORNL-525 (July 28, 1950).

TABLE 5.18

Measurement of Fast Neutrons in the Lid Tank

SHUTTER POSITION	DISTANCE FROM SOURCE (cm)	FAST FLUX, nv
Open	4.7	1.10×10^6
Open	12.0	3.14×10^5
Open	19.6	1.02×10^5
Open	30.3	2.32×10^4
Open	42.0	7.38×10^3
Closed	4.1	7.21×10^4
Closed	18.8	5.54×10^3
Closed	34.2	6.40×10^2

LIQUID-METAL DUCT TEST IN THE THERMAL COLUMN

R. H. Lewis, NEPA
L. J. Frankwitz, KAPL
M. K. Hullings, Physics Division
M. C. Marney, Physics Division

The liquid-metal duct test described in the last quarterly report[14] is now underway. This experiment is designed primarily to determine the reduction in efficiency of a reactor shield when perforated with liquid-metal ducts, with special emphasis on the activation to be expected in a secondary coolant such as sodium. Although KAPL is supplying the duct mock-up, the design is chosen to be of interest to ANP as well as to the Submarine Intermediate Reactor (KAPL project). The sodium in the duct will be simulated by aluminum powder of proper density.

The first leg of the duct has been measured with air in the 6-in. duct as well as the 1-in. annulus. Figures 5.16 and 5.17 show part of the data. Figure 5.16 is the centerline measurement taken in water beyond the end of the duct along its axis. Figure 5.17 shows the traverses on the lucite foil-mounting plates. These plates are mounted perpendicular to the axis of the

(14) ORNL-858, *op. cit.*

DWG. 10083

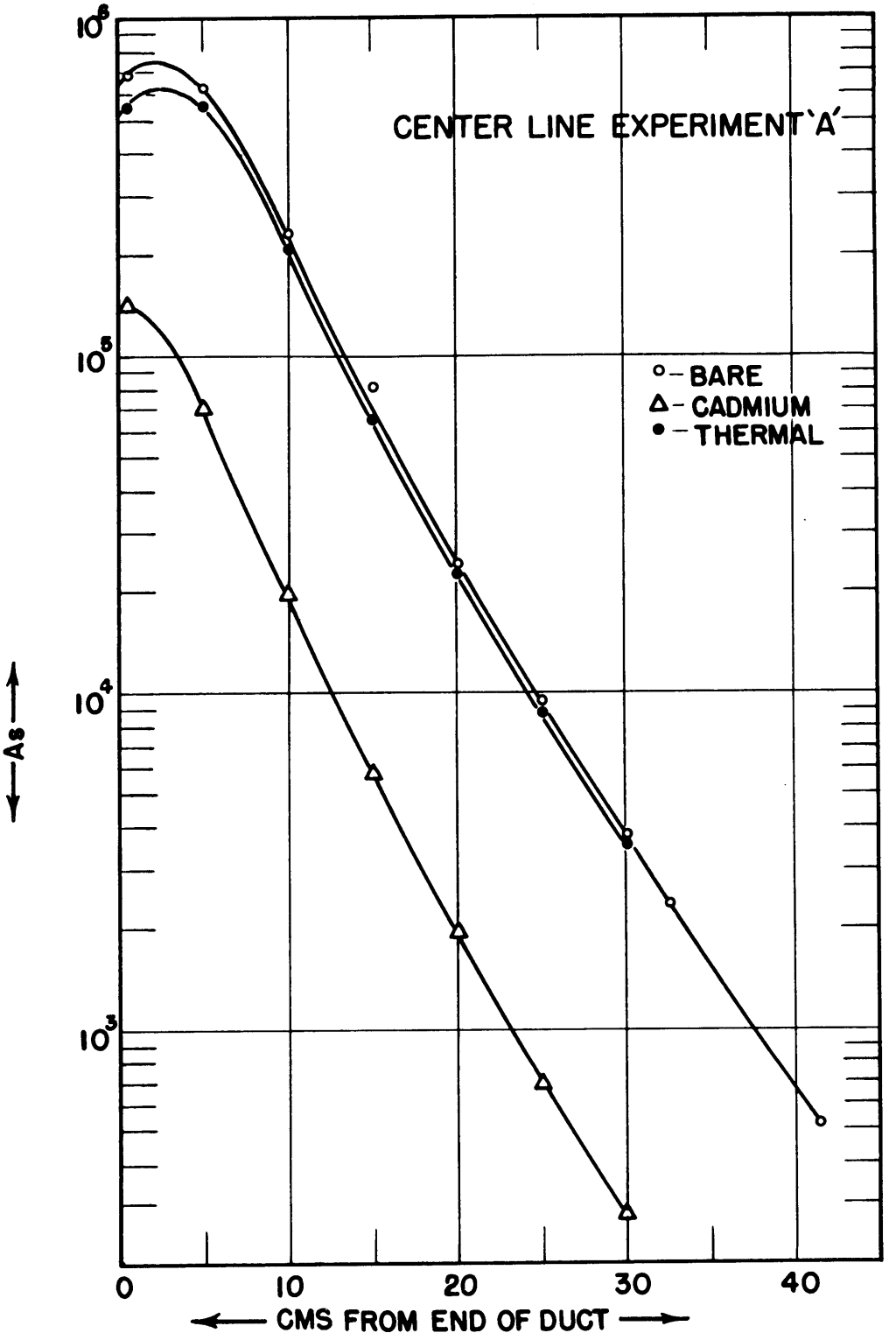

FIGURE 5.16 NEUTRON CENTER LINE MEASUREMENTS FROM END OF DUCT

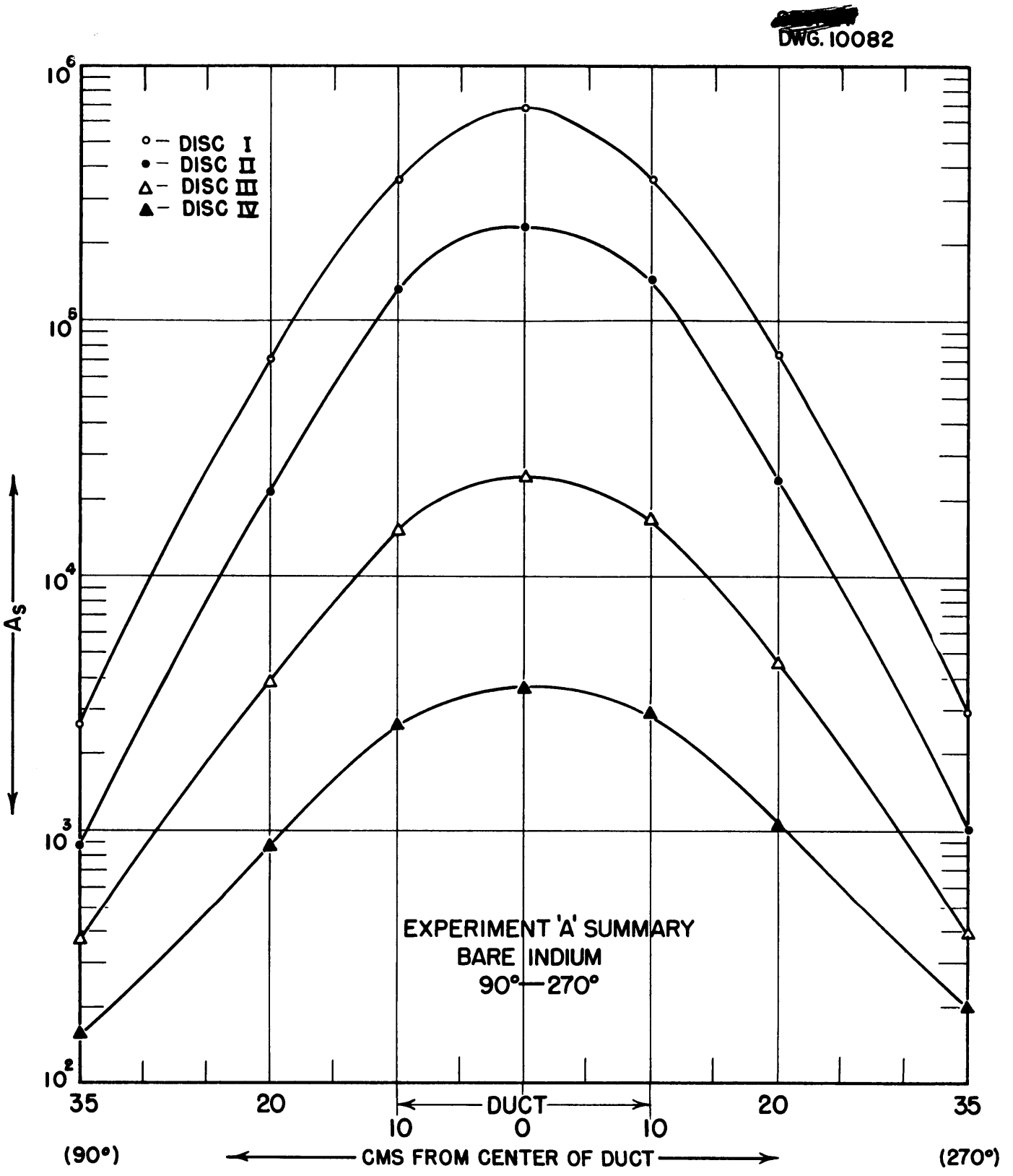

FIGURE 5.17 RADIAL NEUTRON FLUX FROM CENTER OF DUCT

duct at 10-cm intervals. A volume integral of slow-neutron flux obtained from these curves will indicate the total number of neutrons which have come through the duct. A second duct with one right-angle bend has been received, and measurements with air in the duct have been taken but are not yet complete.

The effect of varying the shielding material surrounding the ducts will soon be measured using the B_4C jackets now on hand.

A mapping of the flux distribution over the source box has been made with 1-cm^2 gold foils. The source box contains twenty-four X-10 slugs and provides a secondary source of approximately 10^7 fast neutrons/(cm^2)(sec) from the thermally induced fissions.

The aluminum-filled ducts are expected to arrive from KAPL by December 5. A third duct is now being constructed which will have two right-angle bends. This configuration will complete the types of duct to be measured in this experiment as presently planned.

SHIELD CALCULATIONS

Analysis of Lid Tank Data (S. Podgor, NEPA). The analysis of Pb-H_2O and Fe-H_2O data mentioned in the last quarterly report[15] was completed and is being issued as a separate report.[16] "Effective" fast-neutron cross sections for the metals based on the "one-collision" theory of shielding were obtained.

The procedure consisted in obtaining a good empirical fit to the 100% H_2O data and finding the proper metal cross section that would reproduce the metal-water attenuation data. Analytically this amounted to assuming the following form for the attenuation of a point source of neutrons in water:

$$P(r) = \frac{Ae^{-\alpha r} + Be^{-\beta r}}{4\pi r^2}$$

(15) ORNL-858, *op. cit.*

(16) Podgor, S., *Analysis of Lid Tank Neutron Data for Lead and Iron*, ORNL-895 (Jan. 23, 1951).

where r is the distance from the source and A, B, α, and β are constants for the water. The constants were adjusted so that, on integration of the point kernel over the disk fission source, a fit was obtained to the water attenuation data to within 2%. A constant attenuation for the metal was then inserted to fit the metal-water data. It was possible to do this to within about 5%. The values obtained were 3.4 barns for Pb and 2.0 barns for Fe.

The curves in Figs. 5.18 through 5.20 show the experimental and calculated variation of thermal-neutron flux, at three different distances from the source plate, as successive lead slabs are added. The random variations in the experimental values are probably ascribable to statistical and positioning errors. Two different values for the effective lead cross section are assumed (3.4 and 3.5 barns) and it is clearly seen that no large variation in this quantity is possible.

Analysis of Lid Tank Data on Boron Carbide and Water (R. Zirkind, Reactor Technology School student from Bureau of Aeronautics, U. S. Navy). A preliminary analysis of the Lid Tank data on the attenuation of a 20-in. block of B_4C in H_2O (Expt. 11) was made in accordance with the method described in ORNL-895.

The 20-in. block of B_4C had entrapped about 6% H_2O (by weight). To correct for this, it was assumed that the dry block had its density decreased corresponding to the water content, namely $\rho_{B_4C} = 1.95$. An effective absorption (or removal) cross section of 1.2 barns was taken as a reasonable guess, and the effect of the B_4C on the thermal flux in the water was calculated beyond the B_4C. The results of the calculation are given in Table 5.19.

TABLE 5.19

Comparison of Theoretical and Experimental Attenuation Data

DISTANCE FROM SOURCE (cm)	OBSERVED FLUX	CALCULATED FLUX	APPROXIMATE ERROR (%)
90	9000	7955	15
100	2260	2251	0.5
110	658	650	1
120*	182	190	4

* Data incomplete.

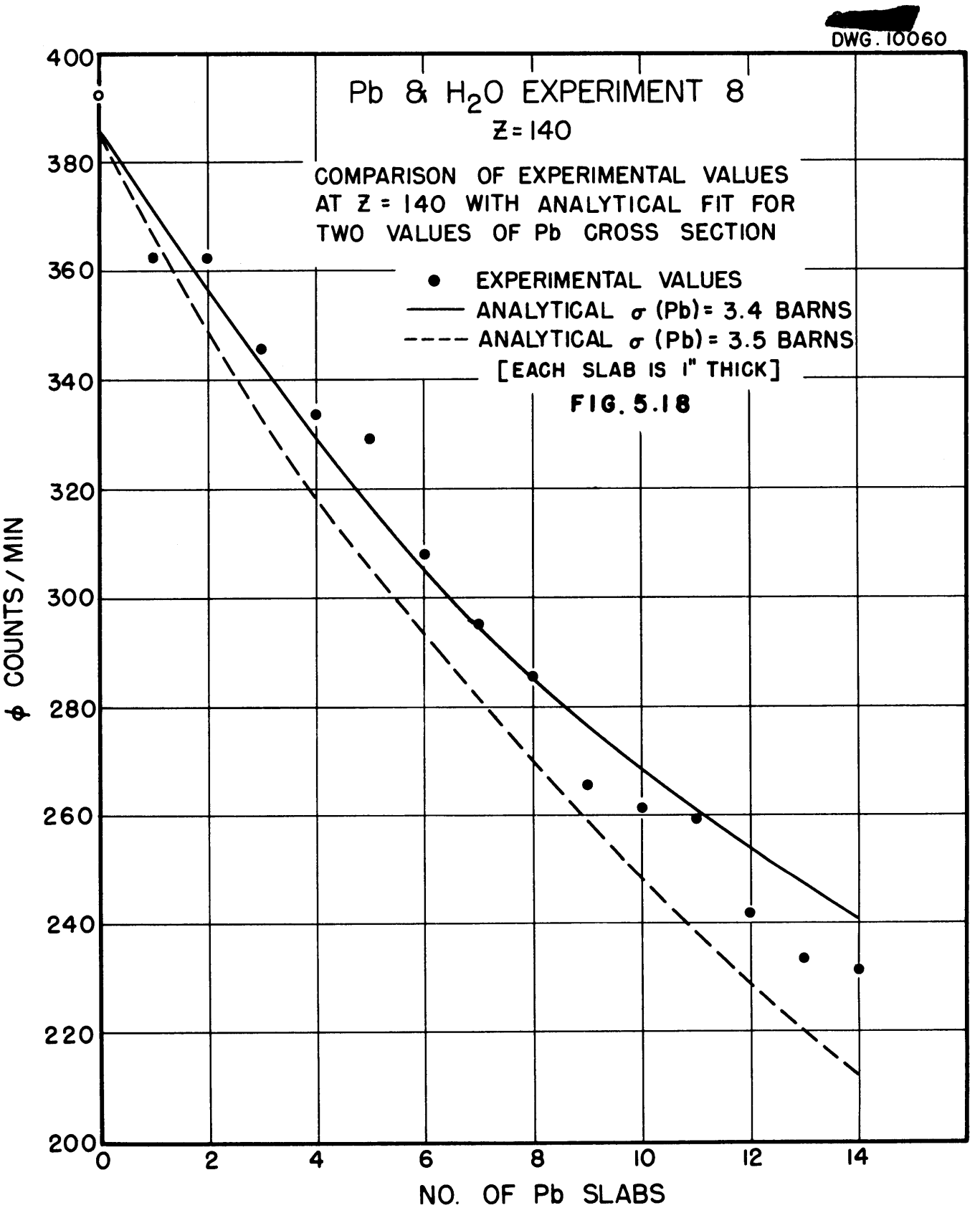
DWG. 10060
Pb & H_2O EXPERIMENT 8
Z = 140
COMPARISON OF EXPERIMENTAL VALUES AT Z = 140 WITH ANALYTICAL FIT FOR TWO VALUES OF Pb CROSS SECTION
EXPERIMENTAL VALUES
ANALYTICAL σ (Pb) = 3.4 BARNS
ANALYTICAL σ (Pb) = 3.5 BARNS
[EACH SLAB IS 1" THICK]
FIG. 5.18
φ COUNTS / MIN
NO. OF Pb SLABS
400
380
360
340
320
300
280
260
240
220
200
0
2
4
6
8
10
12
14

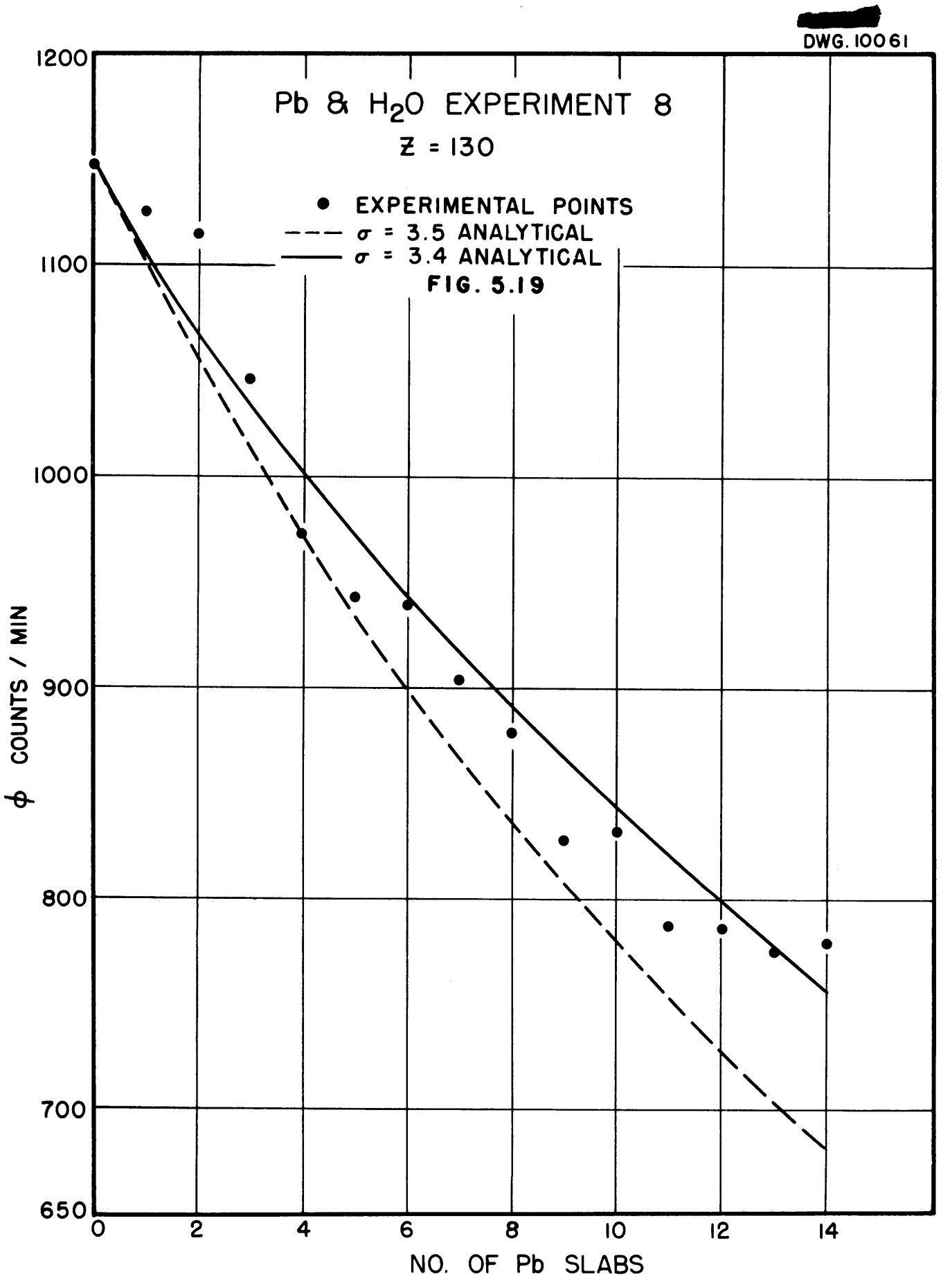
DWG. 10061
Pb & H_2O EXPERIMENT 8
Z = 130
EXPERIMENTAL POINTS
σ = 3.5 ANALYTICAL
σ = 3.4 ANALYTICAL
FIG. 5.19
φ COUNTS / MIN
NO. OF Pb SLABS
1200
1100
1000
900
800
700
650
0
2
4
6
8
10
12
14

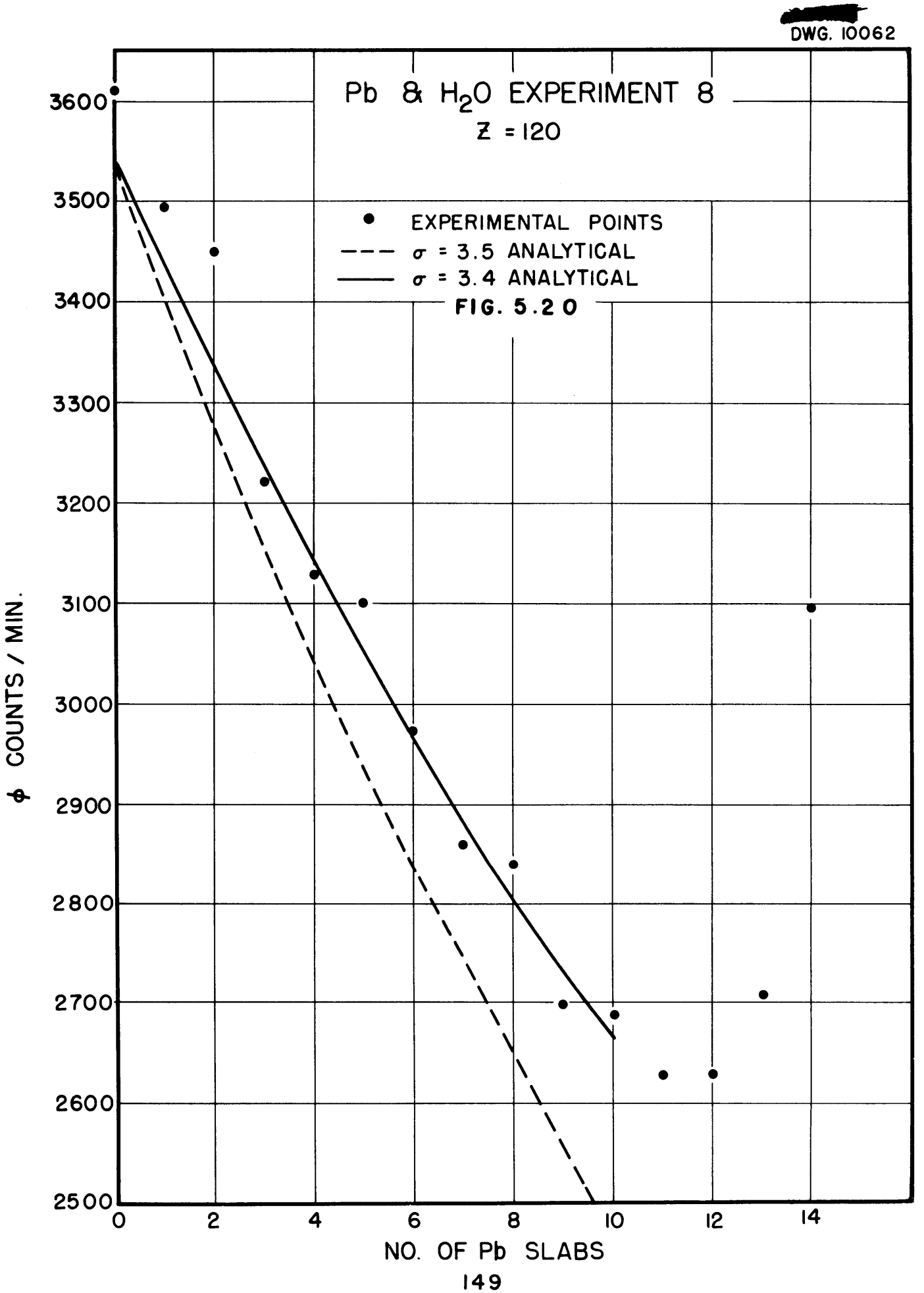
DWG. 10062
Pb & H_2O EXPERIMENT 8
Z = 120
EXPERIMENTAL POINTS
σ = 3.5 ANALYTICAL
σ = 3.4 ANALYTICAL
FIG. 5.20
φ COUNTS / MIN.
3600
3500
3400
3300
3200
3100
3000
2900
2800
2700
2600
2500
0
2
4
6
8
10
12
14
NO. OF Pb SLABS

The agreement for $Z \geq 100$ cm (or 50 cm of H_2O following the B_4C block), where Z is the distance from source to counter, is excellent; however, for $Z \leq 100$, the results become progressively poorer. In fact, for $Z = 70$ cm, or 20 cm of H_2O, the error is 100%. This is readily understandable since the B_4C block produces a large build-up of degraded neutrons, which gives rise to a nonequilibrium region in the initial thickness of the water.

On the basis of the above removal cross section, B_4C of theoretical density, 2.5 g/cc, would exhibit a relaxation length of 6.2 cm. Subsequent measurements on B_4C indicate that the simple picture used for the above analysis may not be completely correct, and consequently the results may not be really meaningful. Work is continuing on experiments to settle this point.

Theory of Neutron Attenuation (F. H. Murray, Physics Division). Several methods are being explored for calculating the neutron attenuation in materials such as B_4C with variable cross sections. In previous calculations for materials with constant cross sections, two terms of the scattering contribution to the Boltzmann equation were usually sufficient, and this result appears to justify a simplified approach by means of a small number of differential equations. Another method based on results for constant cross sections is also being studied.

The general formulas used in the calculations for mixtures of Pb and H_2O were applied to a mixture of equal volumes of Fe and H_2O. A brief analysis of scattering at low energies, $E < 2$ Mev, where inelastic scattering in Fe is relatively unimportant, and with iron considered as a pure scatterer and water as a pure absorber, indicated an appreciably higher attenuation than was present at higher energies. From the analysis based on the assumption of forward scattering in Fe, relaxation lengths for the high-energy flux were obtained as follows:

Z (cm)	λ (cm)	Z (cm)	λ (cm)
35	5.3	85	6.2
45	5.6	95	6.3
55	5.8	105	6.3
65	5.9	115	6.4
75	6.1		

The experimental attenuation between 86 and 120 cm is approximately the same as the calculated high-energy attenuation, but intermediate values show some differences.

Shield Calculation Methods (A. Simon and T. Welton, Physics Division). An attempt is being made to set up a flexible and simple method for predicting shield behavior. Much of the required work was done by the Shielding Group of the TAB, and this work is being extended so that checks can be made with the complete lead-water and iron-water Lid Tank data. In this way, it is hoped to obtain a simple and believable phenomenological shield theory.

A perturbation theory for shields has been set up which allows the calculation of the relaxation length defined by Blizard. This should facilitate the optimization procedure considerably.

Ducting Difference Equations (D. W. Whitcombe, Mathematics Panel). The solution for the neutron flux at all points of a finite or infinite medium which contains a duct cannot be found analytically even for the simplest geometries. However, numerical solutions can be found by replacing the differential equations by the corresponding difference equations. In these computations the medium will be replaced by a grid of area (or volume) elements, and it is desirable that the geometry of the problem correspond to a natural grid.

To illustrate the procedure consider the drawing

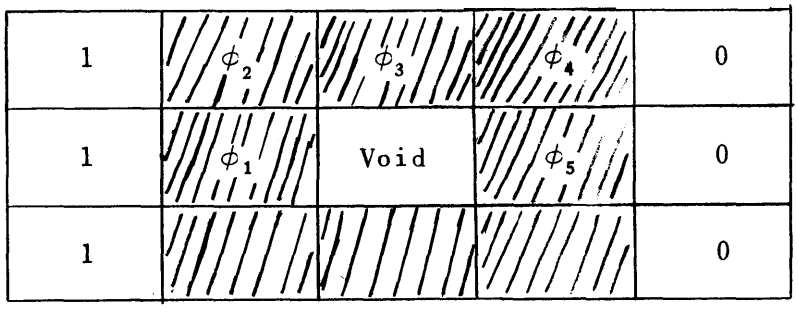

where the shaded material represents concrete, the column of 1's refers to a unit collimated beam source of thermal neutrons, and the column of 0's indicates that the return current on the outside face of the concrete is zero.

The diffusion equation

$$\nabla^2\phi - k^2\phi = 0$$

is replaced by

$$\sigma\phi_p - \sum_n \phi_n = 0, \qquad \sigma = 4 + k^2h^2$$

where h is the lattice spacing, p refers to an arbitrary cell, and $\sum_n$ is the sum of the four neighbors of ϕ_p (i.e., above, below, and on the two sides). To apply these difference equations it is considered that the preceding drawing is a unit cell that is repeated above and below. The results are shown as follows:

1	0.5496	0.3013	0.1483	0
1	0.5286	Air Void	0.1912	0
1	0.5496	0.3013	0.1483	0

Because of the symmetry there are only five equations and five unknowns. When the lattice spacing is taken smaller there will be many more unknowns, and the Fairchild machine will be used to solve the linear equations. A report will soon be issued which will contain an appendix of problems similar to the above but where the Fairchild machine obtained the solutions.

Gamma Activity Due to Fission Fragments (W. K. Ergen, Physics Division). A refinement of existing calculations[17] is needed to determine the gamma activity due to fission fragments in all cases where servicing has to be carried out in the neighborhood of a shutdown reactor which is enclosed in less

(17) Shielding Board Report, ANP-53, *op. cit.*, Appendix I.

than a full ground-safe shield (e.g., reactor in a divided shield, or a partially disassembled unit shield). On the basis of existing literature,[18] refined estimates of the fission-fragment gamma activity can be made now, but an experimental check in the swimming pool is still required, and has been proposed.[19]

Very short-lived gamma activities of fission-fragment decay gammas are of interest in the case of circulating-fuel, or homogeneous, reactors. It has been suggested that they be investigated by means of the pneumatic tube in the ORNL pile. This facility could also measure the Bremsstrahlung from Li^8 betas and settle the question of whether Li^8 emits a gamma upon decay.[20]

A brief calculation was made as a perturbation on the shield for a reactor using sodium as both the primary and intermediate coolant.[21] The perturbation consists in omitting the shutdown tolerance requirements, retaining only the running tolerance specifications. This saves 5¾ in. of lead from the gamma shield around the heat exchanger and 11 in. of B_4C in the neutron shield between the reactor and heat exchanger.

NEW BULK SHIELD TESTING FACILITY

W. M. Breazeale and J. L. Meem, Physics Division

As of December 1 the installation of the reactor and associated equipment was about half completed. Figure 5.21 is a picture of the reactor grid which will hold the fuel elements. The three cylindrical electromagnets shown near the top of the picture will support the safety and control rods. The contractor had not finished the building or installed the overhead traveling crane but hoped to be finished with this work by December 15.

(18) Gillette, P.R., *Final Report, Production Test No. 105-53-P, Measurement of Slug Decay,* HW-17781 (May 15, 1950); Ascoli, G., and Sisman, O., *Absorption of Radiation from an "X" Slug by Lead,* ORNL-53 (May, 1948); Bernstein, S., Talbott, F. L., Leslie, J. K., and Stanford, C. P., *Yield of Photoneutrons from U^{235} Fission Products in Be,* CNL-38 (Feb. 20, 1948); Bernstein, S., Preston, W. M., Wolfe, G., and Slattery, R. E., "Yield of Photoneutrons from U^{235} Fission Products in Heavy Water," *Phys. Rev.* 71, 573 (1947).

(19) Ergen, W. K., *Measurements of Fission Fragment Decay Gammas in the Swimming Pool,* Oak Ridge National Laboratory, Y-12 Site, Y-F20-3 (Nov. 28, 1950).

(20) Hornyak, W. F., and Lauritsen, T., "The Beta-Decay of B^{12} and Li^8," *Phys. Rev.* 77, 160 (1950).

(21) ANP-53, *op. cit.*, Sec. 3.4.

[redacted]
Photo 7290

FIG. 5.21 REACTOR GRID

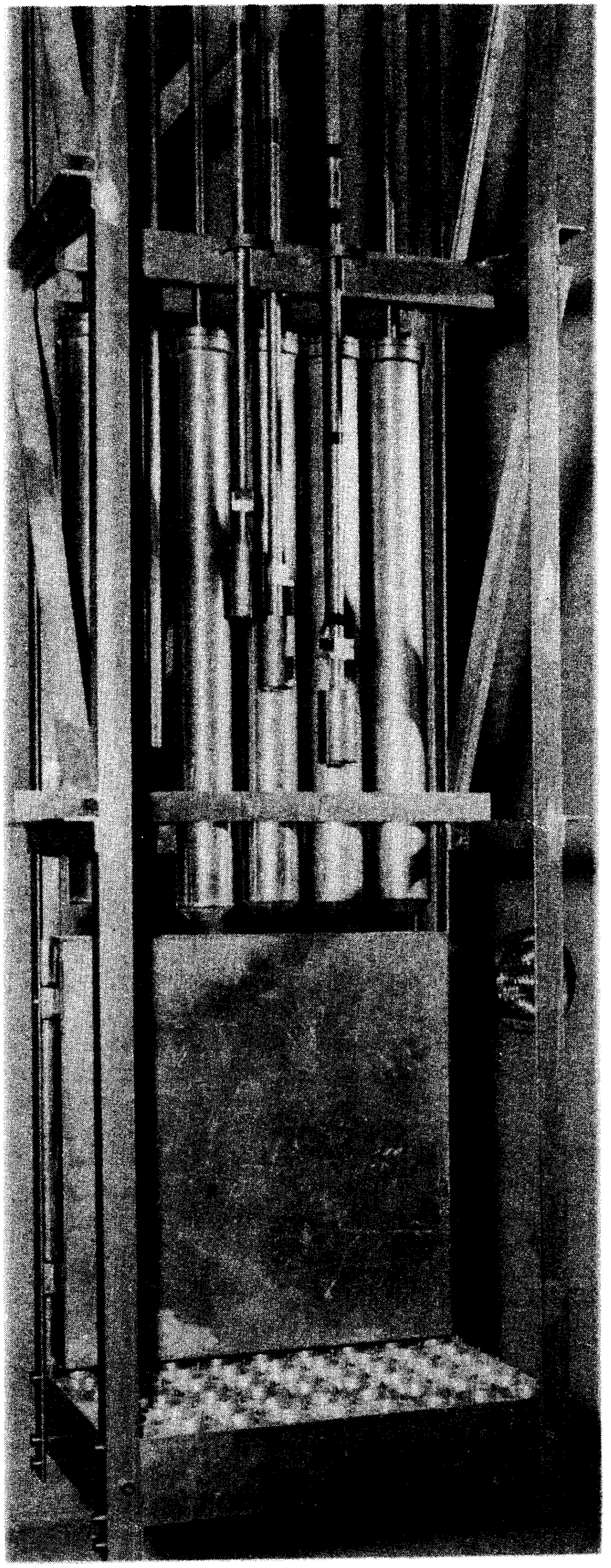

Since it is expected that ordinary filtered water will be used in the "pool," at least at first, the fuel elements are being allodized, i.e., treated with a solution of dichromate salts, to inhibit corrosion of the aluminum. This work is under the supervision of J. L. English and A. R. Olsen.

Design work at NEPA for a mock-up of the reactor part of a divided shield is completed and procurement has started. This mock-up conforms closely to the divided shield described in the Shielding Board Report.[22]

A polonium-beryllium source and nuclear plates are being used to investigate the degradation of the neutron fission spectrum when neutrons are collimated under water. If, as seems probable from work elsewhere, the charge in the spectrum is small, then the problem of providing an underwater collimated beam of neutrons for the proton recoil counter is solved.

A steel water tank 6 ft in diameter and 8 ft high has been installed in one corner of the "pool" room; it will be equipped with a known source and used for standardizing chambers and counters.

MOCK-UP OF UNIT SHIELD

A. S. Kitzes, Reactor Technology Division

Preliminary arrangements have been completed for fabrication of a mock-up of the unit shield which is to be tested in the "swimming pool." The nuclear requirements of the shield have now been well enough established to permit the detailed engineering design to be completed.

The mock-up will be similar to the unit shield described in the Shielding Board Report[23] except that it will correspond to a shield for a 27-in.-diameter spherical reactor. Moving out from the reactor there will be, in order, an approximately 7½-in. air space, 3 in. of iron, and nine 1-in. layers of lead separated by varying thicknesses of borated water.

It is believed that the mock-up can be completed by Mar. 1, 1951, at which time it will be required to fit the current program of the "swimming pool."

(22) ANP-53, *op. cit.*, p. 64.

(23) ANP-53, *op. cit.*, Appendix A.

6. EXPERIMENTAL ENGINEERING

6. EXPERIMENTAL ENGINEERING

H. W. Savage, ANP Division

Implementation of the Experimental Engineering Laboratory in Building 9201-3 at Y-12 has continued throughout the past quarter. Operation of some liquid-metal systems has been possible since mid-September with continuous round-the-clock operation after October 23. All experiments so far performed have tested the compatibility of materials with hot liquid sodium, but preparations are underway for using liquid lead and liquid lithium, and preliminary consideration is being given to systems for sodium hydroxide and for mixed sodium and lithium fluorides. Effort is now shifting toward more complex systems comparable to those anticipated in an ARE installation.

Equipment has been designed and is now being fabricated or installed for inserting test samples of materials in either dynamic or static hot liquid metal for corrosion, erosion, self-welding, and stress-corrosion tests. In certain equipment it will also be possible to move exposed materials with relation to each other, and also to develop adequate pressure, temperature, and flow measuring devices. Pumps, valves, flanges, joints, insulation, instruments, and purification equipment are being developed, and the techniques of pretreating materials and postexperimental examination of used items are being learned.

An adequate power source for electric heating of loops is in process of installation, hoods for adequate ventilation are being fabricated, electromagnetic pumps are on order, tubing for loops is on order, and a small machine shop for experimental fabrication is being installed.

Considerable attention is being given to the hazards involved in handling the coolants proposed, and the Safety Committee, formed during this quarter, is in process of developing adequate protective clothing, fire-fighting equipment, and disposal and cleaning equipment.

Corrosion Tests; Harps (W. C. Tunnell). Corrosion effects of liquid sodium, flowing because of convection, on various metals are being examined in "harps." Each harp is run to failure or for 1000 hr minimum, and the changes

in the metal and the sodium are determined by metallographic and spectrographic analysis.

Operation of the harps filled with liquid sodium has been performed for the ANP Metallurgy Group under mutually agreed-upon specifications, and has required the development of techniques of cleaning, welding, installation, loading, instrumentation, pressurizing, and analysis of used materials. Much of the equipment was obtained from the Metallurgy Group and revised in Y-12 shops to fit local needs. Ten harps were placed in operation for a 1000-hr continuous test on Oct. 23, 1950, and seven others have been placed in operation since. Table 6.1 summarizes the types tested and the characteristics of operation through November 30.

In preparing the first harps for use, it was found that some of the welding had been done without shielding the arc with inert gas and that acid cleaning attached slag inclusions in these welds and resulted in many leaks. Rewelding with heliarc remedied these defects, and cleaning was suspended later since it was suspected to be also attacking the primary metal. It has been necessary to revise the design somewhat, and a procedure was developed to assure consistent treatment, vacuum tightness, and noninclusion of unwanted metals. Degreasing is accomplished with trisodium phosphate; oxide removal appears best accomplished with sodium, since acid pickling often damages the original material although inhibitors may alleviate this situation; and water is removed by a methanol and ether wash and subsequent heating under vacuum.

Samples of the sodium used in each harp are taken at the start and termination of each run and submitted for oxygen and spectrographic analysis. Table 6.2 summarizes the determinations made through November 30. The technique used is patterned after practices at General Electric Co., a sample being drawn into a double-bulbed tube to minimize oxygen contamination. In general the results indicate more oxygen present than can exist in solution in the metal. This may be due to incomplete filtration; consequently the advantages of a 5- instead of a 10-micron filter will be determined.

It appears to be particularly important in preparing any structure for test to have full control of all details of the fabricating process to assure a complete history of the treatment and types of materials included.

TABLE 6.1

Harp Operations Summary (Liquid Sodium)

HARP NO.	MATERIAL	OPERATING TEMPERATURE (°F)	TOTAL TIME TO 12/1/50 (hr)	REMARKS
1	316 stainless steel	1350	764	
2	316 stainless steel	1350	850	
3	316 stainless steel	1500	767	
4	316 stainless steel	1500	625	Failed in middle of hot leg
5	304 stainless steel	1500	349	Failed in top of hot leg below cup
6	L-605 alloy	1500	688	
7	347 stainless steel	1500	795	
8	Low-carbon iron*	1200	579.3	Failed in middle of hot leg; excessive warpage and oxidation outside
9	Nickel	1500	0	Failed; did not reach operating temperature
10	Low-carbon iron	1200	25.4	Failed in side of bottom cup
11	Nickel	1500	13	Failed in top plate of bottom cup
12	Nickel	1500	164.8	Heater failure, appeared to be leak; has been refilled and reoperated
13	Nickel	1500	223.5	Failure in bottom plate of bottom cup
14	347 stainless steel	1350	725	
15	347 stainless steel	1350	894	
16	304 stainless steel	1350	850	
17	304 stainless steel	1350	890	

* See Fig. 6.1

TABLE 6.2

Sodium Samples from Harps

HARP NO.	O_2 IN Na (wt. %)				SPECTROGRAPHIC ANALYSIS (μg/g of Na)					HARP MATERIAL
	AT FILLING		AT TERMINATION							
	Upper	Lower	Upper	Lower	Mn	Ni	Cr	Fe	Mo	
1	0.092	0.082								316 stainless steel
2	0.56	0.13								316 stainless steel
3	0.067	0.087								316 stainless steel
4	0.086		*0.025 **0.039	0.012 0.032	*<10 **<10	<40 <35	<20 <20	50 35	<4 <5	316 stainless steel
5	0.032									304 stainless steel
6	0.038	0.023								L-605 alloy
7	0.020	0.013								347 stainless steel
8	0.021	0.017								Low-carbon iron
9	0.033	0.018								Nickel
10	0.047	0.025	0.025	0.025						Low-carbon iron
11	0.033	0.063				4100 (vertical leg) 245 (bottom pot)				Nickel
12	0.044	0.012	0.016	0.009						Nickel
13	0.027	0.026				8500 (vertical leg) 3300 (bottom leg)				Nickel
14	0.037	0.090								347 stainless steel
15	0.025	0.019								347 stainless steel
16	0.037	0.051								304 stainless steel
17	0.052	0.016								304 stainless steel

* Harp 4 is still in operation; this sample was taken after 12 hr of operation.

** This sample was taken after 14 hr of operation.

Harp operation has been relatively trouble-free except for the final failures and plugging of gas lines by condensation of the sodium. The latter is serious in that it prevents release of the system pressure when a leak occurs, thereby increasing the hazard. No complete solution to the problem has been found.

Failures appear to have occurred at welds exclusively—some completely unexpected because of invisible tube joints. Complete metallographic examination is being performed in the Metallurgy Laboratory. One of the more extreme failures (harp 8) is illustrated in Fig. 6.1.

In addition to the harps, two other convection loops are being operated. These are different from harps in that the liquid metal can be drained from the loop and the liquid is held in position by inert gas pressure without requiring valves. Testing of the device for holding the liquid level automatically is one of the objectives of operating this loop.

Figure-eight Loop (W. C. Tunnell). The figure-eight loop is designed to receive test sections for dynamic corrosion and erosion tests, self-welding tests, and stress-corrosion tests. One such loop has been delivered and is being installed (Fig. 6.2). Seamless tubing was unavailable; consequently satisfactory operation at very high temperatures is not anticipated.

An a-c electromagnetic pump patterned after a General Electric pump was designed for use with this loop. As a part of this problem it was desirable to join copper connectors to the stainless steel pump cell without using soldering alloys and fluxes. A satisfactory joint was made using a type 316 stainless steel rod and building a boss on the stainless steel from the rod to a thickness of about 1/8 in. and heliarc-welding the boss to the copper. The joint was cooled very slowly to prevent cracking.

Test sections for the figure-eight loop are shown in Figs. 6.3 through 6.6. Figure 6.3 shows the method of holding test samples (part 4) in a high-velocity stream for corrosion and erosion studies. Figure 6.4 shows the method of inserting two abutting pieces in the stream with the attachments for applying force to aggravate self-welding by holding the abutting surfaces together under known pressure. Figure 6.5 shows a test piece in the stream subjected to a tensile force and corrosion and erosion effects simultaneously. Figure 6.6 shows details of the foregoing test sections and another modification (item 3)

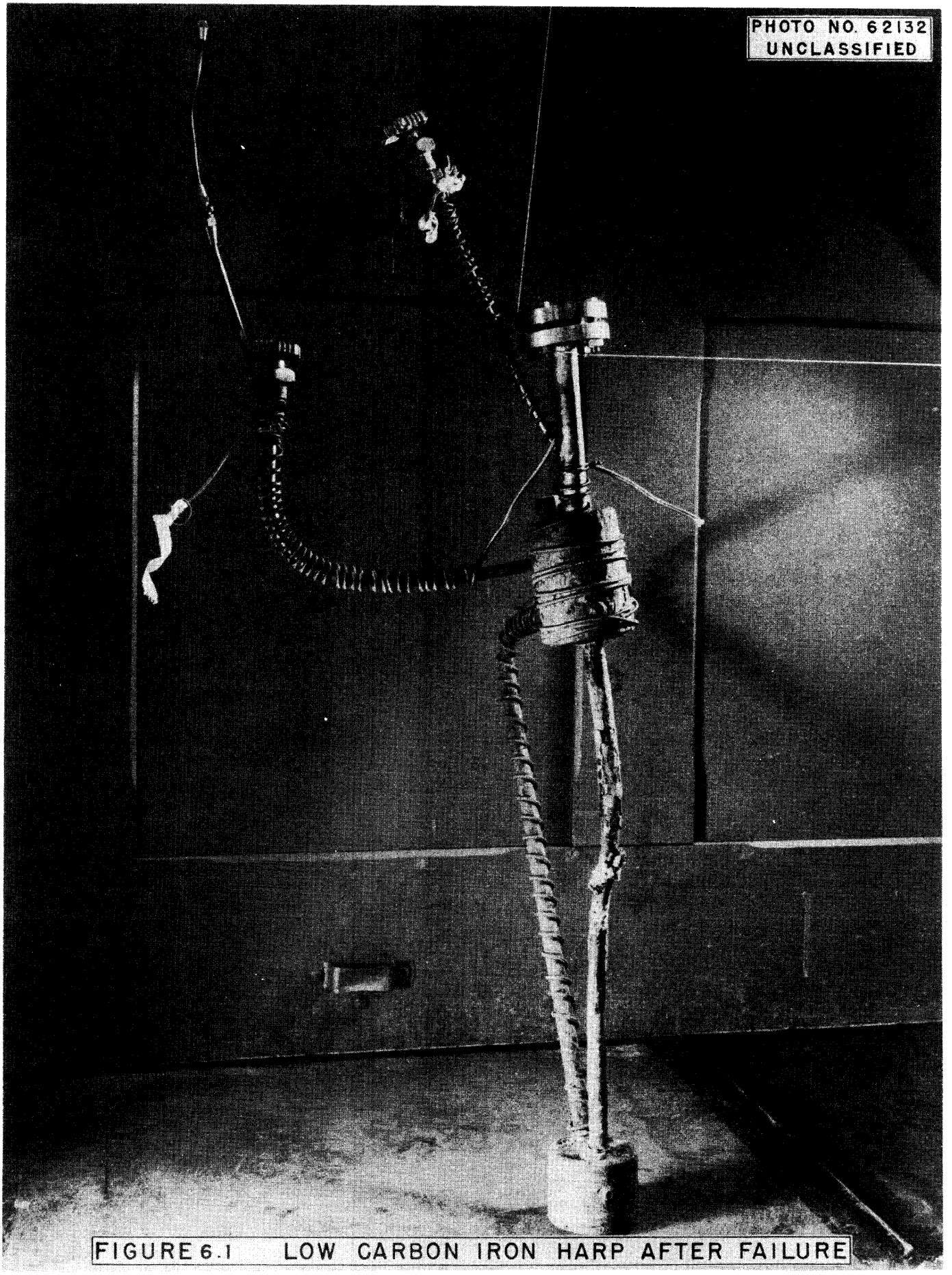

FIGURE 6.1 LOW CARBON IRON HARP AFTER FAILURE

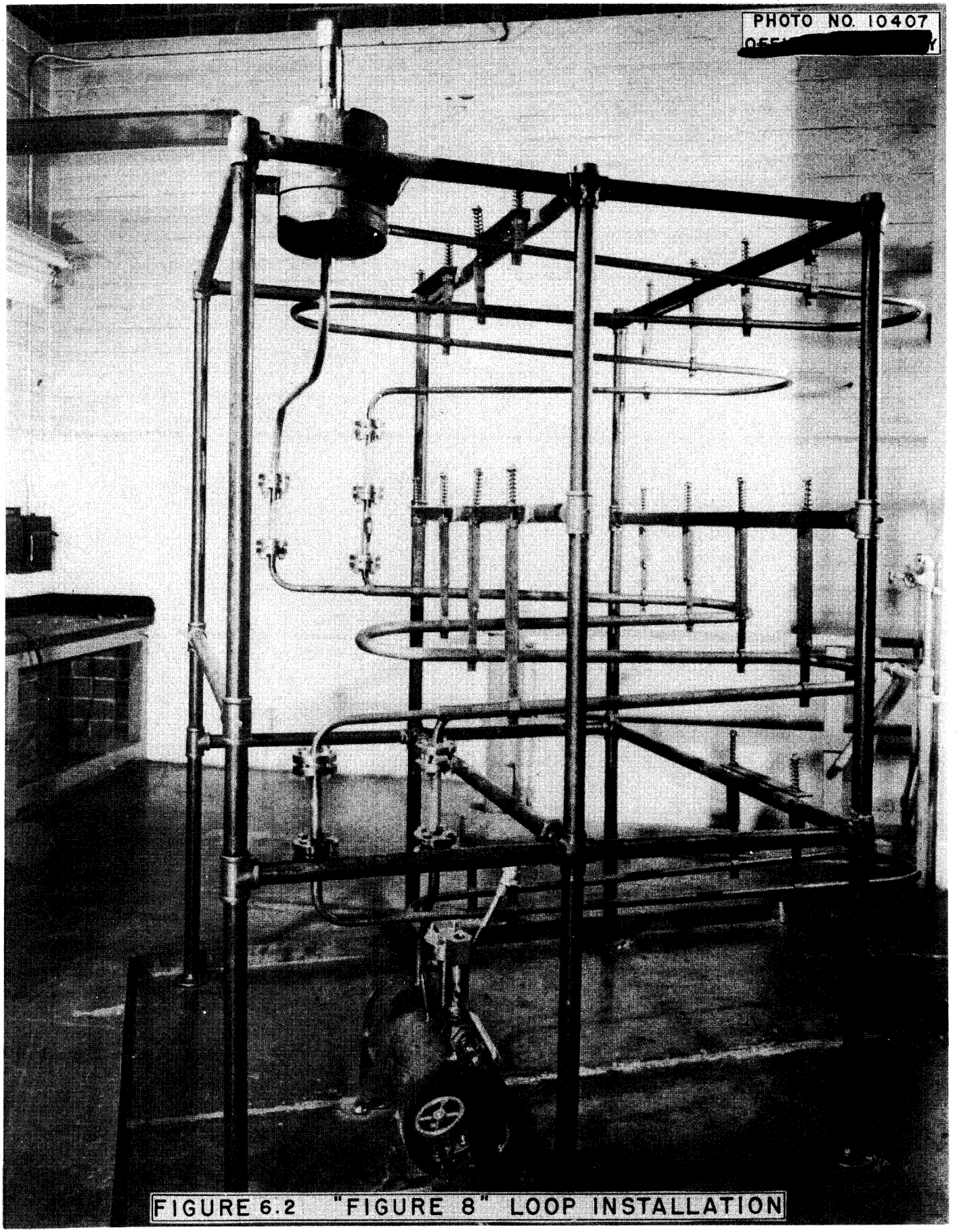

FIGURE 6.2 "FIGURE 8" LOOP INSTALLATION

[redacted]

DRAWING CSK-14316

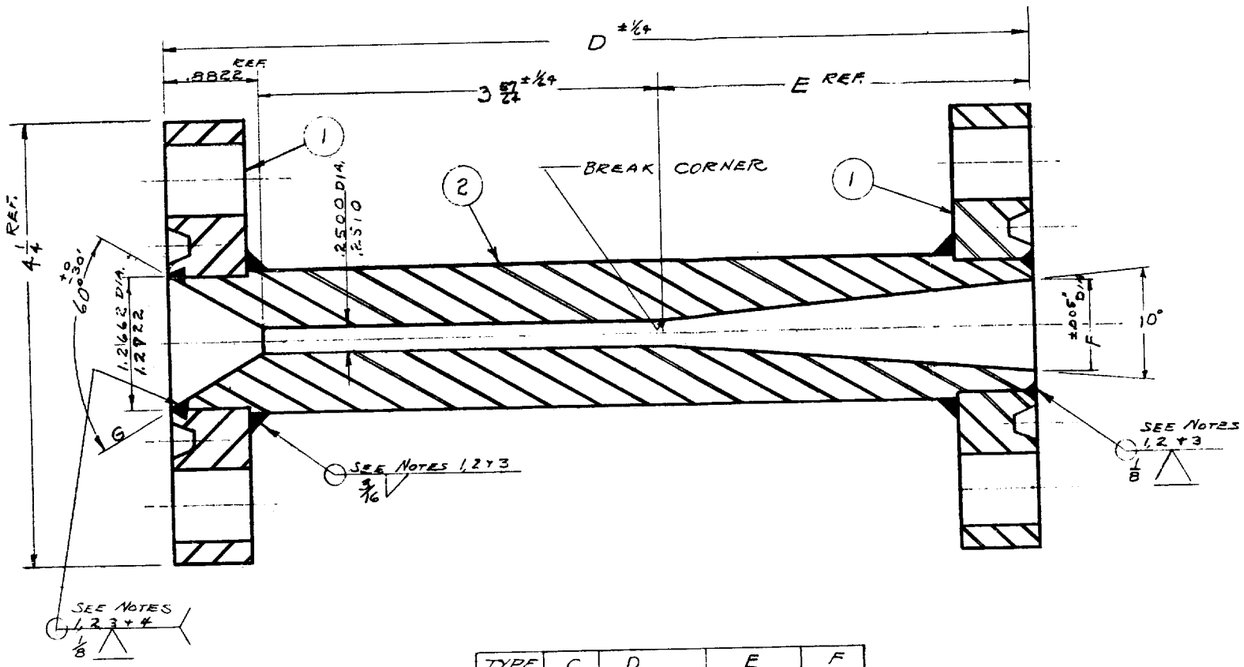

TYPE	C	D	E	F
"C"	8 7/16"	8 5/16"	3.5404	.870"
"D"	6 31/32	6 11/32	1.750	.557"

NOTES:

1. ALL MATERIAL MUST BE DEGREASED BEFORE WELDING.
2. ALL WELDING TO BE DONE BY THE HELI-ARC PROCESS WITH INERT GAS IN THE PIPE
3. ALL WELDS MUST BE VACUUM TIGHT AND TESTED.
4. THE ABOVE MATERIAL FOR ONE UNIT ONLY, TYPE A,
5. MATERIAL IS SAME FOR TYPE "B" EXCEPT LENGTH OF (2) IS 6 13/16

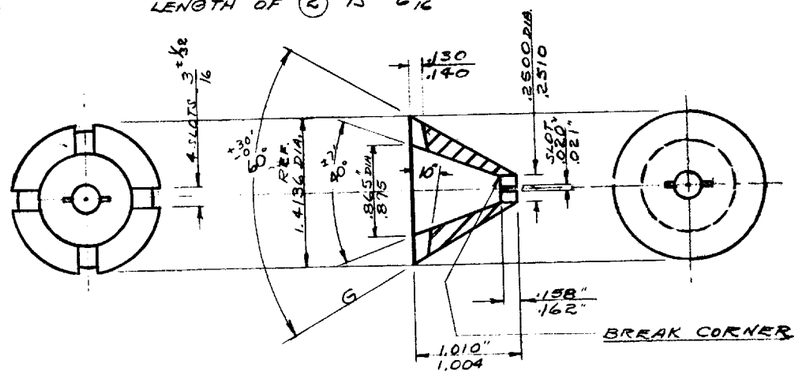

PART No. (3)

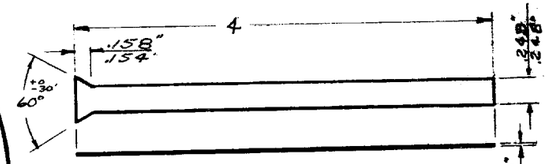

PART No. (4)

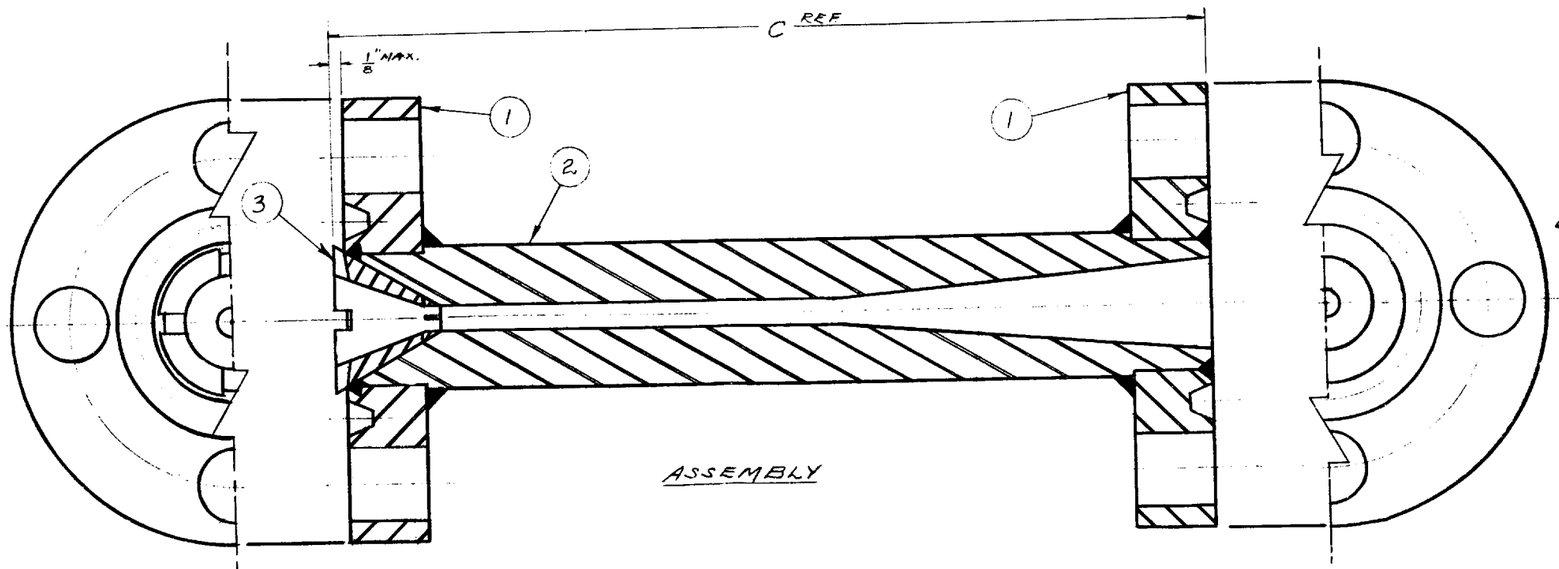

FIGURE 6.3 TEST SECTION FOR CORROSION TESTS IN "FIGURE 8" LOOP

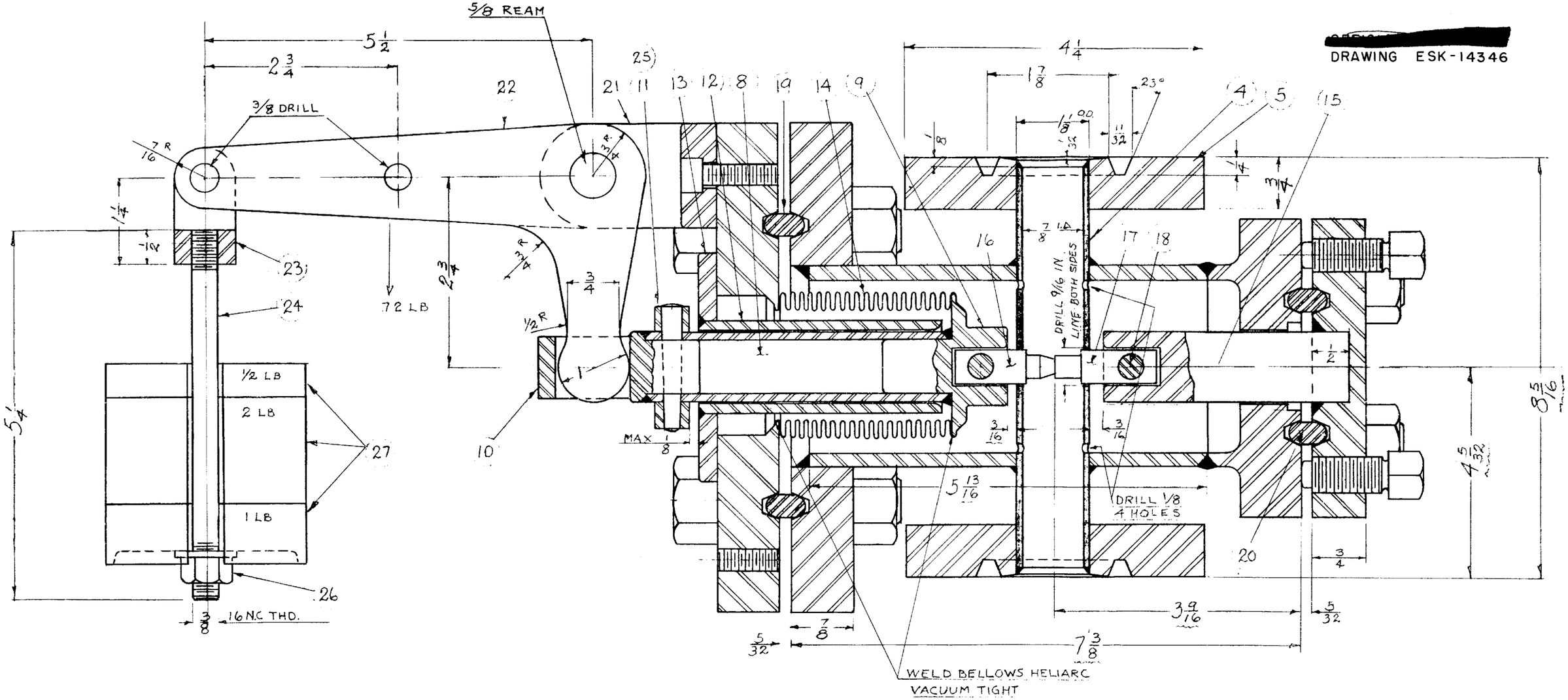

FIGURE 6.4 TEST SECTION FOR SELF-WELDING TESTS IN "FIGURE 8" LOOP

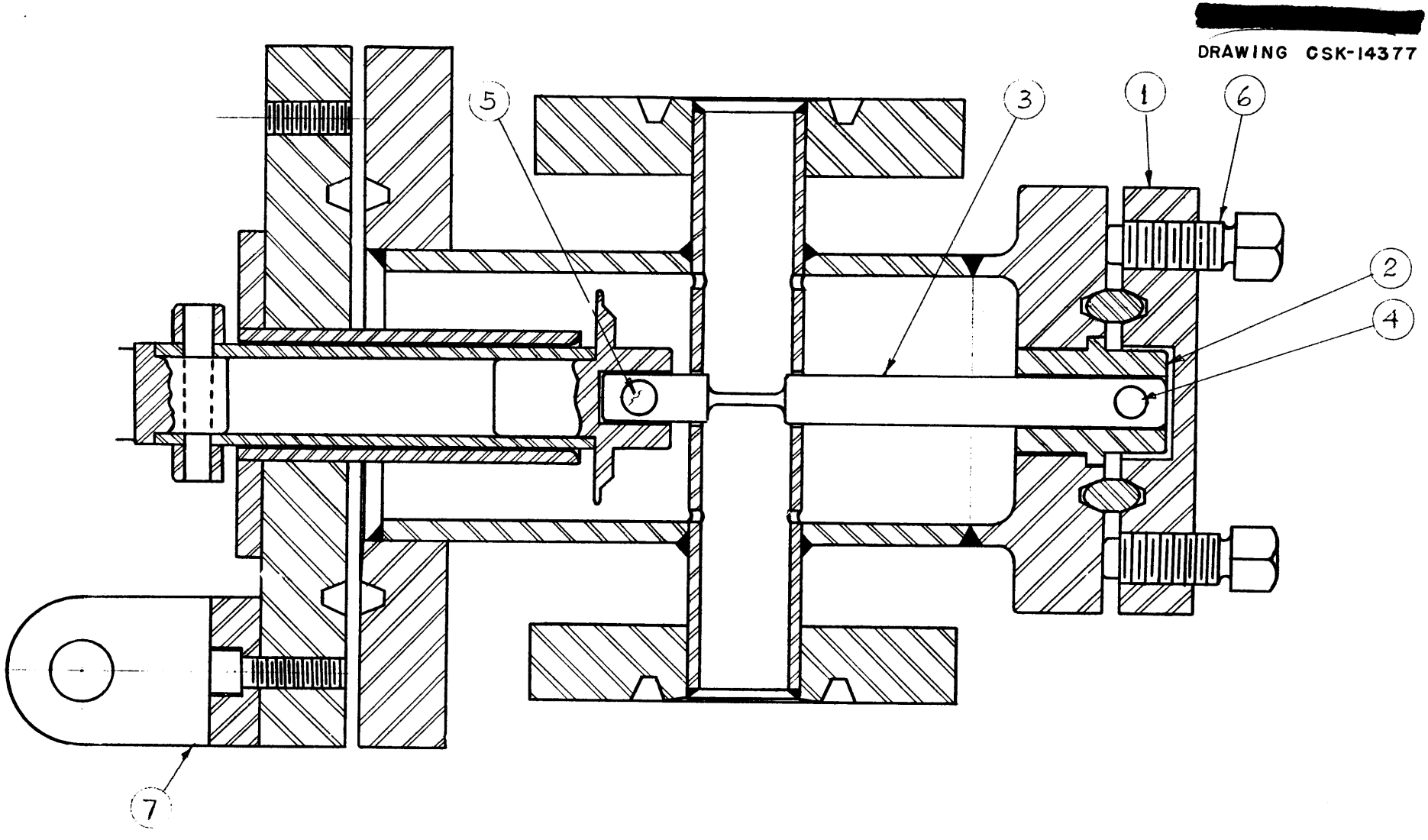

FIGURE 6.5 TEST SECTION FOR STRESS-CORROSION TESTS IN "FIGURE 8" LOOP

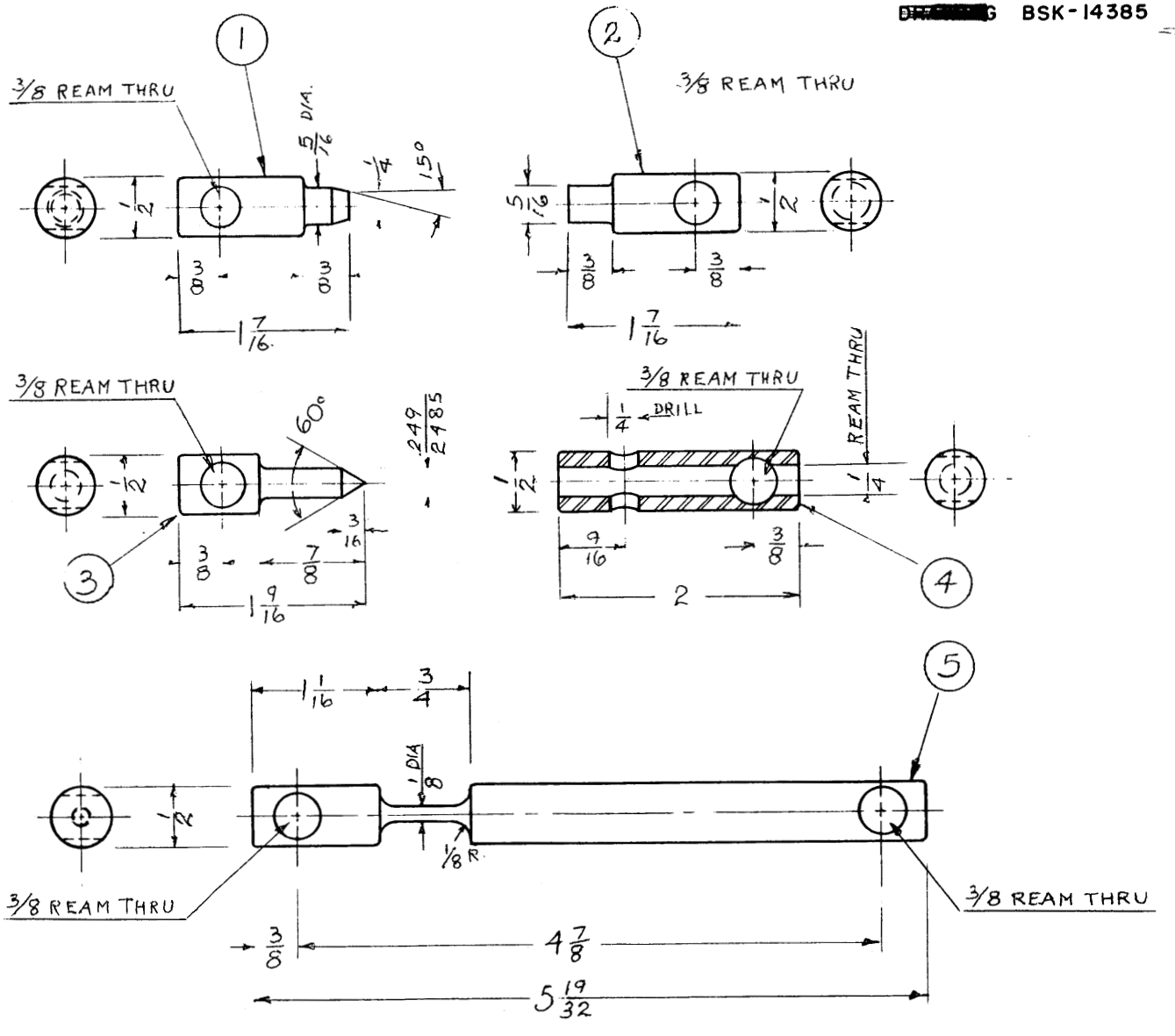

FIGURE 6.6 DETAILS OF PARTS TO BE TESTED IN "FIGURE 8" TEST SECTION

in which two pieces can be moved axially one inside the other, so that while in the stream welding tendencies of oscillating parts can be investigated.

Calibration Loop (W. G. Cobb). An isothermal loop with electromagnetic pump, sump tank, and expansion tank has been designed for the ready insertion of devices for measuring pressures and flow rates (Fig. 6.7). Two venturi meters calibrated on water will be used as standards.

Seal Test Device (J. F. Haines). A device for testing materials to be used as seals is shown in Fig. 6.8. It consists of a sump for molten metal, a vertical overhung shaft, and a holder. One element of the sealing materials is a ring (9) held in the holder and sealed by gaskets to prevent passage of the liquid from outside the holder to the inside. The other element of the seal is a cup (8) attached to the end of the shaft so that it can be rotated; it bears on the stationary ring (9) to form the seal. This type of seal is quite common in other branches of engineering practice, and the effectiveness of the seal in liquid sodium will be determined during operation by visual observation of the well around the shaft through sight glasses.

Bearing Tests (J. F. Haines). A thrust bearing adaptable to the seal test device has been designed, and a radial journal bearing is being designed.

Air Tests (H. Turner). An 800 cfm blower has been set up for the testing of models of the heat exchanger and for testing fuel element configurations for head losses and flow characteristics. Auxiliaries being built for this setup include entrance and exit conduits, entrance orifices for measuring and regulating flow, and a multiple manometer board for pressure determinations. Models for test are being designed, the configurations for which are based on current ARE design concepts.

Insulation Tests (R. T. Schomer). Because of the volume of thermal insulation anticipated for the liquid-metal circulating systems, a number of different types have been subjected to hot liquid sodium to determine the most practical type. Present evaluation indicates the use of a combination insulation composed of an inner layer of either Superex or Hi-Temp No. 19 thick enough to bring the interface temperature down to 1200°F, followed by a layer of lead-mill or steel-mill slag wool thick enough to give the desired heat loss from the pipe. For small pipe (about 2 in.) at 1800°F these thicknesses will

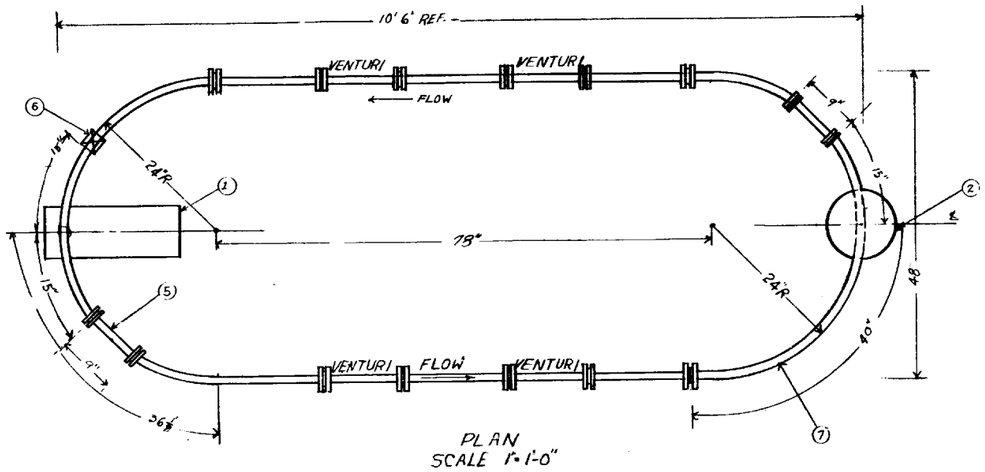

PLAN
SCALE 1"=1'-0"

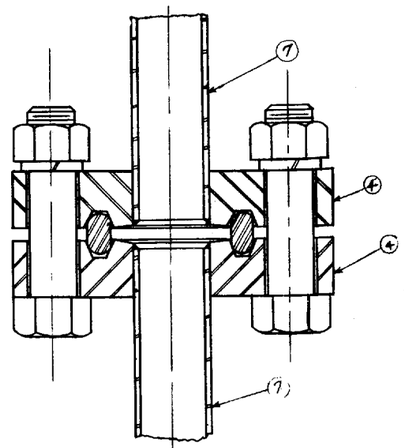

DETAIL "A"

TYPICAL CROSS SECTION OF FLANGED JOINT
SCALE 12"=1'-0"

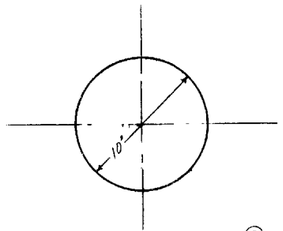

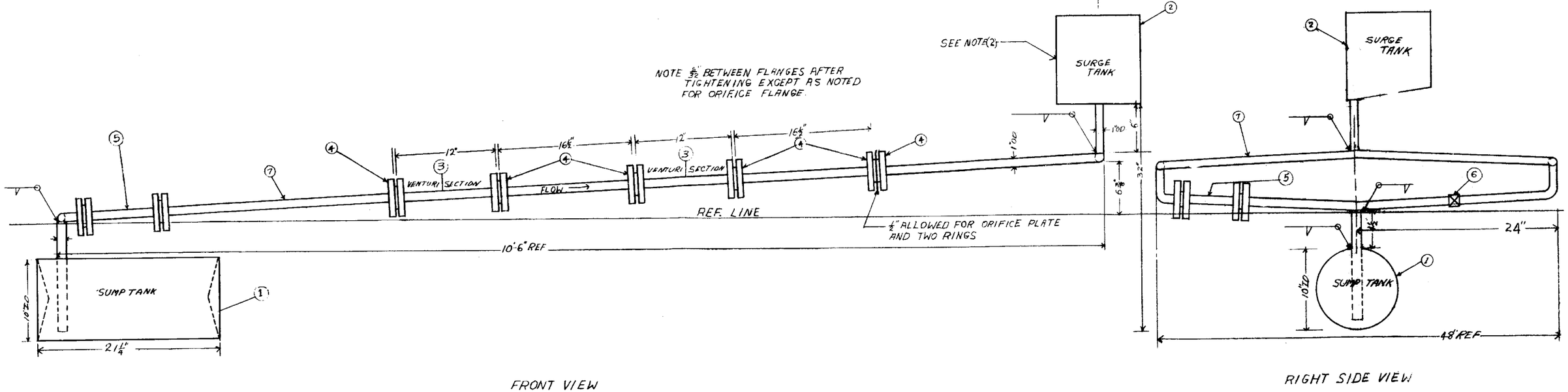

FRONT VIEW

RIGHT SIDE VIEW

FIGURE 6.7 CALIBRATION LOOP

DRAWING DSK 14299

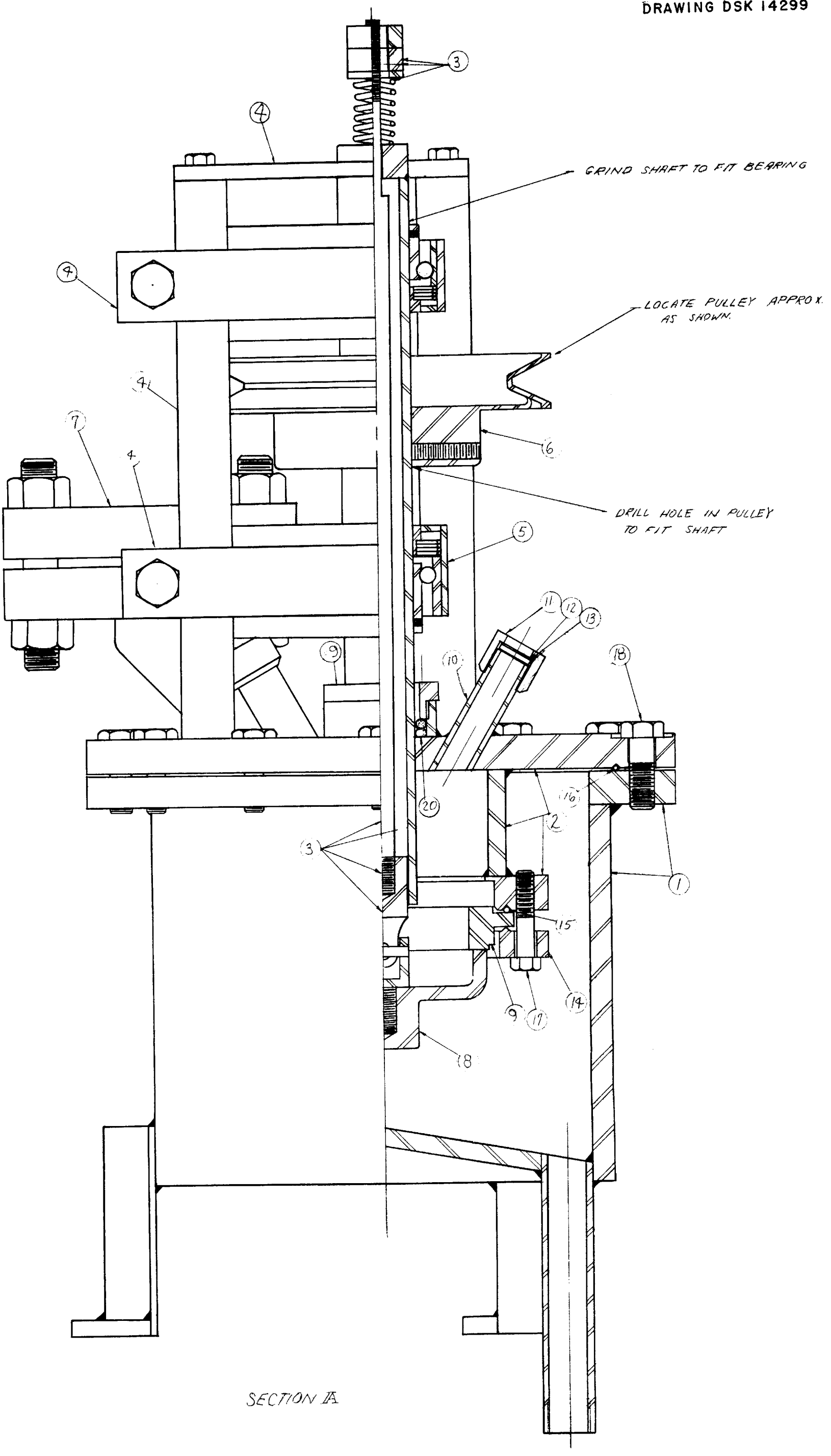

FIGURE 6.8 SEAL TESTING DEVICE

be about 2½ and 3 in., respectively. The basic difficulty with most insulating materials is reaction with the sodium. Table 6.3 summarizes the tests made using the equipment shown in Fig. 6.9.

TABLE 6.3

Insulation Tests

TYPE	PRIMARY CONSTITUENT	PIPE TEMPERATURE (°F)	RESULTS
Johns-Manville RF 300 Thermoflex	Asbestos	1372	Disintegrated
85% Magnesia	MgO	1372	Reacted with Na
Philip-Carey Hi-Temp No. 19	Diatomaceous silica	1100	Gradual hardening; max. penetration ½ in.
Johns-Manville Superex	Diatomaceous silica	1100	Gradual hardening; max. penetration ½ in.
Eagle-Picher DE-85 Block	Diatomaceous earth	1100	Gradual hardening; max. penetration ¾ in.
Baldwin-Hill Neoblock	Lead-mill slag	1100	Caked and crumbly; penetration 7/8 in.
Owens-Selvins Kaylo Block	Lead-silica	1100	Caked and crumbly; penetration 1 in.
Friedrick & Derrick Glass Wool	Glass wool	1100	Fused to steel; penetration ¼ in.
Baldwin-Hill Black Rockwool	Lead-mill slag	Not heated	Penetration less than ¼ in.
Philip-Carey Gray Wool Blanket	Lead-mill slag	Not heated	Penetration less than ¼ in.
Philip-Carey White Wool Blanket Asbestos Board	Blast furnace slag 1 asbestos	Not heated	Violent reaction
Johns-Manville Bauroc Blanket	Steel-mill slag	Not heated	Stuck to metal; penetration less than ¼ in.

Tests of screening of various meshes were also made to determine penetration of a jet of sodium. Single layers of stainless steel screening of 30, 100, and 200 mesh and galvanized screening of 16 mesh did not stop a jet of sodium, whereas a double layer of 200-mesh stainless steel screening was effective.

Pumps (J. F. Haines, W. G. Cobb, and A. P. Fraas). A program of pump development has awaited the definition of types desired as well as the determination of seal and bearing materials. Progress on the latter items has been

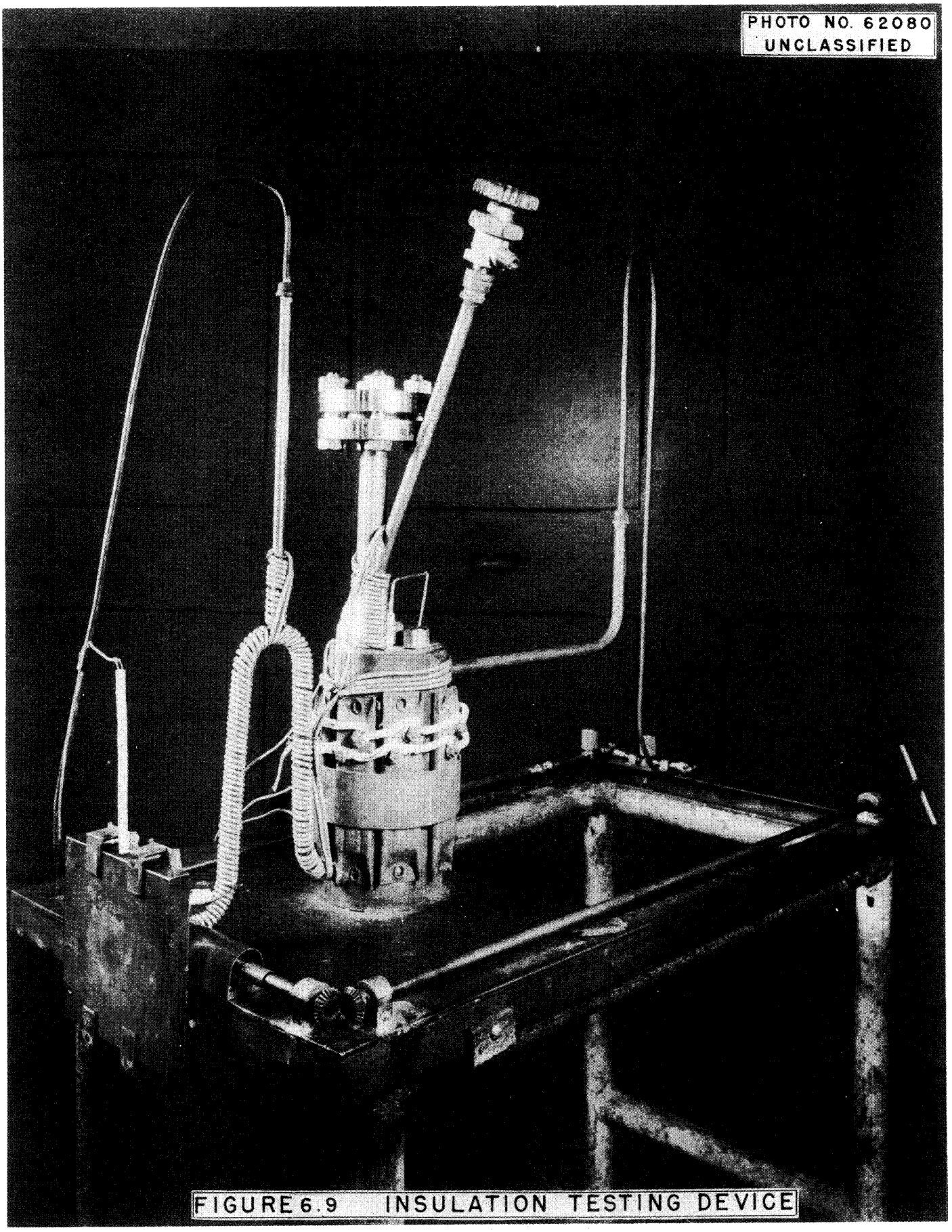

FIGURE 6.9 INSULATION TESTING DEVICE

discussed above.

Both centrifugal and axial flow pumps are now being considered in ARE design, and a program of testing is being set up. In this connection a centrifugal pump has been modified, as shown in Fig. 6.10, to have vanes on the back face of the impeller and a heat dam in the shaft. Initial trial of this pump with water failed for mechanical reasons, and the structure is being repaired. The test stand is shown in Fig. 6.11.

Electromagnetic pumps have been considered adequate for the small-scale test loops and one has been fabricated, some are on order, and one new one has been received. Pump development has been extensively surveyed at Allis-Chalmers Corporation, Milwaukee, Wisconsin, and proposals have been submitted by them. The so-called "centrifugal electromagnetic" pump is being considered as a design possibly suitable for ARE use.

It has been agreed with NEPA to set up a loop by July 1, 1951, capable of testing a 1600-gpm pump to be supplied by them.

Purification (P. L. Hill, USAF). The sodium presently being used in the convection harp tests and to be used in future figure-eight tests is received in dry pack form and is freed of oxygen by filtering at about 250 to 300°F in the process of filling the test apparatus. According to the experience of G.E., this low-temperature filtration removes oxygen to a residual concentration of approximately 10 ppm. The filter medium is a sodium oxide cake deposited on a 10-micron pore size Micrometallic 316 stainless steel filter. No attempt is made to remove trace elements from the sodium as received from DuPont, a typical analysis of which is

Na	99.9%	S	15-20 ppm
B	1-2 ppm	Mg	1 ppm
Ca	110-350 ppm	Ni	2-4 ppm
Cl	190 ppm	P	10-50 ppm
Fe	5-10 ppm		

The lithium will be freed of oxygen and nitrogen by a filtering process the same as that used for sodium. The lithium available at present contains approximately 1% impurities (primarily sodium).

Purification methods for lead, potassium, sodium and potassium hydroxides, and mixed fluorides are being studied with no decision as to the most suitable method having been reached.

[redacted]
DRAWING CSK 14133

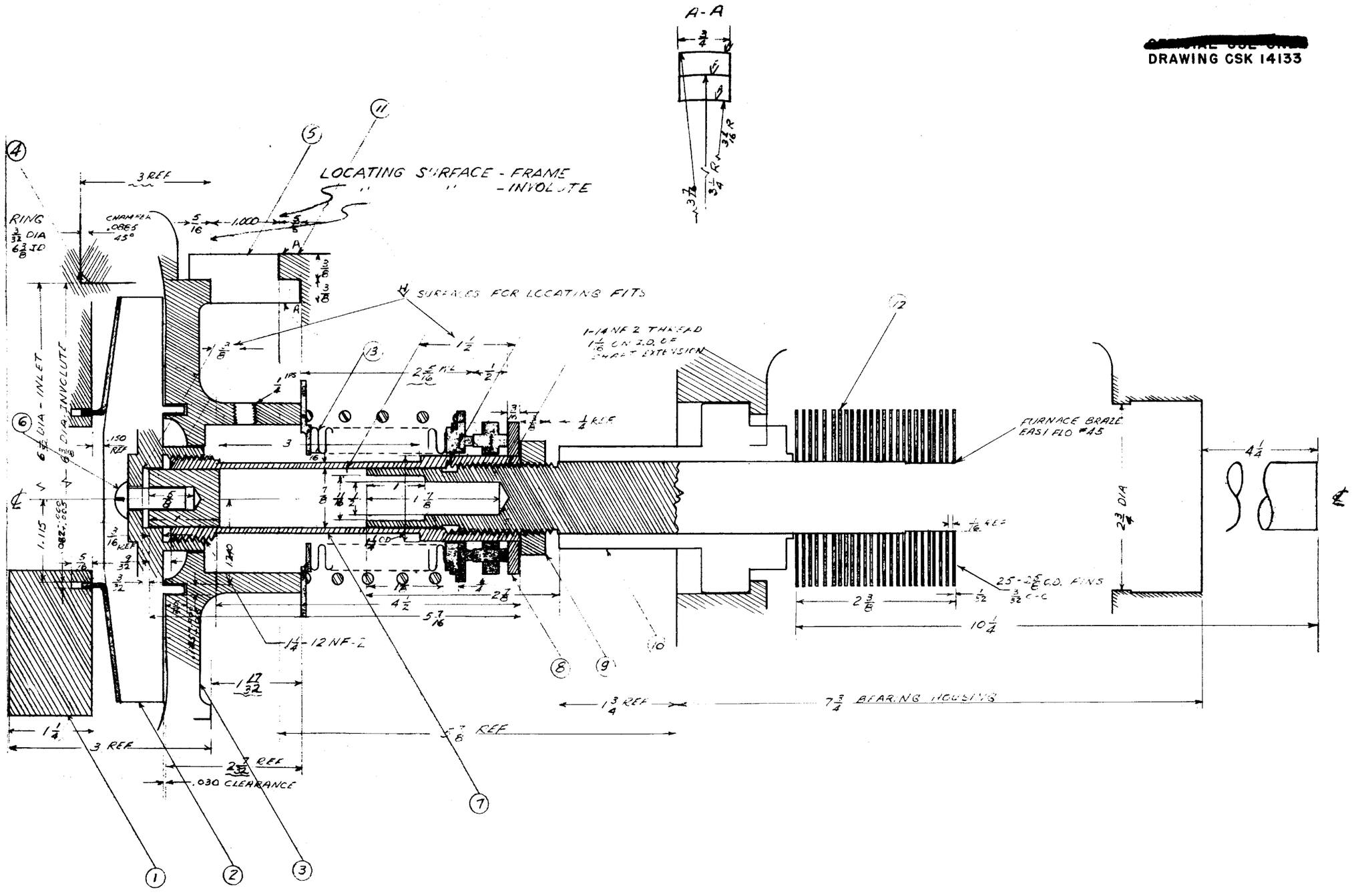

FIGURE 6.10 CENTRIFUGAL PUMP MODIFICATION

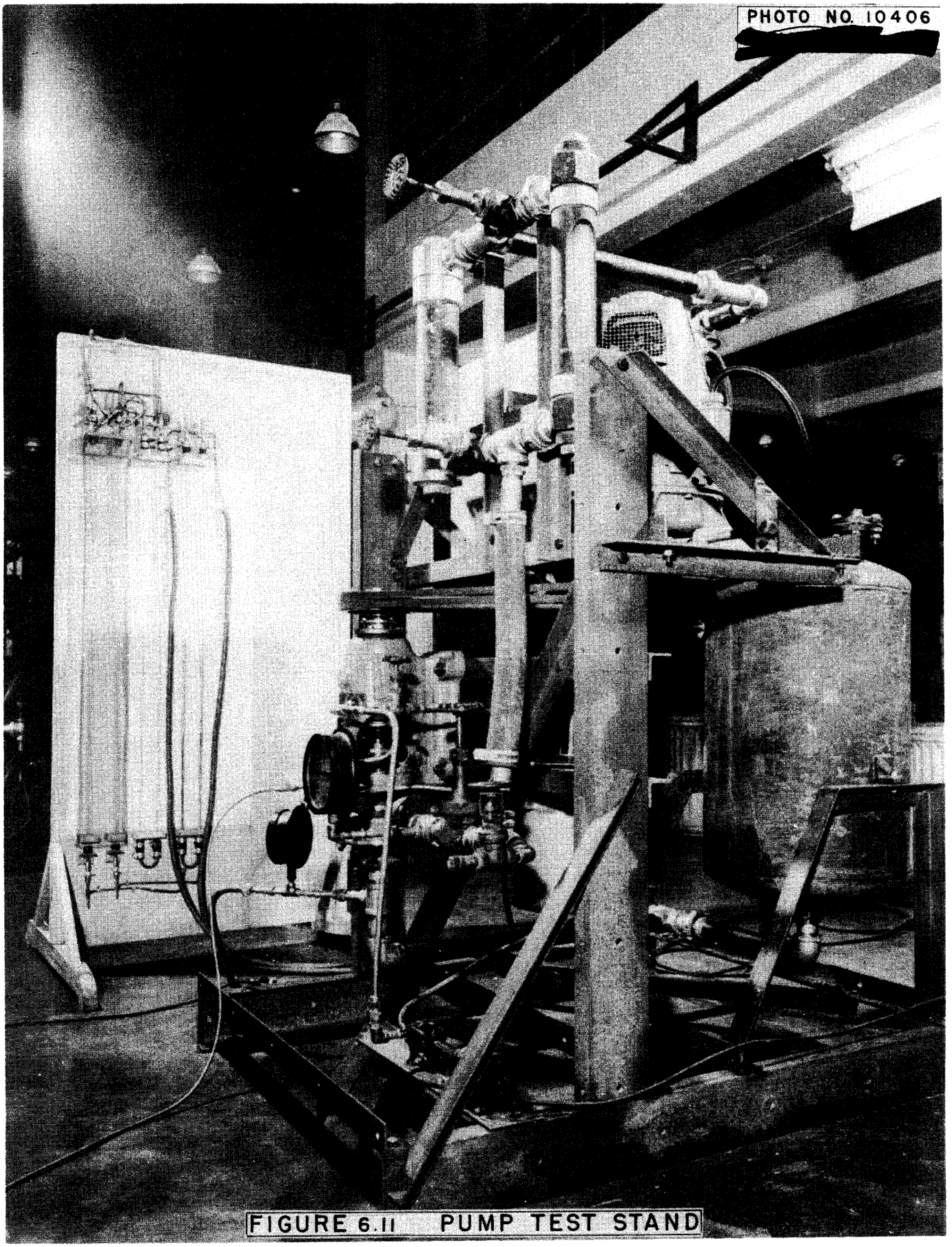

FIGURE 6.11 PUMP TEST STAND

The inert atmosphere used over the present sodium test units has been lamp-grade argon, which is considered oxygen-free. Gas-purification systems will be in operation shortly to ensure the purity of both argon and helium for use as inert atmospheres.

The purification procedure will consist in passing the gas over hot copper turnings to remove the oxygen, through a cold trap to remove water vapor, and then over hot titanium turnings to remove residual oxygen and the nitrogen. In order to prevent impure gas from passing to the test units in case of power failure, a NaK scrubber column is installed after the copper-titanium units, through which the gas will bubble and have the oxygen removed. A second column containing lithium or lithium and NaK will be used to remove the residual nitrogen.

Disposal and Cleaning Facilities (R. Devenish). Small valves and similar pieces of equipment are freed of sodium by immersion in a mixture of butyl and methyl alcohols, followed by water washing to be certain of removing the last traces of sodium. Larger items, such as the convection harps, are freed of sodium by heating above the melting point of the sodium and pouring as much as possible of the metal into a container. The partially cleaned harp is then blown with steam and washed with water or immersed in alcohol and washed with water.

A sodium disposal unit, Fig. 6.12, with a batch capacity of approximately 100 lb of sodium has been designed. The unit is based upon the disposal methods used at Schenectady by General Electric in which molten sodium is jetted under water through a steam nozzle.

The Liquid Metals Safety Committee has recommended a central cleaning and disposal facility for all groups in the Y-12 Area. The facility will be used for removing small quantities of sodium from pieces of equipment and for fumeless disposal of waste sodium.

The cleaning facility will consist of a graveled area upon which will be erected a steel barrier to protect operators and equipment from splashing or from flying pieces in case of explosion. Cleaning will be performed by alcohol immersion, steam blowing, or water washing or a combination of all methods.

DRAWING DSK-14345

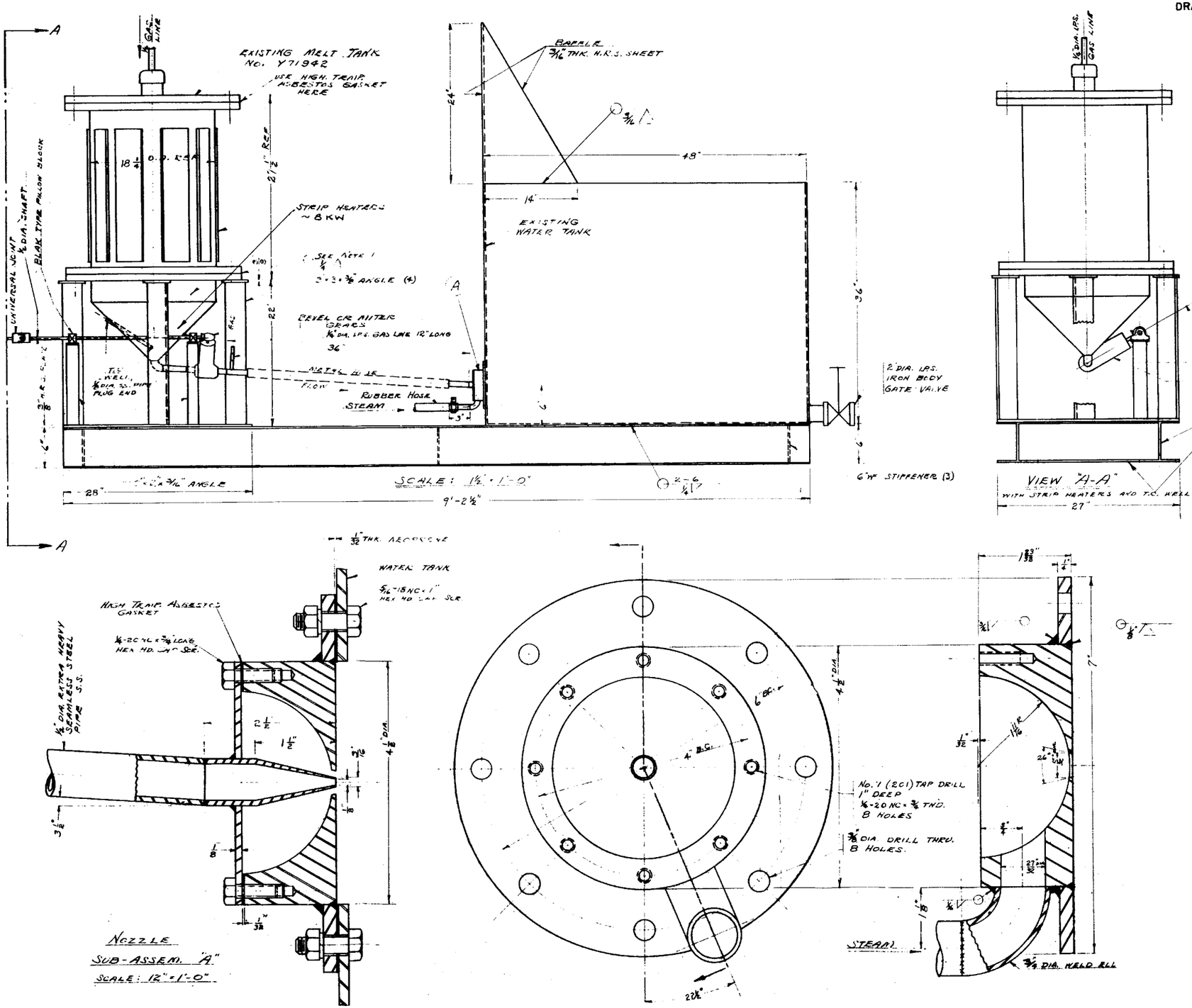

FIGURE 6.12 SODIUM DISPOSAL UNIT

Waste sodium and sodium-contaminated insulation in small quantities will be disposed of in an abandoned quarry if it proves impractical to use the sodium melt unit.

Safety (P. L. Hill, USAF). Experiments performed by various groups with methods of extinguishing liquid-metal fires have indicated that Pyrene G-1 powder is suitable on sodium, potassium, lithium, and calcium fires; Ansul Metal-X is suitable on sodium and potassium fires but is questionable on lithium fires; zirconium silicate is questionable on lithium fires; rust-free iron filings may be suitable on all metal fires; several other materials warrant further tests.

Tests of hot sodium upon protective clothing are still inconclusive but preliminary results indicate that chrome leather may be suitable. Further tests are being carried out.

7. LIQUID-METAL AND HEAT-TRANSFER RESEARCH

7. LIQUID-METAL AND HEAT-TRANSFER RESEARCH

R. N. Lyon and H. F. Poppendiek
Reactor Technology Division

During the past quarter notable progress has been made in heat-transfer research, in the determination of the physical properties of liquids and solids at high temperatures, and in the development of a loop for circulating hot liquid metals through the ORNL reactor.

In the heat-transfer work, final stages have been reached in the construction of the general lithium heat-transfer system and in the high conductance—entrance conductance sodium system. Design of a boiling-liquid-metal heat-transfer system is near enough to completion to start construction, and preliminary designs of a sodium hydroxide heat-transfer system and a system to determine the natural convection in liquid-fuel elements have been completed. Theoretical analyses of heat transfer have been completed on three postulated systems which approximate some of the entrance conditions involved in current ARE core proposals, and a wide range of duct shapes have been analyzed with regard to velocity distribution and heat transfer with liquid metals.

A new physical-properties laboratory has been equipped with benches, lights, and other services. The specific heat of lithium has been found to be 1.0 ± 10% between 550 and 900°C, and redesign of the specific heat equipment to give improved accuracy has been completed. Detailed design of equipment for the thermal conductivity of liquids is complete, as is the overall design of a high-temperature viscosimeter. Consideration has been given to the problem of measuring the densities of high-temperature liquids. Liaison has been established with the Office of Air Research and the Materials Laboratory of the Air Materiel Command, USAF, who have agreed to begin physical-property work in their own laboratories and to contract with other research laboratories for determination of physical properties of materials of interest to the ANP.

As a result of a decision at the last meeting of the Committee on Basic Properties of Liquid Metals, arrangements were made for the rapid dissemination of reportable liquid-metal data. Also, organization of a second edition of the "Liquid Metals Handbook" has started. As with the first edition, the second edition is to be a cooperative effort with other sites, but with the overall editorial responsibility at ORNL.

EXPERIMENTAL LITHIUM HEAT TRANSFER

C. P. Coughlen

As a result of work this quarter, the instruments for the lithium heat-transfer system are now 90% complete, initial design of the heat exchanger has been completed, and the lithium melting tank has been charged with 100 lb of lithium metal. It was found that portions of the system had to be rebuilt because of the penetration into the stainless steel of silver from the brazing metal used in fastening Calrods to the equipment. The rebuilding has been completed. Enough materials have been tested with lithium fires to show the superiority of graphite and Pyrene G-1 powder as extinguishing agents for lithium fires. The instrument panels have been installed and most of the instruments have been mounted. The majority of the electrical connections remain to be made.

In charging 100 lb of lithium into the melt tank, degreasing was found to be ineffective, presumably because of the large amounts of oil either dissolved or absorbed by the lithium slugs. It was necessary to pump the charge at 1100°F at 5 psi absolute pressure for an extended time before the oil was removed.

A test heat-exchanger design has been roughed out, and fabrication will be started in the near future. The design is a simple annulus with mountings such that no interior tube supports are necessary. Uniformity of flow is also furthered by the entrance and exit designs which are essentially annular orifices. It is planned to test the system and calibrate the flow meters before the first test heat exchanger is installed.

During one of the preliminary water tests of the system, a large crack was found in the weld of the pipe that formed the catch tank. After removal of this tank and careful study with the assistance of the Y-12 metallurgists, the crack was found to be caused by penetration of silver into the stainless steel. This silver was introduced by the braze used for mounting Calrod heaters on the outer side of the catch tank. A new catch tank was fabricated and calibrated, and parts of the remainder of the system were replaced. The Calrod heaters are now mounted by tack welding small saddles across the heaters at short intervals and depositing stainless steel by spraying to provide good thermal contact. The Calrods have been remounted by this method at all important points.

Prerequisite to the developing of an adequate fire control for the several hundred pounds of molten lithium to be circulated in this system, practical experience with extinguishing materials had to be obtained. As a result of tests made during the quarter, the only materials considered reasonably satisfactory are powdered graphite and Pyrene G-1 powder, which is largely graphite powder. Sodium- and calcium-containing compounds were reduced to the free metal, which posed a serious disposal problem. Magnesium oxide plaster was rapidly penetrated by burning lithium, while sand and zirconium silicate reacted energetically to form a slag which rapidly attacked stainless steel and frequently resulted in perforation of the stainless steel test pans.

Graphite appears to react with lithium to form the carbide and blanket the metal. The carbide reacts with water to form acetylene in a relatively quiet process.

HEAT-TRANSFER COEFFICIENTS

W. B. Harrison

Construction is about 95% complete on a system designed for two primary purposes: (1) Determination of the highest values of heat-transfer coefficient which are practically attainable with liquid sodium, and (2) exploration of the change in local coefficients resulting from thermal effects in an entrance region. It is expected that heat-transfer coefficients between 200,000 and 500,000 Btu/hr per square foot per degree Fahrenheit will be achieved with reasonable accuracy.

An assembly of the test section is indicated in Fig. 7.1. Liquid sodium at 250°F will be pumped through the 1/32-in.-diameter hole in the center of a copper disk. In order to promote radial heat flow, the disk will be insulated on each side and cooled by water in the tube around its periphery. Observations of disk temperature at various radial locations will be made after steady operation is achieved. From these data and the thermal conductivity of the copper, heat flux and surface temperature at the copper-sodium interface may be computed. Sodium temperature will be measured so as to permit computation of the heat-transfer coefficient. The coefficients computed in this way will be average values over the disk thickness. Disk thickness will be varied from 1/16 to 1/4 in. in order to explore the entrance effects.

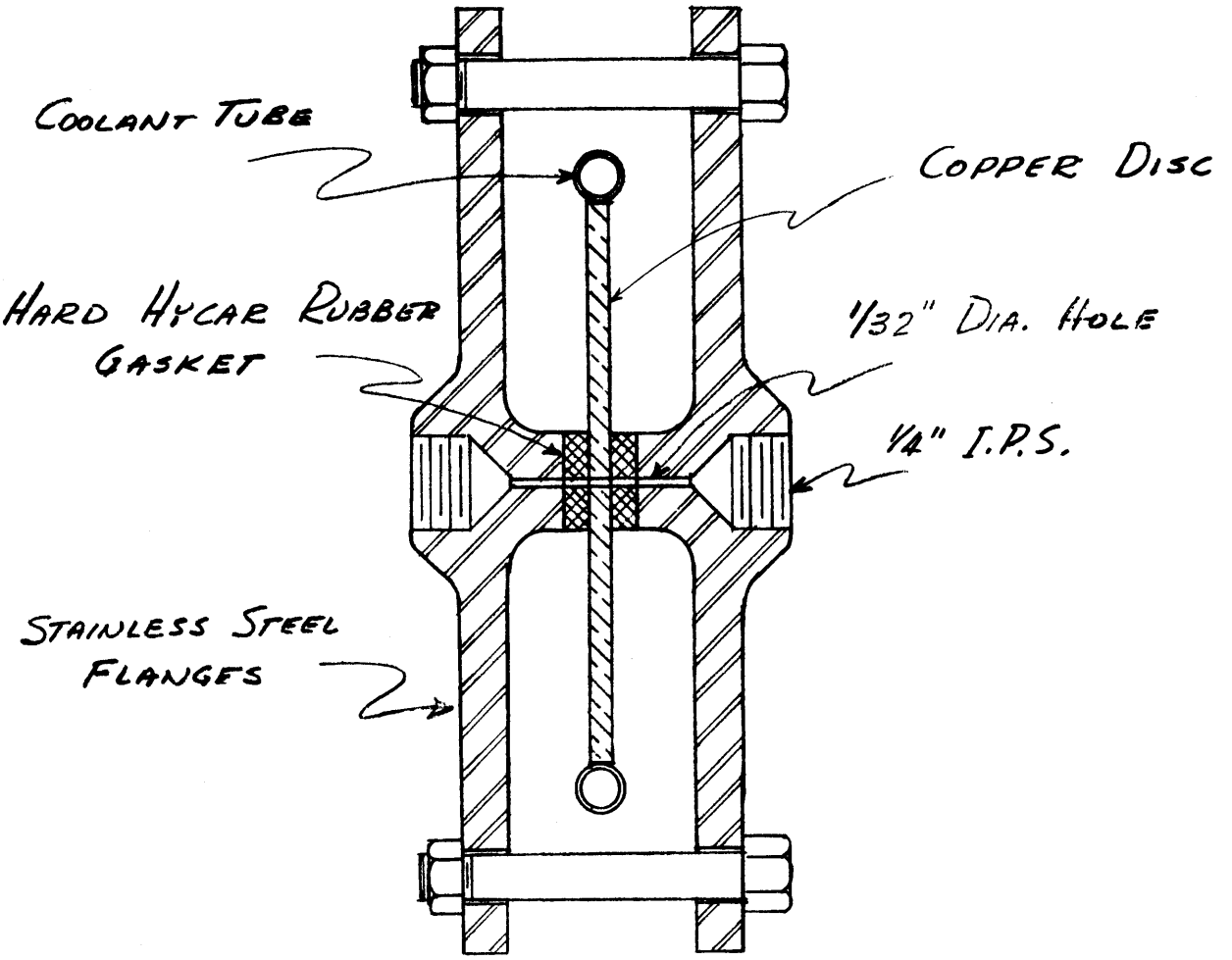

FIGURE 7.1 SECTIONAL VIEW OF PROPOSED TEST SECTION FOR DETERMINING HEAT TRANSFER COEFFICIENT OF LIQUID SODIUM

MEAN CONDUCTANCE DATA USING NaOH

H. W. Hoffman

A tentative design has been made for an apparatus for the determination of the heat-transfer coefficient for a molten sodium hydroxide system under forced convection at temperatures from the melting point (604°F) to 1000°F and possibly higher. The test section will consist of an electrically heated tube, 0.25 in. I.D., 0.375 in. O.D., 25 in. long, with appropriately positioned thermocouples for the measurement of surface temperature. It has been decided to construct the system of "L" nickel. The components of the system and their relative positions are indicated in Fig. 7.2.

The design of a system for the measurement of heat-transfer coefficients can be divided into five major categories; namely, materials of construction, methods of handling and moving the fluid through the system, the design of the test section, methods of introducing and removing heat from the system, and measuring and control instruments.

In this particular investigation both corrosive and high-temperature conditions exist. The handling of materials at high temperatures does not pose too difficult a problem since numerous metals and metal alloys exist which will withstand temperatures well in excess of those expected in this investigation (604 to 1000°F). However, the number of materials able to withstand the corrosive action of molten sodium hydroxide is very limited. In a preliminary test at Battelle Memorial Institute regarding the feasibility of using various materials for containing molten sodium hydroxide, it was found that silver was best with a corrosion rate of approximately 0.1 mg/cm^2/month, with nickel and graphite next at approximately 1.0 mg/cm^2/month. These three are the only materials recommended.

Silver will soften at temperatures in the vicinity of 1000°F and must be used in the form of silver-clad steel tubes. Graphite has the serious disadvantage of having very poor mechanical properties, thus necessitating heavy awkward sections. Nickel possesses none of the disadvantages of the above two, and it has been decided to use "L" nickel for at least the test section of the apparatus.

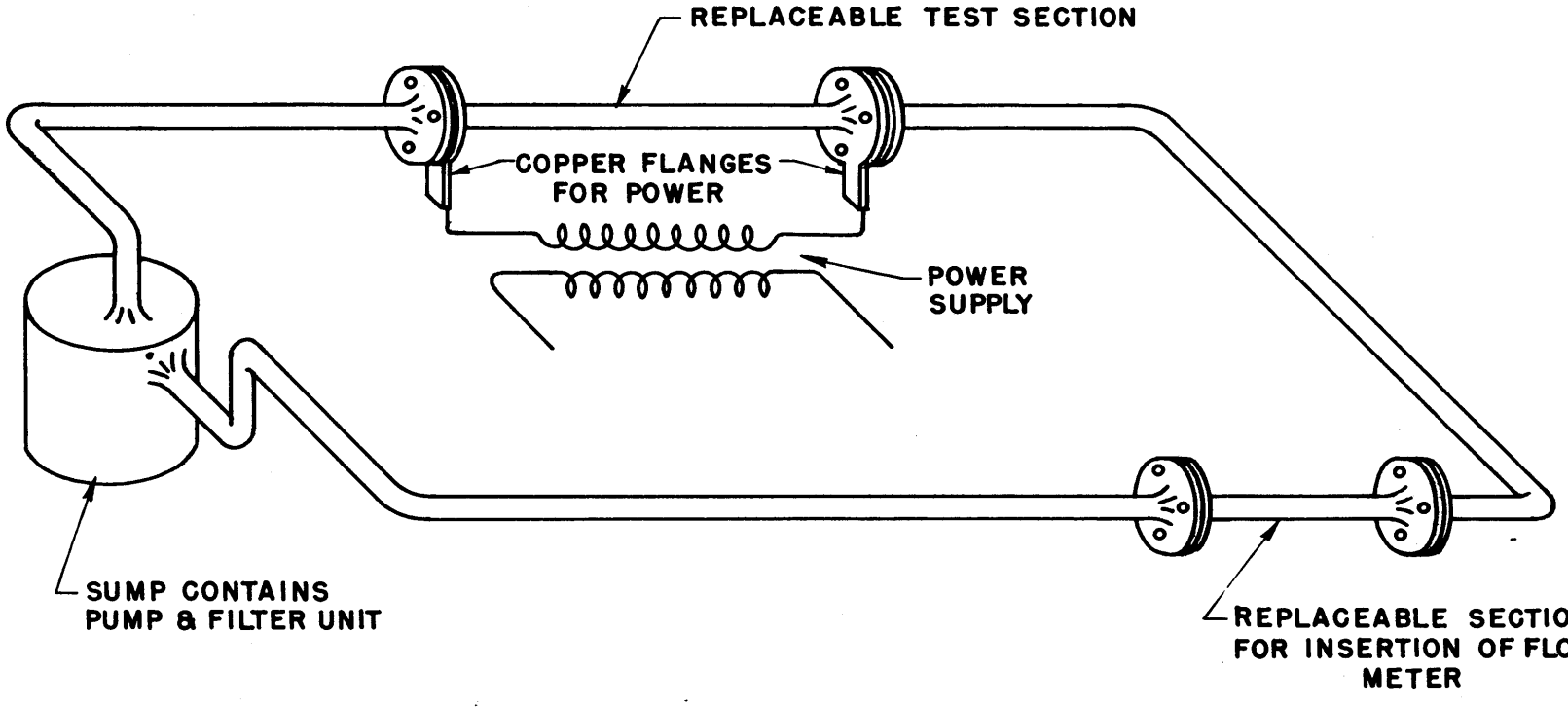

FIGURE 7.2 PROPOSED APPARATUS FOR DETERMINATION OF HEAT TRANSFER COEFFICIENT FOR MOLTEN NaOH

The molten sodium hydroxide will be circulated through the system by a centrifugal sump pump. Since the pump will be in the molten sodium hydroxide, it is necessary that the entire casing, in addition to the impeller, be constructed of nickel. It is planned to use a pump capable of handling 10 gpm at a discharge pressure of 15 psi.

The sodium hydroxide will be melted with the nickel sump tank and maintained at a temperature of about 800°F. Since it is suspected that Na_2CO_3 contributes greatly to the corrosive action of NaOH, it will be necessary to purify the commercial caustic. To prevent formation of Na_2O in the melt, a positive pressure of "forming" gas (10% H_2, 90% N_2) will be maintained over the melt in the sump.

Three tentative designs for the measurement of the flow rate are being considered. Two involve the use of strain gauges in association with an orifice plate. Both of these require calibration because of the variable temperature in the system. The third method uses a volumetrically calibrated catch tank with a magnetic (or radioactive) float.

Several alternatives present themselves in the design of the test section. The following three were considered:

1. Parallel channels of rectangular cross section
2. Concentric channels of circular cross section
3. Electrically heated tube of circular cross section

While all three systems will give information of value, stress has been placed on the third system, primarily because of the simplicity of its construction, the ease of calculation of results, and the elimination of the need for a supplementary system for adding heat. Preliminary calculations indicate that a 15-kw electrical system will be necessary.

Currently, consideration is being given to removing heat by radiation from the system as a whole.

BOILING LIQUID METALS

W. S. Farmer

During the past quarter it has been possible to select an arrangement of apparatus for determining heat-transfer coefficients to boiling liquid

metals. The overall design is 75% complete while detail drawings are 30% complete at this time. A work order for construction will have been issued by the first of December.

The apparatus arrangement finally selected consists of a 12-in. vertical single-tube boiler. Heat is supplied by radiation from a graphite tube, which will be inside and concentric with the molybdenum boiler tube. The metallic vapors produced in the boiler will be condensed in a vertical tubular header consisting of several banks of finned tubes, across which air will be drawn. The design is shown schematically in Fig. 7.3.

Initial experiments will be conducted on natural convection boiling outside a 1-in.-diameter 6-in.-long tube. The flux will be variable up to 10^6 Btu/hr per square foot with existing variable-voltage power equipment. Graphite temperatures up to 5000°F will be required.

NATURAL CONVECTION IN LIQUID-FUEL ELEMENTS

P. C. Zmola

Natural convection will be required in the liquid-fuel elements now under consideration if excessive temperatures are to be avoided at the center of the liquid. Preliminary design has been completed for equipment to determine the extent and the effectiveness of natural convection within the fuel elements. Electric current will be passed through the liquid in a simulated fuel element to generate heat within the liquid itself, and heat will be removed from the surface of the fuel element at fluxes which will exceed 10^6 Btu/hr per square foot.

THEORETICAL THERMAL ENTRANCE ANALYSES

H. F. Poppendiek

Three new sets of analytical solutions have been developed for inclusion in a collection of analytical solutions which is now being compiled. The collection is to consist of solutions for postulated systems which approximate actual heat-transfer systems now under consideration in the ANP reactor development.

UNCLASSIFIED
DRAWING NO. 10281

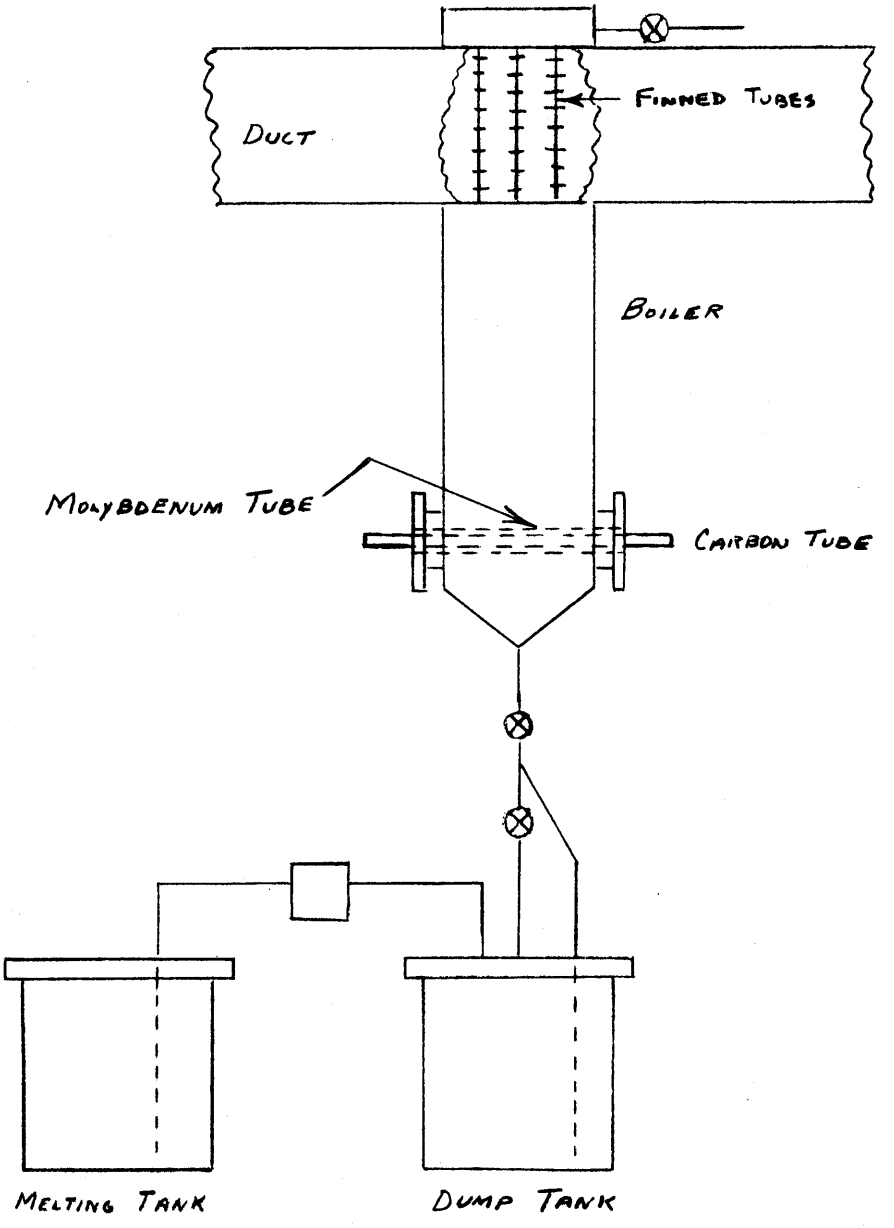

FIGURE 7.3 APPARATUS ARRANGEMENT FOR BOILING LIQUID METALS

An analytical turbulent flow solution has been developed for a system in which (1) a fluid is flowing uniformly (slug flow) between two parallel plates, (2) the initial fluid and wall temperatures are uniform, (3) the fluid suddenly flows over surfaces which are emitting a uniform heat flux to the fluid, and (4) the eddy diffusivity varies linearly with distance from the duct wall (the total thermal diffusivity becomes the thermal molecular diffusivity at the wall). This analysis is in the process of being prepared as a technical report.

Analytical solutions for temperature distributions have been derived for parallel-plate and pipe-duct systems in which (1) the fluid is characterized by a turbulent velocity profile (a power-loss relation) and a high thermal molecular diffusivity compared to the thermal eddy diffusivity, (2) the initial fluid and wall temperatures are uniform, and (3) the fluid suddenly flows over surfaces which are at some new uniform temperature. Local heat flow and convective conductance solutions have also been developed. These analyses are being prepared as a technical report.[1]

An analytical thermal entrance solution has been obtained for a system in which (1) a fluid flowing uniformly between parallel plates is characterized by a high thermal diffusivity compared to the thermal eddy diffusivity and by a symmetrical volume heat source whose strength is a function of distance between the parallel plates, (2) the initial fluid and wall temperatures are uniform, (3) the fluid suddenly flows over surfaces through which heat is lost to a heat-transfer fluid on the other side (the heat-transfer fluid is at a uniform temperature and the duct-wall resistance is not the controlling resistance in the thermal circuit). It is felt that solutions of this type may be useful in describing heat transfer in reactor liquid-fuel elements.

FLUID FLOW AND HEAT TRANSFER IN NONCIRCULAR DUCTS

H. C. Claiborne

Theoretical investigations of fluid flow and heat transfer in noncircular ducts has progressed to a point where a status report[2] is being prepared.

(1) Poppendiek, H. F., *Heat Transfer*, ORNL-913, to be issued.

(2) *Ibid.*

The report will be released before the end of the coming quarter and will contain the following topics: (1) analytical solutions for velocity distribution for laminar or streamline flow in rectangular, equilateral triangular, right isosceles triangular, elliptical, and any circle sector ducts; (2) analytical solutions for the resulting temperature distribution when heat is transferred to a fluid flowing with a square velocity wave (slug flow) through the same type of ducts mentioned above with the duct walls at a constant temperature; (3) analytical solutions for the resulting temperature distribution when heat is transferred to a fluid flowing with a square velocity wave through rectangular, equilateral triangular, any right triangular, elliptical, and 60° circle sector (a general solution has not been obtainable) ducts for the case of constant heat flux from the duct walls.

Average Nusselt's moduli for the case of constant flux were found to be 6, 4, 3, 2, and 0.000386 for rectangular, equilateral triangular, 45°, 30°, and 1° right triangular ducts, respectively, as compared with the value of 8 for a circular pipe.

It can be shown that the slug flow solutions will be reasonable approximations for the case of turbulent flow of liquid metals for Reynolds' moduli below about 10,000, and that heat transfer will be underestimated by these solutions at higher Reynolds' moduli.

Other more complex problems involving noncircular ducts under consideration are entrance solution, effects of finite wall thickness for the case of constant flux to the outer side of the duct wall, heat transfer to a fluid flowing with an established laminar velocity distribution, and some possible approximations for the case of turbulent flow.

PHYSICAL PROPERTIES

A. R. Frithsen, USAF

During the past quarter a laboratory was established for the measurement of physical properties of liquid metals, liquid salts, liquid caustics, structural materials, insulators, and other materials that may be utilized in the design of an aircraft reactor. The design of apparatus for the measurement of specific heats, thermal conductivities, viscosities, and densities

has been initiated. At the time of this writing it was anticipated that the specific heat apparatus would be completed and ready for routine measurements with an accuracy of the order of ±5% by Jan. 1, 1951. It is expected that the thermal conductivity apparatus and the viscosity apparatus will be capable of accuracies of about ±10%, and will be completed by Apr. 1, 1951; and that the density apparatus will be capable of accuracies of about ±2%, and will be completed about Apr. 15, 1951. An approximate value for the specific heat of lithium has been obtained between 550 and 900°C.

In order to avoid unnecessary duplication of effort, personnel of the physical properties laboratory are coordinating their efforts with other agencies also involved in this type of work. As a result of a conference with personnel from the Office of Air Research and the Materials Laboratory of the Air Materiel Command, USAF, these agencies of the USAF will in the near future begin work on the measurement of liquid metals, liquid salts, and other materials at their own laboratories at Wright-Patterson Air Force Base, Dayton, Ohio, and also by contracting with various universities and research organizations. In addition these agencies will contract directly for the development of physical-property-measurement techniques and apparatus in an attempt to develop methods with extremely high accuracies.

A survey shows that the following data already have been obtained by other agencies and are considered acceptable for ARE design studies:

MEASUREMENT	AGENCY	TEMPERATURE (°C)
Specific heat	Bureau of Standards	
Sodium		100 to 800
Potassium		100 to 700
Sodium-potassium eutectic		100 to 700
Beryllium		0 to 900
Viscosity	Naval Research Laboratory	
Sodium		100 to 700
Potassium		100 to 700
Sodium-potassium alloys		100 to 700
Viscosity	Critical Tables	
Lead		441 to 844
Density	NEPA	
Bismuth		m.p. to 1000
Lead		m.p. to 1000
Lithium		m.p. to 1000
Lead-bismuth eutectic		m.p. to 1000

(Continued)

MEASUREMENT	AGENCY	TEMPERATURE (°C)
Density	Naval Research Laboratory	
Sodium		100 to 700
Potassium		100 to 700
Sodium-potassium alloys		100 to 700

In addition to the quantities listed above, it is deemed necessary to determine the specific heats, thermal conductivities, viscosities, and densities of all materials of interest in the design of an aircraft reactor, and, in addition, it will be necessary eventually to extend the above information to 1000°C in each case.

Specific Heat (R. F. Redmond, L. F. Basel, J. Lones, A. Bates,* D. Smith,* W. H. Bowman,* D. James,* and J. Roarty*). The specific heat project has progressed to the stage where the method of determination has been selected and the apparatus has been designed, constructed, and used to determine the specific heat of lithium over the temperature range 550 to 900°C. At present the apparatus, a Bunsen ice calorimeter (Figs. 7.4 and 7.5) is being redesigned.

The enthalpy values for lithium, as obtained experimentally in the temperature range 500 to 1000°C, are shown in Fig. 7.6. A careful statistical analysis of these points in this figure indicates that the best curve through them is a straight line, and, inasmuch as the specific heat is defined as

$$C_{p\ \text{absolute}} = \left[\frac{\partial H}{\partial T}\right]_p$$

then the slope of this straight line, which is 0.964, is the specific heat for lithium over the temperature range. However, the calorimeter was not calibrated, and subsequent experiments with metals of known specific heats showed the calorimeter to be 5 to 8% low. Calibration of this calorimeter by electrical means evidenced excessive heat leakage. Since minor alterations did not materially decrease this leakage, the calorimeter has been redesigned with emphasis given to the improvement of the rate of heat transfer from the heat capsule to the container. The new calorimeter together with refinements in technique will, it is hoped, substantially eliminate the previously encountered experimental errors.

*From MIT Practice School.

UNCLASSIFIED
DRAWING NO. 10282

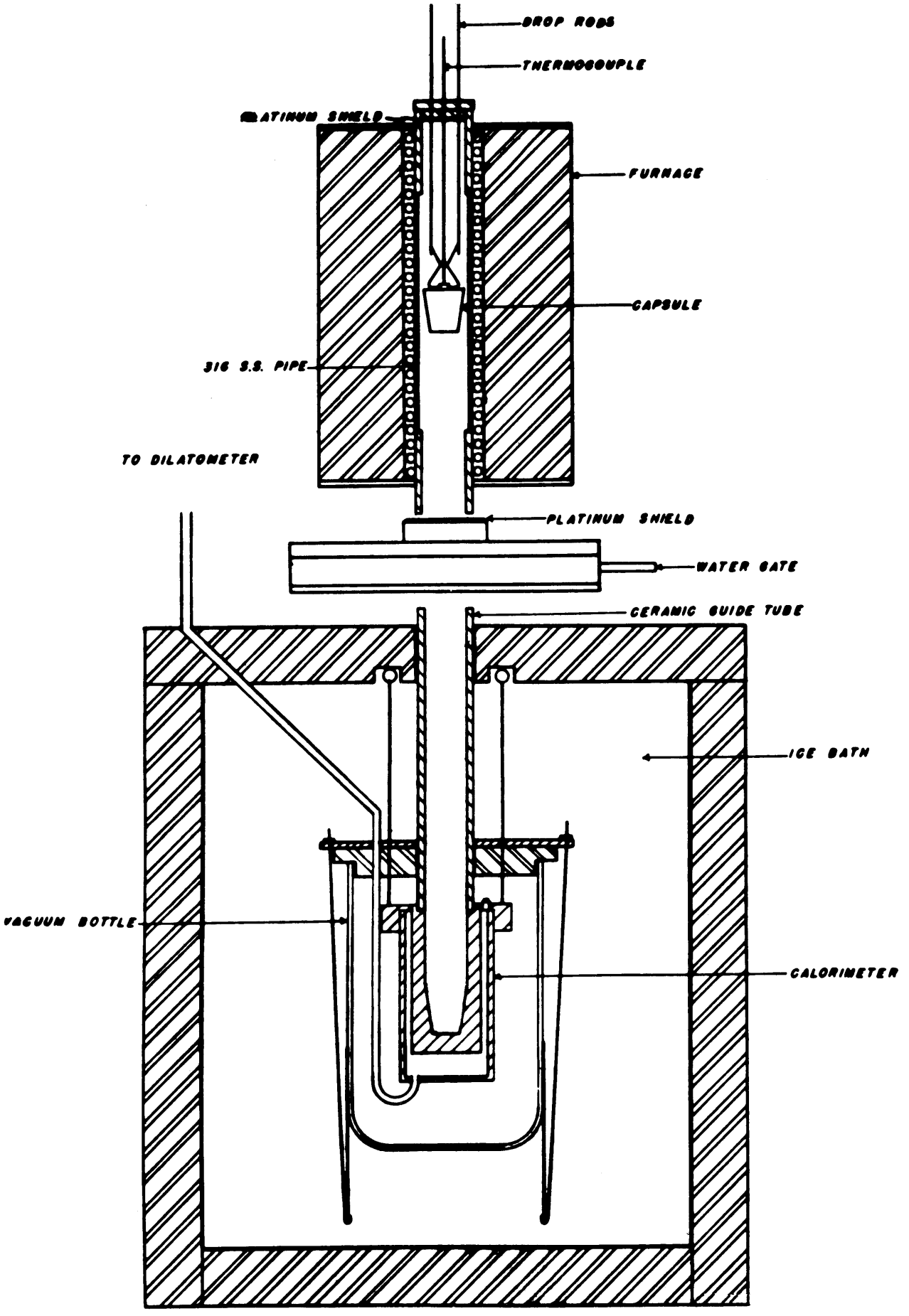

FIGURE 7.4 CALORIMETER ASSEMBLY

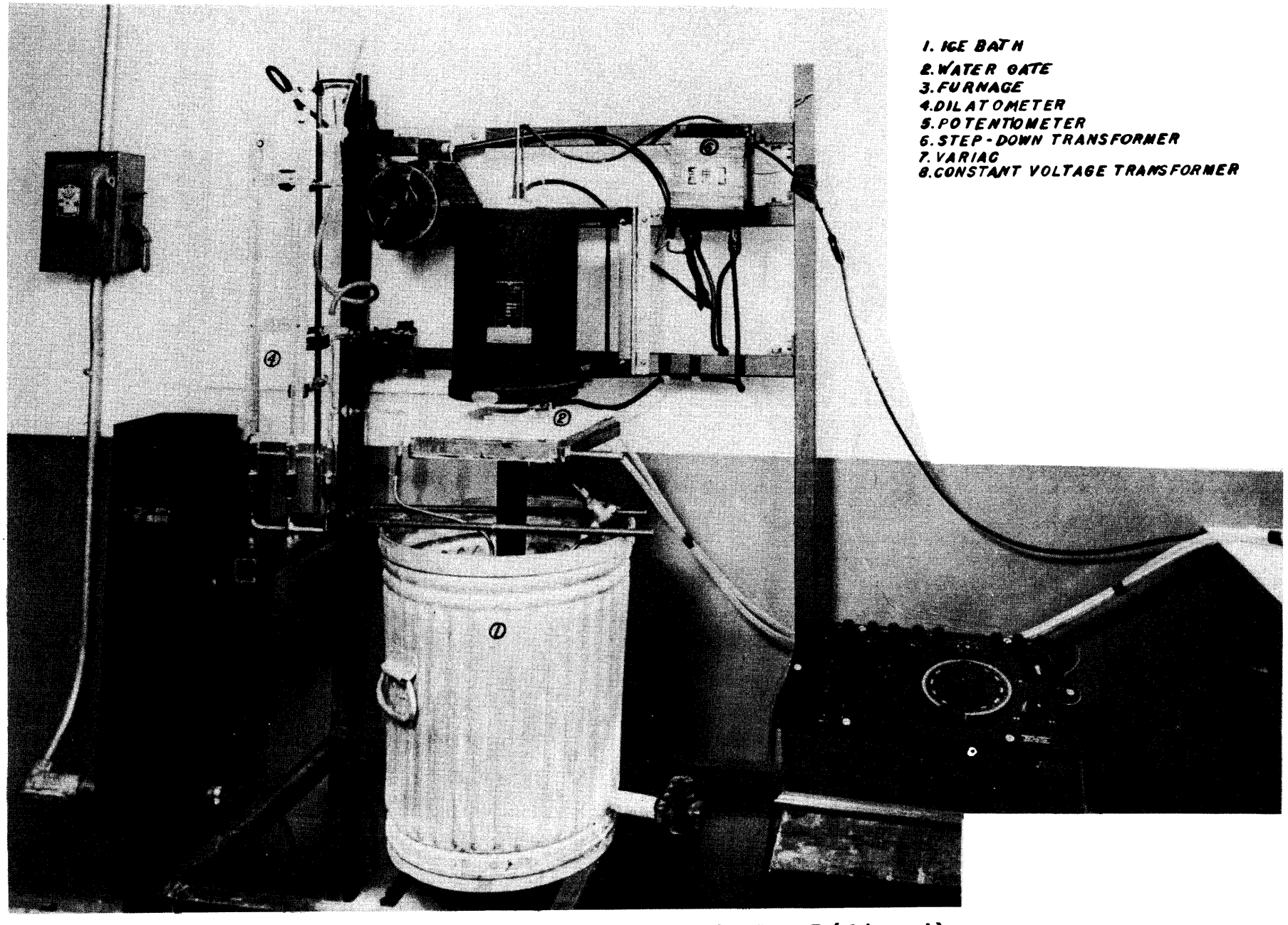

FIGURE 7.5 CALORIMETER (Closed)

UNCLASSIFIED
DRAWING NO. 61940

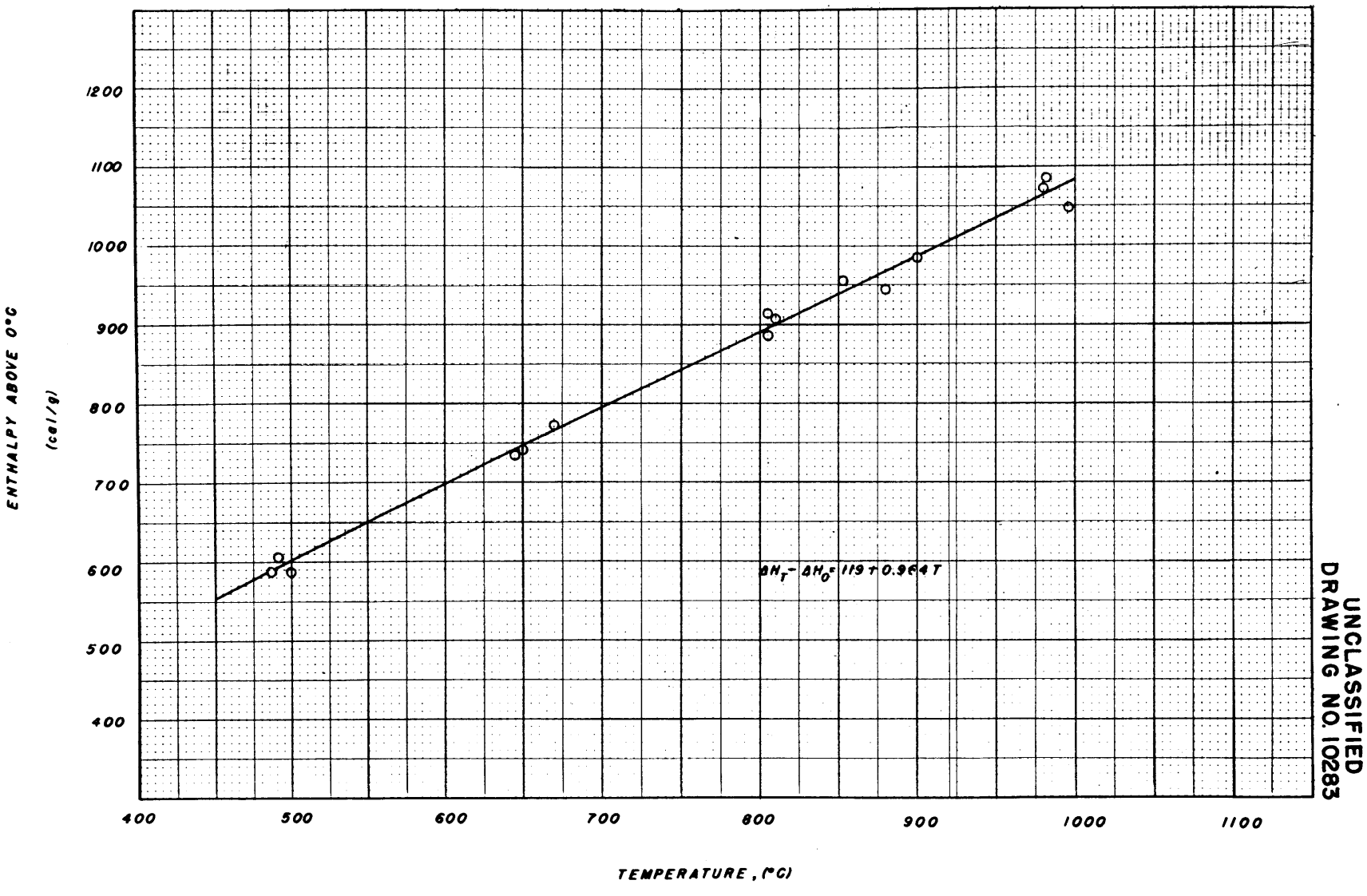

FIGURE 7.6 ENTHALPY OF LIQUID LITHIUM

Thermal Conductivity (L. F. Basel and M. Tobias). As a result of a survey of possible methods for the measurement of thermal conductivities of liquid metals from their melting point to 1000°C, a steady-state linear flow system, similar to one used by Dr. Deem of the Battelle Memorial Institute, has been selected. The design of this equipment is now nearing completion.

A schematic diagram of the Deem apparatus is shown in Fig. 7.7*a*. Heat flows from the upper heating plate down through the liquid, through the Armco-iron standard, to the copper cooling chamber. The heating plate is movable so that the liquid-specimen thickness can be varied. Thermocouples are located in the Armco-iron standard and in the metal surfaces above and below the liquid specimen. The resistance to heat flow between the two specimen thermocouples can be considered to be the sum of the specimen resistance, x/kA, and of the fixed resistance of the two liquid-solid interfaces, F_f.

It is clear that

$$\Delta T_s/Q = R_f + x/kA$$

where

ΔT_s = temperature difference between specimen thermocouples

Q = total heat flow through specimen

R_f = fixed resistances at liquid-metal interfaces

x = specimen thickness

A = specimen cross-sectional area

k = specimen thermal conductivity

By making several runs at different specimen thicknesses but at the same mean temperature, a plot of $A\Delta T_s/Q$ vs. x can be constructed; the slope of the line through the points is the reciprocal of the thermal conductivity.

Tests of an unsteady-state method were made at a temperature of approximately 250°C on Armco ingot iron using the apparatus shown schematically in Fig. 7.7*b*. The block was heated initially to *c* constant temperature and,

UNCLASSIFIED
DRAWING NO. 10284

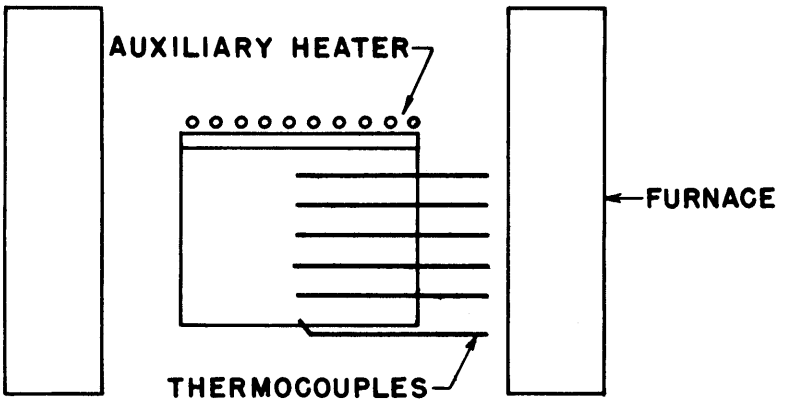

B. UNSTEADY STATE APPARATUS

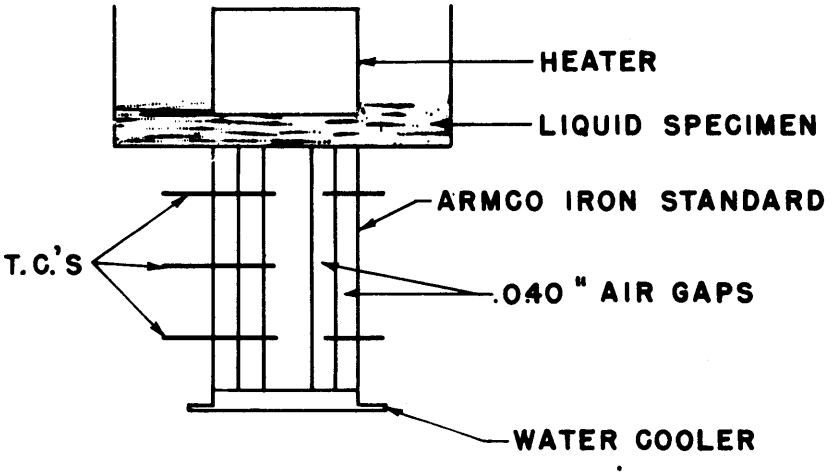

A. DEEM APPARATUS
STEADY STATE

FIGURE 7.7 APPARATUS FOR THE MEASUREMENT OF THE THERMAL CONDUCTIVITY OF LIQUID METALS

at a given time, the auxiliary heater was turned on. Temperatures were recorded at each of the thermocouple positions every few seconds. Ideally, α, the thermal diffusivity, can be calculated from the temperature, time, and distance measurements, since it is given by $\alpha = \frac{\partial T}{\partial \theta} \frac{\partial^2 t}{\partial x^2}$ for unidirectional flow. However, the results were inconclusive because much accuracy was lost in taking first and second derivatives. It is believed that this source of error can be reduced by improved design to give greater precision.

Several other types of unsteady-state systems have been considered, but in most of these systems it is difficult to maintain the proper boundary conditions. Radial heat flow methods cannot be used with liquids because of heat transfer by convection. To maintain a stable system, heat must be conducted unidirectionally from top to bottom of the liquid specimen. A steady state system, similar to that used by Van Dusen of the National Bureau of Standards for metals, has been adapted for use with liquid metals at KAPL. In this apparatus, heat is first conducted through the sample and then through a metal of known thermal conductivity. In the liquid-metal system a thin-walled container holds the sample and a correction is applied for the heat conduction down the wall. This apparatus cannot be used for liquids of low thermal conductivity since the wall correction would be large and the final determination would be inaccurate. Since there is some interest in materials of low conductivity, and since this apparatus appears to be complicated, the method was rejected.

Viscosity (S. I. Kaplan). Several methods of measuring viscosity were considered, including capillary-flow, falling-ball, and rotational viscosimeters. A literature search was made and numerous manufactures were polled on the availability of suitable commercial units, but none were found which would fulfill, without extensive modifications, the requirements peculiar to this project, namely, corrosion resistance, easy cleaning, ready adaptability to various liquids, and the ability to yield results of useful accuracy after brief preparation.

The initial method finally decided upon will employ a falling-ball viscosimeter. Preliminary design of the unit has been completed and fabrication is now in progress. The apparatus consists essentially of a stainless steel tube mounted vertically in a furnace and filled with the liquid being tested. A radioactive ball, of a diameter small compared with that of the

tube, is dropped into the liquid. The time the ball takes to fall a measured distance through the liquid is determined by externally mounted detectors. The viscosity can then be calculated in absolute units from the known relationships given by Stokes' law. The dimensions of the instrument are ample to ensure precise velocity measurements (Fig. 7.8).

As a possible secondary means of measurement, a modification of a commercial viscosimeter employing concentric rotating cylinders is being considered, and correspondence with the manufacturers on adaptation problems is being conducted. A third method, involving measured flow through a capillary, has been used by the Naval Research Laboratory for liquid metals. However, the apparatus is more cumbersome than those proposed, and is more difficult to change over from one liquid to another.

Density. Methods for the determination of the density of high-temperature systems are currently being investigated. Possibilities include the weighing of a suspended bob in the liquid, and determination of the pressure required to force a gas bubble from the mouth of a submerged tube against a known depth of liquid.

DEVELOPMENT OF COMPONENTS FOR EXPERIMENTAL HEAT-TRANSFER SYSTEMS

A. R. Frithsen and M. Richardson

A completely sealed rotary pump has been developed for use with experimental heat-transfer systems. Although the previously reported hydraulic bearings have proved adequate, new bearings which will permit increased flow are being fabricated. Four electromagnetic pumps have been received from G.E. and three Flowrators from Fischer and Porter Co.

Pumps. The main efforts during this quarter have been devoted to continuing the development of a completely sealed rotary type pump since this type appears to show the greatest flexibility for utilization in experimental systems. The hydraulic bearings discussed in detail in the previous quarterly report[3] were tested in the bearing test system and operation proved to be

(3) Frithsen, A. R., "Pump Development for Experimental Systems," *The Aircraft Nuclear Propulsion Project Quarterly Progress Report for Period Ending August 31, 1950*, ORNL-858, 56 (Dec. 4, 1950).

UNCLASSIFIED
DRAWING NO. 10285

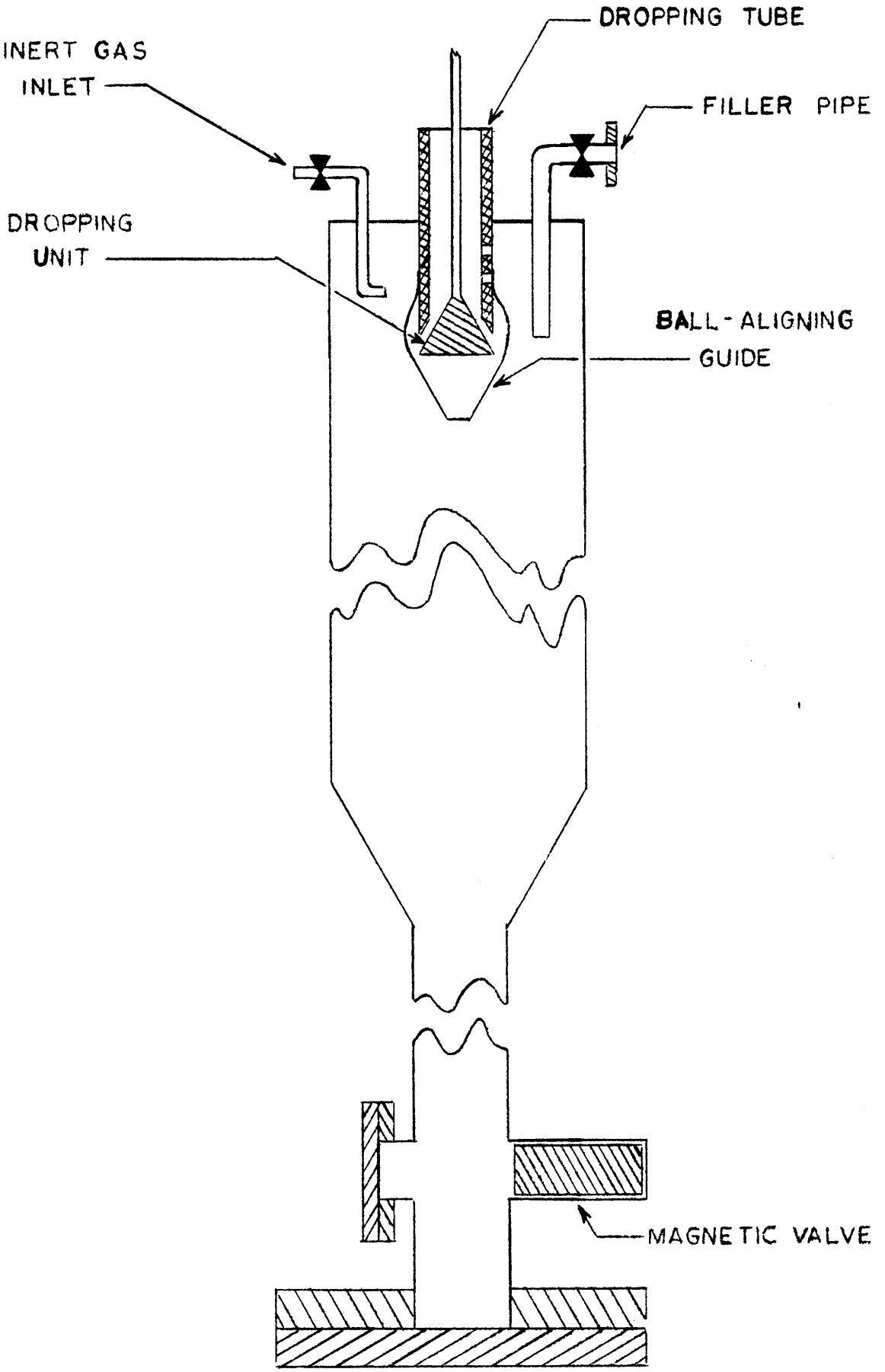

FIGURE 7.8 VISCOSITY MEASURING TUBE

satisfactory. Several runs of ½ to 3 hr duration each were made; however, testing had to be terminated before long-duration runs could be made because of misalignment in the bearing test system.

A new hydraulic bearing has been designed and fabricated, which is similar to those previously described except that two rows of longitudinal pressure slots are used and flow of liquid from each end of these slots is now possible. This latter feature was incorporated owing to the fact that work at Allis-Chalmers Manufacturing Co. on similar type bearings indicates that performance is greatly improved if the flow through the bearing is increased.

The bearing test system has been modified so as to test these new bearings, and initial tests indicate that, although more flow is required in the new type bearings, they will operate at a much lower pressure than the original bearings (i.e., 10 psi as compared with 45 psi). An adapter is now being fabricated which will make it possible to use the same bearing test system to test both types of bearings. Thus it will be possible to obtain a quick comparison of performance of the two types so as to determine the best compromise between efficient operation and simple construction.

The design of a pump using hydraulic bearings and having a capacity of 12 gpm at 230 ft is almost complete. The system for testing this pump up to a temperature of 400°F is in the process of being designed.

Four G.E. electromagnetic pumps have been received and one has been transferred to the Experimental Engineering Section of the ANP Division for use in a liquid-metal corrosion testing system. The other three pumps will be used as the need arises.

Flow Measuring Devices. Three Flowrators (rotameters) have been received from the Fischer and Porter Co. which were designed to meet the following conditions:

Fluid	Lithium or sodium
Operating pressure	100 psi
Operating temperature	100°F
Flow	2 Flowrators for 3.3 to 33.0 gpm
	1 Flowrator for 7.5 to 75.0 gpm

One of the 3.3- to 33.0-gpm Flowrators will be incorporated in the pump test system to test its operation in sodium and sodium-potassium alloys.

LIQUID METALS IN-PILE EXPERIMENTS

R. F. Battistella C. D. Baumann
O. Sisman

The loop for circulating liquid lithium through the pile and most of the auxiliary equipment have been built. Final assembly and testing of this equipment cannot be carried out until the electromagnetic pump and electromagnetic flow meter have been tested and calibrated.

The first calibrating system for the pump and flow meter sprang a leak at a weld about 4 hr after start-up. No damage was caused by the resulting fire, but the system had to be completely dismantled and rebuilt.

A second calibrating system is now ready for operation, a sketch of which is shown in Fig. 7.9. About 2 lb of lithium will be charged into the charging tank, and the entire system will be evacuated before the charging tank heaters are turned on. The molten lithium will be kept under vacuum at 1000°F for several hours to drive off the oil in which the lithium is shipped. The portion of the system between the charging and collector tanks, including three traps, will be heated next, and the molten lithium will be transferred through a micrometallic filter into the metering tank by helium pressure. To calibrate the flow meter, the lithium will be moved from the metering tank to the charging tank by gas pressure. The flow rate will be regulated by regulating the gas pressure at the collector tank, and will be measured by recording the time required to fill up the charging tank between the two probes. Three different size pipes, one with a flat section, are provided for the flow meter to determine which will give the largest signal with the electromagnetic flow meter.

After the flow meter has been calibrated at several temperatures, the lithium will be circulated around the closed system by the pump and the flow at various temperatures will be checked by the flow meter.

If operation of the pump and flow meter is satisfactory, the lithium will be circulated through the system on a 24-hr basis for two weeks or until a leak occurs. If the system holds up for two weeks at 1000°F it will be considered safe to operate the in-pile loop for one week at the same temperature. The in-pile loop will then be tested by circulating lithium through it for 24 hr, and if no leaks occur it will be inserted in the pile.

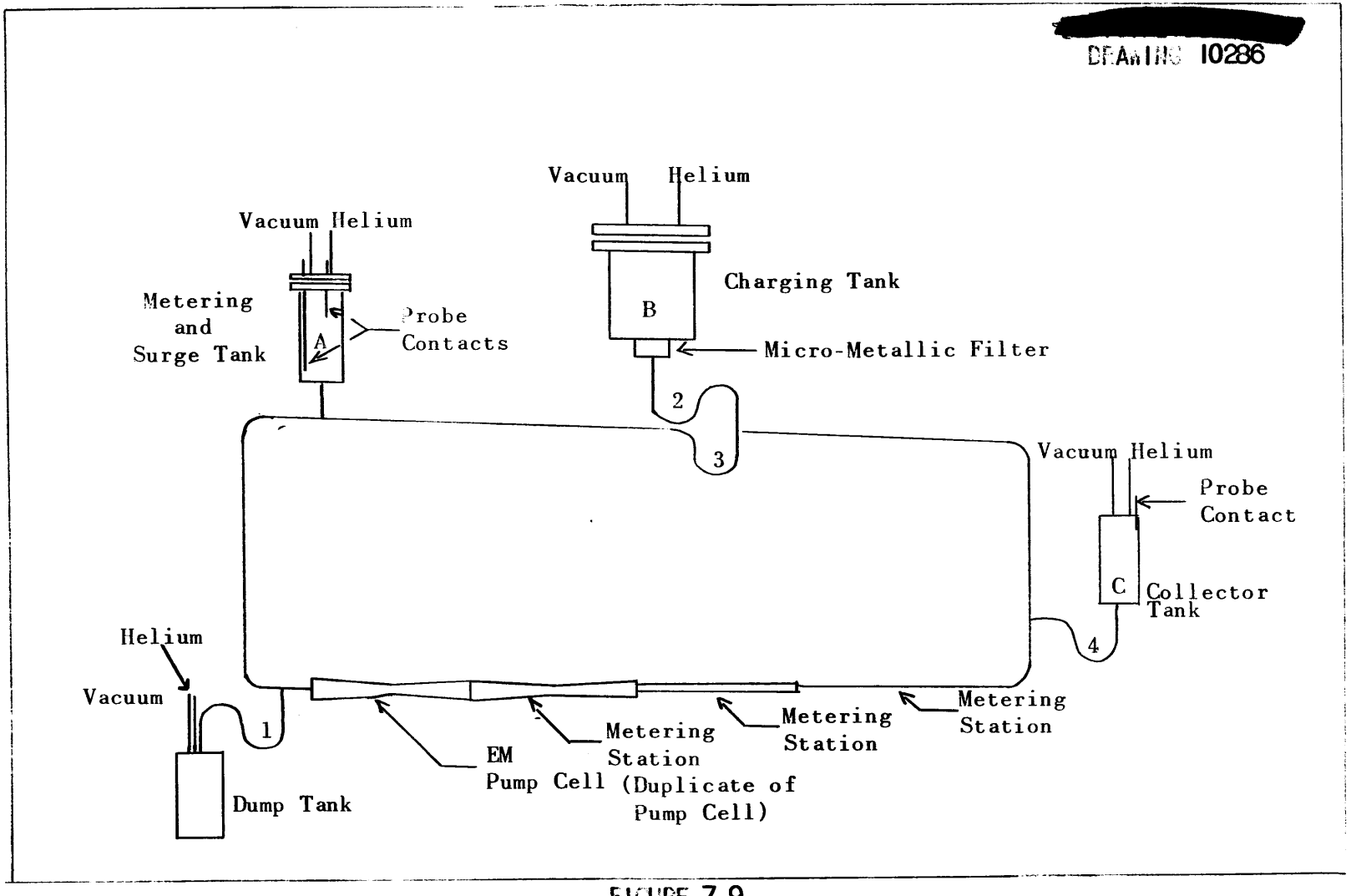

FIGURE 7.9
LITHIUM METERING AND E.M. PUMP LOOP

8. METALLURGY

8. METALLURGY

E. C. Miller, Metallurgy Division

One of the most important requirements of any structure is that the various members be mutually compatible. Very little information is available on the high-temperature compatibility of the various materials now being considered for use in the ARE. Consequently, emphasis has been placed on both static and dynamic corrosion tests of such materials. The static corrosion of metals, particularly the stainless steels, by sodium is being extensively studied; in general, the attack is much milder than similar tests with lithium. Straight iron-chromium alloys or ferritic grades of stainless steel appear to be more resistant than other metals to attack by lead. Similar studies of the corrosive properties of lithium and tests of various metals in a uranium-aluminum alloy are reported.

Dynamic corrosion tests in thermal convection loops are underway but no results are yet available. The laboratory for the fabrication of fuel elements will not be completed before February; nevertheless, it is in operation and some fuel elements have been pressed and extruded. Static corrosion tests were performed on combinations of materials pertinent to this program. The Welding Laboratory and the Creep-Rupture Laboratory are still being set up, although preliminary experiments have been undertaken by both groups.

STATIC CORROSION TESTING

J. E. Cunningham

This initial phase of the liquid-metal corrosion testing program is designed to sort out potential structural materials for use in contact with various coolants. Liquid-metal coolants now being considered for use in the proposed ARE include lithium, sodium, and lead. Because of the contribution this last heat-transfer-fluid would make toward lessening shield weight, the activity on corrosion has been shifted to lead. Testing of materials in sodium and lithium is being continued, but at a reduced effort.

Two important observations made concerning liquid-metal corrosion work in the past six months are: (1) The depth of attack or penetration in liquid-

metal media as measured by metallographic examination is a more reliable criterion for evaluating the corrosion behavior of materials (particularly alloys) than are weight change data; and (2) in many cases, mass transfer effects prevent use of an inert or third material in the test system, and tests must be conducted in tubing containing only the test coolant. On the other hand, information obtained in this manner may be of little value in an application requiring the presence of more than one solid metal.

Materials in Lead. Some of the metallic elements which in the preliminary screening tests showed promise of containing lead were examined metallographically. Tungsten and Armco iron showed no evidence of any form of attack. The refractory elements columbium, molybdenum, and tantalum, which showed an appreciable weight gain after test, were characterized by formation of films or coatings. Columbium and molybdenum exhibited a uniform, duplex type of coating which was rather soft or spongy in nature, while tantalum showed a thin, brittle type of film formation. Elements like nickel, which essentially dissolved during the test, and beryllium and tantalum, which lost appreciable weight, were not examined. Examination of the graphite-melted zirconium, which exhibited a slight weight gain, is incomplete.

Forty-hour tests were performed on several stainless steels (Table 8.1) to determine their corrosion behavior in contact with 1000°C (1832°F) lead. Both the austenitic and straight ferritic type were represented, as well as some extra-low-carbon grades. Wherever possible, tubing served as the test capsule; otherwise a test specimen plus a controlled amount of lead ("Doe Run" grade, 99.99% Pb, as supplied by the National Lead Company) were contained in an evacuated capsule of relatively inert Armco iron. Change in thickness and range of maximum penetration were determined by metallographic examination. All specimens were cut diagonally and mounted with protection bars at the exposed surface to reduce edge-rounding during polishing. Since thickness measurements were made before and after the test, the recorded value gives the total thickness loss resulting from attack on two sides of the test specimen. Penetration refers to the maximum depth of corrosion reached beyond the attacked surface from one side of the specimen only. Six fields were measured and the range was reported.

Results indicate that, with the exception of 316 stainless steel alloy, the austenitic type alloys were characterized by an intergranular type of

TABLE 8.1

Static Corrosion Data on Stainless Steels in 1000°C Lead for 40 hr

STAINLESS STEEL ALLOY	CARBON (%)	SURFACE-VOLUME RATIO (cm^2/cm^3)	WEIGHT CHANGE (mg/cm^2)	METALLOGRAPHIC DATA		
				THICKNESS CHANGE (cm)	RANGE OF MAXIMUM PENETRATION (cm)	REMARKS
304 LC	0.033	1.0	-14.62			No Metallography
304 LC	0.033	1.0	-11.44	-0.004	0.004-0.012	Intergranular type of attack; slight amount of phase transformation $\gamma \rightarrow \alpha$ in attacked grain boundary region
304 LC	0.033	1.0	-1.03	+0.001?	0.004-0.014	Same
304 VLC	0.006	0.7	-10.86	-0.006	0.015-0.024	Grain boundary attack accompanied by phase transformation $\gamma \rightarrow \alpha$; some pitting or hole formation noted in attacked grain boundaries
304 VLC	0.006	0.7	-4.81	-0.004	0.021-0.027	Same
405	0.078	1.0	-9.17	-0.003	0.001-0.003	Light uniform attack
405	0.078	1.0	-13.83	+0.001	0.002-0.003	Light uniform attack
410 ELC	0.041	1.0	+1.21	+0.002	0.003-0.005	Irregular type of attack; formation of blue-gray compound in attacked area, pearlitic type of transformation immediately adjacent to lead-affected zone; parent metal showed an ocicular structure
410 ELC	0.041	1.0	+2.71			Same
410 ELC	0.041	1.0	+2.27			Same
430	0.085	1.0	-2.10	0.000	0.002-0.004	Intergranular type of attack which left surface rough in appearance; pearlitic type of transformation found in attacked grain boundary region; parent metal showed martensitic type structure
430	0.085	1.0	-3.31	0.000	0.002-0.007	Same
430 ELC		0.8	-5.30	-0.002	0.004-0.009	Irregular type of attack which left surface rough in appearance; blue-gray constituent formed in lead-affected zone
430 ELC		0.8	-7.43	-0.002	0.002-0.006	Same
430 ELC		0.8	-7.71	-0.001	0.006-0.008	Same
446	0.084	1.0	-3.73	-0.002	0.006-0.013	Irregular type of attack which resulted in globular holes in lead-affected zone; decarburized to a depth of 0.018 cm

TABLE 8.1 (Cont'd)

STAINLESS STEEL ALLOY	CARBON (%)	SURFACE VOLUME RATIO (cm^2/cm^3)	WEIGHT CHANGE (mg/cm^2)	METALLOGRAPHIC DATA		
				THICKNESS CHANGE (cm)	RANGE OF MAXIMUM PENETRATION (cm)	REMARKS
446	0.084	1.0	-5.03	0.000	0.006-0.009	Same but depth of decarburized zone was 0.014 cm
446 ELC	0.005	1.1	-5.16			No metallography
446 ELC	0.005	1.2	-1.61		0.010-0.018	Irregular type of attack which left large holes concentrated along lead-affected zone; attack did not necessarily follow grain boundaries
446 ELC	0.005	1.2	-7.18			No metallography
446 VLC	0.006	0.7	-7.34	0.003	0.004-0.006	Irregular type of attack which left globular holes spotted randomly throughout lead-affected zone
446 VLC	0.006	0.7	-8.45	-0.003	0.006-0.009	Same
Seamless 310 Tubing					0.011-0.013	Heavy intergranular type of attack to a depth of 0.012 cm; slight amount of decarburization noted
Weldrawn 316 Tubing					0.001-0.003	Extremely mild attack; shallow layer of small grains present at exposed surface; an unidentified precipitate found in grain boundary region of lead-affected zone
Weldrawn 304 ELC Tubing						Essentially no attack; film formed underneath a layer of grains showing an acicular structure
Seamless 446 Tubing						Parent metal showed considerable precipitation, perhaps sigma, at grain boundaries and on crystallographic planes within the grains; lead-affected zone was devoid of precipitate and had appearance of decarburized zone
Seamless 446 Tubing						Attacked surface slightly rough in appearance, but showed no evidence of the precipitate found in test above

attack. Type 304 stainless steel (18-8) showed a phase transformation from gamma to alpha in the attacked grain boundary region. The straight iron-chromium alloys showed an irregular type of attack with formation of an unidentified blue-gray constituent or globular holes in the lead-affected zone. In general, the straight iron-chromium or ferritic grades appeared to be more resistant to attack by lead on the basis of depth of attack and change in weight for short exposures. Numerous cases were encountered, however, in which straight iron-chromium grade tubing collapsed during the test, presumably because of the high temperature and the pressure differential (1 atm) between the inside and outside of the test tube.

Additional work is in progress on 18-8 molybdenum type alloy to check the encouragingly good resistance shown by this high-strength alloy during initial testing. Longer (400-hr) tests have been completed, but metallographic data and interpretation of results are not yet available.

Stainless Steels in Lithium. The study of the corrosion behavior of the commercial stainless steel alloys in 1000°C (1832°F) lithium was largely completed and reported last month. The facts revealed by X-ray and metallographic examination are summarized below:

1. Attack was largely intergranular in nature, but some solution was noted.
2. In the 18-8 type of stainless steel alloy, areas adjacent to attacked grain boundaries and similar exposed surfaces had undergone a phase transformation from austenite to ferrite, presumably as a result of solution or diffusion of an austenite former, such as carbon or nickel, into the lithium.
3. The structure in immediate contact with molten lithium was decarburized.
4. Both the ferritic and austenitic grades showed grain growth with increasing time. The grain coarsening was largely confined to the parent metal with little or no effect on the lithium-affected zone.
5. In general, the straight iron-chromium alloys (ferritic grades) appear somewhat more resistant to 1000°C lithium than do the austenitic grades.

Additional work is in progress to investigate the corrosion behavior of the extra-low-carbon grade alloys.

Metallic Elements in Sodium. Tests were initiated on several elements and alloys to determine their corrosion resistance to sodium at high temperatures. The sodium used was of commercial purity (99.95%) from Merck and Company. The first tests were made with the specimens in Armco-iron capsules, examination of which showed that Armco would not contain sodium as it had apparently leaked through the capsule bottom, sometime during the test period. Metallographic examination showed that these leaks possibly occurred as the result of reaction of sodium with the manganese sulfide stringers. Because of the uncertainty of the length of time the specimens had been exposed to the molten sodium, these tests were discarded.

A trial test was made using nickel for the capsule and it was found that this material would contain sodium barring any imperfect welds. Since this time, the tests in sodium have been in evacuated nickel capsules. Preliminary inspection, on the basis of weight change data only, indicates that nickel has good resistance and that cobalt, molybdenum, tantalum, Alloy N-155, inconel, and inconel X have fair resistance to sodium at 1000°C for 400 hr.

The stainless steels are also being studied extensively in the form of both flat stock and tubing exposed to sodium at high temperatures. The metallographic work on the stainless steel alloys has not been completed although data have been compiled on several special tests that have been run. Two samples of 304 stainless steel (18-8) flat stock, with an extra low carbon content (0.006%) were tested for 40 hr in sodium at 1000°C. Both had a high weight loss. A heavy precipitate was seen at the grain boundaries throughout the specimens and a new phase (possibly sigma) appeared in crystallographic planes as needles. The specimens seemed to be fairly heavily corroded although the attack did not appear selective. A dark, nonadherent, unidentified film formed on the specimens. The corrosion depth was 0.006 to 0.008 cm.

Two ferritic type 446 stainless steel samples with low carbon content (0.006%), flat stock, were also tested in nickel capsules for the same period and temperature. These samples also showed a precipitate both in the grain boundaries and within the grains, but in these it appeared very angular in shape; it also could be sigma. Some irregular corrosion which was also seen was confirmed by the small weight loss. The surface exposed to the sodium was rough and had a blue-gray compound adhering to it. The corrosion depth for type 446 was 0.002 to 0.005 cm.

Two tests were performed on stainless steel tubing filled with sodium. These were heated for 400 hr at 1000°C (1832°F). The sample of type 310 showed an extensive intergranular attack with large voids in the grain boundaries at the exposed surface. The matrix appeared to have complex carbides precipitated both in grain boundaries and along crystallographic planes. The sample of type 420 showed essentially no attack and the structure was that of a typical sample of 420 stainless steel.

In general the tests of stainless steels in sodium indicate a mild attack in comparison to similar tests conducted in lithium.

Compatibility tests were run for possible mass transfer between 316 stainless steel capsules and beryllium, niobium, molybdenum, and L-605 alloy specimens in liquid sodium at 1000°C for 40 hr. The results are incomplete, but essentially no attack was shown by the materials tested except extruded beryllium, which was uniformly attacked and had a general weight loss. Niobium and molybdenum both had films which were very thin and continuous but which have not yet been identified. Alloy L-605 was decarburized slightly but showed no other visible attack. It did show a slight weight gain.

Metals in Uranium-Aluminum Alloy. Some exploratory corrosion tests were run on a few selected pure metals in the hope of finding potential materials to contain molten uranium-aluminum alloy (2 atom % uranium by weight). The test temperature was 1000°C (1832°F) and the time at this temperature was 4 hr.

Tests were performed by immersing samples in the uranium-aluminum bath contained in a BeO crucible under a blanket of inert gas. Metals tested included titanium, iron, zirconium, columbium, and molybdenum. Results indicate that the above materials are not resistant and cannot be used to contain this uranium-bearing coolant at 1000°C.

Macrophotographs of the specimens after the test are shown in Fig. 8.1.

DYNAMIC CORROSION TESTING

Anton Brasiman

The current dynamic corrosion testing has been limited to experimentation on thermal convection loops. The work is being carried out by the ANP Experimental Engineering Group with metallurgical control and examination to be done by

NOT CLASSIFIED
PHOTO NO. Y-2625

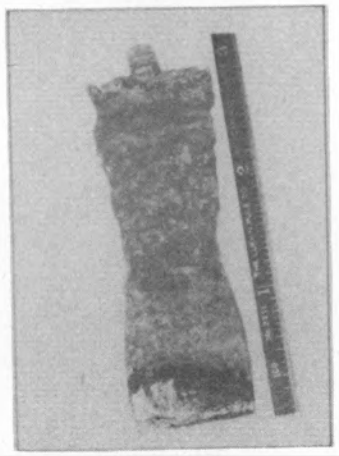

BERYLLIUM

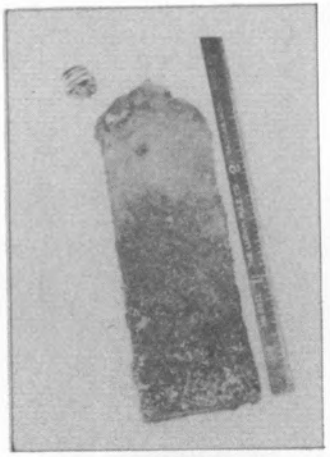

TITANIUM

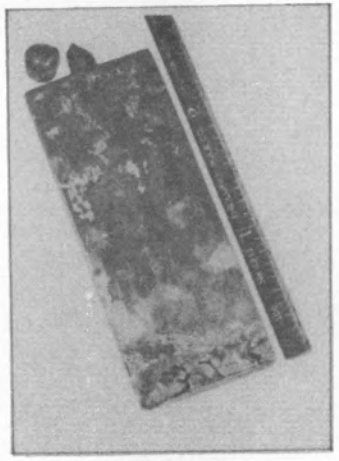

ZIRCONIUM

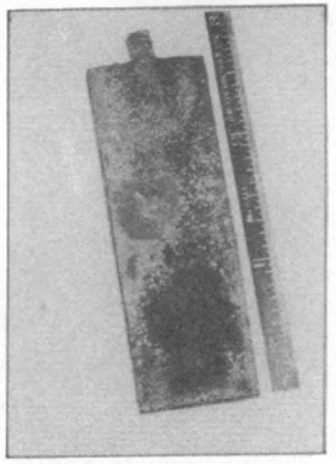

NIOBIUM (COLUMBIUM)

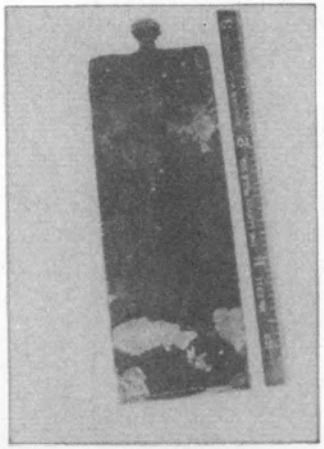

MOLYBDENUM

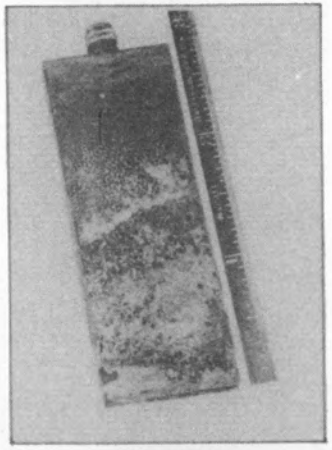

TANTALUM

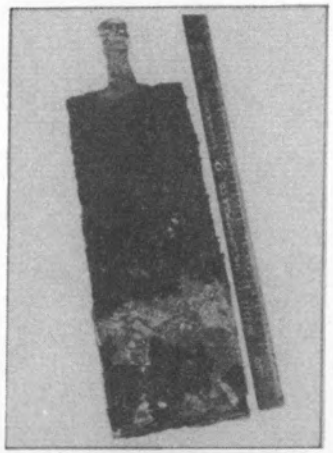

WOLFRAM (TUNGSTEN)

FIGURE 8.1 CORROSION SPECIMENS IN MOLTEN U-AL ALLOY FOUR HOURS AT 1000°C

the ANP Materials Group in the X-10 Metallurgy Division. No results are yet available although 19 loops are being, or have been, operated with sodium at Y-12. So far, no loops have been examined metallographically. More loops are on order.

Thermal Convection Loops. The loops are filled with filtered sodium and operated under a helium atmosphere at temperatures up to 1500°F for 1,000 hr or until failure occurs. At present, temperature differentials between 60 and 100°C are being obtained around the loops.

Immediately after the loops are filled a sample of sodium is taken for determination of oxygen. After the loop has been operated, a sample of sodium is taken from the top cup for determination of oxygen and samples are taken from the top and bottom cups for spectroscopic analyses for carbon and metallic corrosion products. From both the hot and cold zones of the loop metallographic specimens will be taken from the pipe and welds. These samples will be examined for corrosion and any evidence of a local build-up of corrosion products or film formation.

FUEL-ELEMENT FABRICATION

George Adamson

The equipment for the powder metallurgy laboratory is arriving and is being placed in operation. At the time of this writing it was thought that the second room for the laboratory would be available about December 15. The only major piece of equipment now missing is the molybdenum-wound furnace, which is not expected before February.

Some work has started on cold pressing and extrusion of fuel-element components. A series of pellets containing various concentrations of UO_2 and iron have been pressed and sintered. Photomicrographs show that continuous iron networks were obtained with 50 and 70% iron but not with 30%. In all cases the iron and UO_2 tend to agglomerate instead of forming a continuous thin network. The physical properties of these pellets have not yet been determined. Efforts are being made to obtain various sizes of UO_2 particles since all that are available are very fine, being of the order of 10 microns.

Using a 75-ton hydraulic press and makeshift dies, some extrusion work has been attempted. With carbonyl iron powder and a cellulose acetate binder, tubes of 1/8 in. diameter and 0.020-in. walls and containing 30% UO_2 were made. The tolerances were very poor but were all that could be expected with the dies available. A regular extrusion die for a ¼-in.-diameter tube with a 0.020-in. wall has been received from the shop and is being tested with iron powder.

Static Corrosion Tests. The high-temperature compatibility of the various materials now being considered for use in reactors is being examined. This information must be obtained before fuel-element design can advance beyond the preliminary stages. A "quick and dirty" investigation to guide in selection of materials is being made at ORNL, while a more complete long-term program is being launched by NEPA. For this work materials in forms immediately available were assembled in various combinations inside stainless steel tubes. These tubes were evacuated and sealed, swaged at approximately 1000°C to a 40% reduction in area, and then held at 1100°C for 100 hr to allow for diffusion or for reactions to take place. They were then cut and examined metallographically.

The results obtained with these combinations, summarized in the following table, are discussed below. In this discussion the penetration depths are measured from present surfaces since there is no means of determining the position of the original faces. The only stainless steel that has been tested is type 316.

	STAINLESS STEEL 316	Mo	Cb
UO_2	Moderate reaction	No reaction	Moderate reaction
BeO	No reaction	No reaction	Moderate reaction
Mo	Moderate reaction		Not finished
Cb	Moderate reaction	Not finished	
Be	Strong reaction	Not finished	Not finished

(1) *Stainless Steel—UO_2* (Fig. 8.2*a*). There is a reaction at the interface which involves both a general attack and preferential leaching. The preferential attack is shown by the stringers extending about 0.003 in. into the material. The dark spots in the stainless steel are carbides.

(2) *Stainless Steel—BeO.* There appears to be no reaction at this interface. The surface of the stainless steel did contain a considerable number of smooth indentations, but these are thought to be a result of folding during swaging. This conclusion is being confirmed with additional samples.

(3) *Stainless Steel—Molybdenum* (Fig. 8.2*b*). The molybdenum showed a recrystallized structure and in many samples had numerous small tears on the inner periphery adjoining the stainless steel. These are fabrication rather than corrosion defects. A third phase, which extended into both metals, was found in the intersection. Layer depths were of the order of 0.001 in. Some selective leaching is evident in the narrow stringers extending deeper into the steel. The number and depth of these stringers varied tremendously from sample to sample.

(4) *Stainless Steel—Beryllium* (Fig. 8.3*a*). The sample of this compact ruptured after 52 hr at 1100°C. On examination it was evident that an extensive reaction had taken place and that, quite likely, a molten or at least a plastic phase of some type had been present. A series of samples at 800, 900, 1000, and 1100°C was then run. The only one of this series that has been completed is the one at 800°C, which is shown in Fig. 8.3*a*. Even at this temperature considerable reaction had taken place. There is a continuous light diffusion zone of about 0.002 in. around the stainless steel, followed by another zone of indeterminate depth (estimated at 0.0005 in.) which dissolves during etching. The gap between the two phases also contains many broken particles of a reaction product.

(5) *Stainless Steel—Columbium* (Fig. 8.3*b*). The swaging resulted in considerably more deformation of the columbium rods than of the stainless steel matrix tube. A continuous reaction layer of about 0.001 in. is found in the interface. The surface of the stainless steel appears to have been etched quite evenly.

(6) *Molybdenum-UO_2.* Although it was enclosed in a stainless steel tube, the inner surface of the molybdenum was cracked considerably. There did not

[redacted] DRAWING NO. Y-2652

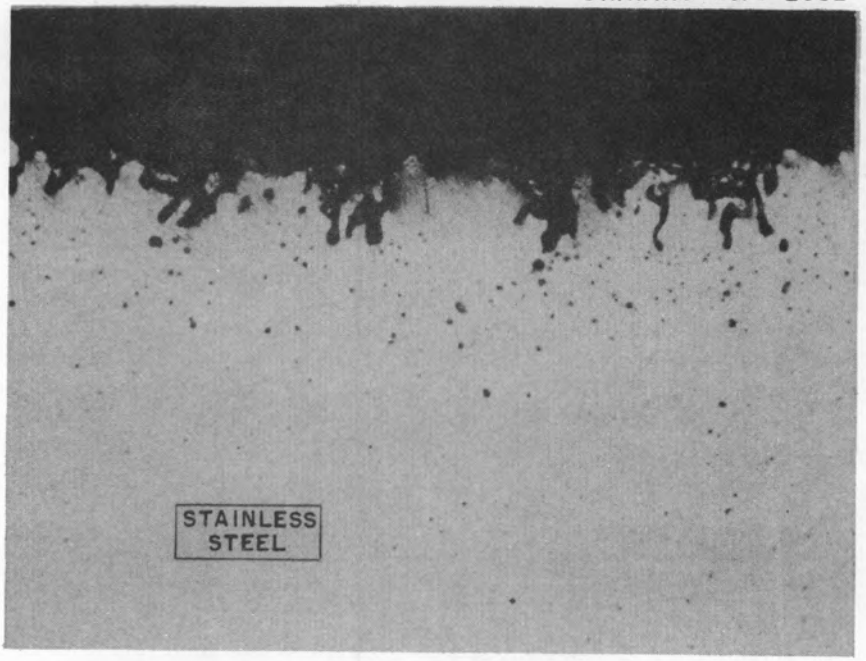

FIGURE a. STAINLESS STEEL & UO_2 HELD 100 HOURS AT 1100°C (mag 250X)

[redacted] DRAWING NO. Y-2519

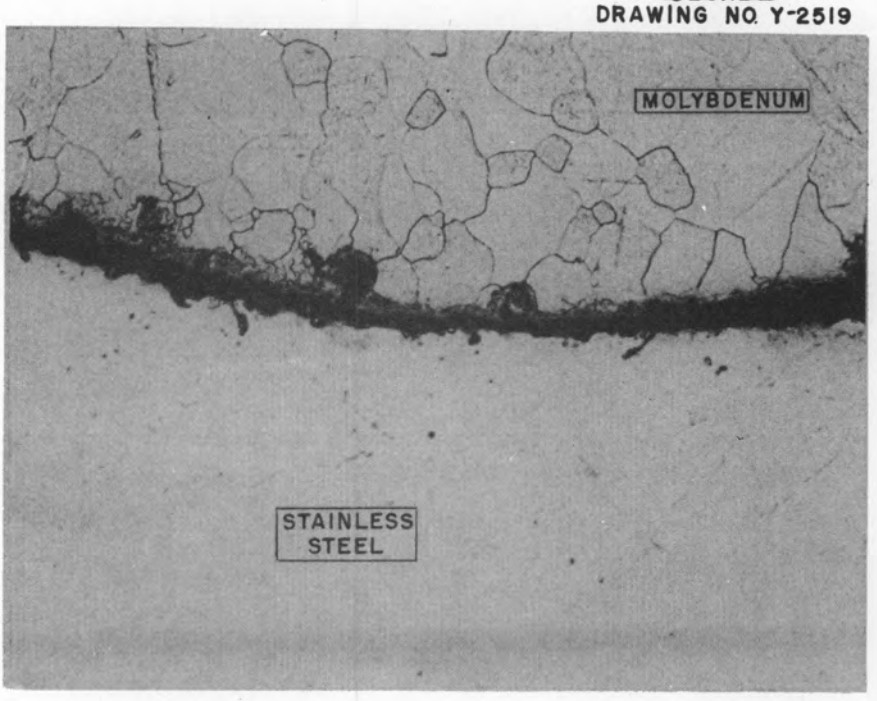

FIGURE b. STAINLESS & MOLYBDENUM HELD 100 HOURS AT 1100°C (mag 250X)

FIGURE 8.2

SECRET

DRAWING NO. Y-2695

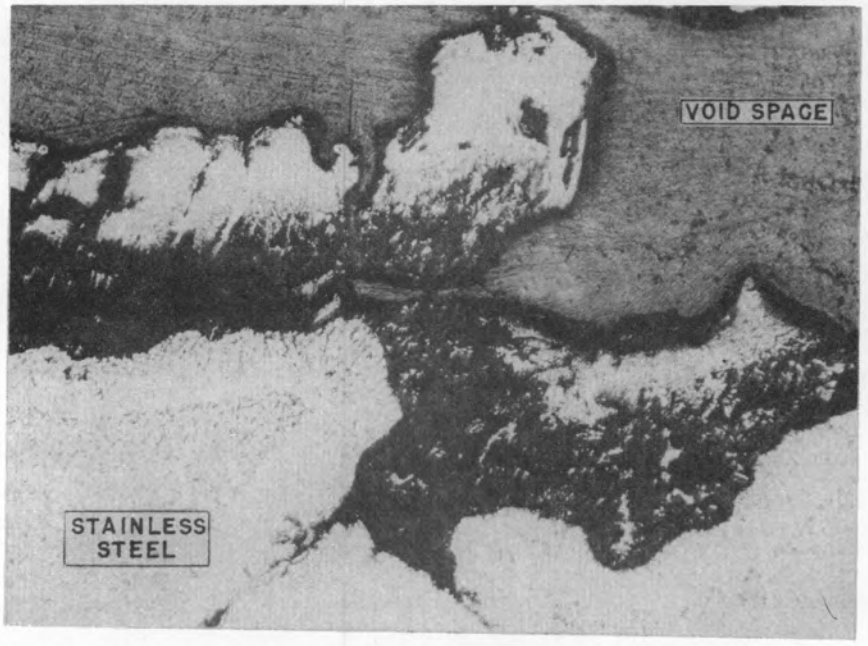

FIGURE a. STAINLESS STEEL & BERYLLIUM HELD 100 HOURS AT 800°C (mag. 250X)

SECRET

DRAWING NO Y-2522

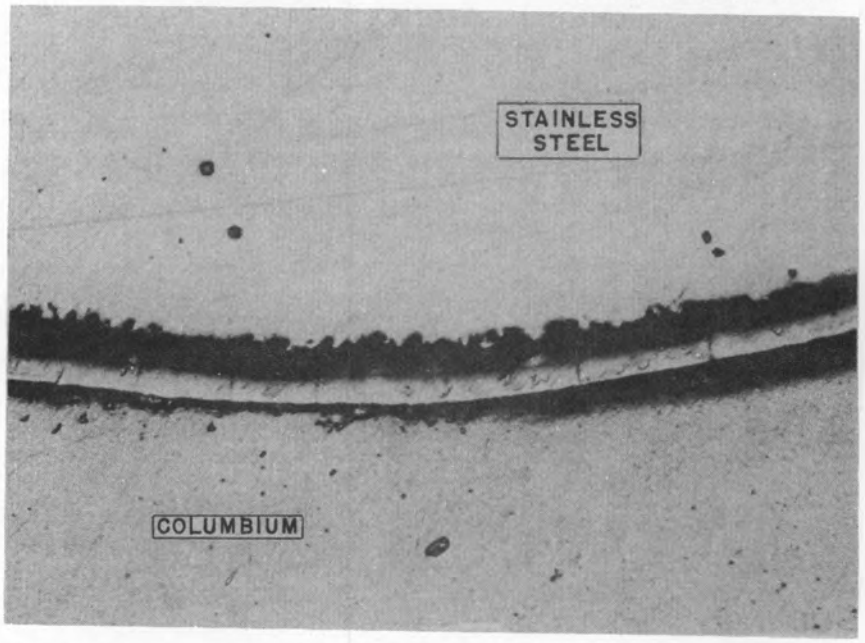

FIGURE b. STAINLESS STEEL & COLUMBIUM HELD 100 HOURS AT 1100°C (mag. 250X)

FIGURE 8.3

seem to be any reaction products or evidences of leaching present. This test will be repeated with a molybdenum rod to avoid breaking-up of the surface.

(7) *Molybdenum-BeO.* The surface of this sample, which was in the same tube as the one discussed above, was also broken but not so badly. There was no evidence of any reaction having taken place.

(8) *Columbium-UO_2* (Fig. 8.4). A reaction is evident on the columbium surface. The reaction products present are of the order of 0.001 in. but there is evidence that an additional layer has been removed in polishing. This is being investigated further.

(9) *Columbium-BeO.* The surface of this interface also shows a thin layer of reaction products. The appearance is identical with that in Fig. 8.4 but the thickness is 0.0005 in.

WELDING LABORATORY

P. Patriarca

Welding research to date has been confined to preliminary experiments, using the welders and existing facilities of the X-10 Research Shops pending the completion of a welding laboratory in the Metallurgy Division. A satisfactory technique for the welding of molybdenum has not yet been developed. Preliminary experiments on welding niobium are more promising. In addition, technical assistance is being supplied to the Dynamic Corrosion Testing group in the welded fabrication of convection loops.

Welding of Molybdenum. All welds were made manually and found to be brittle regardless of the welding process or welding conditions used. A massive copper jig was constructed which permitted a steep thermal gradient during welding in order to minimize recrystallization, this being one of the factors believed to be responsible for the brittleness of molybdenum welds. Ample inert-gas shielding was also provided by the jig by supplementing inert gas flow from the welding torch with a separate inert gas cover of the work within the copper welding jig. Both direct-current straight polarity and alternating current were used with the tungsten-arc process under commercial helium and argon as a shielding gas. Direct-current straight polarity was

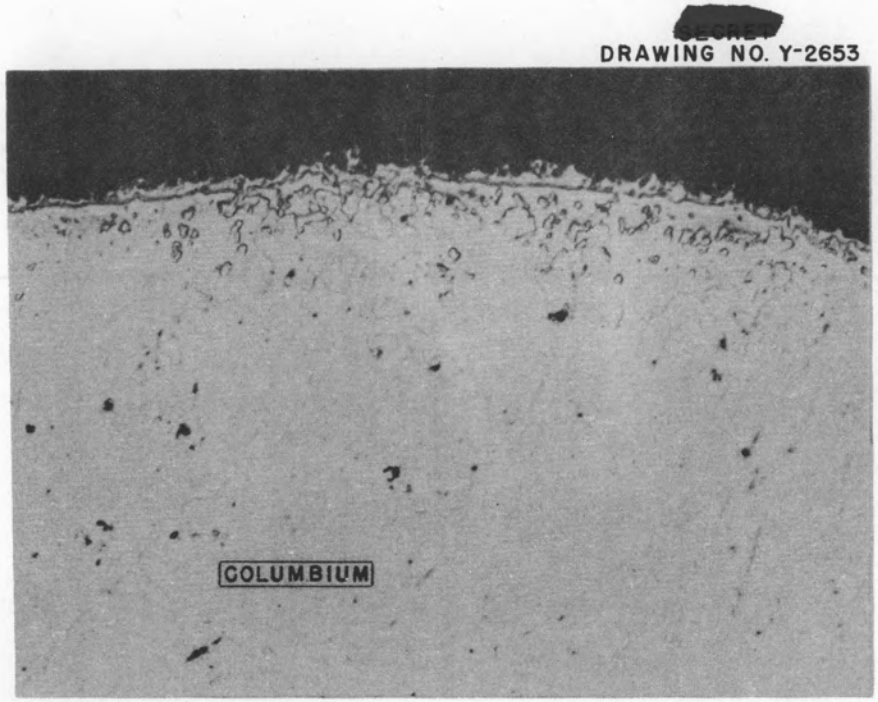

FIGURE 8.4 COLUMBIUM & UO_2 HELD 100 HOURS AT 1000°C
(mag 250 X)

found to provide better control of the weld bead. Atomic-hydrogen welding was also attempted. All welds were edge welds using Fansteel molybdenum sheet 0.020 in. thick. Recent research indicates that present grades of molybdenum must be improved by further purification or by minor alloy additions to render them weldable. Future experiments are contemplated using Climax arc-cast molybdenum and available grades of molybdenum alloyed with minor additions. It is hoped that near-ideal welding conditions can be achieved by conducting future experiments within the confines of an inert-gas-purged dry box.

Welding of Niobium. Preliminary experiments indicate that welding of niobium will not present so imposing a problem as does joining of molybdenum. Welds have been made which demonstrate some ductility. Edge welds made using inert-arc alternating current and inert-arc direct-current straight polarity, using argon and helium, respectively, as inert-gas shields, were relatively strong and ductile as indicated by manual cyclic bend tests.

Fabrication of Thermal Convection Loop. Technical assistance is being supplied to the Liquid Metals Dynamic Corrosion Group in the form of supervision of welded fabrication of all future loops. Written welding specifications and schedules will be set forth on each thermal convection loop and will include specific instructions on edge preparation of component parts, welding sequence, and welding conditions to be used. It is believed that this quality control will minimize premature convection loop failures.

CREEP-RUPTURE LABORATORY

R. E. Oliver

Eight Baldwin lever-arm machines and two Baldwin screw type stress-rupture machines have been received and erected. Six additional lever-arm machines have been designed and are in the process of construction. Sixteen Leeds and Northrup Speedomax-DAT recorder-controller units have been received and installed, and one 56-point precision indicator and one 12-point recorder have been received and installed. Delivery of the power distribution equipment is expected by the middle of December. A 20-kw gasoline driven emergency power plant has been ordered and should be installed by February. The chambers for testing in vacuum or in inert atmosphere have been designed, and production of

these chambers and their accompanying furnaces will be started in the near future.

Since most of the metal going into the reactor and its auxiliaries will be in the form of pipe and tubing, attempts are being made to devise a creep-rupture test for such shapes. Tests will be performed over the range of temperatures expected in service and in the several environments chosen for the conventional creep-rupture tests. It is hoped that a method can be devised to measure the tubing creep, both radially and longitudinally.

The overall ANP Creep-Rupture program will test pipes and tubing in the temperature range from about 600 to 1000°C in air, in liquid metals, and in inert atmospheres. These data will not only indicate possible design stresses but will also give information on stress corrosion in liquid metals and oxidizing atmospheres. The initial effort will be with the austenitic stainless steels with subsequent efforts being indicated by the interim ANP materials studies.

9. RADIATION DAMAGE

9. RADIATION DAMAGE

D. S. Billington, Institute for Solid Studies, Metallurgy Division

Radiation damage experiments are underway at a number of installations. The Y-12 cyclotron is being adapted for such work, and targets are now being constructed. Both stationary and rotating targets are being developed, and initial measurements of creep and resistivity under bombardment will be made. The lithium-iron corrosion experiments in the Berkeley cyclotron will substitute Globe iron for Armco. The Purdue University cyclotron group is preparing to run creep experiments.

Initial experiments on various metals have indicated no significant changes in shape, electrical resistivity, permeability, or hardness after an exposure to a neutron flux of 1.2×10^{12} and while at 400 to 500°F and 1000 psi. In-pile creep tests will be performed on a cantilever type apparatus because of its reliability. Operational techniques with this apparatus are now being perfected.

Y-12 CYCLOTRON EXPERIMENTS

R. S. Livingston, Electromagnetic Research Laboratory

The construction of targets and the adaptation of the 86-in. cyclotron at Y-12 for radiation damage work is well underway. Modifications consist, in the main, of a vacuum lock and handling equipment for the targets. Consideration has also been given to changing the resonance frequency and magnetic field so that low-energy protons of 10 to 15 Mev can be obtained at a larger radius. Initial plans, however, call for using the cyclotron as it is presently operating.

The basic design for the targets consists essentially of two concentric tubes through which a cooling (or heating) fluid is passed (Fig. 9.1). With a large flow of liquid through the system, small variation in beam intensity

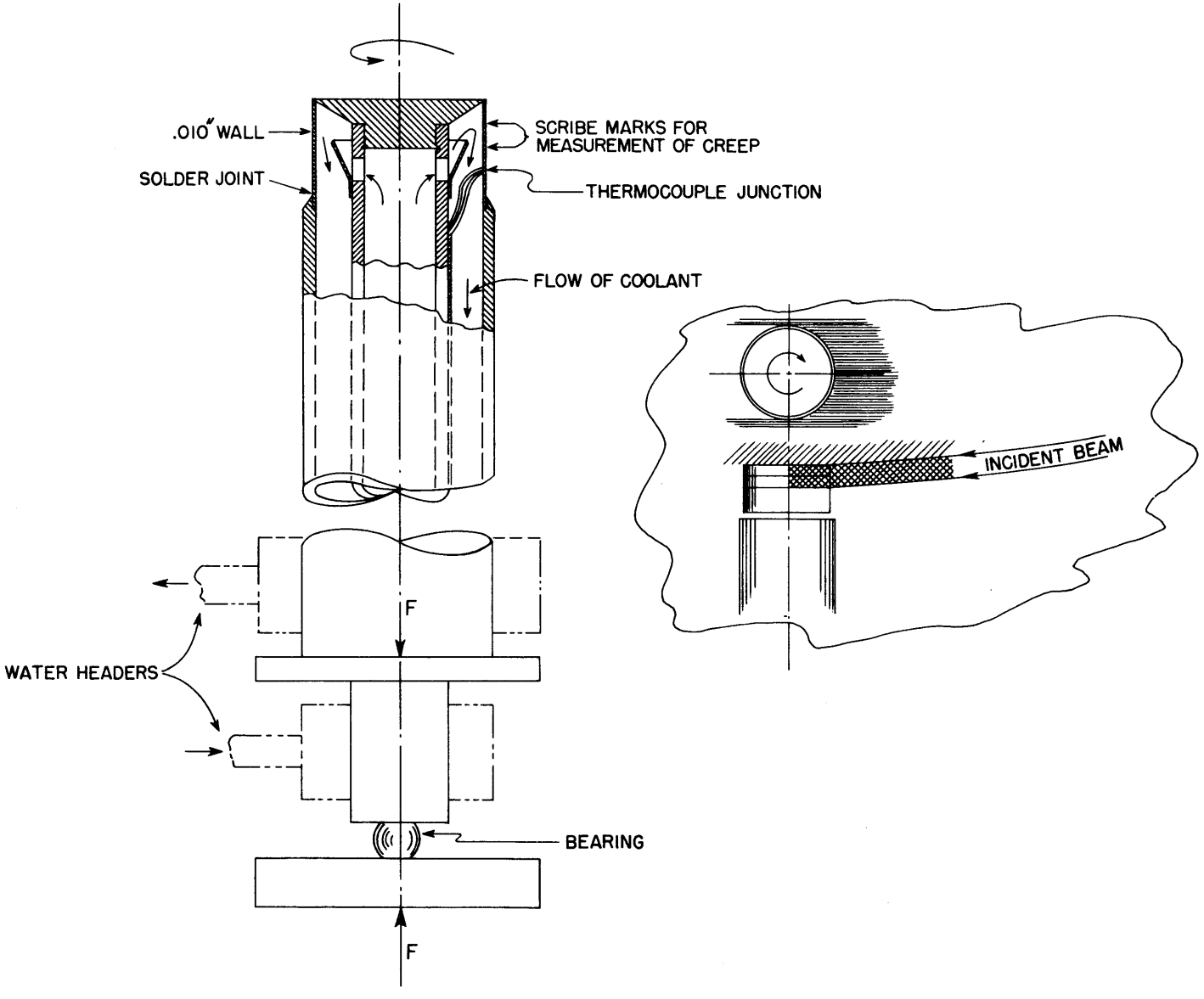

FIGURE 9.1 ROTATING TARGET

DRAWING NO. 10211

is not expected to affect the target temperature seriously. When running at high temperatures and using liquid metals to heat the target, the power input of the beam is small compared to the power used in the fluid. Rotation of the target is achieved by turning the entire assembly through a vacuum seal. The rotation ensures uniform exposure of the target material to the beam.

Controlled stresses must be applied to the target so that creep of the material under bombardment can be measured. The inner "squirt" tube provides not only a path for coolant flow, but also transmits a force which keeps the target area under tension. Creep which may occur under these conditions is determined by marking the target in two places around the circumference. Pictures will be taken of these targets and shown on a calibrated screen. Thermocouples will probably be used for temperature measurements.

In cases in which water-cooled targets are used, the assembly will look essentially the same as that in Fig. 9.1. The water-cooled type of target is under construction; the liquid-metal target is in the design stage. Figure 9.2 illustrates a stationary target to be used for exploration work in the initial stages.

IN PILE CREEP

Data obtained from the creep of a cantilever beam of type 316 stainless steel at 1050°F under a stress of 4000 psi show at least a transient increase in creep rate upon subjecting a creeping specimen to neutron bombardment in the ORNL reactor.

The tensile creep apparatus described earlier[1] proved erratic, mainly because of pulley friction difficulties, and, furthermore, its removal from the pile was hazardous. The cantilever creep test is not commonly used, but

(1) *Aircraft Nuclear Propulsion Project Quarterly Progress Report for Period Ending May 31, 1950*, ORNL-768, p. 96 (Aug. 14, 1950).

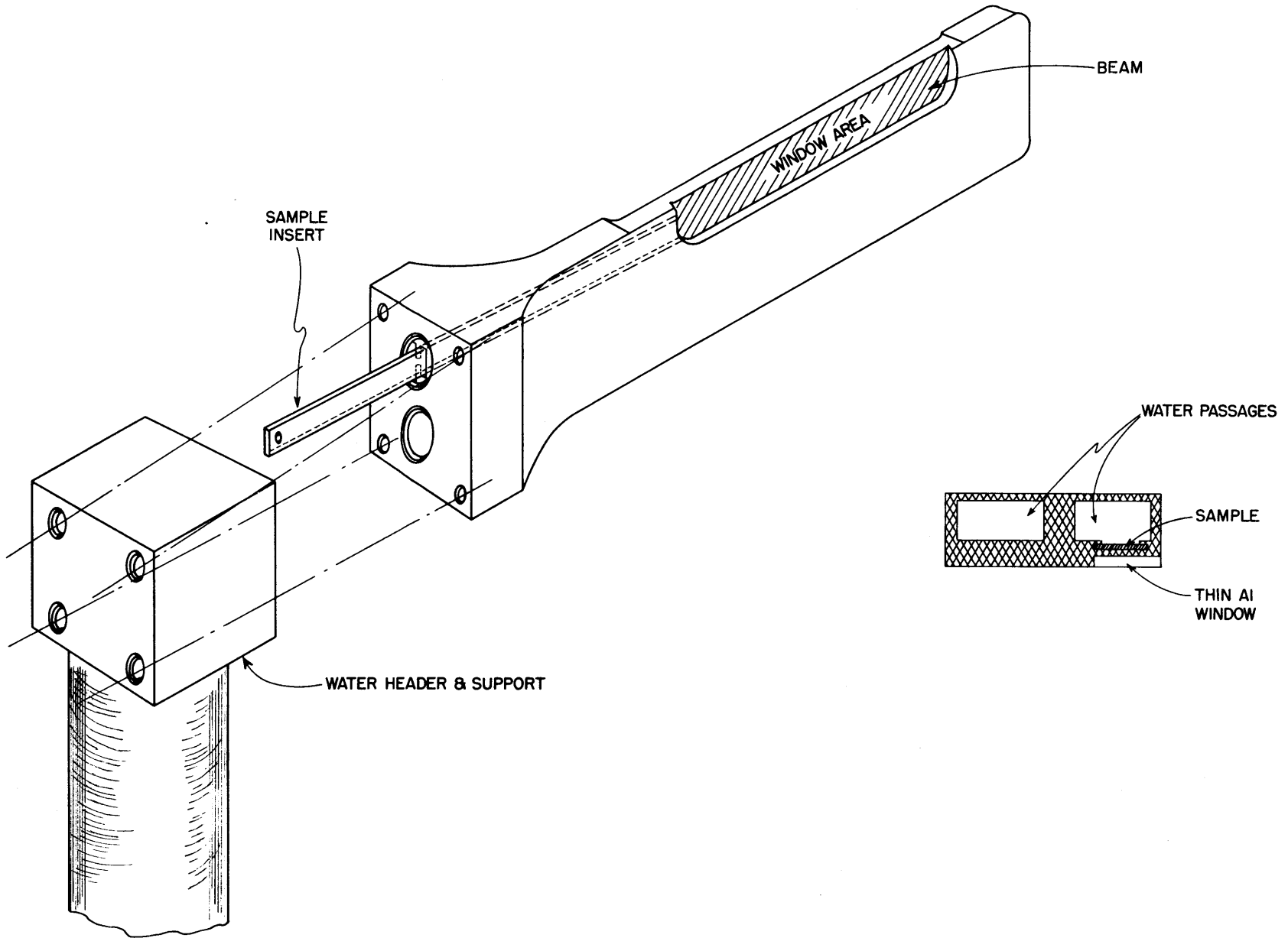

FIGURE 9.2 STATIONARY TARGET

DRAWING NO. 10212

since some correlation between tensile and cantilever creep is possible,[2] it may be used for the determination of tensile creep. From the standpoint of ease of construction and operation the cantilever has much to recommend it for in-pile operation. A very small weight is all that is required for stressing to any reasonable stress level so that only electrical leads need be run to the apparatus in the pile. The strains are magnified mechanically by the long lever arm carrying the weight; furthermore, the effect of temperature on the apparatus (other than the effect on intrinsic creep behavior) is much smaller than for a conventional tensile creep test.

Figure 9.3 shows a partially assembled and unwired apparatus of the type used in these experiments. Supported on a long aluminum base plate are the test specimen with the furnace windings in place, the weight on the end of the beam, and the microformer for the measurement of displacements of the end of the beam. In the foreground are an unmounted specimen, two lavite furnace supports, and the concentric nickel-foil radiation shields which surround the specimen upon assembly. The specimen, its support on the base plate, and the loading beam are integral. The gauge length (approximately ¾ in.) is the reduced portion extending between the loading beam and the support. The furnace windings are nichrome wound around lavite spacers and through ceramic tubes. The furnace is composed of three separate windings to facilitate removal of temperature gradients across the gauge length. Thermocouples are welded directly to sides of the test bar at three points. Figure 9.4 shows the apparatus itself and an outer furnace tube (controlled temperature) to keep the microformer at constant temperature. Control of this temperature also aids in the control of the test bar temperature by its separate controller. This outer furnace is wrapped with aluminum foil and inserted in the rectangular can for insertion in one of the stringer holes in the ORNL reactor.

The apparatus was charged during an extended pile shutdown. Difficulties in removing the temperature gradient across the bar and burnout of one of the furnace sections prevented operation at the anticipated temperature (1500°F) and caused large temperature gradients across one end of the bar. A deflection (strain) time curve plotted from the data showed an increase in strain rate immediately (within 30 sec) upon starting up the pile (to 4400 kw, fast flux approximately 4×10^{10}). The deflection rate for the half hour after the

(2) Harris, G. T., and Child, H. C., "Creep Testing by the Cantilever-bending Method," *J. Iron Steel Inst.* 165, 139 (1950).

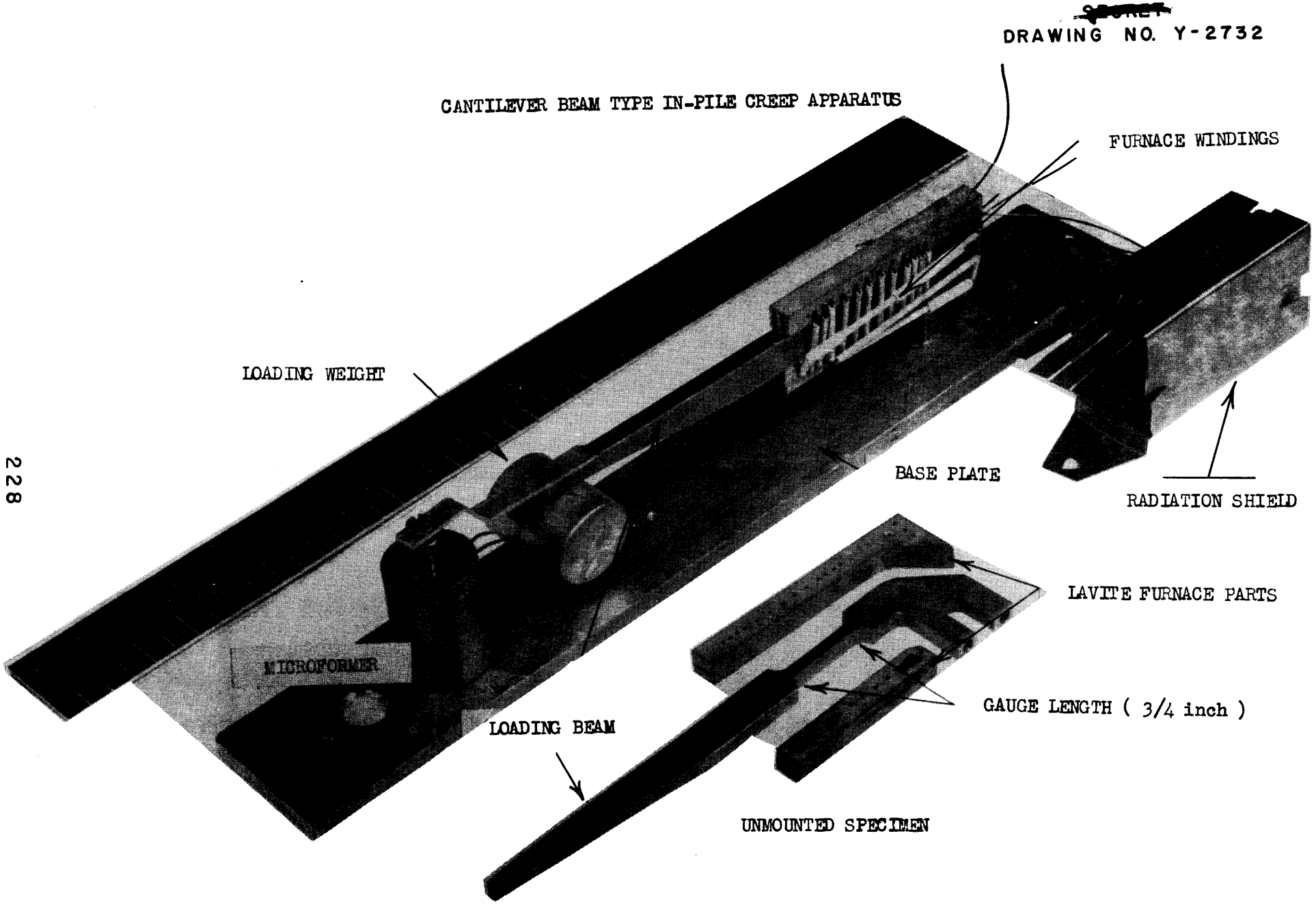
DRAWING NO. Y-2732
CANTILEVER BEAM TYPE IN-PILE CREEP APPARATUS
FURNACE WINDINGS
LOADING WEIGHT
BASE PLATE
RADIATION SHIELD
LAVITE FURNACE PARTS
MICROFORMER
GAUGE LENGTH (3/4 inch)
LOADING BEAM
UNMOUNTED SPECIMEN

FIGURE 9.3

SECRET
DRAWING NO. Y-2731

CANTILEVER BEAM TYPE IN-PILE CREEP APPARATUS

(WITH FURNACE)

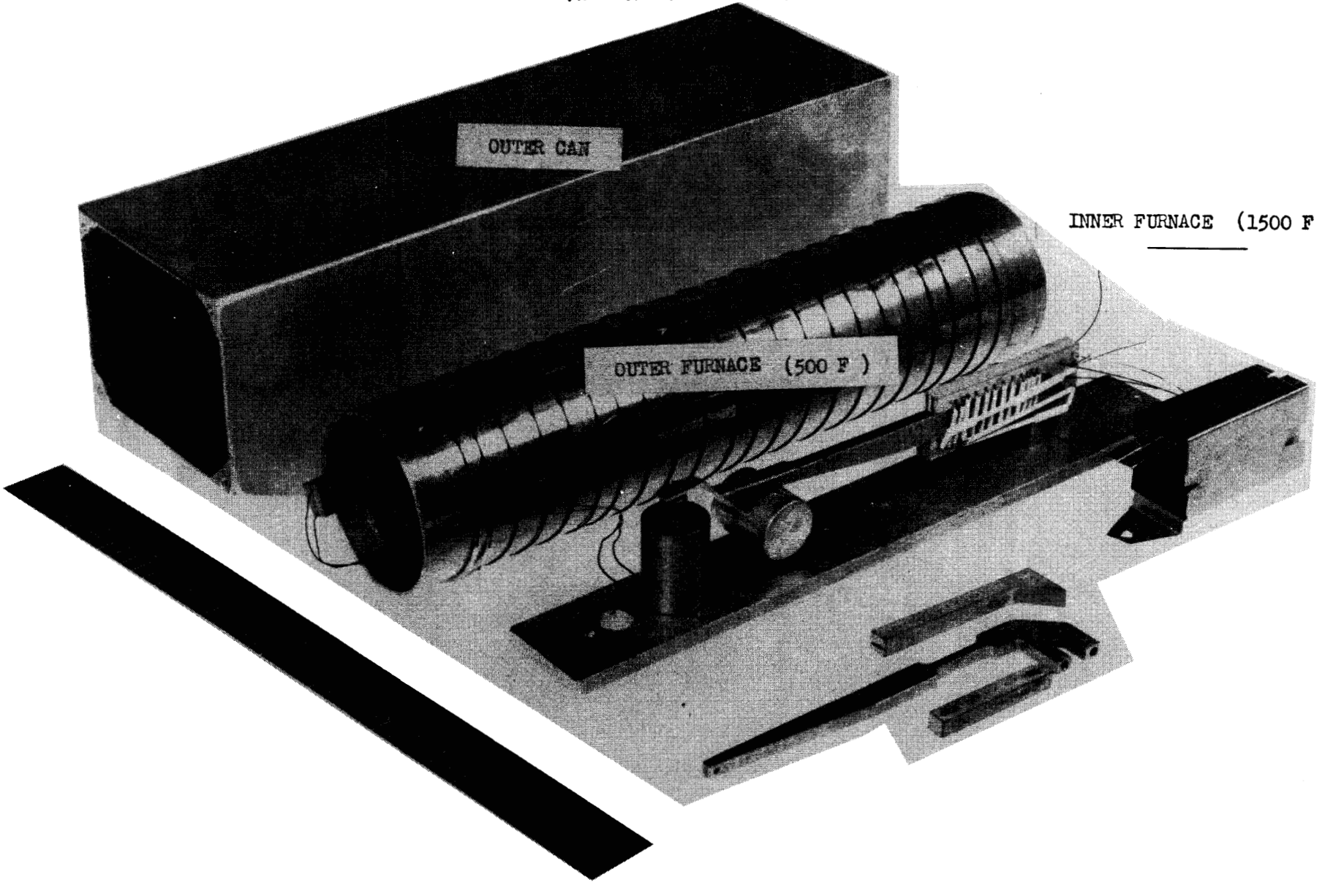

FIGURE 9.4

pile was started was approximately five times the rate in the half hour preceding (pile off). The temperature gradient across the bar and the present lack of correlation between tensile and cantilever creep preclude any quantitative conclusions.

Although the deflection rate fell off with time, subsequent transient increases in deflection rate were again observed upon applying the flux after each pile shutdown during the following week.

Inasmuch as the stress was applied to the specimen all during the heating cycle from pile ambient temperature to operating temperature, and because the amount of time at constant temperature before the pile was operating was short, the state of the metal (whether in so-called "first" or "second" stage of creep) cannot be described with any accuracy.

There is a possibility that the changes in the deflection rate when the pile is started are being caused by gamma or neutron heating of the specimen. However, the behavior of the controllers and the chart record of the temperature indicate no appreciable heating here. The controller on the outer furnace (although unrecorded) and the controller on the inner furnace showed no abnormal variations at the time of pile start-up. The chart on the controller for the inside furnace was unaffected by pile start-up. Separate temperature measurements at three points on the bar showed variations of less than 2°F during the period covered by the measurements described above. The Duration Adjusting type control unit used is very sensitive to temperature variations, and rates of variation, if any existed, would in all probability show up on the chart as changes in the on-off cycle, provided their magnitude was greater than 2°F.

The data obtained are only qualitative to date, and such variations in rate might not be nearly so marked in tensile creep tests. Some theoretical calculations by F. R. N. Nabarro[3] predict that the greatest effect of neutron bombardment on creep rate will occur when there is a stress gradient in the specimen. Of course, the stress gradients in the cantilever test are greater than would be expected in pure tension of a polycrystalline metal. However, most engineering structures have many points of complex stress distribution where gradients exist, so the observations reported above are not

(3) Nabarro, F. R. N., *Report on a Conference on Strength of Solids Held at the H. H. Wills Physical Laboratory, University of Bristol, on 7-9 July 1947*, p. 85, Physical Society, 1948.

without value.

At present a number of bench test rigs are being built to obtain comparative data under conditions free from radiation. The apparatus is being improved to make possible loading of the beam at any time while in the pile and to permit extended operation at 1500°F and higher. Also being investigated are various forms of strain measuring devices, since microformers would be difficult to cool under the conditions of high radiation heating that might be encountered in the MTR.

CORROSION EXPERIMENT OF NORTH AMERICAN AVIATION, INC.*

This group is continuing the lithium–Armco iron accelerator corrosion experiments proposed in the last quarterly report.[4] Plans have been made calling for one or two completed irradiations by January, 1951. It has been decided to substitute Globe iron for Armco because of inherent fabrication difficulties when using thin-walled Armco.

The analyses of Armco and Globe iron are as follows:

ELEMENT	GLOBE IRON	ARMCO IRON
C	0.03	0.015
Mn	0.24	0.035
P	0.015	0.005
S	0.025	0.025
Si	0.01	0.003

The NAA group is also extending their work to include accelerator corrosion experiments with stainless steel and sodium. It is thought that this work can proceed rapidly as there should not be the fabrication difficulties encountered with the Armco iron.

CREEP EXPERIMENTS OF PURDUE UNIVERSITY

The Purdue University group is setting up creep experiments to be run on the Purdue cyclotron. The first materials to be studied will be stainless steel types 316 and 347 and molybdenum.

(4) *Aircraft Nuclear Propulsion Project Quarterly Progress Report for Period Ending August 31, 1950*, ORNL-858, p. 86 (Dec. 4, 1950).

* See also Section 12 of this report, "Vapor-cycle Reactors," where other corrosion experimentation of North American Aviation is discussed.

Much of the preliminary work involving the metallography of molybdenum and the construction of furnaces has been completed. In addition an a-c Hall-coefficient apparatus has been designed.

PROPERTIES OF METALS

The Radiation Damage Group has completed some measurements of samples of stainless steel types 304, 309, 316, and 347, nickel "A," and hastelloy C done in conjunction with the ANL—Naval Reactor Program. The samples were exposed at ORNL for a nvt of 1.2×10^{19} (flux 1.2×10^{12}) at 400 to 500°F and a pressure of 1000 psi. Samples were above 400°F for four months. *Before and after measurements of the electrical resistivity, dimensional stability, magnetic permeability, and hardness showed no significant changes.*

OTHER ACTIVITIES

The Radiation Damage Group is actively studying the problem of conducting experiments in the MTR. The gamma-ray flux is so high that considerable heating will apparently take place in all uncooled samples. The problem of conducting suitable experiments under this condition is not a simple one. Plans have been made for activation of the Thermal Conductivity Group by Jan. 1, 1951.

The samples being exposed at Hanford in the ANL—Naval Reactor test loop will be discharged in January, according to the latest estimate.

10. CHEMISTRY OF LIQUID FUELS

10. CHEMISTRY OF LIQUID FUELS

W. R. Grimes, Materials Chemistry Division

A previous report[1] has discussed some of the general characteristics of liquid-fuel systems and has described the preliminary phases of the research program designed to produce satisfactory liquids. During the past quarter, interest in such liquid fuels has increased materially. Two types of liquid fuels, suspensions of uranium compounds in sodium hydroxide and solutions of UF_4 in alkali and alkaline earth fluorides, have been under intensive study. It is possible at this time to view with optimism the prospect of such a fuel in the reasonably near future; it is true, however, that it is not possible at this time to state the composition of a liquid which will prove suitable.

It has been demonstrated that all uranium materials tested to date react rapidly with sodium hydroxide to form a finely divided material which is almost certainly sodium uranate. Late in the period a satisfactory method for evaluation of the suspensions in terms of settling rate has been established. Studies designed to improve the stability of these suspensions are currently underway.

The equilibrium diagram of the system LiF-UF_4 has been established by thermal analysis techniques, and study of the ternary systems NaF-BeF_2-UF_4, NaF-KF-UF_4, and NaF-LiF-UF_4 is well underway. Of these the NaF-BeF_2-UF_4 system appears the most promising in so far as low melting point and reasonable uranium content are concerned. It must be emphasized, however, that a great deal of effort is still required before these systems are established sufficiently to be recommended for use.

Concurrently, the corrosion of metal immersed in NaF-UF_4 and LiF-UF_4 eutectics has been examined. There is considerable correlation in the corrosive properties of these eutectics, molybdenum, inconel, and hastalloy C (in that order) being the least corroded in the lithium eutectic, and hastelloy C, inconel, and molybdenum the least corroded in the sodium. All other of the many metals under study were far inferior. A test was performed to determine which, and to what extent, fission products react with the proposed eutectic.

(1) "Chemistry of Liquid Fuel Systems," *The Aircraft Nuclear Propulsion Project Quarterly Progress Report for Period Ending August 31, 1950*, ORNL-858, p. 104 (Dec. 4, 1950).

SUSPENSIONS OF URANIUM COMPOUNDS IN SODIUM HYDROXIDE

J. D. Redman D. E. Nicholson
L. G. Overholser

Uranium compounds are not appreciably soluble in sodium hydroxide.[2] It has, however, been established that uranium compounds react with sodium hydroxide to produce finely divided materials. The prime objective of this study is to establish those conditions which will produce a suspension of maximum stability in the temperature range 600 to 900°C. The work to date has been concerned primarily with attempts to determine the stability of these suspensions and the identity of the compound or compounds present.

Preliminary Observation of the Suspensions. Suspensions containing 4 to 5% uranium were prepared from various uranium compounds by adding the uranium compound to sodium hydroxide contained in a silver crucible at 700°C. The suspensions were held at 700°C for 30 min, poured into platinum dishes, and allowed to solidify. The button was removed and portions of the material were examined microscopically. The following compounds were used: ammonium uranyl pentafluoride, uranyl nitrate, uranyl acetate, uranyl formate, uranyl tartrate, uranyl pyrophosphate, sodium peruranate, peruranic acid, ammonium diuranate, potassium diuranate, sodium diuranate, and uranium trioxide (commercial product and specially prepared samples from ammonium diuranate and peruranic acid). Suspensions were also prepared from uranium metal by heating with sodium hydroxide at 500°C in an atmosphere of nitrogen. Uranous chloride and uranous fluoride were similarly treated at 500°C.

An evaluation of these different suspensions, based on very rough settling rate observations and approximate particle size determinations by observation with the microscope, indicated that the suspensions prepared from uranium trioxide and those from uranium metal were probably superior to any of the others; the average particle size in these preparations was approximately 2 microns. Actually, none of the suspensions examined had an average particle size much greater than 10 microns and the majority of them appeared to have about equal particle size. The specially prepared uranium trioxides yielded suspensions comparable to those obtained from the commercial uranium trioxide, indicating that the original particle size is not the most important factor involved in preparing these suspensions.

(2) ORNL-858, *op. cit.*, p. 107.

By the same technique it was demonstrated that use of carbonate-free NaOH, mixtures of Na_2CO_3 and NaOH, and KOH did not yield suspensions which were superior to those described. Mixtures of Na_2O_2 and NaOH yielded suspensions which had definitely larger particles.

A few experiments were performed in which the suspensions were held at 700°C for 24 hr or longer to ascertain whether such treatment promotes growth of the particles. Evidence was found suggesting that such growth does occur on prolonged heating, but the microscopic examination of these materials was complicated by the silver oxide present.

Settling Rate Measurements. Although the microscopic examinations proved useful in the preliminary work, the evaluation of the suspensions by measuring the settling rate appeared to be of more practical value than the approximate particle size determination based upon microscopic examination. Consequently, studies were made using various techniques for measuring the settling rate of the suspensions.

The first method that afforded any degree of success made use of a stainless steel nipple (1 in. I.D. and 3 to 4 in. in length) provided with a cap having a poured silver disk in the bottom to afford a seal against sodium hydroxide. The nipple, with the cap in place, was loaded with 20 g of sodium hydroxide and heated to 700°C before addition of approximately 1 g of the uranium compound. The suspension was heated at 700°C with frequent stirring for 30 min, removed from the furnace, and air cooled (about 10 min was required for the sample to freeze). The cap was removed from the nipple, and the sodium hydroxide plug was driven out. Samples were cut off the plug by use of a hot copper blade. Analyses of sections of the plug for uranium yielded data, of which those shown in Table 10.1 are representative.

These results confirm the earlier observation that the uranium trioxide suspensions are the most stable of any studied and also show rather conclusively that growth of the particles occurs upon aging for 24 hr at 700°C.

Although this method was capable of measuring relative settling rates, it was not so flexible as desired and might be subject to serious error arising from convection currents. Further studies by this method were, therefore, abandoned upon delivery of a silver reactor. The apparatus being used at

TABLE 10.1

Settling Rates of Uranium Suspension Measured in Stainless Steel Nipples

COMPOUND ADDED TO NaOH	PERCENT OF COMPOUND FOUND	
	TOP	BOTTOM
UO_3	4.1	4.7
UO_3	4.2	4.5
UO_3	1.3*	6.2*
UO_3	2.8*	6.0*
U_3O_8	1.7	6.8
U_3O_8	3.9	7.1
U_3O_8	2.9	6.7
U_3O_8	3.2	6.1
$Na_2U_2O_7$	3.0	5.3
$Na_2U_2O_7$	2.0	6.5
$(UO_2)_2P_2O_7$	2.0	6.7
$(UO_2)_2P_2O_7$	3.4	4.5
$(UO_2)_2P_2O_7$	3.5	4.0
$(UO_2)_2P_2O_7$	3.3	4.1
$(UO_2)_2P_2O_7$	1.6	4.1

* Digested for 24 hr at 700°C (no agitation).

present for determining relative settling rates is shown in Fig. 10.1. In using this apparatus the temperature is raised to 700°C, 180 g of sodium hydroxide is added, and, after all water is removed, the uranium compound is carefully added and the suspension is agitated by stirring for the desired length of time. After this time has elapsed, the stirrer is cut off and samples are removed after various intervals of time by inserting a silver rod through a hole in the cover. The silver rods are collared to sample the upper one-fourth of the molten sodium hydroxide. After the silver rods are cooled

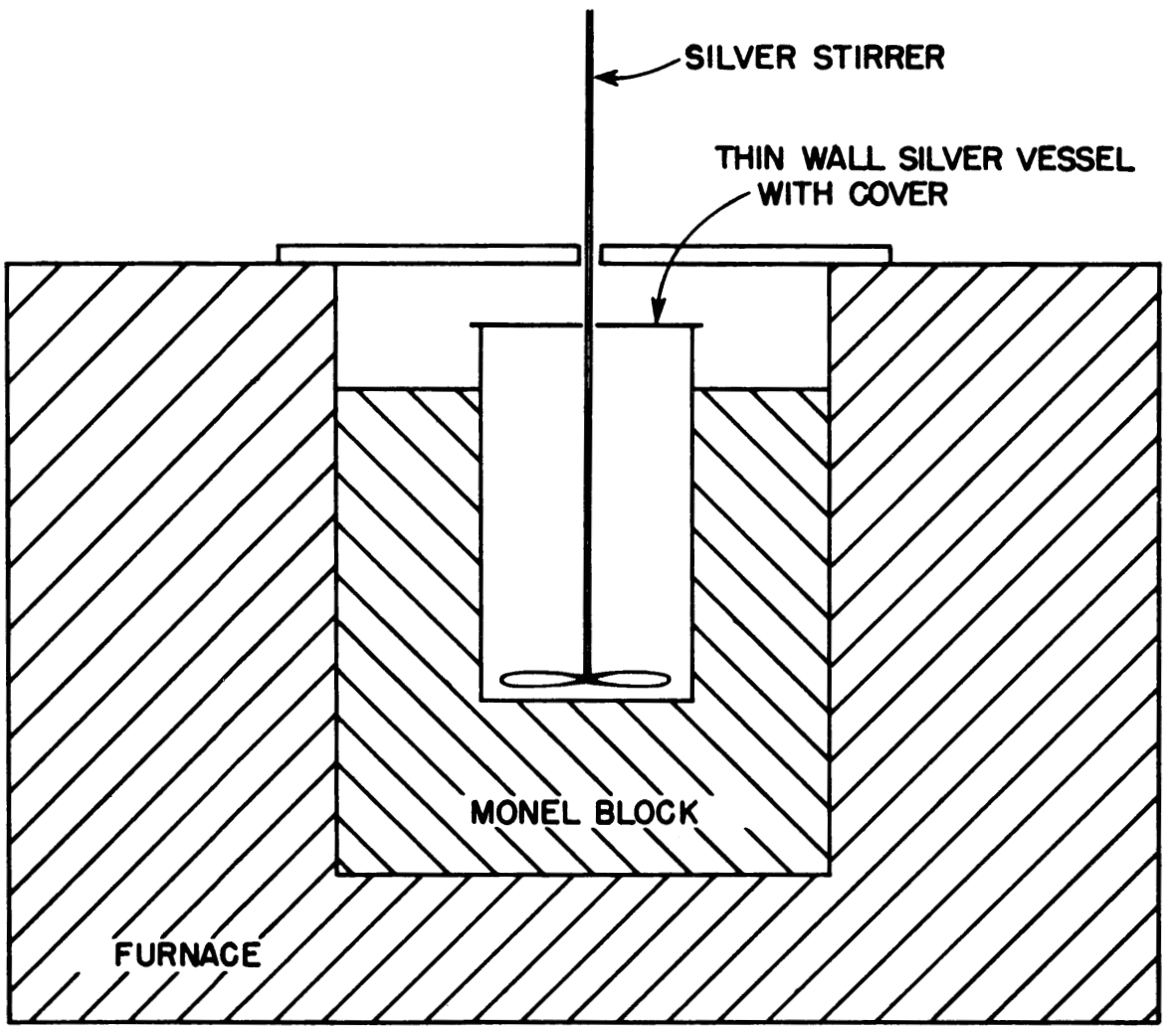

APPARATUS FOR STUDYING URANIUM
SUSPENDED IN MOLTEN SODIUM HYDROXIDE
FIGURE 10.1

DRAWING NO. 10213

and weighed, the uranium is dissolved and the solution is analyzed for uranium. By this method the system may be digested with agitation for any desired period and may be sampled with a minimum of error due to convection currents in the liquid (Table 10.2).

TABLE 10.2

Settling Rates of Uranium Suspensions Measured in the Silver Reactor

SETTLING TIME (min)	DIGESTION TIME, 700°C (hr)	PERCENT OF COMPOUND FOUND		
		UO_3	$Na_2U_2O_7$	$(UO_2)_2P_2O_7$
1	¼	2.4	0.2	0.3
2	¼	1.7		0.1
3	¼	1.6	0.09	0.2
4	¼	0.5	0.04	0.2
5	¼	0.4	0.09	0.2
10	¼	0.2	0.04	
1	1½	3.1	0.08	0.4
2	1½	2.2	0.06	0.3
3	1½	1.3	0.04	0.2
4	1½	0.4	0.04	0.4
5	1½	0.3	0.07	0.4
10	1½	0.2	0.03	
0	4	3.6	2.6	
1	4	2.3		0.2
2	4	1.2		
3	4	1.0		
4	4	0.5		
5	4	0.4		

The results agree with those obtained by use of the steel nipples inasmuch as they show that the uranium trioxide suspensions settle less rapidly than those prepared from the diuranate or pyrophosphate. However, it will be

noted that the settling rate for the uranium trioxide suspensions measured in the silver reactor is greater than that observed by the nipple method. For the best suspension studied in the silver reactor, the upper one-fourth of the molten sodium hydroxide is virtually free of uranium after 3 to 4 min as contrasted to the relatively uniform distribution found in the nipples after 10 min. This suggests that convection currents played an important role in prevention of the settling in the earlier studies.

It is significant to note, however, that only very slight agitation is required to keep the particles well suspended.

Identity of the Uranium Compound. For simplicity, repeated reference has been made in the preceding discussion to uranium trioxide suspensions although the uranium is certainly not present as the trioxide. A program for identification of the uranium compound is still incomplete.

The X-ray diffraction patterns from caustic buttons prepared at 700°C with uranium trioxide or sodium diuranate are identical, but they differ considerably from the patterns for uranium trioxide or sodium diuranate. Caustic buttons (prepared with uranium trioxide), when extracted with anhydrous ethyl alcohol, yield a residue of sodium diuranate; the alcohol extraction alters the X-ray diffraction pattern, indicating that the uranium compound originally present in the caustic cannot be isolated by this technique. Samples of sodium diuranate have also been prepared by precipitation of uranyl nitrate from methyl or ethyl alcohol by sodium hydroxide. Precipitation from ether failed to give the diuranate.

It is believed that sodium monouranate is present in the caustic buttons, but the X-ray diffraction pattern for the monouranate is not available for comparison. Vacuum distillation of the excess sodium hydroxide from the suspensions is being tried, using the apparatus shown in Fig. 10.2. A suspension prepared from uranium trioxide was heated at 800 to 850°C [vapor pressure of NaOH(l), 4.0 mm Hg at 800°C] for approximately 50 hr. The sodium hydroxide distilled off leaving an orange residue in the silver crucible, but this residue was contaminated by particles from the stainless steel pipe fittings and by sodium hydroxide which had fallen back into the crucible. Another run is planned using a cover over the silver crucible to prevent this contamination. Results of X-ray analysis on the first sample are not available, and identification of this orange residue has not as yet been accomplished.

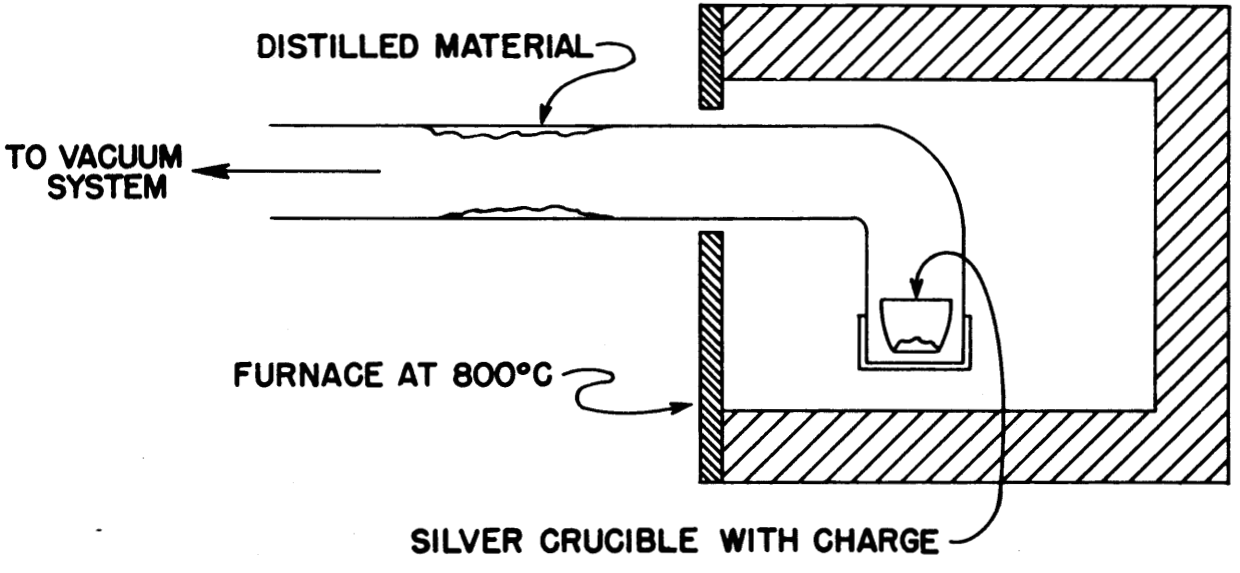

VACUUM DISTILLATION OF SODIUM HYDROXIDE

FIGURE 10.2

LOW-MELTING FLUORIDE SYSTEMS

R. E. Moore J. P. Blakely
G. J. Nessle C. J. Barton

Studies of molten fluoride systems which might serve as fuels have been continued in the directions indicated in the last quarterly report.[3] During the past quarter the equilibrium diagram for the UF_4-LiF system has been established, and considerable progress has been made on the ternary systems UF_4-NaF-BeF_2, UF_4-NaF-KF, and UF_4-NaF-LiF. The equilibrium diagrams for these systems are, however, still far from complete, and it is not as yet possible to state the precise composition of a fuel which would be completely satisfactory from a phase stability point of view. Although the UF_4-NaF-BeF_2 system has shown most promise in preliminary studies, it is not yet certain that this system is best for the purpose. The general characteristics of the systems studied are discussed briefly under individual headings below.

Experimental Methods. The conventional techniques of thermal analysis have been used in virtually all the experiments to date. The procedures and materials are essentially as described earlier[4] although the actual apparatus used has undergone considerable modification since that report was issued.

The melts are still contained in high-density graphite crucibles, but the graphite stirrer—thermocouple well combinations have been replaced by motor-driven stirrers of monel. These stirrers are drilled to serve as a thermocouple sleeve from which the couple is insulated by a ceramic tube. Lubrication of the ceramic tube with graphite permits the stirrer to turn freely without twisting of the thermocouple wire. The stirrer is rotated at about 150 rpm by means of a belt drive which slips without injury to the equipment when the melt solidifies. A graphite sleeve bearing supports the stirrer shaft to facilitate smooth operation of the stirrer.

Cooling curves have usually been recorded by automatic pen-type recorders of the Brown or Leeds and Northrup variety. Manual recording of the curves using type K potentiometers is used to verify points of special importance.

(3) ORNL-858, *op. cit.*, p. 104.

(4) *Ibid.*, p. 110.

Efforts have been made to separate by filtration the phases present under equilibrium conditions. While this has been accomplished at temperatures below 420°C in the NaF-BeF_2-UF_4 system, apparatus difficulties have so far precluded general application of the method.

At low temperatures the melts are essentially without effect on glass equipment, provided the samples are well dried and outgassed. Systems which contain sufficient amounts of liquid near or below 400°C can, therefore, be separated easily by use of the apparatus shown in Fig. 10.3. The materials, which have previously been melted under an inert atmosphere, are placed in the apparatus on the sintered glass disk, and the entire assembly is carefully evacuated. The sample is then heated to the desired temperature while the pumping is continued. After 1 to 2 hr at the desired temperature helium is admitted to the apparatus to accomplish the filtration. The liquid phase that accumulates in the lower tube is removed for analysis.

Apparatus of similar design but with sintered stainless steel filters and of all-metal construction should permit general application of this direct procedure.

Properties of the Fluoride Systems. *Lithium Fluoride—Uranium Fluoride.* This system has been investigated in considerable detail by thermal analysis, and some information has been obtained from X-ray diffraction photographs. While some further study would be necessary to establish with certainty the identity of the compound with incongruent melting point, the main features of the diagram (Fig. 10.4) are well established. Only one eutectic exists in this system; this material, containing 26 mole % UF_4 and melting at 490°C, would be quite interesting as a possible fuel mixture if separated lithium isotopes were available. The compound of incongruent melting point is probably LiF-$3UF_4$ although LiF-$2UF_4$ is a possibility. The compound does undergo a phase transition at about 600°C.

NaF-BeF_2-UF_4 System. The binary NaF-BeF_2 system has been reported as showing a eutectic at 45 mole % BeF_2 which melts at about 360°C. Such a mixture prepared in this laboratory has been shown to melt at 342°C. The purity of the only beryllium fluoride available here is unknown; it is, therefore, quite possible that impurities are responsible for this discrepancy. The extremely low melting point available has encouraged studies of the

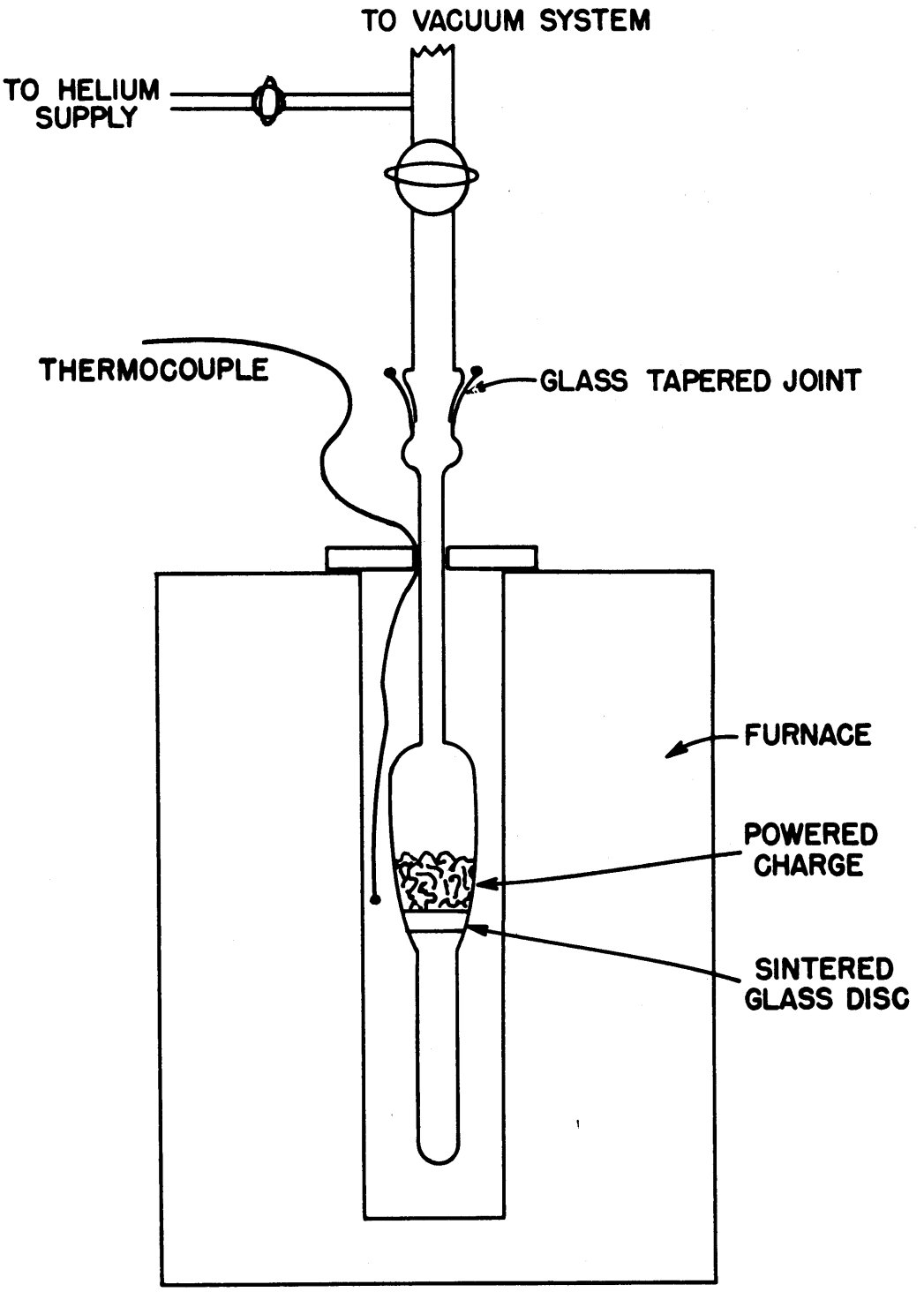

FILTRATION OF LOW-MELTING SYSTEMS

FIGURE 10.3

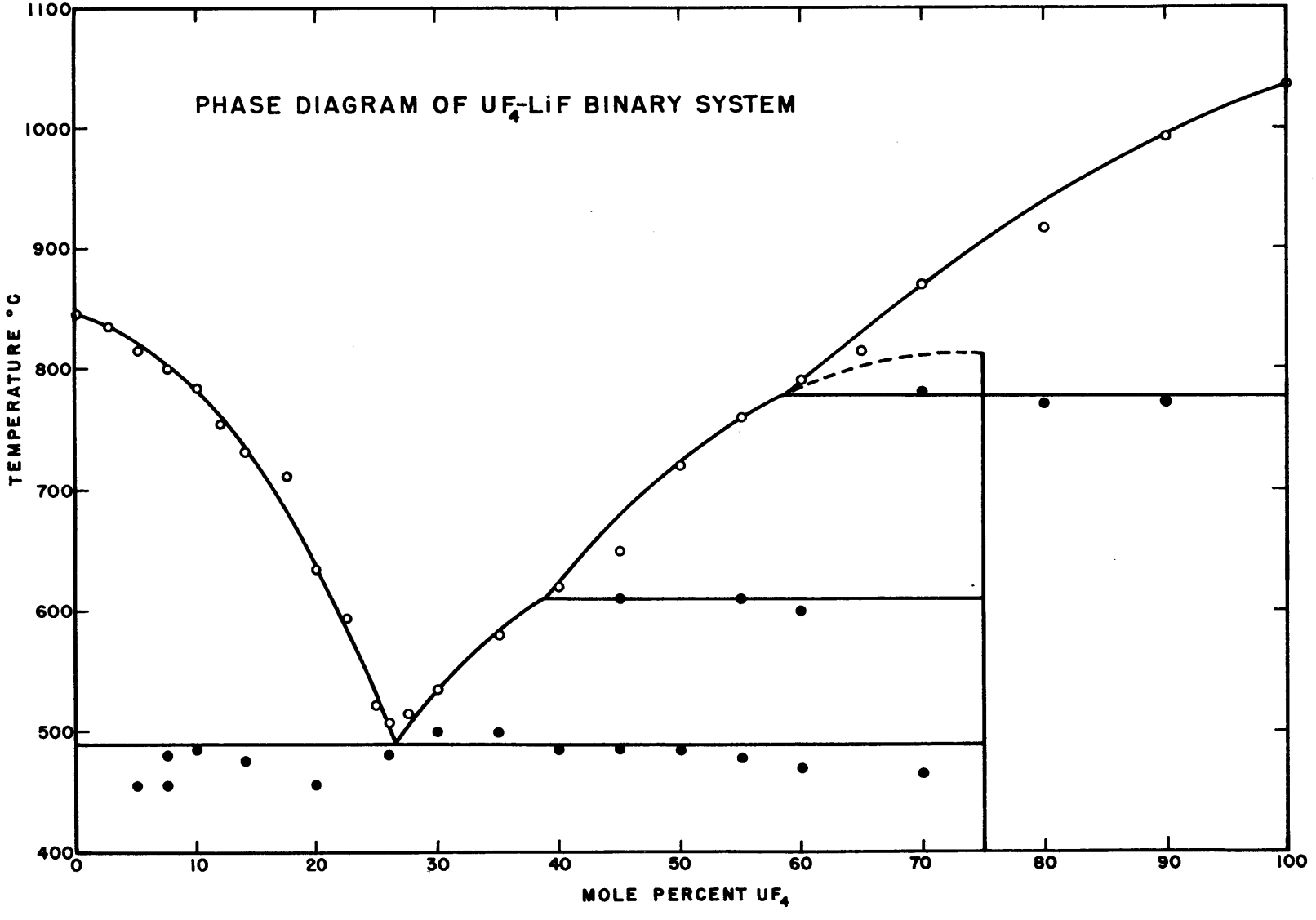

FIGURE 10.4

DRAWING NO. 10216

solubility of UF_4 in this material. It must, however, be recognized that the vapor pressure of BeF_2 at high temperatures is not known and may be relatively high (perhaps as high as a few atmospheres at 1000°C). The well-recognized toxicity of beryllium compounds, especially in the form of air-borne dusts, is a factor which necessarily makes the study a time-consuming one.

Study of this ternary system has been attempted by thermal analysis and by the filtration techniques described above. It has been demonstrated that uranium fluoride dissolves in mixtures of NaF and BeF_2 even at temperatures below 340°C. Unfortunately, however, the uranium content of this liquid phase is less than 5% by weight. Since the volume available for an unmoderated fuel in reactors of current design is limited to about 2 cu ft, such dilute solutions of uranium are of little interest. It is likely that, using reasonable estimates for the density of such liquids, liquids of about 50% UF_4 by weight are required.

Thermal analyses of such mixtures, in the range 10 to 20 mole % UF_4, are far from complete. Such studies as have been completed, however, indicate that mixtures containing 15 to 18 mole % UF_4 and 35 to 45 mole % BeF_2 are completely liquid below 550°C. It is extremely likely that the optimum composition has not yet been reached and that the goal of critical amounts of uranium in 2 cu ft with melting point below 500°C may be realized.

NaF-LiF-UF_4 System. The relatively low temperature (490°C) obtained in the LiF-UF_4 binary system and the known binary eutectics of NaF-KF (640°C) and of NaF-UF_4 (600°C) have encouraged the study of this ternary system. A large number of compositions within this system have been checked by thermal analysis methods. Not all regions of this diagram have been explored as yet. It would appear that the lowest melting point in the system is at a ternary eutectic at 26 mole % UF_4, 48 mole % LiF, and 26 mole % NaF. Material of this composition shows only the eutectic halt at 450°C. It appears that in regions considerably removed from this composition, i.e., 25 mole % UF_4, 45 mole % NaF, and 40 mole % LiF, a new ternary eutectic of higher melting point is observed. A large number of compositions must be investigated before this could be definitely stated.

The uranium concentration of the 450°C ternary eutectic is sufficiently high and the melting point sufficiently low to make it of considerable interest, provided the separated lithium isotopes are available.

NaF-KF-UF_4 System. Studies of this ternary system have been initiated quite recently, and, to date, the few cooling curves available are insufficient to characterize the system. It seems likely, however, that the lowest melting points available are higher than those indicated for the two ternary systems discussed previously. In spite of this fact, there is evidence of a ternary eutectic at 505°C, and samples containing up to 25 mole % UF_4 have remained liquid to 550°C. Determination of the eutectic composition is the object of present efforts.

CORROSION TEST OF METALS

P. J. Hagelston, Isotope Research and Production

The first corrosion test was made to determine the effects of NaF-UF_4 eutectic on various metals and to select the least susceptible for the next test. The samples were cut from sheet materials approximately 1½ by 2 in., weighed, and placed in a reactor containing the molten eutectic at 700°C for approximately 160 hr. The following samples were tested:

Durimet	Inconel
International Ni Special	Stainless steel 316
Illium G	Nickel
Hastelloy A	Tungsten
Hastelloy B	Molybdenum
Hastelloy C	Monel
Hastelloy D	Stainless steel 304
Illium R	Platinum
Tantalum	Stainless steel 347
Inconel X	Zirconium

It was found that tantalum and zirconium disintegrated. Some of the samples lost weight from erosion while others gained weight from penetration by the salts.

The test with LiF (74 mole %) — UF_4 (26 mole %) eutectic was made using samples from the following materials:

Hastelloy A	Illium R
Hastelloy B	Stainless steel 316
Hastelloy C	Stainless steel 321
Nickel	Stainless steel 347
Inconel	Ticonium
Molybdenum	

The samples were placed in a graphite box filled with molten eutectic which was maintained at 700°C. The graphite box was surrounded by a tightly lidded mild-steel "shoe box" through which argon was circulated. The samples were removed and weighed after 24, 68, 134, and 204 hr run time. It was necessary to replenish the eutectic each time the run was interrupted, owing to the creeping of the mixture over the sides of the container. During the final run (134- to 204-hr period), the mild-steel shoe box oxidized and the samples were exposed to the atmosphere. The test was therefore terminated.

It was found that some materials showed an initial weight gain which gradually diminished with time. Scale formations were not removed. In the order of initial weight gain, starting with the least weight gain, these materials were:

Molybdenum
Inconel
Illium R and hastelloy C
Ticonium
Hastelloy A
Nickel
Hastelloy B

Stainless steels 316, 321, and 347 all showed a loss in weight which increased with time. Listed in the order of weight loss, least weight loss first, they are as follows:

Stainless steel 316
Stainless steel 321
Stainless steel 347

The attack on 347 stainless steel represented the extreme case among those tested. Figures 10.5, 10.6, and 10.7 picture this attack.

In order to compare the corrosion effects of $LiF\text{-}UF_4$ and $NaF\text{-}UF_4$ on identical samples, two tests were started on November 30 using the following materials in interior containers made of hastelloy C instead of graphite:

Stainless steel 304 (extra low carbon)
Stainless steel 316 (extra low carbon)
Stainless steel 304
Stainless steel 316
Stainless steel 321
Stainless steel 347
Stainless steel 321
Stainless steel 405
Stainless steel 410
Stainless steel 430
Stainless steel 446
Allegheny 590
Molybdenum
Inconel
Hastelloy C

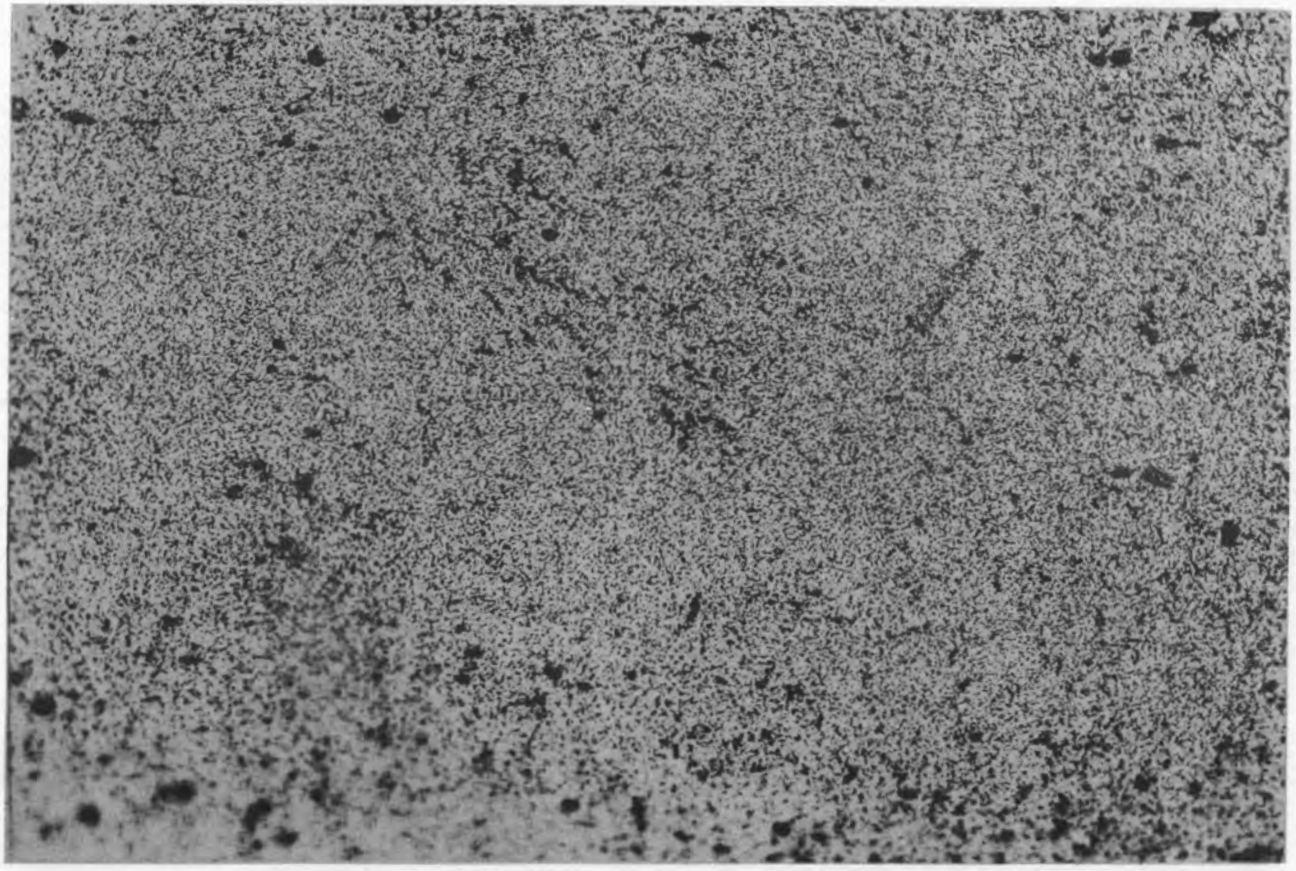

347 STAINLESS STEEL PRIOR TO TEST

FIGURE 10.5 347 STAINLESS STEEL (UNEXPOSED)
(mag. 100X)

DRAWING NO. 10242

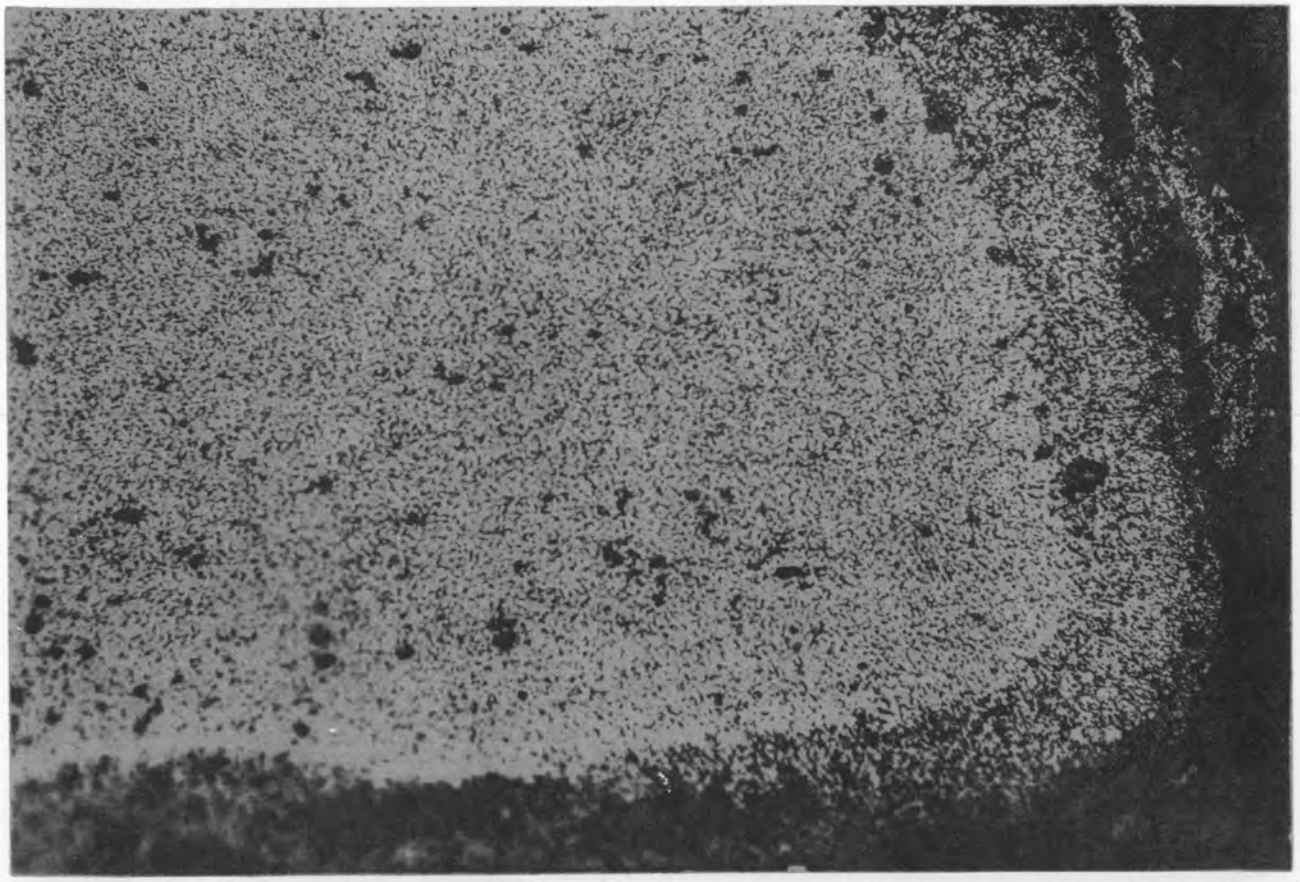

347 STAILESS STEEL, SHOWING ATTACK (DARK OUTER EDGES) AFTER 24 HOURS EXPOSURE TO LiF-UF_4 EUTECTIC

FIGURE 10.6 347 STAINLESS STEEL (24 HR. EXPOSURE) (mag. 100X)

DRAWING NO. 10243

347 STAINLESS STEEL, SHOWING ATTACK AFTER 135 HOURS EXPOSURE TO LiF-UF_4 EUTECTIC

LIGHT SECTION IS UNATTACKED METAL

DRAWING NO. 10244

FIGURE 10.7 347 STAINLESS STEEL (135 HR. EXPOSURE) (mag. 100 X)

Both of these runs were terminated because of oxidization of the mild-steel shoe boxes when the argon lines were plugged by condensation of the vaporized eutectics. The test with LiF-UF_4 eutectic failed after 113 hr, and the one using NaF-UF_4 eutectic failed after 71.25 hr. The samples were removed and cleaned by first dipping into a molten mixture of NaCl and Na_2CO_3 and then into cold water. After washing in water, the samples were free from scales and a fairly accurate weight loss was obtained. Results are summarized in Table 10.3.

TABLE 10.3

Comparison of Material and Eutectic

MATERIAL	WEIGHT LOSS (mg/dm^2/day)	
	LiF-UF_4	NaF-UF_4
Mo	26.1	64.4
Inc	68.5	−44.7*
HaC	198.5	19.67
Al-590	607.0	514.0
304 SS (ELC)	1698.0	876.0
316 SS (ELC)	1732.0	1138.0
347 SS	1850.0	856.0
321 SS	2475.0	1482.0
304 SS	3270.0	2050.0
316 SS	3490.0	2070.0
410 SS	5000.0	3360.0
430 SS	6510.0	3670.0
405 SS	7175.0	4830.0
446 SS	7280.0	5470.0

* Weight gained.

CORROSION TEST OF CERAMICS AND FISSION PRODUCTS

R. O. Hutchinson

A test was performed to determine which, and to what extent, of the better than 1% yield of fission products reacted with the liquid fuel. When the

working fluid is decided upon for the ARE, experiments may be conducted to determine what effect the fission products present in the system will have on the various materials of construction under consideration. Some ceramics were tested to determine which would be least attacked by the liquid fuel at 700°C.

The better than 1% yield of fission products desired as samples were rubidium, strontium, yttrium, zirconium, columbium, molybdenum, technetium, ruthenium, rhodium, palladium, cesium, barium, lanthanum, cerium, praseodymium, neodymium and samarium. Of these metals, only six were found in a slug form. The others were either not available at all or were very expensive. Zirconium, neodymium, palladium, hafnium, barium, and strontium were used. The last two, because of their known activity, were first tested by dropping into a boat containing molten UF_4-LiF eutectic. A spontaneous reaction occurred with both metals.

The remaining four metals were immersed in a boat of molten eutectic and heated up to 1300°F. They were then suspended on molybdenum wire and lowered into the salts. Beryllium metal, BeO, Zircon, lava, and graphite were treated in the same manner. The beryllium metal began immediately to change the salts to a red-looking slag. The slag formed a coating over the zirconium and hafnium, but the palladium and neodymium were gone. The zirconium and hafnium gained about 1 g owing to the slag formation.

The second run was the same as the first except for the ommission of beryllium metal. The four metals were removed at the end of 24 hr. The neodymium and palladium were completely dissolved, and the hafnium metal was still in original shape but completely carbonized when the sample was crushed. The zirconium was also completely dissolved.

Information regarding the weights of samples after 24 hr of immersion is given in Table 10.4.

TABLE 10.4

Corrosion Tests of Ceramics and Fission Products

SAMPLE	WEIGHT (g)		OBSERVATION
	IN	OUT	
FIRST RUN			
Hf	25.4592	26.7331	Slag formed over
Nd	7.8377		90% or better dissolved
Pd	2.4264		90% or better dissolved
Zr	13.8474	12.9677	Slag formed, easily removed
SECOND RUN			
Hf	21.1092		Carbonized 100%
Nd	7.7303		90% dissolved
Pd	1.1102		90% dissolved
Zr	7.7169		Completely dissolved

The molybdenum wire used in the suspension of samples was noted to be much more ductile after subjection to extreme heat and immersion in the bath. After repeated bending, it still remained soft.

The following ceramics were also tested in $LiF\text{-}UF_4$ eutectic at 700°C:

Graphite	ZrO_2
CaF_2	Al_2O_3
Lava A	MgO
Zircon	

After 22 hr CaF_2, ZrO_2, Al_2O_3, and MgO showed signs of complete attack and were eliminated from further test.

A new test was started using graphite, lava, Zircon, and BeO. At the end of 90 hr the Zircon was completely dissolved and the lava badly eroded. The graphite and BeO showed no signs of attack.

After 190 hr the test was terminated; it was found that graphite had lost 1.15% of its original weight, BeO had gained 5.52% owing to formation of slag, and the lava was about 75% dissolved.

11. ANALYTICAL CHEMISTRY

11. ANALYTICAL CHEMISTRY*

C. D. Susano, Analytical Chemistry Division

The Analytical Chemistry Division (Y-12 Section) has assisted in the ANP program by performing service analytical work and by carrying out development, as required, of methods for use, principally, in analyzing materials of construction, liquid-metal coolants, and materials for use in fuel elements. Summaries of the development and analytical activities of this Division which are concerned with the ANP project are here presented.

DETERMINATION OF OXYGEN IN SODIUM

J. C. White and W. J. Ross

Although the method of Pepkowitz and Judd[1] has been adopted for the routine determination of oxygen in sodium, it has not proved entirely satisfactory with regard to precision and it does not permit a spectrographic analysis to be made on the same sample. A search is being made for a reagent other than mercury which will take sodium into solution but will not react with or dissolve sodium monoxide. Of 25 organic liquids tested for this purpose, all except two (ethyl acetoacetic ether and acetonyl acetone) have been eliminated on the grounds of unreactivity with sodium, lack of selectivity of action, high viscosity, or production of insoluble products with sodium. Ethyl acetoacetic ether and acetonyl acetone, together with other as yet untried reagents, will be further investigated.

An additional assembly of the Pepkowitz and Judd type for the determination of oxygen in sodium has been set up and tested. The equipment consists of a purification train and two reactors.

Preparation of Standard Samples (J. C. White and C. M. Boyd). Difficulty was encountered in preparing suitable samples to check the accuracy attained in the determination of sodium monoxide in sodium by the method of Pepkowitz and Judd. Samples were prepared by drawing molten sodium into an evacuated glass vial containing a weighed amount of mercuric oxide. The reaction between sodium and mercuric oxide to produce sodium monoxide was so vigorous that it shattered the glass vial.

* This section, except for minor editorial changes for conformity with other sections, is the same as Report Y-B31-221.

(1) Pepkowitz, L. P., and Judd, W. C., "Determination of Sodium Monoxide in Sodium," *Anal. Chem.* 22, 1283 (1950).

Samples were next prepared by adding sodium and mercuric oxide in separate glass vials to the reactor of the apparatus. After the addition of mercury, the vials were broken and the reaction was allowed to proceed inside the reactor. Test results for samples formed in this manner indicate that the reduction of mercuric oxide is complete and that recovery of the added oxygen is possible. Representative results were as follows:

OXYGEN ADDED (%)	OXYGEN FOUND (%)
0.13	0.14
0.057	0.065
0.17	0.14

Work is continuing on the improvement of the accuracy and precision attainable by the Pepkowitz and Judd method.

Time Study of the Pepkowitz and Judd Method (J. C. White). A detailed study was made of the Pepkowitz and Judd method with regard to the actual time spent in the various operations when the method was performed on a routine basis. It was possible, on the basis of the study, to make several changes designed to speed up the operation. It was concluded that one man could be expected to do eight determinations per day and two men sixteen per day with apparatus consisting of two purification trains and four reactors. A report[2] was written in which the results of the time study, along with a detailed procedure, were given.

MICROANALYSIS OF SILICON CARBIDE

J. C. White and W. J. Ross

Some fourteen samples of irradiated silicon carbide have been submitted for the determination of free silicon and silicon dioxide. Since the average weight of these samples is of the order of 50 mg, a microanalytical method must be used.

A method described in the literature, based on the removal of SiO_2 by treatment with HF and H_2SO_4 and the subsequent removal of silicon by treatment with HF, H_2SO_4, and HNO_3, was shown to be unsuitable. Silicon is not inert to

(2) White, J. C., *Suggested Procedure for the Determination of Oxygen in Sodium by the Pepkowitz and Judd Method*, Memorandum to Dr. R. Rowen, Analytical Chemistry Division, Oak Ridge National Laboratory, Y-12 Site (Nov. 17, 1950).

HF and H_2SO_4, as was supposed by the authors of the method, but undergoes continuous loss in weight

A method has been developed based on the removal of silicon as $SiCl_4$ by reaction with dry chlorine at 350°C and the subsequent removal of SiO_2 by treatment with HF and H_2SO_4. Repeated tests have established that silicon can be quantitatively removed from known synthetic mixtures of the metal and the carbide by this procedure.

Test results representative of those obtained in the analysis of approximately 5-mg portions of the NEPA samples are listed in Table 11.1.

TABLE 11.1

Analyses of Silicon Carbide Samples for Silicon and Silicon Dioxide

SAMPLE	SILICON (%)	SILICON DIOXIDE (%)
Bureau of Standards	1.74	1.63
	1.72	1.90
	1.71	1.35
1	0.95	3.23
	1.09	3.12
2	0.1	2.38
	0.1	2.56
3	0.59	2.61
	0.57	2.45
4	0.12	1.63
	0.17	1.93
6	0.41	0.69
	0.22	0.66

FLAME PHOTOMETRIC ANALYSIS OF LITHIUM

O. Menis

An investigation was made of the flame photometric method for the determination of alkali and alkaline earth metals in a lithium matrix. The principal purpose of the study was to evaluate the previous work done in the Analytical Chemistry Laboratory with a view toward bringing this project to a conclusion.

In brief, the general conclusions and suggestions for further work are as follows: for dilute solutions containing the ions in the range of 1 to 10 ppm, the method as now developed should serve without major modification for the determination of sodium and potassium, but for the determination of calcium, and especially for magnesium, higher temperatures of flame excitation are imperative. The minor constituents should be concentrated by chemical means. A pure lithium standard should be prepared by one of the several methods to be found in the literature. Attention should be given to the following: anion effects, the use of more volatile solvents, choice of wavelength to minimize interference, and proper laboratory conditions to assure instrument stability.

STABILITY OF A SILICONE OIL IN CONTACT WITH SODIUM

J. C. White and W. J. Ross

At the request of the ANP Experimental Engineering Group, an investigation was made of the stability of Dow Corning silicone fluid DC-550 in the presence of sodium at elevated temperatures. This material is a clear, slightly yellowish liquid of exceptional heat stability, high resistance to oxidation, low volatility, and high flash point (600°F, minimum). Because of its favorable properties, it is being considered as a pressure transmitting agent in equipment in which the fluid must be in contact with sodium metal at temperatures of 300 to 350°F. In the event of certain types of failure of the apparatus, however, the oil could come in contact with sodium at considerably higher temperatures.

In order to simulate conditions approaching those which might be encountered in the case of an apparatus breakdown, tests were carried out in

which samples of oil and sodium were heated together at temperatures up to 1050°F. In these experiments the sample was heated under an atmosphere of helium in a test tube which was placed in a lead bath. Temperatures were measured by means of a thermocouple which was inserted in the oil. Two tests were made in which the oil was heated with sodium for 30 min at 1050°F. No violent reaction took place but the oil darkened in color. Upon cooling, the material solidified into a hard, oily, crystal-like mass. A qualitative test showed the presence of sodium.

In a test in which the oil was heated without sodium at 1000°F for 15 min, the only effect was an increase in viscosity and refractive index, apparently due to the loss of some of the lower boiling constituents of the oil.

When the oil was heated for 6 hr with sodium at 400 to 450°F there was no visible change, but the basic reaction shown by a water extract of the oil was evidence that some reaction between oil and sodium may have taken place.

The results of these experiments indicate that silicone oil DC-550 is stable in the presence of sodium at 400 to 450°F for several hours and probably stable at 600 to 700°F for short periods.

SERVICE ANALYSES

J. W. Robinson and L. J. Brady

During this period the analytical work carried out in furtherance of the ANP program consisted chiefly of the determination of minor impurities in liquid metals (coolants) and of the analysis of materials of construction and of uranium compounds and mixtures.

Sodium Analysis (J. M. Peele and L. H. Jenkins). Corrosion-test samples of sodium after exposure to various materials of construction at elevated temperatures were analyzed spectrographically for minor components using the porous cup method, and for oxygen content by the method of Pepkowitz and Judd.

Solutions of test samples and of standard samples were prepared in the chemical laboratories for spectrographic analysis; these solutions were then examined spectrographically in the Physics and Spectrographic Department of the Isotope Research and Production Division.

Analysis of Boron Carbide (J. R. Lund). Acceptable methods have been established for the determination of boron oxide, total boron, carbon, and moisture in boron carbide. The boron oxide is determined by titration of a hot-water leach of the sample. In determining total boron complete dissolution of the sample is required. It was found that the product of a sodium carbonate fusion would dissolve completely only if the material was ground to pass a No. 120 sieve prior to fusion. The resulting solution was titrated for total boron in the usual manner. Carbon was determined by combustion at 1400°C, using copper as an accelerator. Moisture was calculated from loss in weight at 110°C.

Analysis of Ferrous and Nonferrous Alloys (C. K. Talbott). In general, standard methods were used in the analysis of stainless steels and nickel alloys. A number of special alloys such as Co-Ni, Zr-Ni, and Mn-Cu, required less common methods of analysis.

Analysis of Uranium Compounds (E. C. Lynn and A. F. Roemer, Jr.) Sodium and potassium uranate, oxides of uranium, and fusion products containing small amounts of uranium were analyzed for uranium, alkali metal, hydroxide, and carbonates. Potentiometric, colorimetric, or fluorimetric methods—depending on the concentration—were used for the determination of uranium. The alkali metals were determined by means of the flame photometer, carbonates by gas evolution, and hydroxides by titration with acid after precipitation of the carbonate as barium carbonate.

SUMMARY OF SERVICE ANALYSES

A brief summary of the analytical work for the ANP program during the period is tabulated below.

	NO. OF SAMPLES		
	NEPA	Y-12	TOTAL
Backlog of samples 9-16-50	50	1	51
Samples received 9-16-50 to 11-30-50 inclusive	157	71	228
Total	207	72	279
Samples reported 9-16-50 to 11-30-50 inclusive	128	48	176
Backlog as of 12-1-50	79	24	103

	NO. OF DETERMINATIONS
Samples from NEPA	581
Samples from Y-12	128
Total	709

Part II

LONGER RANGE ACTIVITIES

12. VAPOR-CYCLE REACTORS

12. VAPOR-CYCLE REACTORS[1]

North American Aviation, Inc.
C. Starr, A. S. Thompson, and Others

Two types of mercury-vapor compressor jets have been studied. A preliminary design study of aircraft performance indicates that neither type appears suitable for flight at 45,000 ft and Mach 1.5. Even if a very optimistic value of L/D is chosen, indications are that the better of the two is still only marginal.

Some work has been done on a gas-cooled reactor for a turbojet cycle, but no refined weight estimates have yet been made. Two characteristics appear at this stage: (1) The reactor must operate at a very high temperature, and (2) the pumping power required is so great that the turbine size required is several times that required to drive the propulsion duct air compressor.

The corrosiveness of sodium vapor is being measured on potential structural materials of the sodium-vapor cycle reactor. In addition a program has been initiated to study the effects of radiation on corrosion in systems of possible interest to the ANP.

MERCURY-VAPOR COMPRESSOR JET

Two types of mercury-vapor compressor-jet power plants are being studied.[2] The first employs a mercury booster heater downstream of the mercury condenser, and the second employs, instead, a liquid-sodium booster. The mercury turbine cycle which drives the air compressor is the same in each case. Mercury is heated in the intermediate heat exchanger and passes through the turbine to the condenser in the duct air stream. The mercury booster heater draws some of the mercury from the intermediate heat exchanger and condenses it; the sodium booster heater draws sodium directly from the reactor and cools it in the duct air stream. The temperature of the mercury is lower than that of the sodium because of the temperature drop in the intermediate heat exchanger. The reactor wall temperature is 2260°F. The duct air temperature for each case is given in Table 12.1.

(1) See North American Aviation, Inc., *ANP Quarterly Progress Report July 1, 1950 to Sept. 30, 1950*, ANP-56 (Nov. 24, 1950).

(2) See Schwartz, H., Dean, A., and Malone, J. L., *Aircraft Nuclear Propulsion Program Progress Report to July 1, 1950*, NAA-SR-86, p. 23 (Aug. 7, 1950).

TABLE 12.1

Results of Cycle and Weight Analyses

	Hg BOOSTER	Na BOOSTER
Mach No.	1.5	1.5
Altitude (ft)	45,000	45,000
Maximum mercury temperature (°R)	1835	1835
Maximum sodium temperature (°R)	2192	2192
Maximum propulsive duct air temperature (°R)	1601	1849
Specific thrust	37.3	42.2
Reactor power (kw/lb of thrust)	7.44	8.18
Specific power plant weight exclusive of reactor (lb/lb of thrust)	3.8	2.64
Specific power plant weight including reactor (lb/lb of thrust)	5.2	4.04

Weight studies were carried out assuming a power plant having a thrust of 100,000 lb at Mach 1.5 and 45,000 ft. The properties of the power conversion equipment are most sensitive to cycle selection and attention was therefore confined there. For aircraft configuration studies, a figure of 70 tons (for the weight of reactor core and shield) was chosen as a representative value. The results of the cycle and weight analyses are shown in Table 12.1.

Aerodynamic studies and preliminary aircraft design studies were begun as soon as preliminary values for specific thrust, weight, and equipment size were available. The first design study presumed a swept wing, but this proved impractical because of the poor wing-weight distribution and poor aerodynamic characteristics at inlet to the outer engines. Consideration was given to a split wing with no sweep containing a total of 20 engines within the wings. The reactor and intermediate heat exchanger were contained in the fuselage. Some work has also been done on the ducted body configuration but no conclusive results have been obtained as yet.

In considering the practical application of a nuclear power plant to aircraft, the tentative maximum gross weight of 450,000 lb was assumed for preliminary investigations. Planes in excess of this weight could probably be

built, but it was the general opinion that the cost of the necessary facilities for construction would be prohibitive. Of the total weight of power-conversion equipment (264,000 lb) approximately 164,000 lb or about 70% is due to the dry weight of heat exchangers, compressors, turbines, pumps, etc. The balance of 100,000 lb represents the weight of the charge of working fluids, viz., mercury and sodium. Effort is being made to reduce this charge to a realistic minimum but any possible further reduction due to ingenuity in design would not be expected to be significant.

It is the present opinion of the aircraft designers involved that this plane with an L/D of from 4.5 to 5 cannot be built to fly at Mach 1.5 and 45,000 ft unless the power-plant weight including reactor does not exceed 3.4 lb per pound of thrust. Accordingly, it appears that the mercury-vapor compressor-jet cycle even with the sodium booster (estimated specific weight = 4.04) is not suitable for this application. Even if, on the other hand, an L/D of 6 or greater could be realized, and also if a gross weight in excess of 450,000 lb were permissible, then the mercury-vapor cycle would still be marginal. Under these conditions the compressor jet, as compared with a turbojet, would probably not warrant the additional complexity. A more detailed report relative to the mercury-vapor compressor jet is now in preparation.

GASEOUS POWER CYCLE

Preliminary analysis of this turbojet cycle, utilizing a helium-cooled reactor which transfers heat into the propulsion duct through a heat exchanger, indicates that the cycle inherently requires a high temperature. This is because of the gas-to-gas heat exchanger which necessitates high temperature differences to yield useful heat-exchanger weights. Work on this cycle is now concentrated on an effort to arrive at a preliminary design of a heat exchanger which would offer hope for successful application to an aircraft power plant. The analysis is still in such a preliminary stage that refined weight estimates are yet to be made.

Concentrated effort on this compressor-jet cycle is not contemplated until further investigation of the turbojet cycle has been made. It may be that the power to drive the propulsion duct air compressor can be obtained from the turbine driving the gas-circulating compressor by increasing the

turbine size slightly. This is true because of the very large amount of pumping power required.

SODIUM-VAPOR COMPRESSOR JET

Some very rough weight estimates indicate low values of power-plant weight (sp. wt. = 1.1 to 1.3, exclusive of reactor weight). This fact, combined with the relatively high specific thrust (57 to 60) at Mach 1.5 and 45,000 ft, indicates promise for the cycle. The maximum temperatures involved here (3500 to 4000°R) are, of course, much higher than those in the mercury-vapor cycle discussed above (2260°R). Analytical work on this cycle, including aircraft configuration studies, will continue after completion of mercury-vapor and gaseous cycle investigations.

CORROSION EXPERIMENTATION

Current activity in this experimental program is concentrated on the corrosion in systems of probable interest to ANP. Initial results are reported on (1) the corrosive effect of sodium vapor on various potential structural materials in absence of irradiation, and (2) the corrosion in systems (fluids and containers) subjected to irradiation.

Sodium-vapor Corrosion; No Irradiation. The test consists in suspending a weighed sample of the test material from the top of a stainless steel "test tube," evacuating and outgassing the tube, introducing a small quantity of purified sodium, and holding at a temperature of approximately 1650°F for a period of 16 to 24 hr. This bathes the specimen with saturated sodium vapor at a pressure slightly in excess of 1 atm absolute pressure. At the end of the test period, the test tube is opened and the sample is removed, washed, weighed, and subjected to metallographic examination. The techniques involved have now been worked out and one test each has been completed on the following materials:

1. Graphite (AWG). No attack indicated by weighing or by metallographic examination.

2. Stainless steel (type 316). No attack indicated by weighing or by metallographic examination.

3. Tantalum. Attacked at rate of 0.007 in./year as indicated by weight loss. A rerun of this material is planned for the near future since there is evidence that the sodium was contaminated with oxygen.

These tests will be extended to other materials. Upon completion of the relatively low-temperature tests, those materials still in contention will be tested in sodium vapor at higher temperatures. Equipment for these latter tests is now being designed.

Corrosion Tests with Irradiation. Experiments were undertaken to study the effects of radiation on corrosion, in systems of possible interest to ANP, by exposure to charged particles from the 60-in. cyclotron at Berkeley. A comparison of cyclotron and reactor irradiation indicates[3] that accelerated tests are possible on the cyclotron, particularly in regard to corrosion phenomena where ionization energy density is important. Where lattice displacements arising from collisions with the cyclotron beam particles are important, the relative advantage of cyclotron over reactor irradiation is reduced. The systems under study include:

1. Be_2C-air, at elevated temperatures.
2. Pure iron-lithium, at 900°C.
3. Type 316 stainless steel—sodium, at 900°C.

Two samples of beryllium carbide have been irradiated in the Berkeley cyclotron. Both samples definitely contained no free beryllium prior to irradiation. In order to test the applicability of the analytical method to interstitial beryllium, the first irradiations were made in a helium atmosphere at room temperature. The approximate limit of detectability corresponds to an irradiation of 30 μa-hr of 40-Mev alpha particles in which each alpha particle decomposes one Be_2C molecule. Tests made on the 30 μa-hr irradiation sample indicated beryllium present at just about the detectable limit. Improvements in the analytical method, which are in the process of development, will permit more accurate determination. X-ray diffraction studies showed no lattice expansion (as would accompany the presence of interstitial atoms) and indicate that no precipitated phase is present.

Capsules of Armco iron have been prepared for the iron-lithium experiments with the assistance of Dr. W. Parkinson of ORNL. These are to be provided with thin windows of the same metal, filled with pure lithium, and then welded shut. The assembled capsules are to be exposed to 40-Mev alpha particles while being maintained at 900°C in a pure helium atmosphere. It has been possible to make vacuum-tight capsules in only a small percentage of the total

(3) Martin, A. B., and Mills, M. M., *The Application of Particle Accelerators to the Study of Radiation Damage*, NAA-SR-56 (July 24, 1950).

tried because of the difficulty of welding the window to the capsule. Samples of Armco iron were irradiated at 800 and at 850°C in a helium atmosphere, using 40-Mev alpha particles. The duration of the runs was about 2 μa-hr. No change in the metal microstructure was observed in metallographic examination after the irradiation.

Windows and capsules of type 316 stainless steel were fabricated for use in sodium test assemblies in order to determine the feasibility of making the window capsule closure by welding.

INVESTIGATION OF MECHANICAL PROPERTIES AT HIGH TEMPERATURES

Test machines now in the process of design are intended to determine the following properties of various possible high-temperature materials at a maximum of 2000°C (3630°F).

1. Short-time tensile strength.
2. Creep strength.
3. Fatigue strength.

In the tensile machine, stress-versus-strain curves will be determined, and, if desired, tests determining the time to rupture at a fixed stress can be run. After elimination tests at 800°C, it is contemplated that tests will be repeated on the remaining materials at a temperature of approximately 2000°C (3630°F).

13. CIRCULATING-FUEL REACTORS

13. CIRCULATING-FUEL REACTORS*

The H. K. Ferguson Company, Inc.

The design of the major components of the homogeneous NaOH-uranium powered aircraft has progressed to the extent that a fairly definite picture of the aircraft may be presented. The 3-in.-diameter reactor is provided with a single 7-in.-diameter control rod from which extremely rapid action is not required. Xenon is expected to collect in the vapor space provided for the thermal expansion of the fuel and the control problem is thus considerably simplified. NaK is proposed as the coolant and a divided shield is mandatory. The reactor and auxiliary chemical engines (six XJ-53) will fit within the B-52 airframe with no major modifications. Weight and thrust calculations indicate that the nuclear aircraft will exceed the design specification of Mach 0.8 at 35,000 ft.

Reactor. The reactor is spherical, 3 ft in diameter (excluding reflector), and provided with a single 7-in.-diameter control rod. Flow through the reactor is maintained by a single centrifugal pump which delivers the fuel near the periphery with high tangential velocity to promote flow stability.

The reflector consists of 8.5 in. of stainless steel in three concentric shells, which serve as the thermal shield, and the 2-in. pressure vessel. Heat is removed from the thermal shield by partial diversion of fuel flow between the shells. Each shell is made up of pieces which are individually pinned to the vessel wall to permit clearance for thermal expansion. Laminated construction of each piece reduces thermal stress.

The control rod has two separate functions for which mechanisms within the shield will be designed. Shim control will be provided for 7% in $\delta k/k$ which covers the temperature range 1200 to 1500°F (3.5% $\delta k/k$) plus various other contingencies (δm, burn-up, etc.). Lower average slurry temperatures in the reactor are not permissible. Although a homogeneous reactor has considerable stability by reason of the temperature coefficient of reactivity, fine control will still be desirable. This will be obtained by motion of the rod between shim stops (which are set for withdrawal at less than 0.3% δk). Initial calculations on reactor kinetics indicate that neither of these

* This section, except for minor editorial changes for conformity with the rest of the report, is from a letter of Oct. 27, 1950 to Dr. A. M. Weinberg from The H. K. Ferguson Company, Inc. on the current status of their design of a liquid-fuel reactor.

mechanisms will be called on for extremely rapid action. Details of the kinetics depend on pump characteristics, heat-exchanger properties, etc., and are being worked up to determine required characteristics of control response.

Although data on xenon solubility in NaOH are lacking, consideration of analogous systems indicates it to be too low at reactor operating conditions for xenon to be present in solution. Since there will be a vapor space in the circuit for thermal expansion of the fuel, it is expected that the xenon will collect there and will not affect reactivity. The control problem is then considerably simplified; this seems an important advantage for the circulating-fuel type of reactor.

The current estimate of fuel volumes in the primary circuit is as follows:

Core	13.5 cu ft
Reflector cooling channels	3.5 cu ft
External circuit	14.1 cu ft

Thus the ratio of external volume to core volume is 1.05. These figures are based on fairly detailed designs for reactor, pump, and exchanger.

Reactor Coolant. NaK is the preferred coolant for the intermediate heat exchanger. The relatively mild corrosion properties of NaK may eliminate the need for a bimetal heat exchanger to resist both coolant and fuel. The low melting point makes it easy to handle in start-up and shutdown and permits control of the power cycle by by-passing the engine radiators. Although the radiation from this coolant will make a crew shield necessary, the use of divided shielding is desirable for other reasons as well.

An alternate design using lithium as coolant with a unit shield will be prepared for comparison. Some crew shielding may be necessary even in this case.

Shield. The use of NaK as coolant makes the divided shield the only possible choice. Since the divided shield will be considerably lighter than a unit shield, it is a natural choice in any case.

The principal drawback of a divided shield, difficult servicing by the ground crew, is largely obviated by the nature of the fuel. It is comparatively simple to drain and flush both the fuel and the NaK from the power unit

with all necessary connections being made by remote control. With this exception the unit may be serviced as easily as that with a unit shield.

A preliminary study of airplane geometry, weight, and balance shows an advantage in having part of the weight forward. With natural position of the reactor and engines for minimum modification of the contours, up to 25,000 lb can be accommodated at the crew compartment without adverse effect on the airplane balance. Thus the divided shield is consistent with preserving the aerodynamic features of the XB-52 plane.

The reactor shield is designed to fit within the 9- by 12-ft oval of the B-52 fuselage. The weight of everything inside the shield boundary (reactor and contents, coolants, heat exchanger, shield, and structure) is about 75,000 lb. At present the uncertainty is restricted to last-minute changes to fit in the fuselage. The shield at the crew compartment consistent with this shield weighs about 25,000 lb. The calculations are for an air-safe shield only. Full advantage is taken of shadow shielding.

Engine. The plane will be powered by six engines of the XJ-53 type, modified to contain the necessary radiator surface as well as the chemical fuel burners. The cruising conditions (35,000 ft at Mach 0.8) and sea-level climb will be met by nuclear power only, the chemical burners being provided only for take-off and emergency go-around after a missed approach. The chemical fuel burners will have enough capacity to run the plane entirely on chemical fuel, since there is little to be saved by installing partial capacity burners. Aside from addition of the radiator section and lengthening of the drive shaft between compressor and turbine, there will be no essential modification of the XJ-53 engine.

Calculations of thrust, confirmed by similar calculations by G.E., show that the present engine design is satisfactory even with the lower turbine inlet temperature and extra pressure drop between compressor and turbine. Estimated thrust for six engines is as follows:

Altitude	Sea level	35,000 ft
Speed	270 knots	Mach 0.8
Turbine inlet temperature	1200°F	1300°F
Pressure drop, proportion of inlet pressure		
In radiator	12%	13%
In ducts	3%	3%
Thrust	50,400 lb	24,800 lb
Heat to radiators	293,500 kw	145,000 kw

The speed of 270 knots at sea level was picked for best climbing performance (200 ft/min) on nuclear power alone for a 360,000-lb plane. The 24,800-lb thrust available at 35,000 ft is actually more than is required for level flight at Mach 0.8 (approximately 19,200 lb) so that the plane could actually fly somewhat higher or faster.

A radiator of the shell and tube type using internally finned tubes on a triangular lattice is being considered. While this arrangement may not be quite so efficient as the NEPA radiator on a surface-per-unit-volume and pressure-drop basis, it has the advantage of ruggedness and easy construction in almost any geometry. Thus, this type of radiator may be made in the shape of a *U* which can be easily slipped over the drive shaft or can be made in two *D* sections to use the total cross-section area available.

The actual design of the radiator cannot be completed without further details on the XJ-53 compressor, which are expected shortly, but tentative figures show a radiator with frontal area of 7.8 ft^2 and length of 21 in. This size will just fit inside the present XJ-53 shell with no bulge. Inclusion of both radiator and burning section will lengthen the drive shaft about 36 in. and will probably require an additional bearing between compressor and turbine.

Plane Configuration. The best estimates of thrust available per engine and of lift-to-drag ratio show that six engines of the XJ-53 type will be sufficient. An arrangement of six engines immediately behind the reactor in the fuselage has a number of advantages in shielding, piping, and servicing, and may actually result in an improved lift-to-drag ratio even when the increased angle of attack demanded by the additional structural weight in the wing is taken into account. There may be no increase in airplane weight with this arrangement because the fuselage installation of the engines allows a saving of approximately 25,000 lb in piping, insulation, supports, and coolant. Thus the improved lift-to-drag ratio gives a proportional reduction in required thrust.

A further advantage in this compact arrangement is that development and testing of the plane could proceed more quickly. The plane aerodynamics could be checked with a dummy engine group powered by chemical fuel, while the nuclear power plant could be completely designed and tested on the ground.

The final step of installing the nuclear unit in the plane would be relatively uncomplicated.

Ground Facilities. The airport for a nuclear plane must be equipped for certain routine tasks. The plane must be warmed up, filled with fuel and coolant, and checked before flight. Upon returning from a mission it may be completely overhauled or it may need only a few minor repairs, such as changing tires, before taking off on the next flight. Whenever nuclear fuel is in the reactor, its temperature must be in the range 1200 to 1500°F because of control limitations and danger of freezing.

Normal start-up is as follows: The NaK system is first filled and started circulating through an auxiliary heater. The reactor is then heated up by circulating first hot helium and finally hot sodium hydroxide through the reactor—heat-exchanger system. When the system reaches a temperature within the range 1200 to 1500°F, the sodium hydroxide is drained and replaced with fuel preheated to the correct temperature.

When the plane comes in for servicing, it is first located at a dump point at which the fuel and NaK systems are drained and flushed. The plane is then towed to the regular loading buildings for servicing. If the plane is to spend only a short time on the ground, the reactor may be filled with sodium hydroxide and kept hot during the turn-around. The dumped fuel may be replaced "as is" in the reactor or may be chemically processed to remove fission products. The actual cycle will depend on cost and holdup in the chemical cycle and degree of fuel burn-up per flight.

14. SUPERCRITICAL WATER REACTOR

14. SUPERCRITICAL WATER REACTOR

For the past several months various members of the Aircraft Reactor Branch of the Reactor Development Division in the Washington office of the AEC have been developing a design for an aircraft reactor cooled and moderated by supercritical water, along the lines mentioned in the Lexington Report.[1] This work has now been summarized[2] and the Oak Ridge National Laboratory has been asked by the Washington office of the AEC to comment upon the usefulness of such a system for an aircraft reactor. In order to develop the details of the design a little further than they were carried in the Aircraft Reactor Branch Report, WASH-24, ORNL asked its contractor, Nuclear Development Associates, Inc., to prepare an independent design study on this subject. NDA has now submitted an informal interim report[3] stating that it should be possible to construct a reactor substantially the same as the one proposed in WASH-24. It is also felt that it would be no harder to shield this reactor than others considered for aircraft use. However, it was stressed that the difficulties of operating a nuclear aircraft on a supercritical water cycle lie much more in the engine and aircraft phases of the problem than in the reactor.

Both NDA and ORNL are continuing the study of the supercritical water system.

(1) Lexington Project, *Nuclear-powered Flight. A Report to the Atomic Energy Commission*, Lex P-1, Sec. III, p. 57 (Sept. 30, 1948).

(2) Aircraft Reactor Branch of USAEC, *Application of a Water Cooled and Moderated Reactor to Aircraft Propulsion*, WASH-24 (Aug. 18, 1950).

(3) Gruber, A., *Preliminary Comments on Supercritical Water Cycle*, NDA, ANP-55 (Nov. 6, 1950).

15. SUPERSONIC TUG-TOW SYSTEM

15. SUPERSONIC TUG-TOW SYSTEM

During the closing week of the quarter, in response to suggestions by Dr. E. P. Wigner and by Nuclear Development Associates, Inc. (see Appendix A), the Oak Ridge National Laboratory began the study of tug-tow aircraft reactor systems with particular interest in supersonic tug-tow. If, as suggested by NDA, it is possible to build a shield for the tug plane which weighs in the neighborhood of 15,000 lb, then the tug-tow system might permit the use of very small aircraft. Although the operational difficulties of tug-tow might be fairly great, the present international situation does not permit overlooking any systems which could possibly result in a supersonic aircraft of global range within a relatively short time. The investigation of a Supersonic Tug-tow Aircraft Reactor, with its associated engine and planes, is being called Project STAR.

16. LITHIUM-ISOTOPE SEPARATION

16. LITHIUM-ISOTOPE SEPARATION

W. M. Leaders, Materials Chemistry Division

During the last quarter all the research aimed at the separation of lithium isotopes has been concentrated on the electroexchange process, which is the process based on the countercurrent chemical exchange reaction between lithium amalgam and aqueous lithium hydroxide. This process was described in detail in the last quarterly report.[1] Subsequent development of the 48-compartment electroexchanger has eliminated the transport problem through constructed openings and has greatly reduced back-diffusion. With these modifications, samples of 94.5% Li^7 (when operated to enrich Li^7) and 90.3% Li^7 (when operated to enrich Li^6) have been obtained. Other experimental electroexchange apparatus has been designed and built, and is now being operated. The production problems of lithium separation by electroexchange have been studied, and production appears to be feasible; the major difficulty is in reaching sufficiently high reflux ratios in the amalgam-forming section.

Operation of the 48-Compartment Electroexchanger. The 48-compartment apparatus was equipped so that eight of the chambers could be utilized as an internal refluxer for the preparation of amalgam. (This modification further reduced the transport difficulty mentioned above although it did not completely eliminate the deposition of lithium hydroxide.) Operating the equipment with only 40 exchange compartments both as an enricher for Li^7 and as an enricher for Li^6 yielded the following limits of separation:

1. Up to 94.5% Li^7 when operated as a Li^7 enricher.
2. Down to 90.3% Li^7 when operated as a Li^6 enricher (or Li^7 stripper).

Based on an α factor of 1.05, these separations amount to seven stages of enrichment and six stages of stripping. It is considered that the results have definitely established that the fundamental principle of the method is sound for enrichment of either of the isotopes of lithium.

Considerable difficulty was encountered during the early phases of these experiments in effecting the transport of the amalgam through small pipes and

(1) *Aircraft Nuclear Propulsion Project Quarterly Progress Report for Period Ending August 31, 1950*, ORNL-858, p. 122 (Dec. 4, 1950).

other constricted openings. This problem has been diagnosed as being caused by the deposition of solid lithium hydroxide on the surfaces of the pipe and other containing walls which are in contact with the amalgam. It appears that some surface wetting by the aqueous solution is occurring in all parts of the equipment (constructed of lucite and plexiglas) and that reaction with the lithium in the amalgam takes place to such an extent as to exceed the solubility limits of lithium hydroxide in the limited supply of water available. No particular difficulty has been encountered in portions of the equipment being agitated. Larger sized pipes have proved satisfactory for the current experimental program, however, and it is realized that the problem might recur in these larger pipes if the duration of the experiments should be greater than a few hours.

During the course of the experimental work on the 48-compartment apparatus, considerable time was spent in studying the problem of back-diffusion. It is a well-recognized fact that in any apparatus operating on the countercurrent principle, any back-diffusion or countercurrent flow greatly reduces the efficiency of the apparatus. In the 48-compartment apparatus all the cells are in one line. This arrangement is most readily assembled, and this was the deciding factor in the design of this piece of equipment. As originally built, the openings between the cells were all on the center line of the apparatus. The excessive amount of back-diffusion encountered with this particular design of cell dividers necessitated a major revision. Smaller slots (1/16 in.) were cut on alternate sides of the cell dividers to provide the most tortuous path for the liquids. The apparatus was operated in this condition during the most successful runs, the results of which are quoted above. The major difficulty with these small openings was the limit placed on the throughput of the equipment because of the resistance offered by these constrictions to the flow of the liquids. This particular problem should become less troublesome in larger scale equipment.

72 Compartment Electroexchanger. A second device was delivered from the shop during the quarter. This piece of equipment, although more difficult to construct, embodies several features which should reduce if not eliminate some of the difficulties inherent in a straight-line apparatus. This exchanger contains 72 individual compartments, 1 in. in diameter and 2 in. deep. These are arranged in two rows of 36 each and the interconnections between chambers

are arranged to give a zigzag flow through the equipment. The agitators are synchronized by a central worm shaft. Although the connecting canals are ¼ in. wide, the back-diffusion encountered in this device is extremely small when compared to the best results obtained in the 48-chamber in-line model. The apparatus has only recently been reduced to trouble-free operation and no results are as yet available. It is currently being used to determine more accurately the α factor of the method under various rates of production. This may be one of the more reliable methods of definitely establishing the exact value of α for this process.

Alternative Type Electroexchanger. When the decision was made to curtail, at least temporarily, all work on molecular distillation, the group which had been conducting this research turned their attention to the amalgam system. They designed a somewhat different type of apparatus for countercurrent contacting of the amalgam and aqueous solution. A schematic drawing of the current design is shown in Fig. 16.1. The apparatus has only recently been operated for sufficient time to reach isotopic equilibrium. The result from the first successful run showed an increase in Li^7 from 92.5 to 93.6%. One of the features of this type of equipment is the fact that back-diffusion is absolutely eliminated. The only problem from a flow standpoint is the possible short-circuiting of liquid through a chamber before equilibrium has been achieved. As the work progresses it should be possible to evaluate this method more accurately in comparison with the horizontal types of equipment.

Analyses of Production Problems. After it became apparent that the general principle of the electroexchange process was sound, the scale-up problems of production were of major interest. In order to get a more accurate indication of what these problems might be, a large size in-line model exchanger was built. A special baffling device was incorporated in this apparatus in an attempt to reduce back-diffusion. The effectiveness of this baffling device has not been completely established, but preliminary tests indicate that it is quite effective. The apparatus consists of 18 cells operating in groups of 6, one group being used as a Li^7 refluxer for continuous preparation of amalgam, one group as an exchange section, and the third group as a stripping section to remove lithium from amalgam. All agitators are individually powered.

[redacted]
DRAWING NO. 10245

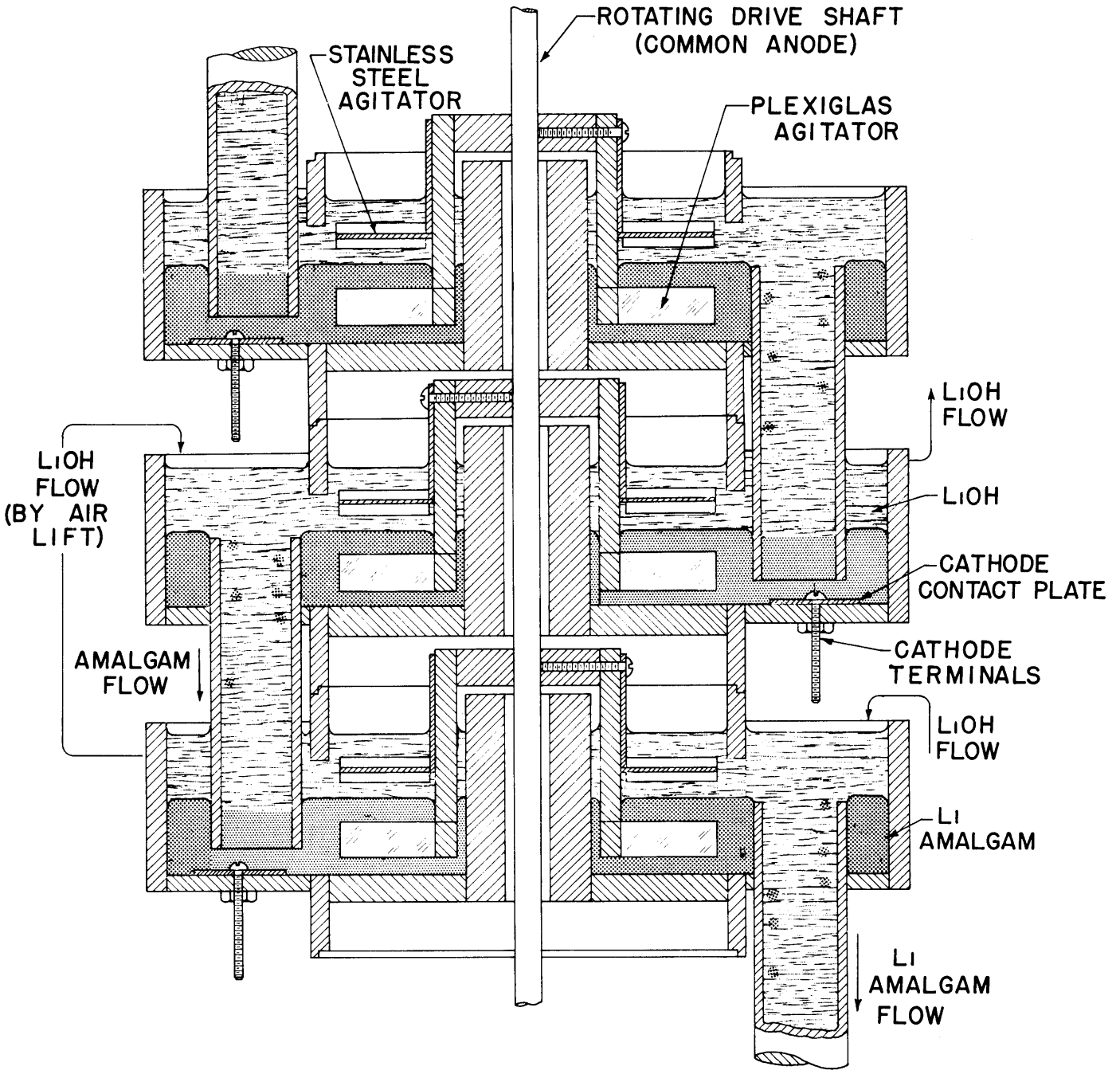

FIGURE 16.1 VERTICAL EXCHANGE APPARATUS
(DIAGRAMMATIC)

Although the work to date has been essentially of a preliminary nature with the purpose of pointing up the major problems with the apparatus, it has indicated that scale-up of the process is feasible. The one major difficulty encountered is the inability of the present apparatus to reach sufficiently high reflux ratios in the amalgam-forming section (Li^7 reflux). Research work is now directed toward finding a solution to this problem.

Considerable research has been done in an effort to find a suitable anode material from the standpoint of cost, electrical properties, and product purity. Platinum is the only material found which is suitable for use in the high-voltage electrolysis section of the Li^7 refluxer. Because of the obvious cost disadvantages of platinum it would be most desirable to find a substitute. In the exchange section of the apparatus, where the potential applied is quite low, it has been found that type 302 stainless steel is a suitable electrode material. An investigation into the possible use of graphite is now underway. To date no sample of graphite has been found which possesses the necessary mechanical properties. It appears from early observations that the gas (O_2) released at the anode is causing the surface to disintegrate as a very fine powder which remains in suspension in the aqueous phase. Research is continuing on this problem.

Recently a closer examination has been made of the factors influencing the product cost in a large-scale plant, and among the several fundamental aspects shown to be of prime importance in future work were the following:

1. The quantities of mercury required will be very large, and every effort must be made to increase plant capacity and reduce mercury holdup. Some study should be made of the probable losses of mercury per cycle since even small losses will add materially to the product cost.

2. Power costs are likely to be fairly high, and every effort should be made to obtain maximum current efficiency. Since most of the power is used in the refluxing sections, this points up the necessity of continuing the effort to design an efficient refluxing mechanism.

APPENDIXES

APPENDIX A

REPORT OF NUCLEAR DEVELOPMENT ASSOCIATES, INC.

Rather than separate the brief discussions of the diverse topics discussed in the "Quarterly Report on ANP Activities"[1] from the Nuclear Development Associates, Inc., they are presented here together, but with identifying paragraph headings.

Xenon Cross-section Computations. Computations on the xenon cross section averaged over a Maxwell distribution, giving the cross section and its temperature derivative as a function of temperature, have been completed and reported (Goertzel, Oppenheim).

Critical Mass of Bare Beryllium-moderated Piles. Calculations on the critical mass of bare Be-moderated piles over a wide range of fuel concentrations, including a perturbation method for finding the effect of added absorbers on fuel requirement, have been carried out and a report is being written (Preiser, Shapiro). A similar study for H-moderated reactors has been started. Some additional considerations pertaining to aircraft reactor control are also intended. Beryllium absorption at thermal (n-γ) and high (n-α) energies, and production (n-2n) at high energies, is being reviewed with Goldstein of the NDA data group and Hughes of Brookhaven.

Supercritical Water Reactor. A preliminary review of the Williams supercritical water proposal has been undertaken. The reactor and shield were looked at briefly, and liaison has been established with United Aircraft which is studying the propulsion system and airplane aspects of the proposal.

Tug-Tow System. The shield weights needed with the Lexington Tug-Tow arrangement appear to be considerably less than the values indicated by the Lexington project. For example, if 40 cm of water (Lex P-1, p. IV B-16) is placed around a 60-cm-radius spherical reactor, and in addition a lead disk of 1 meter radius with a thickness (about 100 g/cm^2) sufficient to provide a γ attenuation of 60 (Lex P-1, p. IV B-14) is provided, the water and lead weight will be a little over 3 metric tons each, or about 7 tons total. Thus relatively midget planes, with midget power outputs and substantially smaller fuel requirements, might be used for tug-tow flight.

(1) Letter to C. B. Ellis from NDA, Nov. 30, 1950.

APPENDIX B

LIST OF REPORTS ISSUED

REPORT NO.	TITLE OF REPORT	AUTHOR(s)	DATE ISSUED
	Design of the ARE		
Y-F8-3	Reactor Maintenance and Disassembly	F. W. Schroeder	10-24-50
Y-F8-4	Evaluation of Coaxial Cylinder Insulation System	S. V. Manson	10-30-50
Y-F8-5	Lecture Notes of Heat Exchanger System of GE Project SIR	S. V. Manson	10-13-50
	Reactor Physics		
ANP-5201	Calculational Procedure for Control Data	N. M. Smith	9-13-50
Y-F10-20	Results of a Test of the Linear Approximating Multigroup Calculations	D. K. Holmes	11-6-50
Y-F10-21	IBM Multigroup Numerical Procedures	D. K. Holmes O. A. Schulze	11-28-50
Y-F10-22	Results of Some Bare Calculations of Critical Mass and Reactivity Effects	J. W. Webster E. T. Macauley	12-1-50
Y-F10-30	Perturbation Equations for the Kinetic Response of a Liquid-fuel Reactor	N. M. Smith T. Rubin M. J. Nielsen R. Coveyou	to be issued
Y-F10-17	Xe Effect in an Epi-thermal Reactor	J. W. Webster	10-10-50
Y-F10-15	Calculation of Average Lifetimes of Neutrons Using the Results of Multigroup Calculations	D. K. Holmes	10-2-50
Y-F10-18	Bare Pile Adjoint Solution	M. J. Nielsen	10-27-50
Y-F10-19	Self-shielding in Uranium	J. W. Webster	11-8-50
Y-F5-22	Numerical Integration of the Multigroup Reactor Equations in Cylindrical Geometry	M. C. Edlund	9-27-50

REPORT NO.	TITLE OF REPORT	AUTHOR(s)	DATE ISSUED
	Critical Experiments		
CF 50-10-115	Fabrication of Fuel Discs for ANP Critical Experiments	A. D. Callihan	10-23-50
CF 50-11-120	Storage and Handling of SF Material for ANP Critical Experiments	A. D. Callihan	11-30-50
	Nuclear Measurements		
CF 50-12-25	Estimate of the Effects of Higher Levels on the Resonance Integral of Xe^{135}	G. E. Arfken T. A. Welton	12-6-50
CF 50-12-45	High Level Sources of 92-hr Xenon	G. W. Parker	12-15-50
	Shielding Research		
ANP-53*	Report of the ANP Shielding Board	NEPA, CRNL, and C&CCD	10-16-50
ORNL-710	Theoretical and Practical Aspects of Shielding	A. S. Kitzes	9-29-50
Y-F15-4	Divided Shields for More Conservative Ground Specifications	T. E. Mitchell	11-20-50
Y-F20-1	Unmanned Nuclear Powered Aircraft and RW	W. K. Ergen	10-10-50
Y-F20-3	Measurements of Fission Fragment Decay Gammas in the Swimming Pool	W. K. Ergen	11-28-50
	Liquid-metal and Heat-transfer Research		
CF 50-9-24	A Survey Concerning the Use of a Liquid Sodium—Austenitic Stainless Steel Heat Transfer Unit Under Conditions Anticipated in Nuclear Aircraft Operations	R. J. Radebaugh	9-7-50

* This report incorporates many earlier reports on various aspects of shielding.

REPORT NO.	TITLE OF REPORT	AUTHOR(s)	DATE ISSUED
Y-F8-6	Theoretical Equations for Estimating Thermal Conductivity of Liquids	S. V. Manson	11-13-50
Y-F8-7	Physical Data for Substances in the Fused State	S. V. Manson	11-20-50
Y-F19-2	Design Charts for Sodium to Lithium and Lead to Lithium Intermediate Exchangers	W. C. Cooley	9-1-50
	Metallurgy		
CF 50-9-83	ANP Materials Projects	E. C. Miller	9-19-50
CF 50-9-127	ANP Materials Program	E. C. Miller	9-26-50
Y-F15-3	Transient Temperature and Thermal Stress in an Infinitely Long Solid Cylindrical Rod with Surface Temperature Changing at a Constant Rate	J. G. Duffy	10-27-50
	Circulating Fuel Reactors		
HKF-109	Homogeneous Reactor for Subsonic Aircraft	H. K. Ferguson Company	12-15-50
	Supercritical Water Reactor		
ANP-55	Preliminary Comments on Supercritical Water Cycle	A. R. Gruber(NDA)	11-6-50
	Miscellaneous		
ANP-54	Interim Report of the ANP Control Board	NEPA, ORNL, and C&CCD	11-1-50